



HAL
open science

Thermodynamic modeling of mixed-solvent electrolytes for process simulators

Saifuddin Ahmed

► **To cite this version:**

Saifuddin Ahmed. Thermodynamic modeling of mixed-solvent electrolytes for process simulators. Chemical and Process Engineering. Sorbonne Université, 2018. English. NNT : 2018SORUS002 . tel-02049398

HAL Id: tel-02049398

<https://theses.hal.science/tel-02049398>

Submitted on 26 Feb 2019

HAL is a multi-disciplinary open access archive for the deposit and dissemination of scientific research documents, whether they are published or not. The documents may come from teaching and research institutions in France or abroad, or from public or private research centers.

L'archive ouverte pluridisciplinaire **HAL**, est destinée au dépôt et à la diffusion de documents scientifiques de niveau recherche, publiés ou non, émanant des établissements d'enseignement et de recherche français ou étrangers, des laboratoires publics ou privés.

Sorbonne Université

Faculté des Sciences et Ingénierie

ED 388 : Ecole doctorale de Chimie Physique
et de Chimie Analytique de Paris Centre



Modélisation thermodynamique des mélanges électrolytiques multi-solvants pour les simulateurs de procédés

par

Saifuddin Ahmed

Thèse de doctorat

Discipline : Génie des Procédés

Dirigée par Jean-Charles de Hemptinne

Présentée et soutenue publiquement le 1 Mars 2018

Devant un jury composé de:

Prof.	DUSSAP Claude-Gilles	Rapporteur	Laboratoire de génie des procédés Université Clermont Auvergne
Prof.	GALINDO Amparo	Rapporteur	Département de génie des procédés L'Imperial College Londres
Prof.	ECONOMOU Ioannis	Examineur	Département de génie des procédés Université Texas A&M à Qatar
Dr.	NOINVILLE Sylvie	Examineur	Laboratoire MONARIS, CNRS Sorbonne Université
Dr.	SIMONIN Jean-Pierre	Examineur	Laboratoire PHENIX, CNRS Sorbonne Université
Prof.	de HEMPTINNE Jean-Charles	Directeur de thèse	IFP Energies Nouvelles, IFP School
Dr.	BERNARD Olivier	Invité	Laboratoire PHENIX, CNRS Sorbonne Université
Dr.	FERRANDO Nicolas	Invité	IFP Energies Nouvelles
M.	BAUDOIN Olivier	Invité	ProSim SA

Thermodynamic modeling of mixed-solvent electrolytes for process simulators

by

Saifuddin Ahmed

Ph.D. thesis

Discipline : Chemical Engineering

Directed by: Jean-Charles de Hemptinne

presented and defended publicly on 1 March 2018

in front of jury:

Prof.	DUSSAP Claude-Gilles	Reviewer	Laboratory of Chemical Engineering Clermont Auvergne University
Prof.	GALINDO Amparo	Reviewer	Department of Chemical Engineering Imperial College London
Prof.	ECONOMOU Ioannis	Examiner	Department of Chemical Engineering Texas A&M University at Qatar
Dr.	NOINVILLE Sylvie	Examiner	Laboratory MONARIS, CNRS Sorbonne University
Dr.	SIMONIN Jean-Pierre	Examiner	Laboratory PHENIX, CNRS Sorbonne University
Prof.	de HEMPTINNE Jean-Charles	Thesis supervisor	IFP Energies Nouvelles, IFP School Laboratoire PHENIX, CNRS
Dr.	BERNARD Olivier	Invited	Sorbonne Université
Dr.	FERRANDO Nicolas	Invited	IFP Energies Nouvelles
Mr.	BAUDOIN Olivier	Invited	ProSim SA

میں اس تحقیق کو اپنے والدین کو نظر کرتا ہوں

मेरे माता पिता को समर्पित

Dedicated to my parents

Dédié à mes parents

Acknowledgements

This thesis is written for the requirement for the PhD degree in chemical engineering at Sorbonne University, Paris, France. The research work was done at the Department of Thermodynamics and Molecular Modeling at IFP Energies Nouvelles (IFPEN) in collaboration with ProSim company and National Center for Scientific Research (CNRS) from March 2015 to March 2018. I would like to thank Véronique Ruffier-Meray and Pascal Mougin for providing an opportunity at IFPEN for carrying out this research work.

I would like to convey my deepest and sincere gratitude to Jean-Charles de-Hemptinne as the main supervisor and Nicolas Ferrando as co-supervisor of this thesis at IFPEN. They have been an excellent guide for the research journey which involved numerous scientific discussion while realizing the goals of this thesis. I would also like to extend this gratitude to Jean-Pierre Simonin, Olivier Bernard for their excellent guidance during this thesis which involved several discussion deep down into electrolyte thermodynamics. To Olivier Baudouin for his continuous and productive collaboration involving several discussions with him that has made this thesis highly important to industry. I extend my expression of sincere gratitude to the jury of this thesis for their time and effort in examining this thesis.

I would like to extend my heartiest thanks to my colleagues and friends Angela, Annabelle, Aurélie, Benoit, Brigitte, Carlos, Catherine, Camilo, David, Germain, Isabelle, Leo, Martha, Mona, Salah, Sebastien, Michel, Theo, Veronique, Xavier.

Finally, I must express my very profound gratitude to my parents and to my siblings for providing me with support and encouragement throughout these years. This accomplishment would not have been possible without them.

Thank you all for you encouragement!

Résumé

Avec le développement de nouvelles technologies dans les procédés, les solvants mixtes électrolytiques présentent un intérêt croissant. Cependant, les performances des modèles thermodynamiques actuels sont assez limitées sur ce type de système. Cela est dû aux interactions complexes que ces systèmes présentent. Par conséquent, l'objectif de ce travail est d'étendre les capacités du modèle thermodynamique eGC-PPC-SAFT aux solvants mixtes électrolytiques. Ceci est fait en plusieurs étapes. Dans une première étape, le modèle PPC-SAFT existant est amélioré pour l'eau pure et des solvants usuels, et une modélisation de leurs équilibres de phase en mélange est proposée. Une modification du diamètre consistant à introduire une dépendance en température a ainsi été proposée pour améliorer la précision du modèle. Dans une seconde étape, ce modèle amélioré est utilisé pour étudier les coefficients d'activité et les densités des systèmes contenant des électrolytes forts et les équilibres VLE des solvants mixtes électrolytiques. Cela est réalisé en proposant une stratégie de paramétrage des ions pouvant prédire au mieux ces propriétés et les phénomènes de « salting-out ». Cela implique également d'étudier l'importance de la constante diélectrique dans le cadre de la modélisation thermodynamique de ces systèmes. Dans la troisième étape, le modèle final est utilisé pour étudier les équilibre liquide-liquide des solvants mixtes électrolytiques. Cela a été réalisé en étudiant les coefficients de partition de chacune des espèces dans le système. Pour cela, une stratégie de paramétrage des paramètres binaires ion-solvant a été développée, qui implique l'évaluation de l'impact de chacune des contributions individuelles du modèle ePPC-SAFT sur les coefficients de partition. Par ailleurs, une nouvelle méthode de traitement de la condition d'électroneutralité dans les systèmes électrolytiques liquide-liquide a été proposée, impliquant une correction directe du coefficient de fugacité. Enfin, une nouvelle règle de mélange pour la constante diélectrique du solvant mixte comprenant un paramètre binaire est proposée afin de fournir la meilleure description possible des équilibres LLE de ces systèmes. Au final, le modèle développé est capable de décrire les coefficients d'activité ainsi que les équilibres VLE et LLE des systèmes solvants mixtes électrolytiques.

Abstract

With the advent of new and advanced process technologies, mixed solvent electrolytes are finding increased utility. However, the capabilities of the current thermodynamic models are quite limited in dealing with such systems. This is due to the complex interactions that these systems exhibit. Therefore, the objective of this work is, to extend the capabilities of eGC-PPC-SAFT model to mixed solvent electrolytes mixtures. This is done in several steps. In the first step, the existing PPC-SAFT model is improved for pure water and solvents, and subsequently modeling their phase behavior. A modification in the temperature dependent diameter was proposed which then improves the description of mixed-solvent systems. In the second step, the improved model is utilized to study activity coefficients and densities of strong electrolyte systems and VLE of mixed solvent electrolyte system while proposing an ion-parameterization strategy that best describes these systems, and describe the salting-out phenomena. This also involves investigating the importance of the dielectric constant in the mixed solvent electrolyte thermodynamic framework. In the third step, the final model is used to study the liquid-liquid equilibrium of the mixed-solvent electrolyte system. This was done by looking at the partition coefficients of the individual species in the systems. In doing so, a parameterization strategy was developed for ion-solvent binaries that involves assessing the impact of the individual ePPC-SAFT contribution on the partitioning of individual species. A new method for dealing with the condition of electroneutrality in liquid-liquid ionic systems was proposed that involves a direct correction on the fugacity coefficient. A new mixing rule for the dielectric constant of mixed solvent including a binary parameter is proposed to provide the best description of LLE of mixed solvent electrolyte. The final model is capable of describing, the activity coefficient, VLE, and LLE of mixed-solvent electrolyte systems.

Table of contents

List of figures	xvii
List of tables	xxiii
Nomenclature	xxvii
1 Setting up stage	1
1.1 Introduction	1
1.2 A very brief history of thermodynamics	3
1.3 Motivation for this work	4
1.4 Roles of Electrolytes in Various Industries: Scope of this work	8
1.4.1 Biorefining industry	8
1.4.2 Oil and Gas industry	9
1.4.3 Carbon capture and sequestration (CCS)	11
1.4.4 Acid gas injection	11
1.4.5 Pharmaceutical industry	11
1.4.6 Other uses of electrolytes	11
1.5 Aqueous two-phase systems	12
1.6 Objectives of this research	12
2 Electrolyte thermodynamic model and the State of the art	15
2.1 Introduction	16
2.2 Activity coefficient models vs EoS	17
2.3 Interactions in electrolyte systems and theories	18
2.3.1 Discharge	19
2.3.2 Repulsion and dispersion	20
2.3.3 The Structure-forming step	20
2.3.4 Electrolyte terms	21

2.4	Review of the existing electrolyte and mixed-solvent electrolyte EoS . . .	27
2.4.1	State of the art	27
2.4.2	Choice of thermodynamic model	30
2.5	Statistical associating fluid theory (SAFT)	30
2.5.1	Perturbation theory	30
2.5.2	History of Statistical Associating Fluid Theory (SAFT)	31
2.5.3	Mathematical description of PC-SAFT	32
2.5.4	Various terms of ePPC-SAFT	33
2.5.5	Group contribution approach	38
2.5.6	Cross association parameters	38
3	Modified model of PC-SAFT for water	41
3.1	Abstract	42
3.2	Introduction	43
3.3	Model	43
3.3.1	Previous Descriptions of Water with the PC-SAFT EoS	47
3.3.2	A new Temperature Dependence of Water Diameter	48
3.4	Results for binary mixtures	51
3.4.1	Mutual solubilities	51
3.4.2	Octanol/Water Partition coefficient	65
3.4.3	Gibbs energy of Hydrogen Bonding	66
3.4.4	Conclusion	68
4	Modeling of strong electrolytes	69
4.1	Abstract	70
4.2	Introduction	70
4.3	Some thoughts and arguments related to the choices made in this work	71
4.3.1	What is solvation?	71
4.3.2	Specificities related to the GC-ePPC-SAFT model	76
4.3.3	Parameters from previous work	77
4.4	Ion parameterization procedure	79
4.5	Regression Results	83
4.5.1	Correlation results for Alkali halide brines	83
4.5.2	Solvation Gibbs energies for Alkali halide brines	89
4.6	Alkanes and acid gases with brines: salting out effect in presence of organic compounds	90

4.7	Mixed solvent electrolytes	93
4.8	Conclusion	98
5	Modeling LLE of mixed-solvent electrolytes	101
5.1	Introduction	102
5.2	Algorithmic issue: Electroneutrality	103
5.2.1	Generalities	103
5.2.2	Current state: without electroneutrality	104
5.2.3	A new method for electroneutrality: Modifying the fugacity coefficient	104
5.3	The machinery	109
5.3.1	Prediction of the LLE by the non-parameterized model	109
5.3.2	Partition coefficient of salts	111
5.4	Parameterizing mixed solvent salt systems using available data	117
5.4.1	Dielectric constant of mixed-solvents	118
5.4.2	MIAC of mixed solvent electrolyte systems: Analysis	121
5.4.3	Approach for parameterization of mixed-solvent salt systems	122
5.4.4	Result of MIAC for mixed solvent electrolytes	126
5.4.5	Parameter for 1-Butanol-water-salt systems from LLE data	132
5.5	Final results	133
5.6	Conclusion	138
6	Conclusions and recommendations for future work	141
6.1	Conclusion	141
6.2	Recommendations for future work	143
	Bibliography	145
	Appendix A Variants of the MSA theory	167
A.1	Mean spherical approximation (MSA) theory	167
A.1.1	Primitive MSA	167
A.1.2	Non-restricted primitive	167
A.1.3	Restricted primitive	169
A.1.4	Helmholtz energy expression	169
A.2	Non-Primitive MSA	170

Appendix B LLE phase diagrams of mixed-solvent salt systems	173
B.1 1-Butanol-water-salts	173
B.2 2-Butanol-water-salts	176
B.3 Propanol-water-salts	176

List of figures

1.1	A very simplified view of a chemical industry	2
1.2	Process simulation using process simulation software ProSimPlus ®	3
1.3	Timline for major milestones in the history of thermodynamics	4
1.4	History of modern thermodynamics (Green colored label are those which will continue to dominate the future of chemical engineering thermodynamics)	5
1.5	Plot of liquid-liquid phase split in water-NaCl-propanol mixture and limited capability of the predictive model [17]	7
1.7	Various objective statements of this PhD thesis in order to obtain the ePPC-SAFT model for mixed solvent electrolytes	13
2.1	Thermodynamic cycle representing steps in forming an electrolyte thermodynamic equation of state	19
2.2	Radial distribution function (rdf) and coordination number (CN)between Na+/O pairs and Cl-/O pairs obtained from Monte Carlo simulations [67]	21
2.3	Solvation interaction in an electrolyte solution, salt crystals gets dissolved and salt gets dissociated into ions, solvent molecules surround cations and anions	22
2.4	A schematic representation of various contribution in PPC-SAFT	31
3.1	Deviation (%) in vapor pressure (old model  , new model ) and saturated liquid volume (old model  , new model ) of pure water using our approach	47

3.2	Plot of the temperature dependent segment diameter $\sigma_{T,W}(T)$. Symbols indicate optimized values of sigma on small temperature intervals of 10K. The line indicates the correlation (equation 3.3), but this correlation has final parameters which are optimized again on saturated liquid density and vapor pressure of pure water and LLE of n-hexane in the temperature range 273.15K-550K.	50
3.3	Deviations in aqueous and organic solubility of various water-alkane mixtures from current model in comparison to results from NguyenHuynh <i>et al.</i> [152]	55
3.4	● Solubility in aqueous phase and ● solubility in organic phase of n-pentane, points are experimental data and lines are calculation from model	55
3.5	Deviations in aqueous and organic solubility of various water-alkylbenzene mixtures from current model in comparison to results from NguyenHuynh <i>et al.</i> [152]	56
3.6	Deviations in aqueous and organic solubility of various water-alcohol mixtures from current model [152] in comparison to results from NguyenHuynh <i>et al.</i> [152]	57
3.7	Water-Ethanol VLE at 2 different temperatures	58
3.8	Water-hexanol vapor liquid equilibrium at 313.15K (solid line) and 294.15K (dashed lined), lines are prediction from the new model and symbols are experimental data)	58
3.9	Water-butanol vapor liquid equilibrium at 323.15K (solid line) and 298.15K (dashed lined), lines are prediction from the new model and symbols are experimental data)	59
3.10	Butanol-ethanol-water liquid-liquid phase diagram at 298K, 1 bar as a comparison of model prediction with experiemntal data. Green circles represent the model and the res squares represents the experimental data [177]	59
3.11	Deviations in aqueous solubility of various water-aldehyde mixtures from current model in comparison to results from NguyenHuynh <i>et al.</i> [130] . .	60
3.12	Deviations in organic solubility of various water-aldehydes mixtures from current model in comparison to results from NguyenHuynh <i>et al.</i> [130] . .	60
3.13	Deviations in aqueous solubility of various water-ketone mixtures from current model in comparison to results from NguyenHuynh <i>et al.</i> [130] . .	61
3.14	Deviations in organic solubility of various water-ketone mixtures from current model in comparison to results from NguyenHuynh <i>et al.</i> [130] . .	62

3.15	Deviations in aqueous solubility of various water-ether mixtures from current model in comparison to results from NguyenHuynh <i>et al.</i> [130]	63
3.16	Deviations in organic solubility of various water-ether mixtures from current model in comparison to results from NguyenHuynh <i>et al.</i> [130]	63
3.17	Deviations in aqueous and aqueous solubility of various water-ester mixtures from current model	64
3.18	Deviations in aqueous and organic solubility of various water-ester mixtures from current model	64
3.19	Octanol/water partition coefficient for alkanes, alcohols, aldehydes, ketones, ethers, and esters from our models compared to experimental data	65
3.20	Gibbs energy of hydrogen bonding calculated with this model	67
4.1	Contribution of Helmholtz free energy $\frac{\partial A^{res}}{\partial n_i}$ (Y-axis) for each term of PC-SAFT and for each ion at infinite dilution.	72
4.2	Effect of the various terms on the logarithm of the mean ionic activity coefficient (MIAC) for NaCl at 298.15K. The model used is that presented in section 3 along with the parameters presented in table 4.6	75
4.3	Trend of regressed parameters in comparison to Pauling diameters. (a) MSA diameters vs Pauling diameters (b) association energy. Blue (cations), orange (anions)	83
4.4	MIAC of aqueous salt solutions at 298.15K for alkali halides. The lines represent calculation from model and circles represent experimental data both in the order from top to bottom (LiX, NaX, KX, RbX, CSX) where X is the alkali halide ion except for fluorides where this order is reversed (no LiF salt not taken)	85
4.5	Effect of the various terms on the logarithm of the mean ionic activity coefficient (MIAC) for NaF salt	86
4.6	Densities (kg/m ³) (Y axis) of aqueous salt solutions at 298.15K for alkali halides. The lines represent calculation from model and circles represent experimental data both in the order from bottom to top (LiX, NaX, KX, RbX, CSX) where X is the alkali halide ion	86
4.7	MIAC of salt aqueous solutions at various temperatures for (a) aq. NaCl (273.15K 323.15K 348.15K 373.15K 423.15K) top to bottom (b) aq. KCl (273.15K 291.15K 308.15K 323.15K) top to bottom. The lines represent calculation from model and circles represent experimental	87

4.8	Liquid density(kg/m ³) of salt aqueous solutions at various temperatures. The lines represent calculation from model and circles represent experimental.(273.15K 323.15K 373.15K 423.15K 473.15K)	88
4.9	Liquid densities of aqueous (a) NaCl + KCl system and aqueous (b) NaCl + KBr system 298.15K and varying salt molalities. The figure is plotted against mole fraction of NaCl while each line is at fixed total salt concentration. Points are experimental data [226] and lines are prediction from model	88
4.10	Solubility of alkanes and acid gases in water at two different salt concentrations red(0 molal) blue (1 molal) green (4 molal) for systems (a) CH ₄ -H ₂ O-NaCl system at 324 K (b) C ₂ H ₆ -H ₂ O-NaCl system at 353K (c) CO ₂ -H ₂ O-KCl system at 313K (d) H ₂ S-H ₂ O-NaCl system at 393K . . .	92
4.11	Isobaric Vapor-liquid equilibrium of Methanol-Water-salt system at 1 bar. Lines are prediction from model and point are experimental data. (a) water-methanol-NaCl system at varying salt molalities (upto 2.56 molal) (blue line indicates salt-free systems (water-methanol) (b) water-methanol-KCl system at varying salt molalities (0.1-2 molal) in experimental data the model prediction at 2 molal concentration of salt to obtain a smooth curve at uniform salt concentration. (c) water-methanol-NaF system at varying salt molalities(0.2-0.5) in experimental data but model prediction at 0.5 molal concentration of salt to obtain a smooth curve at uniform salt concentration. (d) water-methanol-NaBr system at varying salt molalities(0.01-3.5 molal) in experimental data but model prediction at 2.0 molal concentration of salt to obtain a smooth curve at uniform salt concentration	96
4.12	Isothermal Vapor-liquid equilibrium of Ethanol-Water-NaI system at 298.15K. Lines are prediction from model at 0.5 molal and point are experimental data at varying molalities (upto 1.35) (blue line indicates no salt systems (water-ethanol) (b) water-ethanol-NaF system at varying salt molalities (up to 0.82) at 1 bar	97
5.1	Various methods for imposing the condition of electroneutrality in a thermodynamic framework	103
5.2	Current flash procedure without respecting electroneutrality	104
5.3	Creation of electrostatic phase potential	105

5.4	Theoretical representation of the condition of electroneutrality	106
5.5	Procedure for implementing the new method of electroneutrality	108
5.6	Partition coefficient of Na^+ and Cl^- in two phase ionic system before and after implementing the new method for electroneutrality	109
5.7	Current state of parameterization in mixed solvent electrolyte systems . .	110
5.8	Partition coefficients of 1-Butanol - Water - CsCl system at 293.15K . . .	111
5.9	Partition coefficients of 1-Butanol - Water - LiCl system at 293.15K . . .	111
5.10	Contributions of the various terms on the partition coefficient of salts, cations and anions for 1-Butanol-water-KCl at 298.15K	114
5.11	Contributions of the various terms on the partition coefficient of salts, cations and anions for 1-Butanol-water-CsCl at 298.15K	115
5.12	Contributions of the various terms on the partition coefficient of salts, cations and anions for 1-Butanol-water-NaF at 298.15K	115
5.13	Contributions of the various terms on the partition coefficient of salts, cations and anions for 1-Butanol-water-LiF at 298.15K	115
5.14	Contributions of the various terms on the partition coefficient of salts, cations and anions for 1-Butanol-water-NaI at 298.15K	116
5.15	Contributions of the various terms on the partition coefficient of salts, cations and anions for 1-Butanol-water-NaCl at 298.15K	116
5.16	Contributions of the various terms on the partition coefficient of salts, cations and anions for 1-Butanol-water-RbCl at 298.15K	116
5.17	Dielectric constant of Alcohol-water mixture at 298.15K, comparison from model vs experimental data (adjusted binary parameter D_{ij} for model) .	120
5.18	Mean Ionic activity coefficients experimental data trend for mixed solvent methanol, ethanol, 1-Propanol, and butanol - salt systems systems at varying weight fraction (w_m) (10% —, 20% —, 30% —, 40% —) . .	122
5.19	Plot of the regressed alcohol-ion parameter u_{ij} against Pauling diameters: Case(a)	126
5.21	Plot of the regressed alcohol-ion parameter l_{ij} ● and u_{ij} □ against Pauling diameters: Case(b)	126
5.20	Plot of the regressed alcohol-ion parameter l_{ij} against Pauling diameters: Case(b)	127
5.22	Mean Ionic activity coefficients of Methanol-water-NaCl systems at varying weight fraction (w_m) (10% —, 20% —, 30% —, 40% —), points: experimental data, full lines: case (c)	128

5.23	Mean Ionic activity coefficients of Ethanol-water-NaCl systems at varying weight fraction(w_m) (10% — , 20% — , 30% — , 40% —), points: experimental data, full lines: case (c)	130
5.24	Mean Ionic activity coefficients of Propanol/ Butanol-water-NaCl systems at varying weight fraction (w_m) (10% — , 20% — , 30% — , 40% —), points: experimental data, full lines: case (c)	131
5.25	Partition coefficients of 1-Butanol - Water - CsCl system at 293.15K . . .	134
5.26	Partition coefficients of 1-Butanol - Water - LiCl system at 293.15K . . .	134
5.27	Partition coefficients of 1-Butanol - Water - KCl system at 298.15K . . .	134
5.28	Partition coefficients of 1-Butanol - Water - NaCl system at 293.15K and 303.15K	135
5.29	Partition coefficients of 1-Butanol - Water - NaCl system at 298.15K . .	135
5.30	Partition coefficients of 1-Butanol - Water - NaF system at 293.15K . . .	135
5.31	Partition coefficients of 1-Butanol - Water - NaI system at 293.15K . . .	136
5.32	Partition coefficients of 1-Butanol - Water - LiF system at 293.15K . . .	136
5.33	Partition coefficients of 1-Butanol - Water - KF system at 293.15K . . .	136
5.34	Partition coefficients of 1-Butanol - Water - RbCl system at 293.15K . .	137
B.1	Liquid-Liquid equilibrium in 1-Butanol-Water-Salt systems at various temperatures, Points are experimental data, line is the calculation from model. Axes represent the mole fraction of the respective component, some axes are scaled.	173
B.2	Liquid-Liquid equilibrium in 2-Butanol-Water-Salt systems at 298.15K, Points are experimental data (NaCl [268], KCl [268]) line is the calculation from model. Axes represent the mole fraction of the respective component, some axes are scaled.	176
B.3	Liquid-Liquid equilibrium in 1-Propanol-Water-Salt systems at 298.15K, Points are experimental data(NaCl [281], NaBr [281], KF [282],KCl [283]), RbCl [284]) line is the calculation from model. Axes represent the mole fraction of the respective component, some axes are scaled.	177

List of tables

2.1	Traditional classification of thermodynamic models and EoS	16
2.2	Review of the existing electrolyte thermodynamics models	28
2.3	Review of the mixed-solvent electrolyte thermodynamics models	29
3.1	Group Contribution parameters for alkanes, alkylbenzenes, alcohols, ketones, aldehydes, ethers and esters for use with GC-PPC-SAFT ^a	45
3.2	Pure component parameters of water used in this work.	50
3.3	Compressibility factor Z in the supercritical region from the new model and from NIST database	51
3.4	Optimized water-group interaction parameters using approaches (a) and (b)	52
3.5	Deviations between experimental and calculated mutual solubilities	53
3.6	Binary interaction parameter k_{ij} between molecules for approach (b)	54
3.7	Average absolute deviation (%) in K_{OW} over whole hydrocarbon/oxygenate family as a comparison between Nguyen <i>et al.</i> [130] and our model	66
3.8	Comparison of Gibbs energy of hydrogen bonding between water and a solute at 298.15 K from this work (GC-PPC-SAFT model) and the experimentally-based methodology of Sedov <i>et al.</i> [178–181]	67
4.1	Correlations for calculating dielectric constants of the pure solvent, regressed on experimental dielectric constant (273–423 K and densities upto 63 mol/dm ³)	77
4.2	Pure component parameters of water used in this work taken from our previous work [196].	78
4.3	Pure component parameters of alkanes and alcohols used in this taken from [152] work	78
4.4	Number of association sites (N_s) for ions in different electrolyte models	78

4.5	Apparent Molar Volumes (AMV), Mean Ionic Activity Coefficients (MIAC), and densities at 298 K, experimental Data, correlations, and calculations	80
4.6	Final ion parameters sets, $\sigma_{HS}(\text{\AA})$ are fixed equal to Pauling diameter . .	83
4.7	Gibbs energy of solvation $\Delta_{Gs,salt}$ for alkali halides. Experimental data compared to calculation from the model (our model vs SAFT-VR+DE [127] vs SAFT-VRE [71] vs SAFT-VRE [123]).	90
4.8	Table for AAD, binary and ternary system parameter for alkane/acid gases-water-salt systems	94
4.9	Table for AAD, binary system parameter for VLE of alcohol-water-salt systems	98
5.1	Dominant PC-SAFT contribution in partitioning of salt in LLE of mixed solvent electrolytes and their parameter	113
5.2	Correlations for calculating dielectric constants of the pure solvent [123] .	118
5.3	Experimental MIAC data at 298.15K of mixed solvent salt systems used for ion-solvent parameter regression, deviations from calculation using case(c) are reported in % AAD of MIAC	124
5.4	Solvent-ion parameters for mixed-solvent salt systems (Case a: Association parameter tuning u_{ij})	125
5.5	Solvent-ion parameters for mixed-solvent salt systems (Case b: Repulsion parameter tuning l_{ij})	125
5.6	Solvent-ion parameters for mixed-solvent salt systems (Case c: Association parameter u_{ij} and Repulsion parameter tuning l_{ij})	126
5.7	Experimental LLE data of mixed solvent salt systems used in the current work	132
5.8	Final solvent ion-parameters for propanol/butanol - water - salt systems	133

Nomenclature

List of symbols

ΔV Electrostatic phase potential difference between two phases

$\Delta^{A_i B_j}$ Association strength

Γ MSA closure parameter

γ_i Activity coefficient of component i

κ^{-1} Debye screening length

$\kappa^{A_i B_j}$ Association volume

λ Sphere softness

μ Dipole moment

μ_i Chemical potential of a component i

μ_i^α Chemical potential of component i in phase α

μ_i^{ref} Chemical potential of a component i at the reference state

ψ_i Electric potential around a component i

ρ Molar density

ρ_i^Q Volumetric charge density of component i

σ_i Solvation diameter of an ion (used in Born term)

σ_{ij} Diameter of the segment

$\tilde{\mu}_i^\alpha$ Electrochemical potential of component i in phase α

$\tilde{\varphi}_i^\alpha$	Fugacity coefficient of component i in phase α in an electroneutral system
\tilde{K}_i	Partition coefficient of component i in an electroneutral system
ε^{AB}	Association energy
ε_0	Permittivity of free space
ε_r	Relative static permittivity
ε_{ij}/k	Dispersion energy parameter
φ_i	Fugacity coefficient of component i
φ_i^α	Fugacity coefficient of component i in phase α in a non-electroneutral system
A^{res}	residual Helmholtz energy
$d(T)$	Temperature dependent diameter
F	Faraday's constant
f_i	fugacity of the component i
f_i^{ref}	fugacity of the component i in the reference state
g_{ii}^{seg}	Hard sphere radial distribution function
J	Pseudo-ionization energy
k_{ij}	Binary interaction parameter
K_i	Partition coefficient of component i in a non-electroneutral system
l_{ij}	Correction of cross diameter
M	Number of association sites
m_i	the chain length
P	Pressure
R	Ideal gas constant
σ	Segment diameter

T	Temperature
V^α	Electrostatic phase potential of phase α
X^A	Non-bonded fraction to site A
x_i	Mole fraction of component i
x_p	fraction of polar hard spheres
z_i	Charge of component i
z_i	Charge on ion
A^{NAS}	Residual Helmholtz energy contribution for Non-additive Segment (NAS)
A^{SWC}	Residual Helmholtz energy contribution for ordinary Square Well Chains (SWC)

List of physical constants

$\kappa_B = 1.3806503 \times 10^{-23}$	J K ⁻¹	Boltzmann constant
$N_A = 6.0221415 \times 10^{23}$	mol ⁻¹	Avogadro's constant
$N_A = 6.0221415 \times 10^{23}$	mol ⁻¹	Avogadro's constant
$R = k_B N_A = 8.314472$	Pa m ³ mol ⁻¹ K ⁻¹	Ideal gas constant
$e = 1.60217646 \times 10^{-19}$	C	Elementary charge
$F = e \times N_A = 96485.33$	C mol ⁻¹	Faraday constant
$\varepsilon_0 = 8.854187 \times 10^{-12}$	F m ⁻¹	Vacuum permittivity

Chapter 1

Setting up stage

1.1	Introduction	1
1.2	A very brief history of thermodynamics	3
1.3	Motivation for this work	4
1.4	Roles of Electrolytes in Various Industries: Scope of this work	8
1.4.1	Biorefining industry	8
1.4.2	Oil and Gas industry	9
1.4.3	Carbon capture and sequestration (CCS)	11
1.4.4	Acid gas injection	11
1.4.5	Pharmaceutical industry	11
1.4.6	Other uses of electrolytes	11
1.5	Aqueous two-phase systems	12
1.6	Objectives of this research	12

1.1 Introduction

Our daily life is surrounded by fascinating chemical products, for instance, the paper on which this text is printed or perhaps the screen on which you are reading this thesis, or the chair on which you are sitting, are all chemical products in part or as a whole. There are umpteen numbers of objects around us that qualify as a chemical product. But, have you ever wondered how these chemical products are made?. An obvious reply to this question would be that *“these products are made in a chemical industry or factories”*. This is correct in a broad sense, however, a chemical industry involves several

complicated operations. In figure 1.1 we present a very simplified picture of a complex chemical industry. This figure presents two main operations, a conversion operation (conversion of raw material into products) and then there is a separation operation (separating unconverted material from converted material to form the pure product). This research is applied on the second step “the purification process”. Purification of a mixture containing two or more chemical components in an industry is inevitable and is done using separation operations like distillation, extraction, and filtration. Distillation involves separating chemical components based on their differences in boiling temperatures (volatilities). While extraction is done using the difference in the affinities (solubilities) of the compounds in a third chemical compound.

The separation process is vitally dependent on the availability of thermodynamic data which helps in designing a separation column specific to the mixtures needed to be separated. Since each material differs from the other in the physical properties such as density, vapor pressure, and boiling point, it is necessary to know this information before designing a suitable separation equipment. This information can be extracted in a laboratory setting by certain experimental techniques for the same material of interest. Thus, it is clear that physical properties or thermodynamics are essential for designing a process.

The design of the process equipment is thus central to the efficiency of the overall process. A famous chemical engineer and businessman Bodo Linhoff said and I quote:

"Most chemical process are a network of different pieces of equipment. Usually, even the best pieces of equipment will give a poor overall process if linked up inappropriately in the network"

The integration of process equipment thus becomes crucial. The design of the process network and the process equipment is done using process simulation software. Figure 1.2 is presented below which shows how a process is designed using process simulator (the linking up of various pieces of equipment involves complicated heat and mass balances and process engineering in the background). This software rely on the availability of

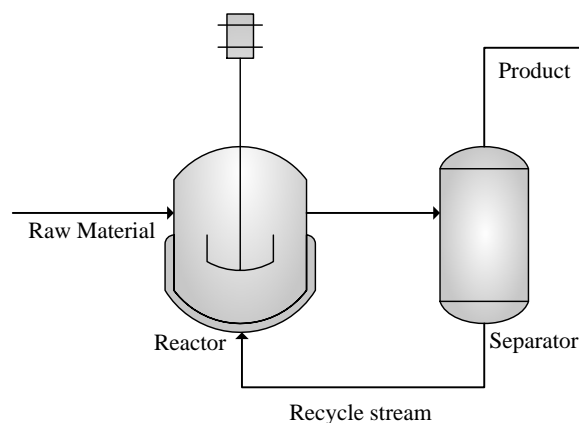


Figure 1.1: A very simplified view of a chemical industry

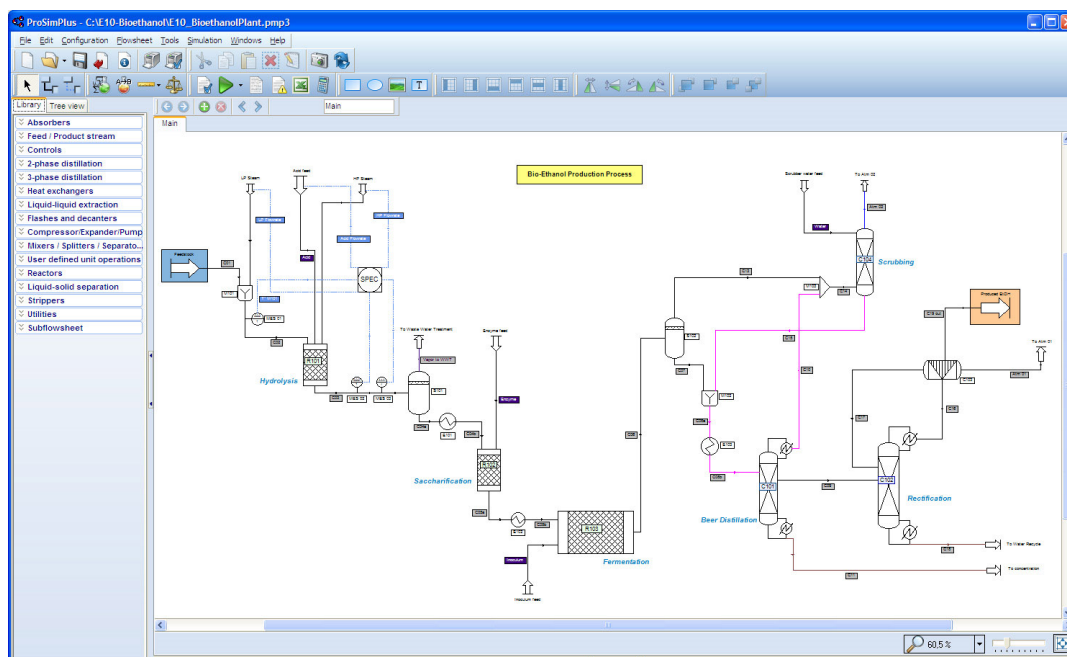


Figure 1.2: Process simulation using process simulation software ProSimPlus ®

thermodynamic information to the extent that the success of an efficient process simulator depends on the efficiency of the thermodynamic framework integrated into.

To this end, accurate thermodynamic information is necessary for efficient process equipment design. After the oil crisis of 1970's, much of the interest was put on improving the design in order to optimize energy utilization, thus reducing the operational cost. The focus was shifted on the need of accurate thermodynamic models and equation of states in process simulation software that would better represent physicochemical properties of materials in the process.

Before moving on further to talk about the motivation of this work, it is important to take a brief look at the history of thermodynamics. This is also important because it will allow to draw a connect between the “industrial age” and the “evolution of thermodynamics”.

1.2 A very brief history of thermodynamics

As already said, chemical engineers utilize thermodynamics for process calculations and particularly balances of material and energy streams. However, it would be incorrect to say that before the advent of the industrial age, thermodynamics was an “unknown science”. The invention of the thermometer and the manometer to measure physically

quantified relative values of temperature and pressure marked the beginning of the thermodynamic science in mid-1600's. Two centuries later, Avogadro proposed that *"equal volumes of all gases, at same temperature and pressure, have the same number of molecules"*, which later on led to the development of ideal gas law (the first thermodynamic Equation of state (EoS)). In those times, interest in measuring and correlating Pressure-Volume-Temperature relationships grew. In 1873 J.D. van der Waals proposed a pressure-volume and temperature EoS for real gases, which marked the beginning of modern day thermodynamics and the birth of new EoS, that took into account intermolecular interactions. In the figure 1.3 we present some major events that took place in history and led to the development of present-day thermodynamics. In fig 1.4 we present the major models/ theories/ EoS that has been developed in the last century and will continue to dominate the future of thermodynamics.

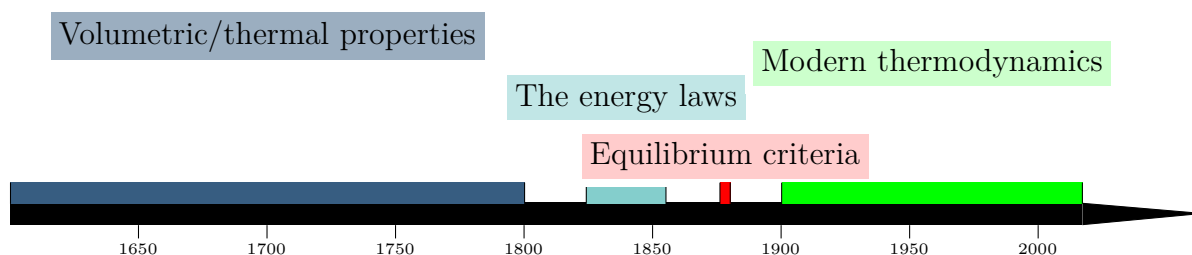


Figure 1.3: Timline for major milestones in the history of thermodynamics

1.3 Motivation for this work

For obtaining the thermodynamic information, several theoretical thermodynamic frameworks exist, such as activity coefficient models and equation of state (Chapter 2). These frameworks are still popular when it comes to obtaining thermophysical properties and phase equilibrium of simple fluids in the process industry. Cubic EoS [1–3] are simple and deliver fast calculations, applicable over wide ranges of temperature and pressure. They can provide satisfactory results for hydrocarbons, gases and non-polar compounds using binary interaction parameters. However, predictive capabilities of Cubic EoS are limited, they rely on fitted binary interaction parameters (k_{ij}) which require extensive experimental data. Moreover, for complex polar compounds, the correlative capability is also poor even with fitted binary interaction parameters. Kontogeorgis in his book has extensively discussed merits and demerits of Cubic EoS [4]. Activity coefficient models

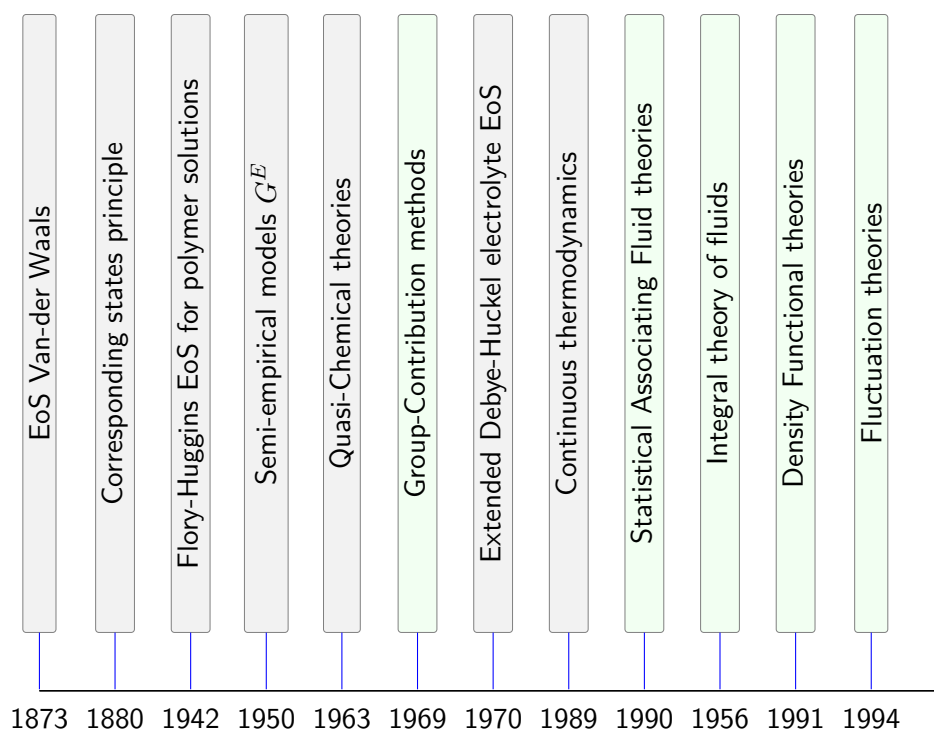


Figure 1.4: History of modern thermodynamics (Green colored label are those which will continue to dominate the future of chemical engineering thermodynamics)

are applicable at low pressure and are successful for polar fluids, polymers/oligomers, and electrolytes. However, these models too have restricted predictive capability. In a nutshell these models and cubic EoS act as correlative tools to reproduce experimental data while their extrapolation outside the range of "fitted experimental data" is often unreliable.

Industrial processes involving complex mixtures of polar, non-polar, ionic species, and species that are capable of forming a hydrogen bond, need better and reliable thermodynamic frameworks. These mixtures are ubiquitous in various chemical, biochemical processes such as the production of biofuels, acid-gas treatment, waste-water treatment and various distillation and fractional crystallization processes [4, 5] (Section 1.4). More specifically, chemical engineers need to know phase equilibrium between species and enthalpies to accurately design separation processes such as distillation columns, extractive distillations, liquid-liquid extractions, etc. [4-6].

When salts are introduced in mixtures of polar solvents such as water they split into ions and the resulting solution is called an electrolyte solution. Various interactions are observed in these electrolyte solutions, the solvent molecules which are polar and

often associating in nature exhibit various dipolar/quadrupolar and hydrogen bonding interactions. The charged species (ions) on the other hand exhibit ion-ion long-ranged electrostatic interactions which are coulombic in nature. These ions may further coalesce resulting in phenomena known as ion-pairing. Short range interaction between ion and solvent (depending on the orientation of the dipoles of solvent molecules) leads to modification of existing solvent structure.

Presence of ions in solution reduces the activity of water which results in lowering the freezing point of the mixture. The presence of ions also affects the volume and the heat capacity. Many activity coefficient models like e-UNIQUAC [7] or e-NRTL [8–10] can correlate fairly well, the data, but, they are mostly reliant on empirical techniques, which renders them ineffective when used for predicting the behavior of a new mixture [11].

Due to a large number of species involved and varying operating conditions, accurate thermodynamic data are often missing, which leads to inefficient design both in terms of energy efficiency and product purity. In this context, the development of a predictive thermodynamic equation of state is of primary importance [4, 6, 12–16]. The availability of liquid-liquid equilibrium data for electrolytes is scarce and it is often impossible to predict it correctly. For instance, an illustration is shown in fig. 1.5 shows the liquid-liquid equilibrium in Water – NaCl – Propanol mixture, while Water-Propanol mixtures without salt are completely miscible.

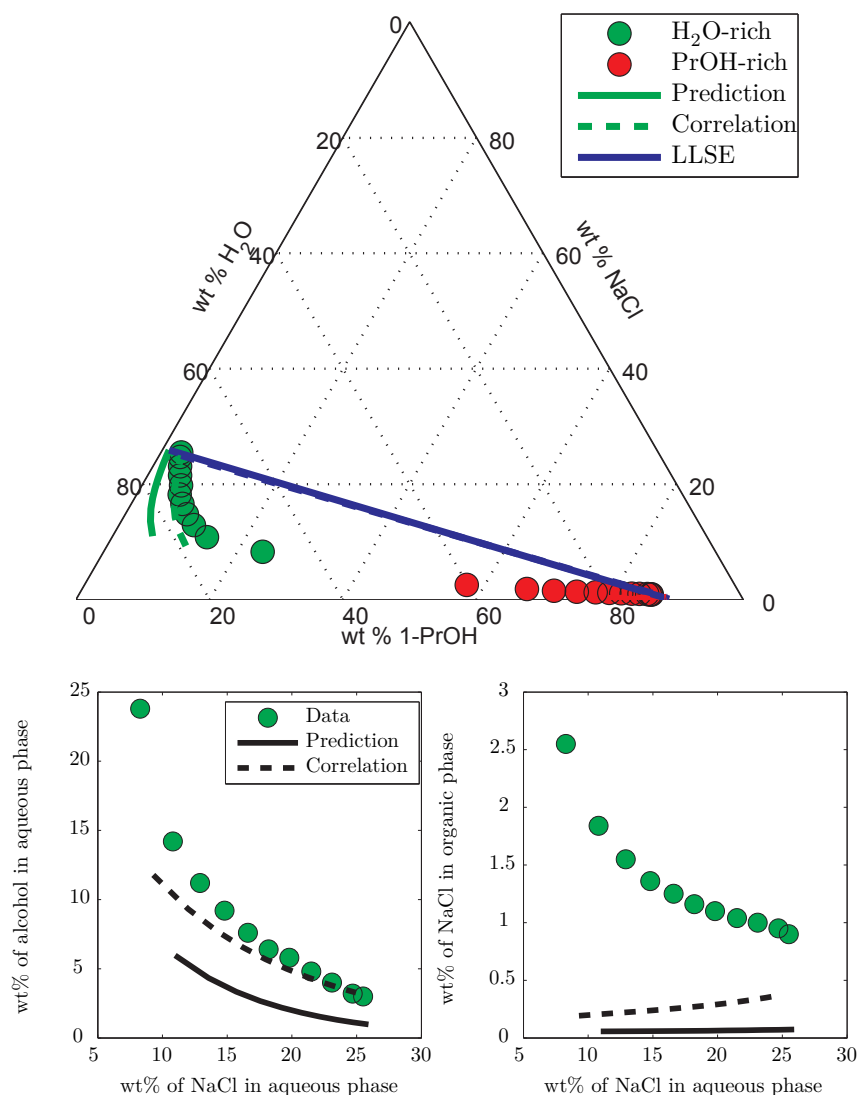


Figure 1.5: Plot of liquid-liquid phase split in water-NaCl-propanol mixture and limited capability of the predictive model [17]

The capabilities of the existing thermodynamic models to represent these systems are poor and still far from actual data [17]. As of now, it is almost impossible to predict such behavior using current thermodynamic models due to their limited capabilities. A recent publication by the Working Party of Thermodynamic and Transport Properties of the European Federation of Chemical Engineers (EFCE) addressed a finding on industrial needs within thermodynamic and transport properties through a questionnaire involving 28 different companies in the areas of oil and gas, chemical, and pharmaceutical/biotechnol-

ogy sector. One of the key findings of electrolytes revealed that all industries recognized that [6]:

"The predictive capability of thermodynamic models for electrolyte mixtures lag years behind their non-electrolytes counterparts and there is an industry-wide consensus that new predictive (rather than correlative) models are strongly needed. The models must be able to handle to all types phase behavior (VLE/LLE/SLE) and thermal properties of electrolyte in mixed solvents with hydrocarbons over a wide range of temperature and pressure."

At this stage, it becomes clear that the current capabilities of thermodynamic models for modeling mixed-solvent electrolytes are restricted. But before presenting the details of this work it is important to look at its scope of this work in the industrial context.

1.4 Roles of Electrolytes in Various Industries: Scope of this work

The electrolyte along with other solvents are present in the following industry and there are several problems associated with them as mentioned in the following sections. The following discussion will put forth the problems whose solution demands an accurate thermodynamic framework for the mixed-solvent electrolyte.

1.4.1 Biorefining industry

Biorefining industry involves the conversion of biomass or organic material into fuel grade bio-diesel or bio-gasoline. The pre-treated biomass (feed for bio-refinery) units is a complex mixture of oxygenated hydrocarbons and water, a strongly polar solvent which forms a non-ideal mixture with the oxygenated chemicals. Water is also responsible for degradation of processing equipment and worsening of product quality so it needs to be separated.

Aqueous solutions of salts have shown promising trends to aid in separation of these complex molecules encountered during the biofuel generation. The electrolyte causes a significant change in the equilibrium composition (especially liquid-liquid equilibrium), by altering the hydrogen bonding structure and other intermolecular forces. Hence, due to the addition of salt, the mutual solubilities of the solvents change in either phase (water-rich phase and hydrocarbon-rich phase). These phenomena may be used in various industries (Biorefining, Pharmaceuticals, and water treatment) for separation of hydrocarbons. To this end, an accurate representation of mutual solubilities of oxygenated compounds and

water in organic and aqueous solvents including salts is of utmost importance. Often, the lack of experimental thermodynamic data for such complex mixtures results in a need for procuring such knowledge from predictive thermodynamic approaches that must be both accurate and efficient at the same time.

1.4.2 Oil and Gas industry

Corrosion

The transportation of oil and gas over long distance is advantageous in terms of cost and operation if multiphase well streams can be transported without pre-processing to onshore refining facilities and chemical plants. The presence of the corrosive components such as CO_2 and H_2S from the well stream can significantly prohibit the use of carbon steel, which is prone to corrosion. However, the use of corrosion resistant steel increases the cost of pipe installation which is already high. The problem of corrosion in oil transportation poses a grave concern from the environmental point of view in addition to economic loss. The corrosion of pipeline can lead to an oil leak (or spill in case of oil-tanks) which can cause irreversible damage to surrounding ecosystem. Corrosion is also ubiquitous in downstream refining and petrochemical industry. It is estimated that a cost of corrosion is USD 15 billion globally. Generally, the petroleum distillates and refinery product stream are not corrosive, however, the presence of water and presence of salts even as low as 15 ppm (chlorides, sulfates, nitrates) can lead to significant levels of corrosion in refinery process equipment [18, 19].

Corrosion is almost unavoidable, however, it is the rate of corrosion that can be controlled and reduced, if the information related to the condition of corrosion with respect to temperature, water content, pH and flow velocity are known. It is also required to know the condition at which the formed iron carbonate Fe_2CO_3 will precipitate because this acts as a protective layer to the steel surface. Localized corrosion is more serious problem since it can lead to high corrosion rates which is further aggravated by the changing composition of the well stream over time. The presence of salts dissolved in the well fluid can further complicate the phenomena and affects the rate of corrosion.

Hydrate formation

Hydrates are crystalline ice-like substances that plug pipelines in oil and gas industry and are formed when a guest molecule (natural gas) is trapped by surrounding host molecules(water) in a hydrogen bonded structure. During transportation of oil and gas, the hydrate formation will block the flow thus stopping the operation until the formed hydrate is cleared. Clearly, oil and gas transportation industry require combatting

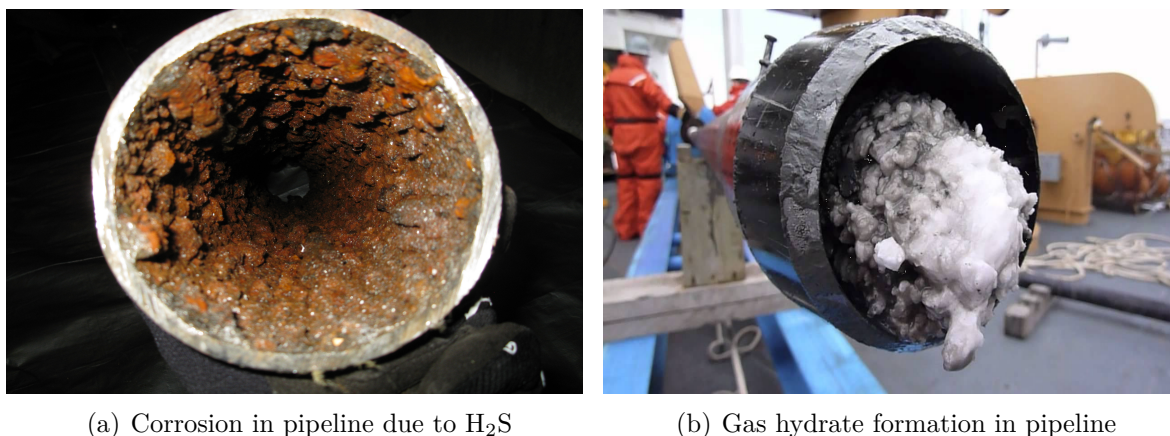


Figure 1.6: Corrosion and gas hydrates problem associated in oil and gas industry ¹

hydrate formation (Figure 1.6). For this purpose, there are several methods, chemical, hydraulic, mechanical and thermal methods. Particularly, chemical methods make use of thermodynamic inhibitors either to shift the equilibrium temperature of hydrate formation or to be used as a kinetic inhibitor/ dispersant. Some of the well-known inhibitors are methanol, glycols or solutions of electrolytes [20–22]. Presence of salts causes the salting-out effect of hydrocarbons from the salt solution. This reduces the solubility of the hydrocarbons in comparison to water, also, the inhibitory effect of salt aids in the structure making and breaking phenomena of ice (gas hydrates) in pipe-lines hence is effective in avoiding blocking of gas pipelines [4].

Produced water treatment

In oil and gas industry, the produced water is that water which is trapped in underground formation but brought to the surface along with oil exploration and production. This water contains several dissolved hydrocarbon components of oil along with a large amount of salt. Stringent government policies and rising environmental concern require this water to be treated before it can be discharged [23]. To this end, before developing an efficient desalination process for treating produced water it is necessary to model the thermodynamic phase behavior for process simulation calculations (heat and mass balances) [24] of the chemical species involved (a mixture of complex hydrocarbons and water).

¹<http://www.restreamsolutions.com/technology/>

¹<http://www.ipt.ntnu.no/jsg/undervisning/naturgass/oppgaver/Oppgaver2014/14Gama.pdf>

1.4.3 Carbon capture and sequestration (CCS)

Carbon capture and sequestration (capture-transport-storage) is a technology aimed at reducing the release of carbon dioxide into the atmosphere from power plants and other industries. Sequestration or storage of trapped CO₂ is often done in unminable coalbed methane reservoirs or deep saline aquifers [25]. For designing CCS process, it is very important to possess an accurate knowledge of various primary and derivative thermodynamic properties of various compounds that are encountered [26].

1.4.4 Acid gas injection

Acid gas comprises of CO₂ and H₂S which is a by-product of natural gas treatment process. The acid gases separated from the natural gas is at low pressure and must be compressed in order to achieve injection pressures. The use of an aqueous solvent in gas sweetening process results in the acid gas mixtures saturated in water which is a major concern in the injection process. A high concentration of water can lead to formation of a separated liquid phase or hydrate formation. Acid gases often contain dissolved hydrocarbons up to 5 mole percent.

The efficient design of acid gas injection process relies on the availability of reliable thermodynamic models that can calculate phase boundaries of systems containing a large amount of water, CO₂, and H₂S. For instance, efficient design of compression and cooling system is dependent on the ability of the thermodynamic model to accurately calculate dew temperatures and dew pressures [27].

1.4.5 Pharmaceutical industry

Drug solubility in water and organic solvent has a key role in drug discovery and formulation in pharmaceutical processes that comprise of several stages such as design, synthesis, extraction, purification, formulation, absorption, and distribution in body fluids [28]. Electrolytes are quite commonly found in pharmaceutical industry processes at various stages. The pharmaceutical industry thus demands calculative models to predict or provide knowledge of the solubility in mixture of solvents in presence of salts.

1.4.6 Other uses of electrolytes

Electrolyte solutions have an important role in biological and chemical engineering. Other important areas which involve electrolytes are sewage-water and drinking water treatment

and fertilizer production [29]. Various separation processes such as wet flue gas scrubbing, reverse osmosis, and reactive distillation find an application of electrolytic solutions [30]. Apart from these, electrolytes find applicability in CO₂ and H₂S removal by absorption using aqueous solutions of alkanolamines and ammonia. Ionic liquids find increasing importance in various separation and catalytic applications in Pharmaceutical industries including biotechnology.

1.5 Aqueous two-phase systems

Aqueous two-phase systems (ATPS) are solutions containing water with polymer/two polymer mixtures and salts at a specific concentration range. The systems are specific to salt and polymer pairs and not all polymer-salt pairs form a phase-separated ATPS. The two different liquid phases are both rich in water (approximately 85% w/w). Albertsson in mid-1950's showed that biological solutes go in the two liquid phases with varying composition. This makes them a good choice in separation industry involving bio-material.

Thermodynamic modeling of ATPS systems is a hot area of interest, however not new. A classical formulation for modeling ATPS has been proposed by some authors [31–34] but quantitative results were not of good quality.

1.6 Objectives of this research

There is an abundance of electrolyte thermodynamic models that are capable of calculating activity coefficient and other physicochemical properties with a reasonable level of accuracy. Yet, these models have limited capability when it comes to modeling VLE and LLE mixed solvent electrolyte and aqueous two-phase systems. The major grey areas that need to be investigated for forming an efficient mixed-solvent electrolyte models are:

- Evaluating the performance of the thermodynamic EoS for solvents (water, alcohols, etc). It was found that our earlier version of the model [35] had significant deviations in correlating liquid density of pure water. This was investigated and an improved version of the model was formulated. In chapter 3 we present the finding of our investigation along with details of the modification.
- Since we are intended on formulating an ion based electrolyte model, it becomes necessary to take a holistic approach in parameterizing ions. Parameterization should be physically meaningful and be based on certain evidently arguments, since

several interactions play a predominant role in the fluid system character. The parameterized model must be able to clearly represent thermodynamic properties of aqueous salt systems and mixed solvent salt systems. To this end, results from our investigations of the mean ionic activity coefficients (MIAC) and the vapor liquid equilibrium (VLE) calculations are presented in the chapter 4.

- The parameterized electrolyte thermodynamic model should be combined with a robust and clear model for dielectric constant for studying phase equilibrium of mixed-solvent electrolyte systems. The results of liquid-liquid equilibrium (LLE) and MIAC are presented in chapter 5.

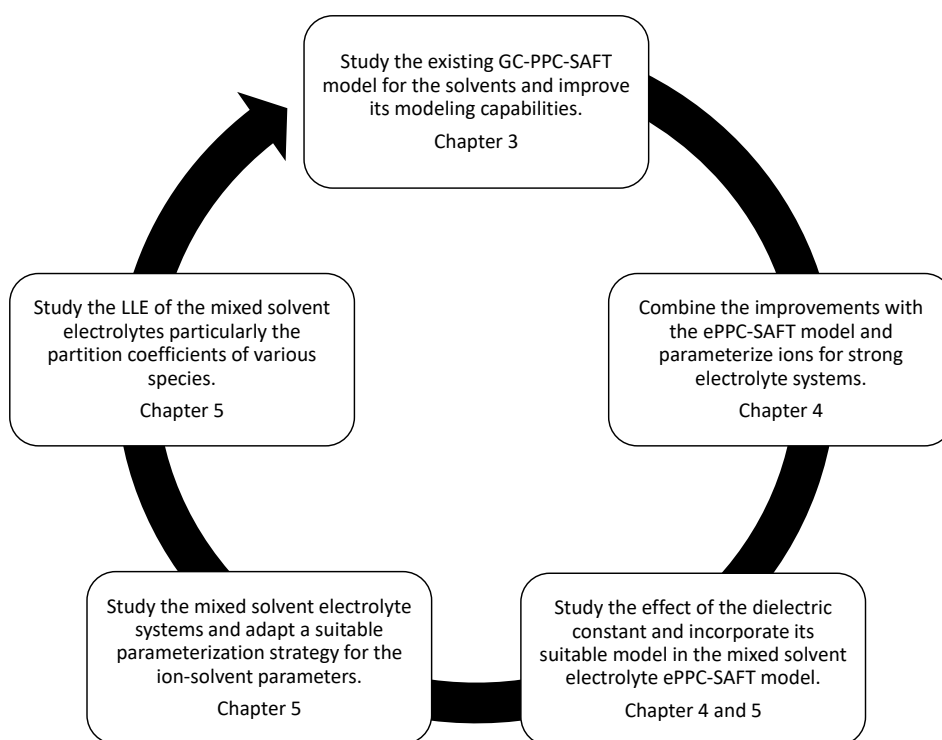


Figure 1.7: Various objective statements of this PhD thesis in order to obtain the ePPC-SAFT model for mixed solvent electrolytes

Chapter 2

Electrolyte thermodynamic model and the State of the art

2.1	Introduction	16
2.2	Activity coefficient models vs EoS	17
2.3	Interactions in electrolyte systems and theories	18
2.3.1	Discharge	19
2.3.2	Repulsion and dispersion	20
2.3.3	The Structure-forming step	20
2.3.4	Electrolyte terms	21
2.4	Review of the existing electrolyte and mixed-solvent electrolyte EoS	27
2.4.1	State of the art	27
2.4.2	Choice of thermodynamic model	30
2.5	Statistical associating fluid theory (SAFT)	30
2.5.1	Perturbation theory	30
2.5.2	History of Statistical Associating Fluid Theory (SAFT)	31
2.5.3	Mathematical description of PC-SAFT	32
2.5.4	Various terms of ePPC-SAFT	33
2.5.5	Group contribution approach	38
2.5.6	Cross association parameters	38

2.1 Introduction

When it comes to describing phase behavior of complex fluids and electrolytes, activity coefficient models are often used (the models based on $\gamma - \varphi$ approach). To this end, numerous activity coefficient models have been developed for describing the vapor-liquid equilibrium (VLE) and the liquid-liquid equilibrium (LLE) that are fast, simple, and can be easily deployed in process simulators. For instance, eNRTL models work fairly well for many systems including those with reactive species and mixed solvents as for example with mixed acids and mixed alkanolamine systems [36]. While the models are pertinent to specific fluid systems and physical condition, there is not a single model that can be successfully applied to all systems, at all conditions, for procuring all types of thermodynamic data. An elaborate review on the use of activity coefficient models and cubic EoS with their capabilities and limitations on application to the various system is already done [36].

For modeling the phase equilibrium we require mathematical correlations for activity coefficient γ or fugacity coefficient φ (computed from the equation of state (EoS) or some equation from which these relationships can be deduced (section 2.2)). Phase equilibrium is then computed using either $(\gamma - \varphi)$ or $(\varphi - \varphi)$ approaches. The *gamma-phi* ($\gamma - \varphi$) approach uses activity coefficient models for the liquid phase and an EoS for the vapor phase. The *phi-phi* ($\varphi - \varphi$) approaches utilize EoS for all phases.

Another classification can be made, distinguishing predictive and correlative methods. Correlative approaches are simple, they rely heavily on large amounts of high-quality experimental data. The predictive approaches are based on “physics-based equations” that may be complex. Yet, the predictive approaches have an edge in terms of usability since they are less dependent on experimental data and are transferable to other fluid systems. Table 2.1 presents a few examples of the few model on these classification and different approaches.

Table 2.1: Traditional classification of thermodynamic models and EoS

	Activity coefficient models	EoS
Correlative	NRTL, UNIQUAC	Cubic EoS + G^E mixing rules
Predictive	UNIFAC/COSMO	GC-EoS

So, it becomes clear that chemical engineering thermodynamics need advanced predictive thermodynamic models. Models that take into account various intermolecular interactions present in complex fluid systems in the present process industry are needed.

This is essential for better product and process design [16, 36, 37]. A review on the choice of thermodynamic models for process industry along with their associated problem areas is proposed by Chen and Mathias [16]. A guide for practicing process simulation engineers on the choice and application of thermodynamic models is a book written by de Hemptinne [38]

In the current chapter, we are going to present a thermodynamic framework that we have adapted for modeling our systems of interest.

Before presenting the framework of our choice, it is necessary to look at various existing competing frameworks in order to draw a conclusive argument regarding the merits of our choice. We have broadly divided this chapter into three parts.

Section 2.3: To begin with, we will first introduce the theory behind electrolyte contributions and mathematical models that describe that interaction.

Section 2.4: In this part, we will present a comprehensive review of the state-of-the art.

Section 2.5: Finally, we will present the mathematical model of the thermodynamic framework that we have chosen. The description of ePPC-SAFT EoS [39]

2.2 Activity coefficient models vs EoS

For phase equilibrium calculations, the main property that needs to be computed is the chemical potential, which is defined as:

$$\mu_i = \mu_i^{ref}(T_0, P_0) + RT \ln \frac{f_i}{f_i^{ref}} \quad (2.1)$$

where the reference state is generally taken either as the pure liquid solvent or as the fluid mixture in the ideal gas state at the same pressure and temperature. In the first case, the equation becomes:

$$\mu_i = \mu_i^*(T, P) + RT \ln x_i \gamma_i \quad (2.2)$$

where γ_i is the activity coefficient, which requires the use of a suitable model (e.g. Pitzer [40–42], eNRTL [8–10], eUNIQUAC [7]). The reference state (indicated by a “*”) is generally taken, for neutral molecules, at its vapor pressure, while for ions, infinite dilution in the solvent, which is most often pure water. The drawback of this approach

is that the pressure is not taken into account. Since the activity coefficient models are generally pressure independent. In the second case, we have:

$$\mu_i = \mu_i^\#(T, P, x) + RT \ln \varphi_i \quad (2.3)$$

where φ_i is the fugacity coefficient that requires an equation of state. The reference state (here indicated by “#”) is then the fluid mixture taken as an ideal gas at the same temperature T and pressure P as the fluid mixture (x : vector of composition). The logarithm of the fugacity coefficient is obtained using the mole number derivative of the volume-based residual Helmholtz energy [43]:

$$RT \ln \varphi = \frac{\partial A^{res}(T, V)}{\partial n_i} - RT \ln(Z) \quad (2.4)$$

where Z is the compressibility factor. The relationship between the two approaches can be obtained using the definition of activity coefficients:

$$\gamma = \frac{\varphi_i}{\varphi_i^*} \quad (2.5)$$

The models most often used in industry [44] are based on activity coefficients (most known are Pitzer [40–42], eNRTL [8–10], eUNIQUAC [7], as well as MSE [45, 46]). In addition to their low-pressure limitation, these models rely on adjusting many interaction parameters against the available experimental data. Their predictive capability is therefore very weak. Today, many researchers try to develop electrolyte EoS [36, 47, 48] which use the notion of fugacity coefficient. They are able to account for pressure effects and allow combining the emerging statistical thermodynamic models (as the SAFT EoS based on Wertheim’s association theory [49–52]) with electrolyte thermodynamics. As such, they make it possible to describe simultaneously complex molecular interactions as those occurring in bio-systems [53–57], for example, electrolytic effects [54, 58–61]. Yet their capabilities in modeling multi-solvent electrolyte systems are limited [45].

2.3 Interactions in electrolyte systems and theories

Electrolyte solutions are characterized by high thermodynamic non-ideality, which makes it even more important to model their thermodynamic properties. However, modeling such systems requires taking into account long-range electrostatic interactions in addition to short-range interactions that result from van der Waals attraction, polar, or association

forces. Considering the various theories that are available for treating electrolytes in an EoS, a selection must be made. Hence, the aim of this section is to present theories and models that would best describe the behavior of electrolytic solution and finalize the construction of an electrolyte equation of state.

Thermodynamic models are often constructed using a thermodynamic cycle, where each transformation, which corresponds to a specific interaction being turned on, brings in an additive contribution to the total Gibbs energy (in the case of activity coefficient models) or Helmholtz energy (in the case of equations of state). In the case of an equation of state, the residual Helmholtz energy at given volume and temperature is computed. We can then use as an example the thermodynamic cycle (figure 2.1) that is proposed by Rozmus [62]:

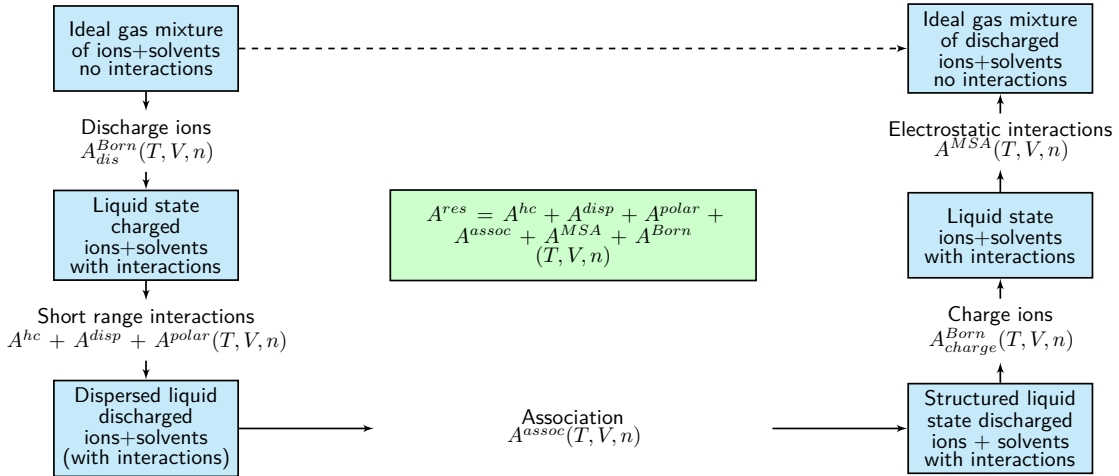


Figure 2.1: Thermodynamic cycle representing steps in forming an electrolyte thermodynamic equation of state

$$A^{res} = A^{hc} + A^{disp} + A^{polar} + A^{assoc} + A^{MSA} + A^{Born} \quad (2.6)$$

The starting point is the mixture containing all species considered but in its ideal gas state. This means that the species have no volume and no interactions. They only have kinetic energy.

2.3.1 Discharge

In the first step, the ions are discharged so as to yield the same mixture but without charge. The energy associated with this transformation is generally described using the

Born term [63] by the equation 2.7:

$$\frac{\Delta A_{dis}^{Born}(T, V, n)}{RT} = -\frac{N_A e^2}{4\pi\epsilon_0 RT} \sum_i^{ions} \frac{n_i z_i^2}{\sigma_i^{solv}} \quad (2.7)$$

Where σ_i is the solvation diameter of the ion, z_i is the charge on the ion, ϵ_0 is the permittivity of vacuum, e is the electronic charge and R is the universal gas constant. A detailed discussion is made in chapter 4 on the role and the significance of Born term.

2.3.2 Repulsion and dispersion

In a second step, repulsive interactions and attractive interactions are turned on (the species are given a volume and van der Waals interaction). This step can be modeled with any equation of state. In fact, electrolyte equations of state have been proposed since the 90's using the cubic equations of state (SRK with Fürst & Renon [64], Zuo *et al.* [65], Lin *et al.* [47], or PR with Myers *et al.* [66]). More recent works are based on either CPA [44] or one of the SAFT versions (see Table 2.2).

2.3.3 The Structure-forming step

Note that in this third step, the ions, though they remain present throughout the cycle, are considered in the same way as neutral molecules, which means that their only interactions are short-range repulsion and attraction. No specific structure is created. This is obviously not the case, so the next transformation that must be considered is the structure-forming of the ions: water molecules will cluster around the ions to form the so-called "solvation shell". This phenomenon is also called "hydration". Water, a polar molecule, tends to align its negative center around a cation, which forms a hydration shell.

Many molecular simulation studies exhibited this structure-forming phenomenon. As an example, figure 2.2 shows the radial distribution functions (rdf) in an aqueous NaCl solution at 1 mol/kg and 298.15K between the pairs Na^+/O and Cl^-/O (where O is the oxygen atom of the water molecules) obtained from Monte Carlo simulations [67]. On this figure is also plotted corresponding coordination numbers (integral of the non-normalized-rdf) : these coordination numbers shows that in the first solvation shell of water-ion there are approximately the same number of water molecules surrounding the ion (6-7). The structure of water-ion mixtures is discussed at length in [68]. Fürst & Renon [69] used a specific "short range" term to describe solvation phenomenon, but Inchekel [70] showed some inconsistencies with this term and proposed, as many others, to use the Born term

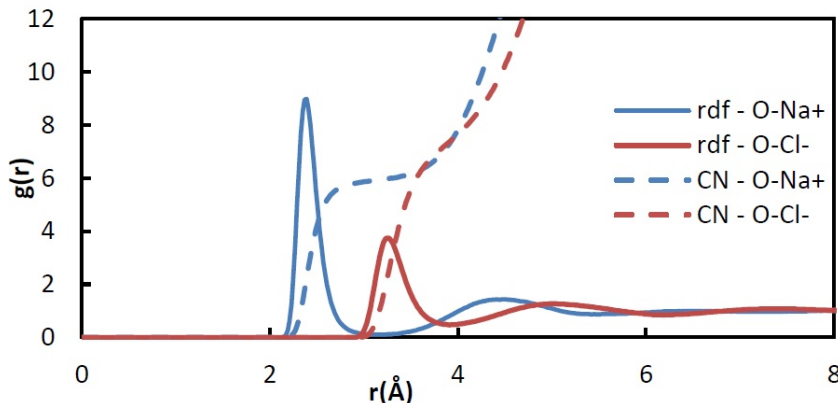


Figure 2.2: Radial distribution function (rdf) and coordination number (CN) between Na⁺/O pairs and Cl⁻/O pairs obtained from Monte Carlo simulations [67]

instead. Yet, as we demonstrate here, the objective of the Born term is different from describing the structuring effect of ions. Several other authors [53, 59, 71–73] adjust a binary interaction parameter for the dispersion term to model this phenomenon. Several authors (e.g., Rozmus *et al.* [39] and Herzog *et al.* [74]) use the Wertheim association term for describing this phenomenon: it allows describing the disruption of the water-water hydrogen bonds and the formation of hydration interactions in the presence of ions. This choice is also made in the present work. The short-range nature and the strong hydration interactions make the use of the SAFT association term a natural choice to model this phenomenon. The complexity comes in the selection of the number of sites on each ion. As is discussed in chapter 3, we have compared two different hydration numbers one from Bockris and Reddy [68] and other from molecular simulations to find the most suitable hydration numbers.

2.3.4 Electrolyte terms

In the current section, we will discuss predominantly two aspects of ionic interaction, ion-ion interaction and ion-solvent interactions. These two aspects are crucial in comprehending electrolyte thermodynamics: how ions interact with the solvent (most often water), move within the solvent; how they associate with the solvent and sometimes form dimers. A pictorial representation is shown in figure 2.3 presents a brief idea about the dissolution of a salt crystal in water, its dissociation into ions and how those ions interact with water molecules.

Since ions are charged species, long range coulombic interaction govern several properties and phenomena of salt systems. According to Debye-Hückel theory 2.3.4.1,

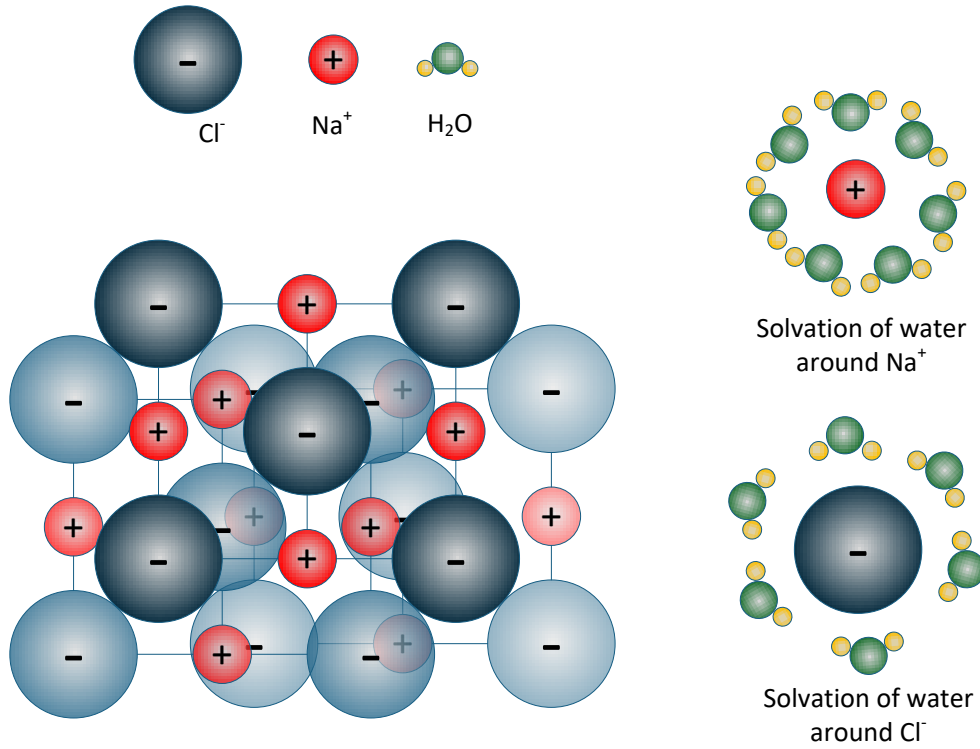


Figure 2.3: Solvation interaction in an electrolyte solution, salt crystals gets dissolved and salt gets dissociated into ions, solvent molecules surround cations and anions

forces acting on a charged particle j separated by distance r_{ij} from the central ion i , is given as:

$$F_{ij}^{el} = \frac{e^2 z_i z_j}{4\pi \epsilon_0 \epsilon_r r_{ij}^2} \quad (2.8)$$

where z_i is the charge of the ion, e is the electronic charge, r_{ij} is the distance between the two ions, ϵ_0 is the static permittivity of the vacuum. Relative static permittivity ϵ_r plays an important role in the strength of the electrostatic force. When the concentration of salt increases in the system there is a reduction in the value of relative static permittivity which increases the force between the ions.

The next two transformations (figure 2.1) are related to the presence of the charge on the ions: the charging effect of every single ion, and the energy related to the long-range ion-ion interactions. Although these two phenomena are related, as far as we know, some theories exist that take into account these phenomena, however, they are complex and

rather not easy to use in process simulation context. All other existing models propose a sum of the two effects.

1. The Born term is used again to describe the energy related to the turning “on” of a point charge on each individual ion. It is identical to equation 2.7, except for the sign and the fact that now the actual liquid solution dielectric constant is used

$$\frac{\Delta A_{charge}^{Born}(T, V, n)}{RT} = -\frac{N_A e^2}{4\pi\epsilon_0\epsilon RT} \sum_i^{ions} \frac{n_i Z_i^2}{\sigma_i} \quad (2.9)$$

This makes that the global Born contribution becomes:

$$\frac{A^{Born}}{RT} = -\frac{N_A e^2}{4\pi\epsilon_0 RT} \left(1 - \frac{1}{\epsilon}\right) \sum_i^{ions} \frac{n_i Z_i^2}{\sigma_i} \quad (2.10)$$

2. Either the Debye-Hückel (DH) [75] or Mean Spherical Approximation (MSA) [76] the term is employed to describe ion-ion long-range interactions.

A specific note should be made regarding this latter type of interaction. The model(s) accounting for coulombic interaction in electrolytes systems are generally developed based on the following approaches

- **Primitive models:** These models assume that the ions are surrounded in a solvent which is represented as a dielectric continuum, and the value of the dielectric constant is equal to that of the solvent. These models thus require the value of the dielectric constant of the solvent to be supplied from outside (from experimental data, correlation or association based models). Examples are the Debye Huckel and primitive MSA
- **Non-Primitive models:** These models assume that the ions are surrounded in a solvent which is represented as dipolar hard spheres and not as a dielectric continuum. As a result, it is possible to quantify at once three different types of interaction, between, ion-ion, ion-dipoles, and dipoles-dipoles. These models do not require the value of the dielectric constant of the solvent. In fact they provide an ability to predict its value. However, the predicted value may not be very accurate. In addition to the above categories, additional subcategories are often used:
 - **Restricted models:** Also called implicit models, they are based on an assumption that all ions have the same ionic diameter and in case of non-primitive version this diameter is taken equal to the diameter of the solvent hard sphere.

- **Semi-restricted models:** This is similar to the restricted models where all ions have same ionic diameters but the solvent dipolar hard sphere are of different diameter.
- **Non-restricted models:** Also called explicit models, they are based on the assumption that different ions have different ionic diameters.

The choice between primitive and non-primitive version is rather important. Our choice is the non-restricted primitive approach. It has been recognized by many authors [77, 78] as a good representation of the physical phenomenon. However, we have our own argument for choosing the primitive model over the non-primitive model. The non-primitive model accounts for three different types of contributions in the system, ion-ion, ion-dipole and dipole-dipole. While the former two contributions are clearly essential the latter “dipole-dipole” contribution is an extra contribution that is already taken into account in the ePPC-SAFT equation. In our framework, dipolar interactions are already taken into account using dipolar term by Jog and Chapman [79, 80].

However, it is worthwhile to look at the various primitive models and their mathematical formulation. There are two theories that describe these ionic interactions, Debye Hückel and MSA. The fundamental difference between the two theories is that the DH theory is based on ion described as point charges, but assuming a minimum distance of separation σ_i between the ion and solvent molecules. The MSA theory, however, assigns this σ_i as the diameter to ions and treats them as hard spheres. Both theories are comparable and may yield similar results (depends on which versions are compared) [81].

The restricted models do not have the capability to tune the ionic parameters for specific salts under investigation but assume that all diameter is equal to that of the solvent. This is not the case in our thermodynamic framework where we use parameters for each component (independently) and use the pure component parameters transferable onto other mixtures. The use of the restricted approach in our case would limit such possibility and require re-tuning of the hard sphere diameters for water again on salt systems. This would lead to several hard sphere diameters for water or several binary interaction parameters, thus limiting the predictive capability.

2.3.4.1 Debye Hückel theory

The Debye-Hückel (DH) [75] theory is one of the oldest models which is capable of describing long-range electrostatic interactions between ions. It uses the Poisson’s

equation 2.11 to express the energy resulting from the presence of a point charge in a cloud of charges. The DH theory is based on a few assumptions such as, non-random distribution of ionic species in a continuum of dielectric, electroneutrality of solvent, treatment of ions as a hard spheres of radius σ_i (not the ionic radius but the distance of closest approach by a counter-ions) with a point charge placed at its centre, and surrounding of an ion by its counter ions. The final mathematical expression in terms of Helmholtz energy is obtained by solving Poisson's equation and Boltzmann distribution function for volumetric charge density around a central ion.

$$\frac{1}{r^2} \frac{d}{dr} \left(r^2 \frac{d\psi_i}{dr} \right) = -\frac{\rho_i^Q}{\varepsilon_0 D} \quad (2.11)$$

where ψ_i is the electrostatic potential in polar coordinates as a function of distance r_i from the central ion i . While the Boltzmann distribution of volumetric charge density (ρ_i^Q) for an ion i can be expressed as:

$$\rho_i^Q = eN_A \sum_i^{\text{ions}} \frac{n_j z_j}{nV} g_{ij}(r) \quad (2.12)$$

$$g_{ij}(r) = \exp \left[-\frac{e z_i \psi_i(r)}{k_B T} \right] \quad (2.13)$$

where g_{ij} (radial distribution function) is the function of electric potential $\psi_i(r)$, whereby combining eq. 2.11 and eq. 2.12 the following equation 2.14 can be obtained.

$$\frac{1}{r^2} \frac{d}{dr} \left(r^2 \frac{d\psi_i}{dr} \right) = \kappa^2 \psi_i \quad (2.14)$$

According to investigations made by Onsager [82] for electrolytes with non-symmetric charged salts the above equation does not hold true as $\rho_i g_{i,j}(r) = \rho_j g_{j,i}(r)$ cannot be validated. This limits the use of Debye-Huckel theory for only symmetrically charged salts. However, by using the Pitzer equation this limitation can be overcome. However, the Pitzer equation itself includes hard-sphere repulsion contribution which is already accounted in the PC-SAFT framework.

The important property here is the Debye screening length (κ), the inverse of which has a physically important significance, It is the limiting-range of electrostatic interactions, beyond which they (electrostatic interactions) can be ignored. It is expressed as follows:

$$\kappa^2 = \frac{e^2}{k_B T \varepsilon_r \varepsilon_0} \sum_j^{ions} \frac{n_j}{V} z_j^2 \quad (2.15)$$

The final expression of the DH Helmholtz energy is written as:

$$\frac{A^{DH}}{RT} = -\frac{1}{4\pi\varepsilon RT} \sum_i \frac{x_i q_i^2}{(\kappa\sigma_i)^3} \kappa \left[\frac{3}{2} + \ln(1 + \kappa\sigma_i) - 2(1 + \kappa\sigma_i) + \frac{1}{2}(1 + \kappa\sigma_i)^2 \right] \quad (2.16)$$

2.3.4.2 Mean spherical approximation theory (MSA)

The MSA theory is based on the perturbation of polar fluids where the reference system is in the Percus-Yevick approximation using the Ornstein-Zernike equation as a specific closure. MSA theory has both an implicit and an explicit version, the explicit (restricted) version is simple and uses a common ion diameter whereas implicit (non-restricted) version is solved iteratively [36]. According to some findings, it is said that MSA theory (section 2.3.4.2) has an edge over DH theory (section 2.3.4.1). Galindo *et al.* [71] compared the MSA and DH theories for describing short-range interactions and reported that at a higher salt concentration of NaCl densities were more accurately represented by MSA than by DH. However, for the representation of vapor pressure, the performance was nearly the same. A Taylor series expansion and the comparison of the mathematical form of both these theories by Lin *et al.* [47] showed that there are very little differences when assuming the same ion diameters. A recent comparison made by MariboMogensen *et al.* [81] showed that the two theories (DH vs NP-MSA) when compared numerically in terms of screening length gave similar results. Since we are adapting a non-restricted primitive version of MSA we present the final expression in terms of Helmholtz energy below:

$$\frac{A^{MSA}}{RT} = -\frac{e^2 N_A}{4\pi\varepsilon_r \varepsilon_0 RT} \left[\Gamma \sum_i \frac{z_i^2}{1 + \Gamma\sigma_i} \right] + \frac{V\Gamma^3}{3\pi} kT \quad (2.17)$$

$$4\Gamma = \frac{e^2 N_A^2}{\varepsilon_0 \varepsilon_r RT} \sum_i^{ions} \frac{n_i}{V} \left[\frac{z_i}{1 + \Theta\sigma_i} \right] \quad (2.18)$$

Where Γ or $(2\Gamma)^{-1}$ (shielding parameter) is equivalent to the inverse screening length κ^{-1} in the Debye Huckel theory, e is the electronic charge, σ_i is the diameter of the ionic species.

2.4 Review of the existing electrolyte and mixed-solvent electrolyte EoS

2.4.1 State of the art

A good review of the electrolyte thermodynamics is made by Loehe and Donohue [83], that included models from 1985-1997. Another review by Prausnitz [84] presented a brief account of electrolyte thermodynamics including their applicability in the biotechnology industry. A short review by Pinsky and Takano [85] presents some local composition models emphasizing computational details of activity coefficient models. Lin *et al.* [47] and Tan *et al.* [86] presented an account on electrolyte equation of state in conjunction with SAFT and electrolytic theories. In addition to these, Michelsen and Mollerup [43] presented a thorough discussion including a derivation of modern Debye-Hückel theory and the theories of dipolar ions.

Similarly, many authors have investigated equations of state and also several electrolyte thermodynamic equations of state have been developed. An extensive review is already presented by Kontogeorgis [36] and MariboMogensen [87]. An extension of those reviews including some newer ones is presented herein tables 2.2 and 2.3. These tables present the models with a mention of their parent/base model, the type of Coulombic term employed, whether a Born term is used, and the functional form of the dielectric constant if needed (i.e. density-dependent – indicated with V; salt concentration-dependent – indicated with i) used for the electrolyte terms, the presence of ion-ion or ion-solvent association.

This table shows that the models differ on the incorporation of short-range [7, 88–90] and long-range forces as Debye-Hückel (DH) or mean spherical approximation(MSA).

Table 2.2: Review of the existing electrolyte thermodynamics models

Model	Ref	Parent model	Electrolyte model	Solvation	ϵ	Property and systems studied
e-PACT (salt specific)	Jin and Donohue [83, 91]	PACT	PE ion-ion	PE ion-dipole	T	MIAC, VLE, SLE of strong and weak electrolytes
e-SRK (ion specific)	Furst and Renon [69]	Modified SRK+SR2	nrPMSA	-	T, V, i	Osmotic coefficients for strong electrolytes
	Zuo <i>et al.</i> [92]	Modified SRK+SR2	nrPMSA	-	T	vapor pressures of single non-aqueous electrolytes
	Lin <i>et al.</i> [47]	DH	nrPMSA	Born	T, V	MIAC, osmotic coefficients, densities and SLE of several electrolyte systems
	Simon <i>et al.</i> [93]	SRK	DH	Born	T, V, i	activity coefficients of NaCl/MgCl ₂ and VLE of Methanol-water-NaCl
e-PR (salt specific)	Myers <i>et al.</i> [66]	PR with volume translation	rPMSA	Born	T, V	activity coefficients for 138 electrolytes, osmotic coefficients and densities certain salt systems
e-PR (ion specific)	Wu and Prausnitz [94]	PR + association from SAFT	nrPMSA	Born	T, n	VLE of water hydrocarbon and salts
e-CPA (ion specific)	Inchekel <i>et al.</i> [70]	CPA+SR2	iMSA	Born	T, V, i	activity coefficients and densities for strong electrolytes
	Schlaikjer <i>et al.</i> [95]	CPA	DH	Born	T, V, i, -	MIAC, osmotic coefficients of several single aqueous salt systems.
	MariboMogensen <i>et al.</i> [87]	CPA	DH	Born	T, V, i, -	MIAC, osmotic coefficients, VLE, LLE, SLE of aqueous single salt systems and mixed solvent
	Courtialet <i>et al.</i>	CPA	nrPMSA	Born	T, V, i, -	solubility of CO ₂ in aqueous NaCl with methane
e-CPA (salt specific)	Haghighi <i>et al.</i> [96]	CPA	DHF	-	T, V	freezing point depression of binary and ternary aqueous salt systems
e-SAFT(ion specific)	Galindo <i>et al.</i> [71]	SAFT-VR	rpMSA	-	T	vapor pressures and densities of certain alkali halide systems
	Sadowski <i>et al.</i> [60, 61, 61, 97, 98]	PC-SAFT	DH	-	T, n	MIAC, densities and VLE of aqueous salt systems
	Radosz <i>et al.</i> [86]	SAFT1	rPMSA	-	T	MIAC, density, osmotic coefficient, and vapor pressure of several aqueous alkali halide solutions
	Radosz <i>et al.</i> [99? -103]	SAFT2	rPMSA	-	T	osmotic coefficients, densities, and vapor pressures of several aqueous single and multiple salt systems
	Lee and Kim [104]	PC-SAFT	rPMSA	Born	T	MIAC, densities, and osmotic coefficients of single aqueous salt systems
	Rozmus [39]	PPC-SAFT	iMSA	Born	T, V, i	activity coefficients and densities of strong electrolytes
	Herzog Gross <i>et al.</i> [74]	PC-SAFT	nPMSA	-	-	MIAC and densities of alkali halides
	Galindo <i>et al.</i> [71]	SAFT-VR	rpMSA	-	T	vapor pressures and densities of certain alkali halide systems
e-SAFT(salt specific)	W.Liu <i>et al.</i> [105]	LJ-SAFT	npMSA	-	-	MIAC of 30 electrolytes
	Z.Liu <i>et al.</i> [106]	LJ-SAFT	npMSA	-	-	MIAC, osmotic coefficient and densities of aqueous NaCl
	Radosz <i>et al.</i> [107]	SAFT1	rpMSA	-	T	osmotic coefficients of certain binary, ternary and quaternary salt systems
	Najafloo <i>et al.</i> [108, 109]	SAFT-HR	rpMSA	Born	T	MIAC, osmotic coefficient and densities 61 strong electrolytes

Table 2.3: Review of the mixed-solvent electrolyte thermodynamics models

Model	Ref	Parent model	Electrolyte model	Solvation term	Dielectric constant	Systems studied
ALS EoS [110]	Aasberg-Petersen <i>et al.</i> [111]	ALS	DH	-	T, n	CO ₂ , CH ₄ , N ₂ , Nat. gas with water+salt
eCPA	Carvalho <i>et al.</i> [112]	RKSA EoS	DH	-	T	CO ₂ salting-out effect
eWilson+DH	Chou and Tanika <i>et al.</i> [113]	Wilson	DH	DH modified	T, n	VLE Alcohol-water-salt
PR	Wu and Prausnitz <i>et al.</i> [94]	NRTL	DH	Born	T, n	VLE of water-hydrocarbons-salts
excess GE models	Lee <i>et al.</i> [114]	excess GE	DH	-	T, n	VLE Methanol-water-salts
	Kosinski <i>et al.</i> [46]	excess GE	Pitzer-DH	SR	T, n	acid-base equilibria, VLE of MEG-H ₂ O-salt
Gibbs Duhem equation	Lee <i>et al.</i> [114]	Duhem equation	DH	-	T, n	VLE Alcohols-water-salts
NRTL	Rastogi and Tassios <i>et al.</i> [115]	NRTL	DH	-	T, n	VLE Methanol-water-salts
	Hou <i>et al.</i> [116]	PR	DH	-	T, n	VLE CO ₂ -water-salts
UNIQUAC	Rousseau and Boone [117]	UNIQUAC	-	-	T, n	VLE of mixed alcohols+salt(compared Wilson and UNIQUAC performance)
	Fosbol [118]	UNIQUAC	DH	-	T, n	VLE and SLE of mixed solvent and mixed salt(compared Wilson and UNIQUAC performance)
Barker-Henderson	Iliuta [119]	UNIQUAC	DH	-	T, n	VLE, LLE of methanol-water-salt systems
	harvey and Prasnitz [120]	BH	DH	Born	T, V, n	VLE of CO ₂ , N ₂ , CH ₄ with salts
	Reschke <i>et al.</i> [55]	PC-SAFT	DH	-	T, n	ATPS (PEG+salts)
	Reschke <i>et al.</i> [56]	PC-SAFT	DH	-	T, n	ATPS (polymers+salts)
	Reschke <i>et al.</i> [57]	PC-SAFT	DH	-	T, n	VLE of water-alcohol-salt
eSAFT	Ji <i>et al.</i> [121]	SAFT1-RPM	DH	-	T, n	VLE and densities of CO ₂ -water-salt
	Patel <i>et al.</i> [122]	SAFT-VR	rpMSA	-	T	solubility of alkanes in aqueous salt systems
	Schreckenberg <i>et al.</i> [123]	SAFT-VR	nrpMSA	Born	T, V	MIAC, osmotic coefficient
	Eriksen <i>et al.</i> [124]	SAFT-VR-Mie	nrpMSA	Born	T, V	MIAC, osmotic coefficient, and solubility limits of salts
	Monir <i>et al.</i> [125]	SAFT-VR	nrpMSA	Born	T, V	activity coefficients and solubility of amino acids in aqueous salt systems.
	Das <i>et al.</i> [126, 127]	SAFT-VR+DE	npMSA	-	-	activity coefficients, osmotic coefficient, and density of strong electrolyte systems..

2.4.2 Choice of thermodynamic model

The objective of the IFPEN investigation is to develop, for use in process simulation, a predictive model that eventually will allow describing systems containing complex molecular structures together with electrolytes. The GC-PPC-SAFT has shown promising results in that context [128–130] and has already been extended to simple electrolyte systems by Rozmus *et al.* [39]. The objective of this work is to further improve it so as to have a better description of the aqueous phase density and allow liquid-liquid phase split description in the presence of mixed solvents. The need is to adapt EoS applicable at high pressures, applicable to complex oxygenated compounds, GC-PPC-SAFT is one of the theories that takes into account various interactions between molecules as a perturbation term. An illustration below (Figure 2.4) describes these interactions (section 2.5.4) in a non-electrolyte system.

The choice of the model eGC-PPC-SAFT for studying the liquid-liquid equilibrium of electrolytes is because of its successful predictive nature for non-electrolyte systems [128, 128, 131, 132]. When it comes to electrolytes, the e-PPC-SAFT model has proved to be promising as investigated by Rozmus *et al.* [39] by taking into account the ion-ion and ion-solvent(hydration) interactions 2.3.4: with a very small number of parameters (association energy of ions), she showed that the model is capable to describe the behavior of the MIAC and other electrolyte properties in extrapolation up to high temperatures. The GC-PPC-SAFT model is thus a promising model to combine non-electrolyte and electrolyte contribution and be a successful electrolyte predictive thermodynamic model. The choice will be strongly supported after going through the details of GC-PPC-SAFT which are covered in the later sections of this chapter.

2.5 Statistical associating fluid theory (SAFT)

In the current section, we present details about SAFT. The reasons for choosing SAFT as a basis for this work is due to its success in describing non-electrolyte systems. This section will provide a theoretical background followed by various developments made in SAFT.

2.5.1 Perturbation theory

Perturbation theory is a mathematical theory which provides an approximate solution to a problem. The solution is obtained by adding values obtained by approximating

perturbation terms to the solution of exact terms as in a Taylor series expansion. The mathematical expression describing the residual Helmholtz energy is given as in equation 2.19.

$$A^{res} = A^{ref} + A^{perturbation} \quad (2.19)$$

Where A^{ref} refers to the Helmholtz energy of reference state is often the hard sphere fluid. The perturbation term accounts for various interactions such as repulsion, chain, dispersion, association, polar (figure 2.4) and in the current work for electrolytic contributions.

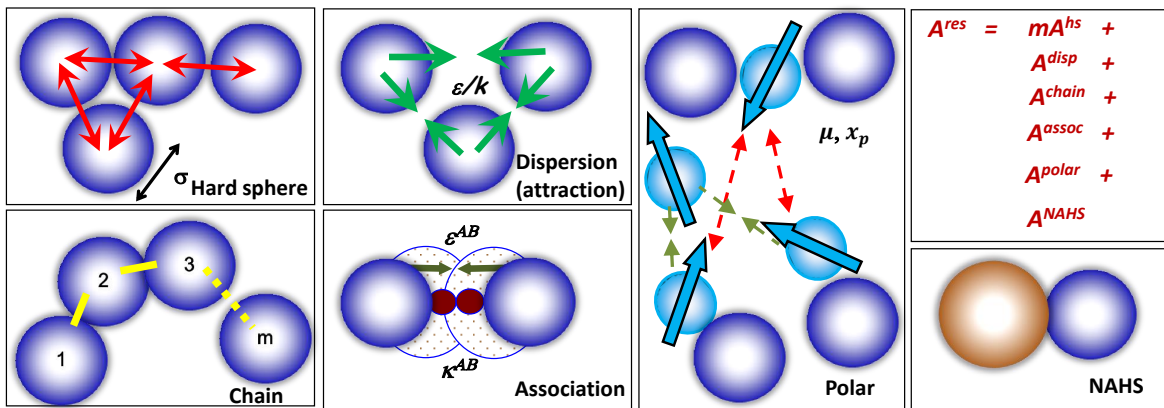


Figure 2.4: A schematic representation of various contribution in PPC-SAFT

2.5.2 History of Statistical Associating Fluid Theory (SAFT)

Several developments that took place in the last century in the areas of atomistic simulation, integral equation theories, radial distribution functions, perturbation and statistical association theories have paved a way for developing statistical associating fluid theory (SAFT). For a long time the development of equations of state was based on polynomial correlations, however, with the development of molecular simulation tools, the use of statistical mechanics made it possible to describe the molecular interactions more explicitly. The SAFT EoS was first developed by Chapman, Gubbins and Jackson, and Radosz is based on the work published by Wertheim in his four articles on perturbation theory [49–52].

In the last decades, extensive research efforts are made in developing SAFT which is believed to have a promising potential to be a predictive and robust thermodynamic model. Many versions of SAFT have appeared since then such as PC-SAFT [133], VR-SAFT [134], SAFT- γ [135] and Simplified-SAFT [136]. The main difference between

these various versions concerns their treatment of the dispersion term (section 2.5.4.3) and the choice of the reference fluids. There are several extensive reviews related to various versions of SAFT presented by some well-known authors: Economou [137], Sadus [138] Prausnitz and Tavares [139] and Tan *et al.* [48] published. Von Solms *et al.* [140] and Arlt *et al.* [141] provided detailed account of various applications based on PC-SAFT. De-Hemptinne *et al.* [142] gave the various petroleum-based application of three models viz. CPA, PC-SAFT, and VR-SAFT. Paricaud *et al.* [77] and Muller and Gubbins [143] provided an extensive review of various SAFT versions, including those pertaining to the electrolyte and proposed improvements in the current SAFT model.

Various polar versions of SAFT (i.e. including a polar term as a specific contribution) have appeared, for instance, CK-SAFT for dipolar molecules employing Jog and Chapman dipole theory (section 2.5.4). The PC-SAFT polar versions include one dipolar by Tumakaka and Sadowski [144], quadrupolar by Gross *et al.* [145], dipolar and induced dipolar by Karakatsani *et al.* [146], and polar and polarizable dipole by Kleiner and Gross [147].

One such model which is based on group contribution theory of Tamouza [148] and extended to polar molecules by Nguyen [128, 149], based on PPC-SAFT, is known as the Group Contribution Polar-Perturbed Chain Statistical associating Fluid theory (GC-PPC-SAFT) [62, 129–132, 150–155].

2.5.3 Mathematical description of PC-SAFT

In SAFT, the interactions between the molecules are accounted as perturbations. The physical picture of SAFT is based on the statistical perturbation theory. The reference is most often the hard sphere, except for PC-SAFT where it is the hard chain. The perturbation applied to this reference is based on some picture of the pair potential (Lennard-Jones, square well or other) and is called the dispersive contribution. The hard spheres are assumed to contain association sites, making it possible, using Wertheim's theory, to construct a perturbation related to association interactions. Considering infinite association strengths between some selected sites, it is possible to construct a chain with its specific perturbation term. The representative equation 2.20 for final residual Helmholtz energy is given as a follows. Figure 2.4 illustrates the interactions and construction of GC-PPC-SAFT.

$$\frac{A^{res}}{RT} = \frac{A^{hs}}{RT} + \frac{A^{chain}}{RT} + \frac{A^{disp}}{RT} + \frac{A^{assoc}}{RT} + \frac{A^{polar}}{RT} + \frac{A^{NAHS}}{RT} + \frac{A^{electrolyte}}{RT} \quad (2.20)$$

2.5.4 Various terms of ePPC-SAFT

2.5.4.1 The hard sphere term

The hard sphere reference contribution of Helmholtz energy is given as follows. This term account for the hard sphere repulsion interaction energy.

$$\frac{A^{hs}}{RT} = \frac{6}{\rho\pi} \left[\left(\frac{\zeta_2^3}{\zeta_3^2} - \zeta_0 \right) \ln(1 - \zeta_3) + \frac{3\zeta_1\zeta_2}{1 - \zeta_3} + \frac{\zeta_2^3}{\zeta_3(1 - \zeta_3)^2} \right] \quad (2.21)$$

$$\zeta_k = \frac{\pi N_A \rho}{6} \sum_{i=1}^n x_i m_i (d_{ii})^k \quad (2.22)$$

$$d_{ii}(T) = \sigma_{ii} \left[1 - \lambda_i \exp \left(-3 \frac{\varepsilon_{ii}}{kT} \right) \right] \quad (2.23)$$

where, ρ is the molar density, σ_{ii} is the segment diameter, ε_i is the dispersive parameter, λ is the softness parameter which is often equal to 0.12, where $k = 1, 2, 3..$ and N_A is the Avagadro's number, d_{ii} : the hard sphere diameter which is given by equation 2.23 [156].

2.5.4.2 The chain term

Chapman *et al.* [157] developed an EoS based on the Wertheim's perturbation theory of first order by assuming homonuclear chains of m number of segments where the association energy is considered infinite. This led to the formulation of chain term (equation. 2.24). The radial distribution function $g_{ii}^{seg}(d_{ii})$ (equation 2.25 is given by Boublik and Mansoori [158, 159]).

$$\frac{A^{chain}}{RT} = \sum_{i=1}^n x_i (1 - m_i) \ln(g_{ii}^{seg}(d_{ii})) \quad (2.24)$$

$$g_{ii}^{seg} = \frac{1}{1 - \zeta_3} + 3 \frac{d_{ij}}{(1 - \zeta_3)^2} + 2 \frac{(d_{ij}\zeta_2)^2}{(1 - \zeta_3)^3} \quad (2.25)$$

$$d_{ij} = \frac{d_i d_j}{d_i + d_j} \quad (2.26)$$

where x_i is the mole fraction of the chains of component i , m_i is the number of chain segments for component i , ρ represents the total number density of the molecules

($\rho = \frac{N}{V}$), g_{ii}^{hs} is the radial distribution function at contact in the hard sphere system for component i .

2.5.4.3 The dispersion term

The dispersion terms in PC-SAFT is accounted for as a perturbation on hard chain. In order to do so, the Lennard-Jones potential with a radial distribution function for inter-chain is assumed. The Helmholtz energy for dispersion is given as:

$$\frac{A^{disp}}{NkT} = \frac{A_1}{NkT} + \frac{A_2}{NkT} \quad (2.27)$$

where,

$$\frac{A_1}{NkT} = -2\pi m^2 \left(\frac{\epsilon}{kT}\right) \sigma^3 \int_1^\infty \tilde{u}(x)^2 g^{hc} \left(m; \frac{x\sigma}{d}\right) x^2 dx \quad (2.28)$$

$$\frac{A_2}{NkT} = -\pi \rho m \left(1 + Z^{hc} + \sigma \frac{\partial Z^{hc}}{\partial \rho}\right)^{-1} m^2 \left(\frac{\epsilon}{kT}\right)^2 \sigma^3 \frac{\partial}{\partial \rho} \left[\rho \int_1^\infty \tilde{u}(x)^2 g^{hc} \left(m; \frac{x\sigma}{d}\right) x^2 dx\right] \quad (2.29)$$

Gross *et al.* [133] used mixture parameter $\overline{m^2 \epsilon \sigma^3}$ and $\overline{m^2 \epsilon^2 \sigma^3}$ to calculate the integrals appearing in above equations.

$$\overline{m^2 \epsilon \sigma^3} = \sum_i^n \sum_j^n x_i x_j m_i m_j \left(\frac{\epsilon_{ij}}{kT}\right) \sigma_{ij}^3 \quad (2.30)$$

$$\overline{m^2 \epsilon^2 \sigma^3} = \sum_i^n \sum_j^n x_i x_j m_i m_j \left(\frac{\epsilon_{ij}}{kT}\right)^2 \sigma_{ij}^3 \quad (2.31)$$

These average function are calculated using coomon specific parameters:

ϵ_{ij}/k : the dispersion energy parameter

σ_{ij} : the diameter of the segment

m_i : the chain length

It is worth mentioning here that these parameters are tunable in our thermodynamic framework. They are usually fitted using the PVT data of pure compounds. These parameters are always present for all types of molecules, irrespective of their nature.

2.5.4.4 The binary interaction parameters

Mixtures can be modeled by PC-SAFT using Van der Waals one-fluid theory and modified Lorentz-Berthelot combining rules that relate parameters ε_{ij} and σ_{ij} between segments of molecules. These correlations are given as follows.

$$\varepsilon_{ij} = (1 - k_{ij})\sqrt{\varepsilon_{ii}\varepsilon_{jj}} \quad (2.32)$$

$$\sigma_{ij} = \left(\frac{\sigma_{ii} + \sigma_{jj}}{2} \right) \quad (2.33)$$

A non-zero binary interaction parameter is necessary for representing a real phase equilibrium behavior of the molecules presented in this work. A correlation was proposed for k_{ij} on the basis of London-dispersion forces by introducing an adjustable parameter J_i (pseudo-ionization energy). The correlation is as follows.

$$1 - k_{ij} = \frac{2\sqrt{J_i J_j}}{(J_i + J_j)} \quad (2.34)$$

So, the following parameter can be tuned for mixtures.

k_{ij} : binary interaction parameter

J_i : pseudo-ionization energy

where subscripts i and j refer to molecules i and j .

2.5.4.5 The association term

The association term in the equation is given as follows:

$$\frac{A^{assoc}}{NkT} = \sum_{A_i} \left(\ln X^A - \frac{X^A}{2} \right) + \frac{1}{2}M \quad (2.35)$$

$$X^A = \left[1 + N_{AV} \sum_B \varrho X^B \Delta^{AB} \right]^{-1} \quad (2.36)$$

$$\Delta^{A_i B_j} = g_{ii}^{seg} \left[\exp \left(\frac{\varepsilon^{A_i B_j}}{kT} \right) - 1 \right] d_{ij}^3 \kappa^{A_i B_j} \quad (2.37)$$

where, g^{hs} is calculated by equation 2.25 X^A : The fraction of un-bonded associations sites A, M : The number of association sites in a molecule, Δ^{AB} : The association strength between two sites A and B, The two adjustable parameters are:

$\varepsilon^{A_i B_j}$: association energy
 $\kappa^{A_i B_j}$: association volume respectively.

2.5.4.6 The polar term

Jog and Chapman [160] proposed a term that was successfully able to describe the long-range electrostatic interactions within the systems. The SAFT term describing the change in free energy contributing to the dipolar interaction, is taken by dissolving all bonds in a chain and forming a mixture of non-bonded segments of both polar and non-polar segments. Finally, the contribution of Helmholtz free energy describing the polar interactions are given as.

$$A^{polar} = \frac{A_2^{polar}}{1 - \frac{A_3^{polar}}{A_2^{polar}}} \quad (2.38)$$

$$A_2^{polar} = -\frac{2\pi}{9} \frac{\rho}{(kT)^2} \sum_i \sum_j x_i x_j m_i m_j x_{pi} x_{pj} \frac{\mu_i^2 \mu_j^2}{d_{ij}^3} I_{2,ij} \quad (2.39)$$

$$A_3^{polar} = -\frac{15}{9} \pi^2 \frac{\rho^2}{(kT)^3} \sum_i \sum_j \sum_k x_i x_j x_k m_i m_j m_k x_{pi} x_{pj} x_{pk} \frac{\mu_i^2 \mu_j^2 \mu_k^2}{d_{ij} d_{jk} d_{ik}} I_{3,ijk} \quad (2.40)$$

Here μ_i is the dipole moment, and the following is the tunable parameter for pure polar components. I_2, I_3 are correlations representing integrals over statistical properties.

x_{pi} : the fraction of the polar hard spheres of molecule i
 μ : the dipole moment of component i

2.5.4.7 The non-additive hard sphere term

The non-additive contribution by Trinh *et al.* [161], is an extension to GC-PPC-SAFT that was designed to model the hydrogen solubility of oxygenated compounds. This extension consists in an additional perturbation term. The mathematical description of the term is as follows. This term models the deformation of a hard sphere when it is close to another hard sphere. As ionic solutions are dense and due to strong electrostatic

interactions, ions can be affect the diameter of the neighbouring molecules. Hence, this term NAHS can be useful in our model.

Based on the work of Malakhov and [162] an equation of state of non-additive square well chains was developed. The deviation from the square well chain behaviours is attributed to Non Additive Segment (NAS) perturbation and is written as follows.

$$\frac{A}{NkT} = \frac{A^{SWC}}{NkT} + \frac{A^{NAHS}}{NkT} \quad (2.41)$$

A^{SWC} denotes the additive contributions for ordinary Square Well Chains (SWC) i.e. the PC-SAFT equation and A^{NAS} represents the correction to the additive behavior. The interaction potential between segment i and segment j of two non-additive homonuclear chain molecules is defined as.

$$u_{ij} = \begin{cases} \infty & r < d_{ij} \\ -\varepsilon_{ij} & d_{ij} \leq r < \lambda d_{ij} \\ 0 & r \geq \lambda d_{ij} \end{cases} \quad (2.42)$$

where r is the distance between the two segments, σ_{ij} is the cross diameter, ε_{ij} denotes the depth of the potential well and λ is the reduced well depth. The correction parameter for cross diameter is introduced as follows.

$$d_{ij} = \frac{d_{ii} + d_{jj}}{2}(1 - l_{ij}) \quad (2.43)$$

where d_{ii} and d_{jj} is computed from eqn 2.23.

l_{ij} is correction for cross diameter.

$$\frac{A^{NAHS}}{RT} = -2\pi\rho \sum_i \sum_j x_i m_i x_j m_j d_{ij}^3 l_{ij} g_{ij}^{SWC} \quad (2.44)$$

where g_{ij} : is computed from inter-segment distribution function of a fluid of ordinary square well chains. x_i, x_j : represents the mole fractions of molecules i and j ; m_i, m_j : are the constitutive segments or the length of chain of molecules i and j ; ρ : is the total molecular density. The calculation of g_{ij}^{SWC} is based on method suggested by Paredes *et al.* [163] and its expression is given by [161].

2.5.5 Group contribution approach

The pure component parameters for the higher members of the same homologous series may be calculated using group contribution correlation [148] developed for, ε_k , σ_k and m . These expressions were inspired by the Lorentz-Berthelot combining rules and are as follows.

$$\varepsilon = \sum_{k=1}^{n_{groups}} n_k \sqrt{\left(\prod_{k=1}^{n_{groups}} \varepsilon_k^{n_k} \right)} \quad (2.45)$$

$$\sigma = \frac{\sum_{k=1}^{n_{groups}} n_k \sigma_k}{\sum_{k=1}^{n_{groups}} n_k} \quad (2.46)$$

$$m = \sum_{k=1}^{n_{groups}} n_k R_k \quad (2.47)$$

Where n_k is the number of groups k in the molecule comprising of n_{groups} non-identical groups. A group contribution method was also devised for calculating pseudo-ionization energies and is given by the following relation.

$$J_i = \left(\sum_{k=1}^{n_{groups}} n_k \right)^n \sqrt{\prod_{k=1}^{n_{groups}} J_k^{n_k}} \quad (2.48)$$

J_k represents the contribution of the group k to the pseudo-ionization energy of the segments of the molecule under consideration. This relation is applicable to members in a homologous series except for the starting first or second members. It is however recommended to use molecular pseudo-ionization energy for aromatic molecules.

The binary interaction l_{ij} can be computed from group contribution as follows.

$$l_{ij} = \frac{1}{n_i^{group} n_j^{group}} \sum_{\alpha} \sum_{\beta} n_i^{group\alpha} n_j^{group\beta} l^{\alpha\beta} \quad (2.49)$$

$l_{\alpha\beta}$: correction for the diameter (between two groups)

2.5.6 Cross association parameters

If the current GC-PPC-SAFT model is to be extended to associating species, well-defined combining rules must be applied for cross association parameters. For this purpose, the so-called CR1 combining rules by Derawi *et al.* [164] were utilized to calculate cross

association parameters. In GC-PPC SAFT model the association is considered between groups rather than between the molecules which allow specific treatment for polyfunctional groups (for example alkanolamines and alkanediols [62]). A combining rule must be explicitly defined for each group and for each association parameter (section 2.5.4.5). The equations are as follows.

$$\varepsilon_{\alpha\beta}^{AB} = (1 - w_{\alpha\beta}) \left(\frac{\varepsilon_{\alpha}^{AB} + \varepsilon_{\beta}^{AB}}{2} \right) \quad (2.50)$$

$$\kappa_{\alpha\beta}^{AB} = (1 - u_{\alpha\beta}) \sqrt{\kappa_{\alpha}^{AB} \cdot \kappa_{\beta}^{AB}} \quad (2.51)$$

The parameters $w_{\alpha\beta}$ and $u_{\alpha\beta}$ are adjustable group-group interaction parameters that allow adjusting the combining rules when needed. Note that subscripts $\alpha\beta$ are different from i and j above because association between groups is considered here rather than molecules.

$w_{\alpha\beta}$: correction for the association energy (between two groups)

$u_{\alpha\beta}$: is correction for the association volume (between two groups)

Chapter 3

Modified model of PC-SAFT for water

3.1	Abstract	42
3.2	Introduction	43
3.3	Model	43
3.3.1	Previous Descriptions of Water with the PC-SAFT EoS	47
3.3.2	A new Temperature Dependence of Water Diameter	48
3.4	Results for binary mixtures	51
3.4.1	Mutual solubilities	51
3.4.2	Octanol/Water Partition coefficient	65
3.4.3	Gibbs energy of Hydrogen Bonding	66
3.4.4	Conclusion	68

A New PC-SAFT Model for Pure Water, Water-Hydrocarbons and Water-Oxygenates Systems and Subsequent Modeling of VLE, VLLE and LLE.

J. Chem. Eng. Data, **2016**, 61 (12), pp 4178–4190

DOI: [10.1021/acs.jced.6b00565](https://doi.org/10.1021/acs.jced.6b00565)

3.1 Abstract

Before dealing with the electrolytic systems it is necessary to have a model describing correct phase equilibrium and volumetric properties of the pure solvent and the mixture of solvents. Water is, of course, the important solvent to be investigated, As the main objective of this thesis is to deal with the mixed solvent electrolyte systems, it is of primary importance to have an accurate modeling of phase equilibrium of mixtures involving water and organic compounds.

Accurate analytic thermodynamic modeling of water and its mixtures with hydrocarbon and oxygenates is difficult even with new and advanced equations of state such as PC-SAFT. Several attempts have been made in the past by various authors to solve this issue. However, current models generally fail to describe simultaneously and accurately pure water properties (especially its liquid density) and liquid-liquid equilibria for mixtures involving water, hydrocarbons and oxygenates. In the current work, this problem is dealt by a modification in the fundamental structure of the model. It was established that the temperature dependent diameter $d(T)$ does not behave in the same way for water as it is inscribed in the original model. Hence, a modification was proposed for $d(T)$ of water in order to correctly represent the phase behaviour of pure water and its mixtures with hydrocarbons and oxygenates. Thus, the deviation in saturated liquid densities and vapour pressure for pure water were reduced to 0.6% and 2.2% respectively in a large temperature range. The results for LLE, VLE, and VLLE of various water-hydrocarbons and oxygenates show the accuracy of this new model and its predictive capability when coupled with a group contribution approach. For certain oxygenated mixtures such as water with aldehydes, ketones, ethers, and esters a new contribution to the Helmholtz energy, known as “non-additive hard sphere” contribution, was used. The cross-interaction parameters obtained for mixtures were validated qualitatively by calculating octanol/water partition coefficients and the Gibbs free energy of hydrogen bonding (ΔG_{HB}). Results are found in good agreement with experimental data.

3.2 Introduction

Water is a strongly polar solvent that forms strongly non-ideal mixtures with hydrocarbons and oxygenated chemicals present in the biomass. It is also responsible for degradation of processing equipment and worsening of product quality. An accurate representation of mutual solubilities of these hydrocarbons and oxygenated compounds in water is consequently very important. This information plays a vital role in the design and optimization of processes such as bio-refineries, which are the epicenter of the second-generation biofuel conversion process. The lack of experimental thermodynamic data for these complex mixtures results in the need to develop predictive thermodynamic approaches that must be accurate and efficient at the same time. A lot of authors have proposed models for calculating the mutual solubility of hydrocarbon and water mixtures. However, a very low mutual solubility of hydrocarbons and water makes it difficult to predict, and empirical approaches are often required, such as heterogeneous approaches using activity coefficient models coupled with Henry's constant correlations [165, 166]. Concerning the homogeneous approaches, much attention has been paid to Cubic Equation of State (CEoS), as in the work of Kabadi and Danner [167], and of Soreide and Whitson [168] for hydrocarbons + water mixtures. More recently, advanced equations of state have been proposed, such as the Cubic Plus Association (CPA) model [169–171] which uses Wertheim's association theory [49–52] for hydrogen bonding in water.

The aim of this work is to make PC-SAFT model more accurate in terms of prediction of pure water properties (saturated liquid densities and vapour pressures) and liquid-liquid-vapour phase equilibria for mixtures involving water, hydrocarbons and oxygenates.

The framework of this model is already presented in chapter 2. In this chapter, the modification brought in the diameter calculations to improve pure water properties predictions are presented in section 3.3. In section 3.4, binary mixtures are investigated. In section 3.4.2 a focus is made on the octanol-water partition coefficients, which is a ternary property of primary importance for industrial applications. Finally, our model will be evaluated in term of Gibbs energy of hydrogen bonding (section 3.4.3).

3.3 Model

The details pertaining to the mathematical model of PC-SAFT have already been discussed in section 2.5.3. To recall, the GC-PPC-SAFT Equation of State used in this work has been developed from PPC-SAFT (Polar Perturbed Chain SAFT) EoS [133,

172]. It utilizes group contribution correlations of Tamouza [148, 173], for calculating parameters that represent a pure component, chain length (m), segment diameter (σ), and dispersive energy ε/k . These three parameters are always present, irrespective of the type of molecule. For associative components, there are 2 additional parameters, ε^{AB}/k : association energy and κ^{AB} : association volume. A specific term is added which describes dipolar and quadrupolar effects for polar compounds such as water, alcohols, aldehydes, ketones, esters, and ethers. The parameters are x_p^μ : dipolar fraction of the molecule, along with the dipole moment μ for the dipolar molecules. For quadrupolar compounds such as aromatics, similar term quadrupolar fraction x_p^Q along with quadrupolar moment Q are employed. Finally, another parameter for pure compounds should be mentioned here: the diameter softness λ that relates to the temperature dependent diameter $d(T)$ with σ in the following way.

$$d(T) = \sigma \left[1 - \lambda \exp\left(-3\frac{\varepsilon}{kT}\right) \right] \quad (3.1)$$

The value of this parameter (λ) is fixed to be 0.12 in PC-SAFT. However, it is of significance in the work to see the effect of changing the value of the diameter $d(T)$ in equation 3.1. To recall, the GC-PPC-SAFT parameters for a large number of groups have been determined by several authors and are provided in Table 3.1. The parameters have been obtained based on regressing pure component vapour pressure and saturated liquid densities covering the reduced temperature range from 0.4 to 1.0. For details pertaining to parameterization, readers are referred to NguyenHuynh *et. al.* [152].

Table 3.1: Group Contribution parameters for alkanes, alkylbenzenes, alcohols, ketones, aldehydes, ethers and esters for use with GC-PPC-SAFT ^a

Family	Groups	$\varepsilon/k(\mathbf{K})$	$\sigma(\text{\AA})$	\mathbf{R}/m^b	$\varepsilon^{AB}/\mathbf{k}$	κ^{AB}	$\mu(\text{\AA})$	$x_{p,\mathbf{m}}$	$\mathbf{J}(\text{ev})$	Reference
Alkanes	CH ₃	189.9628	3.4873	0.7866					22.755 ^b	[148]
			0.7866 (para)							
			0.8593 (ortho)							
Alkyl Benzenes	CH ₂	261.0866	3.9308	0.3821					6.254 ^b	
	(C) _{AB} or (C<) _{aro}	391.5410	4.2783	0.0016						[128]
	(C) _{BR} or (CH<) _{aro}	294.2235	3.7572	0.3805						[132]
Alcohols	Ring	-	-	-	1000 ^d	0.01986	7.0 ^b	0.25 ^c		[132]
	(OH) ₁	307.5094	2.8138	0.8318	2143.29	0.0088 ^d	1.7, 1.83 ^g	0.6	28.008	[152]
	(OH) ₂			0.3573		0.0044				
	(OH) ₃			0.2694						
	(OH) ₄			0.2649						
Ketones	-CO	480.73	3.7495	0.5229	2143.29 ^d	0.0088 ^d	2.7	0.57	6.5	[152]
				0.5154						
Aldehydes				0.4539						
				0.2731						
Esters				0.4088						
	-CHO	397.67	3.8538	0.718	2143.29 ^d	0.0088 ^d	3.16 ^f	0.6	6.5	[152]
	-COO	362.82	33448	0	2143.29 ^d	0.0088 ^d		2.018 ^e	14	[128]
Ethers				0.8274						
				0.8116						
				0.7279						
Ethers				0.7279						
	-O-	280.96	3.5764	0.5084	2143.29 ^d	0.0088 ^d	1.2	1.2	6.5	[152]
				0.3101						
				0.2173						
				0.1592						
				0.1378						

- ^a The first parameter ε/k is the dispersive energy, is the segment diameter R is the chain length which may depend on the group position within the molecule. The association parameters mentioned here (ε_{AB} for association energy and κ^{AB} for association volume) all refers to the single electron donor site, except for alkanols which have 3B association scheme. The polar parameters are group parameters (μ for dipole and Q for quadrupole) and are accompanied by their respective fraction (x_{pm} : amount of polar group in the molecule). The group contribution value used for contributing pseudo-ionization energies are also provided (K), even in many cases a specific molecular value was needed.
- ^b The pseudo-ionization energies from Mourah *et al.* [153]. The alkyl-benzene quadrupole moment is a molecular property that is taken equal to 7B for all alkyl Benzene except those listed in Table(2) of [132] and in Nguyen-Huynh *et al.* [128]
- ^c The quadrupolar fraction is also a molecular property (i.e. it refers to the benzene ring and not to the individual aromatic groups).
- ^d The association parameters mentioned here are not used for self-association, but only in the case of cross-association, in which case they are used in combination with equations 2.50 and 2.51.
- ^e The dipole moment of esters depend on the position as discussed in NguyenHuynh *et al.* [149]
- ^f The dipole moment of aldehydes depends on the chain length as discussed in the NguyenHuynh *et al.* [149]
- ^g The dipole moment of the group used separately for ethanol. ^h R_m , m represents position of the group in the molecule. for $k_{i,j}$ on the basis of London dispersion forces by introducing an adjustable parameter J_i (pseudo-ionization energy) [151] and modifying the expression of Hudson and McCoubey [174] based on semi-empirical grounds. The correlation is as follows.

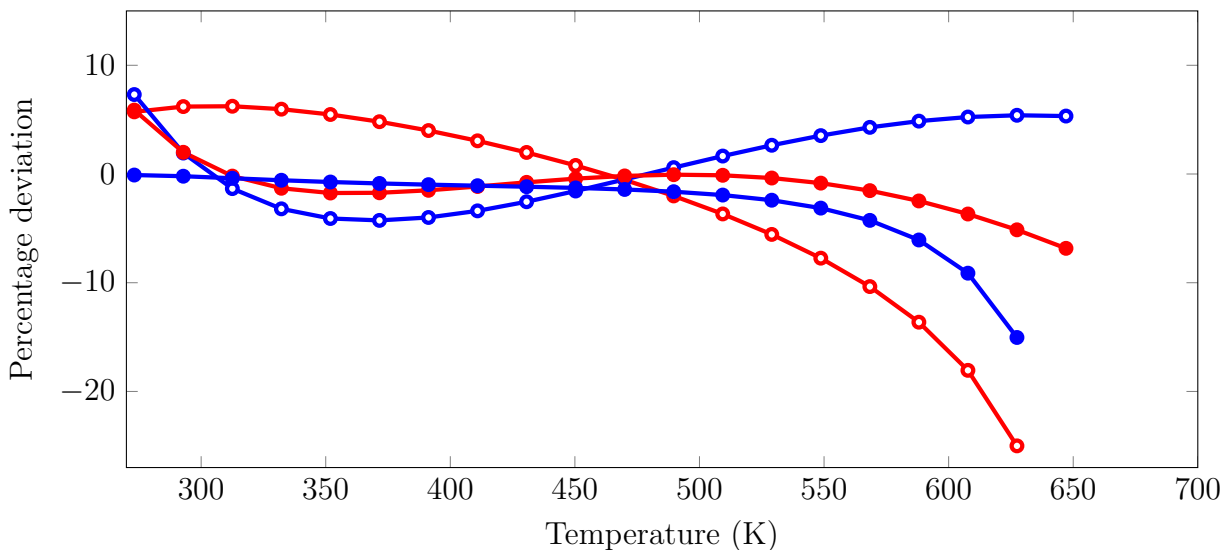


Figure 3.1: Deviation (%) in vapor pressure (old model \circ , new model \bullet) and saturated liquid volume (old model \circ , new model \bullet) of pure water using our approach

If the current GC-PPC-SAFT model is to be extended to associating species, well-defined combining rule must be applied for cross-association parameters. For this purpose, the so-called CR1 combining rule by Derawi *et al.* [164] was utilized to calculate cross association parameters. In GC-PPC SAFT model the association is considered among groups and not among molecules with sometimes specific treatment for polyfunctional molecules (for example alkanolamines and alkanediols [175]). A combining rule must be explicitly defined for each group and for each association parameter. The equation is as follows for these rules are given by eqn 2.50-2.51

3.3.1 Previous Descriptions of Water with the PC-SAFT EoS

3.3.1.1 Former GC-PPC-SAFT Parameters

Water is a polar solvent which has strong association tendency. It readily forms hydrogen bonds to itself and to other molecules capable of forming such bond. In current GC-PPC-SAFT prior to modification, water is viewed as polar associating component, however, there has been significant deviations in predicting liquid densities of pure water. NguyenHuynh [152] has described pure water according to a 4C association scheme and a dipolar character. The deviations in liquid densities of pure water were 4.74% for liquid volume and 3.36% for vapor pressure. Moreover, at room temperature, these deviations remained significantly high, around 10% (Figure 3.1).

3.3.1.2 Cameretti *et al.* approach

Some authors like Cameretti [73], Sadowski and Held [60] have reduced the deviation in liquid densities of water by introducing a modification to the temperature independent segment diameter σ_w (subscript w represents that this modification is exclusive for water). Their modification was based on an empirical correlation consisting of two similar exponential terms, with four temperature dependent coefficients, as shown in the equation below which is coupled to equation 3.1 to yield the temperature dependent $d(T)$.

$$\sigma_{T,w} = \sigma_w + T_{dep,1} \times \exp(T_{dep,2} \cdot T) + T_{dep,3} \times \exp(T_{dep,4} \cdot T) \quad (3.2)$$

where σ_w is the temperature independent segment diameter and $\sigma_{T,w}$ is the temperature dependent segment diameter. $T_{dep,1}, \dots, T_{dep,4}$ are coefficients whose values were determined by fitting experimental liquid densities and vapor pressure. Reportedly, they obtained an AAD in saturated liquid volumes of 0.06%. However, their approach is based on a small range of temperatures from 0 to 100°C. Moreover, they used the 2B association model while the association is best described by 4C in the case of water. Using 2B association approach leads to significant deviations in predicting solubilities of mixtures containing water and oxygenated hydrocarbons [176]. Moreover, their modification failed when used for higher temperature range (373.15 to 550 K) where much higher deviations were observed in the liquid volume and the vapor pressure of water.

3.3.2 A new Temperature Dependence of Water Diameter

After an exhaustive investigation, it was clear that accurate modeling of liquid densities in water cannot be obtained without modification of its temperature independent diameter σ_w (equation 3.3), which was also reported by Held and Sadowski [60]. However, the expression proposed by Held is corrective in nature and contains 4 regressed parameters valid on a reduced temperature range. It appears that a very small change in the value of this parameter may change the resulting densities significantly. This is coherent with observations made by NguyenHuynh *et al.* [152]. Thus, it was important to identify the exact behavior of the optimal water diameter with our model, on a larger temperature range and then systematically incorporate that behavior in the model. To that end, the optimal diameter was fitted on both vapor pressure and saturated liquid molar volume (data originating from DIPPR correlation). The segment diameter σ was regressed at short temperature intervals (~ 10 K) of vapor pressure and saturated liquid volume data. This process was repeated over entire range of temperatures from 273.15 to 550 K and the regressed values were plotted as a function of temperature (average of the temperature

intervals on which it was regressed). As shown in figure 3.2, this clearly exhibits that the segment diameter of water should increase with temperature if we want it to match accurately and simultaneously liquid densities and vapour pressures. The functional form that was chosen to fit the observed behaviour is as follows:

$$\sigma_{T,W} = \sigma_W + T_{dep,1} \cdot \exp(T_{dep,2} \times T) + \frac{T_{dep,3}}{T^2} \quad (3.3)$$

An advantage of this functional form is that it allows a continuous increase of the segment diameter with temperature, which makes a smooth extrapolation at higher temperatures possible (supercritical region included, see table 3.3). The four parameters of this function (σ_W , T_{dep1} , T_{dep2} and T_{dep3}) and four other parameter of the GC-PPC-SAFT model (segment number m , dispersion energy ε/k , association volume κ^{AB} and sphere softness λ) have been adjusted to the full temperature range to fit water vapour pressures, liquid molar volumes and LLE of water + n-hexane (solubilities of alkanes in the aqueous phase and water in the organic phase). The optimal value of m was found close to 1, since water could be reasonably modeled as having 1 segment. Note that the association energy ε^{AB} is not regressed since its value is directly the value obtained from spectroscopic experimental data [152]. The value of the dipole moment is also taken equal to its experimental value in vacuum [152]. The value of the dipolar fraction x_p^μ is kept equal to the value used in the former GC-PPC-SAFT model [152]. The final optimized parameters proposed are given in table 3.2. It was observed that the vapor pressure deviations were very sensitive to the value of σ_w . With this new model, the average absolute deviation in liquid densities was brought down to 0.72% and in vapour pressure to 2.32% based on DIPPR experimental database on the 273 to 550K temperature range, as illustrated in figure 3.1.

After successful parameterization of pure water based on vapour pressure, liquid densities and mutual solubilities of water and n-alkanes, it is required to validate the model for predicting solubilities of other hydrocarbons (aromatics) and oxygenates in water. The results of predicting liquid-liquid equilibria would provide deeper insight into the accuracy of the model. In the following section 3.4.1, results of mutual solubilities of water with alkanes, aromatics, alcohols, aldehydes, ketones, ethers, and esters are provided.

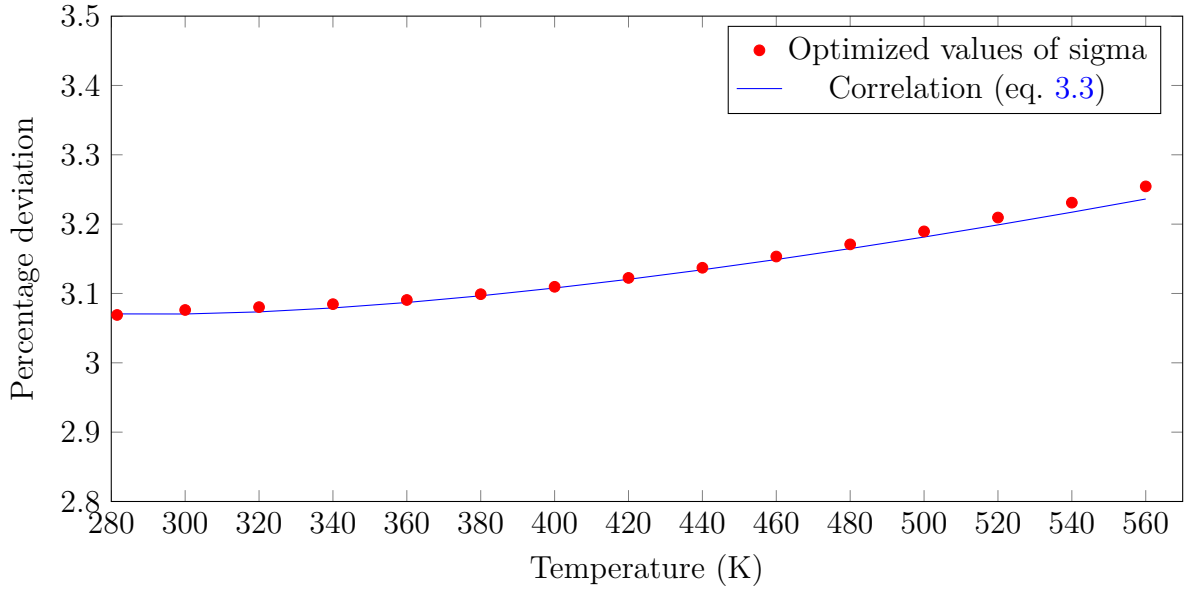


Figure 3.2: Plot of the temperature dependent segment diameter $\sigma_{T,W}(T)$. Symbols indicate optimized values of sigma on small temperature intervals of 10K. The line indicates the correlation (equation 3.3), but this correlation has final parameters which are optimized again on saturated liquid density and vapor pressure of pure water and LLE of n-hexane in the temperature range 273.15K-550K.

Table 3.2: Pure component parameters of water used in this work.

Parameters	Unit	abbreviation	Parameters (current work)
Segment number	-	m	1.02122
Segment diameter	Å	σ_w	2.2423
$T_{dep,1}$	Å	$T_{dep,1}$	0.51212
$T_{dep,2}$	-	$T_{dep,2}$	0.001126
$T_{dep,3}$	K ²	$T_{dep,3}$	9904.13
Dispersion energy	K	ε/k_B	201.747
Association energy	K	ε^{AB}/k_B	1813
Association volume	-	κ^{AB}	0.044394
Association type	-	-	4C
Sphere Softness*	-	λ	0.203
Dipole Moment	D	μ	1.85
Dipole fraction	-	x_p	0.276

*Bold indicates regressed parameters over liquid densities and vapor pressure of pure water from 273.15-550 K also on the LLE of water-n-alkanes. *This parameter (softness of diameter) is fixed as 0.12 in original PC-SAFT model, however it is made adjustable in the present version of GC-PPC-SAFT*

Table 3.3: Compressibility factor Z in the supercritical region from the new model and from NIST database

$T(\text{K})$	Pressure (MPa)	Z (model)	Z (experimental)(NIST database)
700	100	0.440	0.474
800	100	0.611	0.561
900	100	0.788	0.700

3.4 Results for binary mixtures

3.4.1 Mutual solubilities

When not mentioned otherwise, the k_{ij} binary parameters were computed using the predictive approach (2.5.4.4). Except for alkanes, all chemicals studied in this section can be cross-associated with water (aromatic hydrocarbons, alcohols, ketones, aldehydes, ethers, and esters). Two approaches to model these associative mixtures were investigated (in all cases we used the experimental data correlations for mutual solubilities from Nguyen *et al.* [130]):

- (a) Regression of group-group cross association parameters only, that are $w_{\alpha\beta}$ and $u_{\alpha\beta}$ (eqn. 2.50 and 2.51). Note that this is equivalent to regressing directly the cross-association energy, ε^{AB} and the cross-association volume κ^{AB} . It may be argued that these two parameters are correlated, but in fact, the energy affects the temperature dependence of the cross-association, while the volume affects more directly its amplitude. It was observed that they have not the same effect on the mutual solubilities. In some water-oxygenates systems, in addition to these two parameters, another group-group parameter for the NAHS term is also regressed ($l_{\alpha\beta}$, see equation 2.49) simultaneously.
- (b) Regression of the molecule-molecule interaction binary parameter k_{ij} , in addition to the group-group $w_{\alpha\beta}$ and $u_{\alpha\beta}$ parameters.

In what follows, approach (a) was privileged since it is only based on the interaction between groups. It allows for extending the computation to other oxygenated solvents of the same family, using the group contribution concept. On the contrary, approach (b) is purely correlative and it does not allow for such an extension unless some trend can be identified in the k_{ij} parameter.

With approach (a), we observed that regressing only $w_{\alpha\beta}$ and $u_{\alpha\beta}$ leads to an acceptable accuracy for water + aromatic and water + alcohol systems. For the other

systems (water + aldehydes, water + ketones, water + esters and water + ether), the regression of the $l_{\alpha\beta}$ interaction parameter involved in the NAHS contribution is also required.

Wherever feasible the results from the new model are compared to the previously reported results such as [130, 132]. The optimized group-group interaction parameters are summarized in table 3.4. Details for each chemical family are given further. The deviations between experimental and calculated mutual solubilities are provided in table 3.5 (the term "aqueous solubility" represents the solubility of organic compound in the aqueous phase and the term "organic solubility" represents the solubility of water in the organic phase, their deviations are denoted by X^{aq} and X^{org} respectively).

Table 3.6 also shows the numerical values of the k_{ij} parameters for approach (b). A trend towards smaller k_{ij} absolute values with increasing molecular weight can be observed, but all values are negative, which is in contrast with the theoretical meaning of this binary interaction parameter as stated by NguyenHuynh *et al.* [129]. Hence, no physically meaningful correlation can be developed using these results. This is the reason why approach (b) was not further considered.

Table 3.4: Optimized water-group interaction parameters using approaches (a) and (b)

Group	Approach (a)			Approach (b)		
	$\varepsilon^{AB}(K)$	κ^{AB}	$l^{\alpha\beta}$	$\varepsilon^{AB}(K)$	κ^{AB}	Specific k_{ij}
Aromatic ring	853.26	0.1056	-	-	-	-
OH (ethanol)	1685.87	0.04781	-	-	-	-
OH (alcohols)	1968.82	0.02314	-	-	-	-
CHO (aldehydes)	1605.65	0.02314	0.03045	1844.83	0.023137	See table 3.6
CO (ketones)	1728.15	0.03681	0.08501	1793.98	0.02079	See table 3.6
COO (esters)	1577.05	0.06298	0.04855	1637.68	0.03112	See table 3.6
O (ethers)	2275.90	0.00406	0.10674	1775.17	0.03061	See table 3.6

Table 3.5: Deviations between experimental and calculated mutual solubilities

Family	System (Water +)	Deviation(%(AAD))			
		approach(a)		approach(b)	
		X^{aq}	X^{org}	X^{aq}	X^{org}
Alkanes ^a	Pentane	42.72	19.60	-	-
	Hexane	44.89	19.07	-	-
	Heptane	46.18	12.14	-	-
	Octane	47.68	8.64	-	-
	Nonane	32.33	16.13	-	-
Alkylbenzenes	Toluene	31.00	5.74	-	-
	Propyl Benzene	26.00	21.61	-	-
	Butyl Benzene	42.70	22.84	-	-
	Hexyl Benzene	43.20	18.99	-	-
	m-Xylene	34.30	11.46	-	-
	p-Xylene	32.20	10.57	-	-
Alcohols ^b	Butanol	31.81	9.78	-	-
	Pentanol	20.07	2.91	-	-
	Hexanol	18.19	16.1	-	-
	Heptanol	28.28	23.06	-	-
Aldehydes	Propanal	48.6	21.8	-	-
	Butanal	23.1	24.0	-	-
	Pentanal	35.4	14.3	-	-
	Hexanal	34.7	12.5	-	-
	Heptanal	31.7	9.4	-	-
	Octanal	19.2	6.6	-	-
	Nonanal	5.6	3.3	-	-
Ketones	2-Butanone	28.7	72.02	9.8	67.9
	2-Pentanone	27.0	31.49	11.8	28.9
	2-Hexanone	24.51	39.8	20.0	32.7
	2-Heptanone	47.4	29.2	23.0	20.8
	3-Heptanone	37.5	9.8	29.7	16.9
	4-Heptanone	36.58	31.95	27.4	29.2
Ethers	Diethyl Ether	38.9	26.9	30.0	8.1
	Ethyl Propyl Ether	38.1	13.9	14.7	8.9
	Methyl isoButyl Ether	23.3	39.8	25.5	22.8
	Methyl n-Butyl Ether	23.3	39.8	15.1	31.8
	Methyl sec-Butyl Ether	28.0	39.8	99.9	13.9
	Diisopropyl Ether	51.8	28.6	51.5	16.6
Esters	Methyl Propionate	44.8	9.0	11.0	19.4
	Ethyl Propionate	22.7	15.9	9.8	17.7
	n-Propyl Propionate	31.9	29.2	24.4	29.8
	n-Butyl Propionate	47.6	28.8	8.7	7.8
	Methyl n-Butyrate	31.4	18.0	18.6	13.0
	Ethyl n-Butyrate	29.7	26.2	14.8	12.7
	n-Propyl n-Butyrate	83.5	29.1	8.7	18.9
	n-Butyl n-Butyrate	69.1	34.4	17.9	20.7
	Ethyl Acetate	11.0	5.6	31.6	39.5
	n-Propyl Acetate	18.2	13.1	24.4	29.9
	n-Butyl Acetate	43.8	16.1	18.9	21.8
	n-Pentyl Acetate	60.4	20.7	24.1	22.4
	n-Hexyl Acetate	74.5	22.1	12.7	5.5
n-Heptyl Acetate	85.9	38.1	12.4	5.8	

^anote that for alkanes, no regression at all have been performed: the results are entirely predicted.

^bFor alcohols there was no need to regress k_{ij} which explains why approach(b) is not documented.

Table 3.6: Binary interaction parameter k_{ij} between molecules for approach (b)

Family	System (Water +)	Binary Parameters k_{ij} (approach b)
Aldehydes	Propanal	-0.02199
	Butanal	-0.01032
	Pentanal	-0.00112
	Hexanal	-0.00173
	Heptanal	-0.00317
	Octanal	-0.00318
	Ketones	2-Butanone
2-Pentanone		-0.04572
2-Hexanone		-0.03818
2-Heptanone		-0.03214
3-Heptanone		-0.02627
4-Heptanone		-0.01493
Ethers	Diethyl Ether	-0.07063
	Ethyl Propyl Ether	-0.07735
	Methyl isoButyl Ether	-0.05850
	Methyl n-Butyl Ether	-0.06578
	Methyl sec-Butyl Ether	-0.07787
	Diisopropyl Ether	-0.03728
Esters	Methyl Propionate	-0.00449
	Ethyl Propionate	-0.00335
	n-Propyl Propionate	-0.00607
	n-Butyl Propionate	-0.00122
	Methyl n-Butyrate	-0.00434
	Ethyl n-Butyrate	-0.02912
	n-Propyl n-Butyrate	-0.00758
	n-Butyl n-Butyrate	-0.00743
	Ethyl Acetate	-0.01191
	n-Propyl Acetate	-0.01295
	n-Butyl Acetate	-0.01287
	n-Pentyl Acetate	-0.01265
	n-Hexyl Acetate	-0.01339
n-Heptyl Acetate	-0.02438	

3.4.1.1 Water - Alkanes

Alkanes are characterized by very low solubility in water because of the absence of polarity and any functional groups that can associate with water. Moreover, the presence of hydrocarbon chain that is hydrophobic in nature makes the process of solubility less profitable in terms of energy. Solubility decreases with increase in chain length. The current model is entirely predictive for these mixtures (k_{ij} is computed from equation

9 and 10) and performs fairly well in terms of deviations, as shown for the example of n-pentane in Figure 3.3(a)-3.4. A comparison with results reported by NguyenHuynh *et al.* [132] shows considerable improvement for water and organic solubilities.

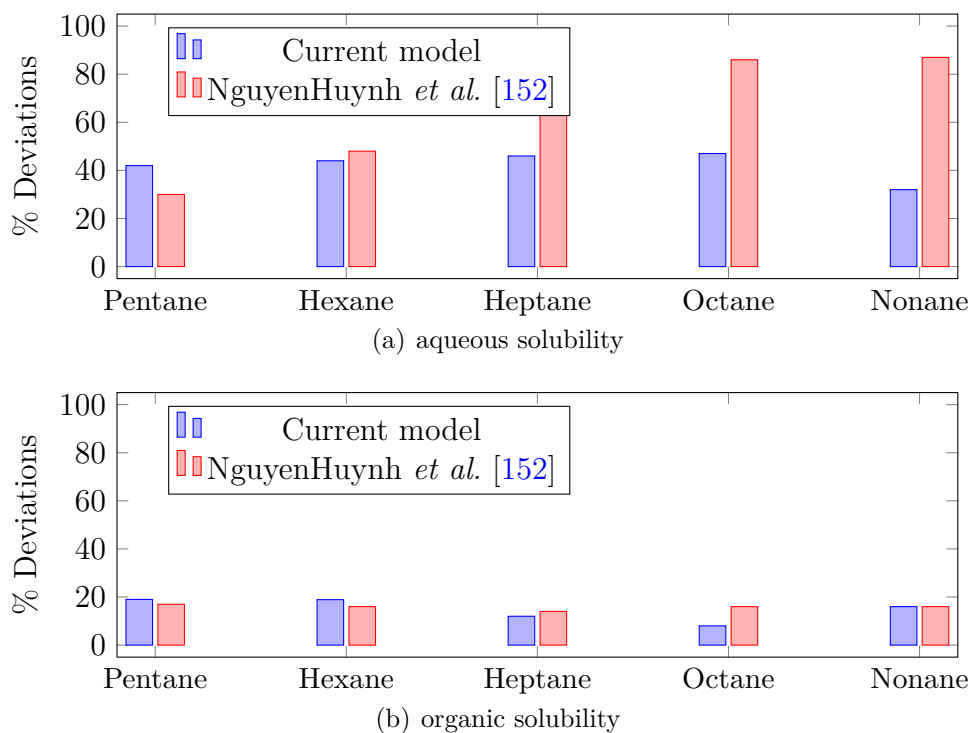


Figure 3.3: Deviations in aqueous and organic solubility of various water-alkane mixtures from current model in comparison to results from NguyenHuynh *et al.* [152]

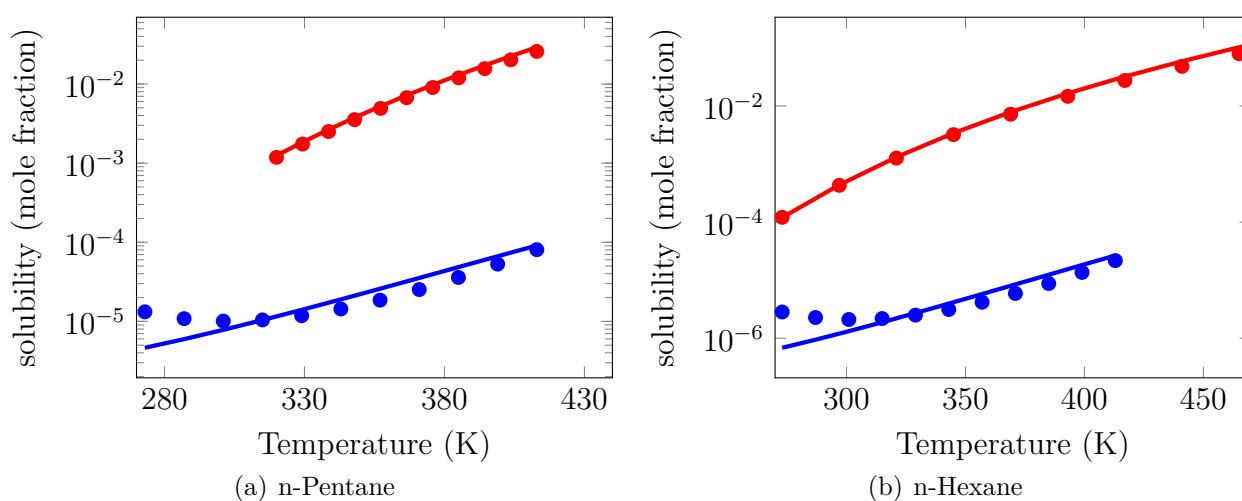


Figure 3.4: ● Solubility in aqueous phase and ● solubility in organic phase of n-pentane, points are experimental data and lines are calculation from model

3.4.1.2 Water - Alkylbenzenes

Alkylbenzenes are associative compounds due to the presence of aromatic rings and they are capable of forming hydrogen bonds with water. Still, they are characterized by low solubilities with water due to the significant hydrophobic part present in the chain. However, with increasing temperatures solubility tends to increase, with a minimum at 290 K.

The solubility of some alkylbenzenes is investigated in the following section using the proposed model. One association site is positioned on the benzene ring as suggested by NguyenHuynh *et al.* [152]. Approach (a) was used: the cross-association parameters between water and the aromatic alkylbenzene ring was then adjusted. The regressed values are $\varepsilon^{AB} = 853.26$ and $\kappa^{AB} = 0.10558$ and results obtained were within fairly satisfactory range, shown in fig 3.5. However, slightly higher deviations were observed in comparison to results by NguyenHuynh *et al.* [152], such deviations could be viewed as a good tradeoff when deviations in liquid densities of pure water were reduced to very low values. The deviations obtained are in the same order of magnitude as those for n-alkanes.

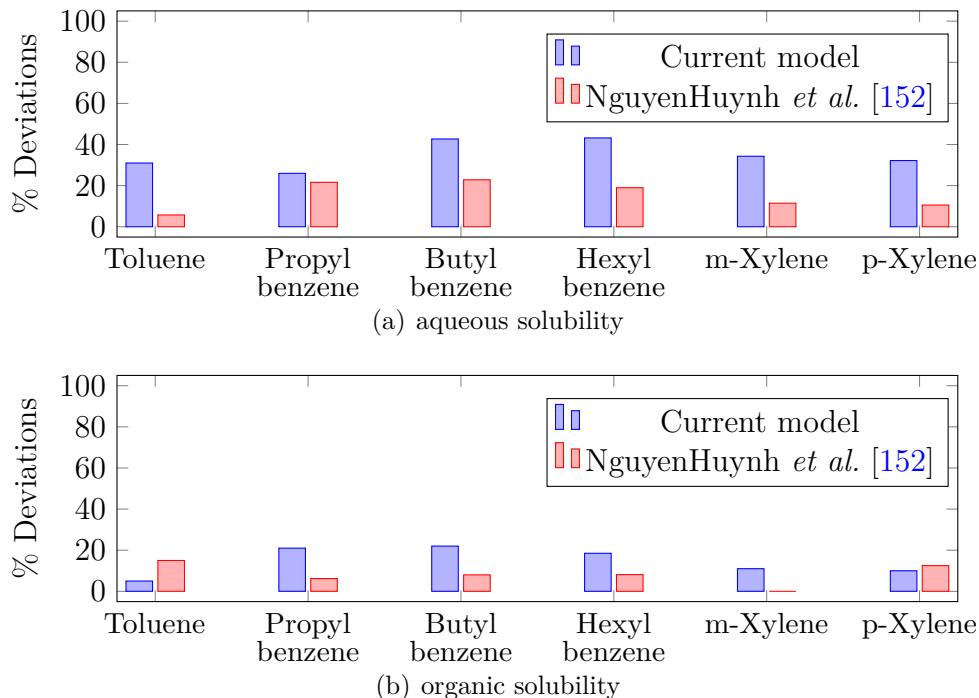


Figure 3.5: Deviations in aqueous and organic solubility of various water-alkylbenzene mixtures from current model in comparison to results from NguyenHuynh *et al.* [152]

3.4.1.3 Water - Alcohols

Alcohols are oxygen bearing hydrocarbons which consist of a hydrocarbon chain and a terminal OH group. They have a tendency to form hydrogen bonds with themselves and with water. Because of the strength of attraction of the OH group, the first three alcohols (methanol, ethanol, propanol) are completely miscible in water. They dissolve in water in all proportions. However, the hydrocarbon chain in alcohol is water repellent and hence above n-butanol alcohols are immiscible in the liquid phase.

The cross association parameters between water and the hydroxyl group (OH) were regressed on mutual solubility data of 1-butanol to 1-heptanol as well as VLE data for 1-hexanol and 1-butanol, using approach (a). The optimized values are $\varepsilon^{AB} = 1968.82$ and $\kappa^{AB} = 0.02317$. Deviations (figure 3.6) are within satisfactory ranges and in fact improved in contrast to deviations reported by NguyenHuynh *et al.* [152]. The dipole moment for ethanol is slightly higher than for other members of the alcohol family, hence a separate group (ethanol molecule is defined by group contribution method) was defined just for ethanol, with different dipole moment (refer to Table 1). The cross association parameters between water and the OH group of ethanol is adjusted separately on VLE data of the water-ethanol system. The optimized values are $w_{\alpha\beta} = 0.147753$ and $u_{\alpha\beta} = -1.41225$. The results of VLE of water-ethanol, water-butanol and also VLLE of water-hexanol are presented in figure 3.8 and 3.9. Predictive computation of the liquid-liquid phase equilibrium on the ternary water - 1-butanol - ethanol system (figure 3.10) is represented correctly and the tie lines have correct inclinations. Yet, as is often observed with the model, the critical point is overestimated.

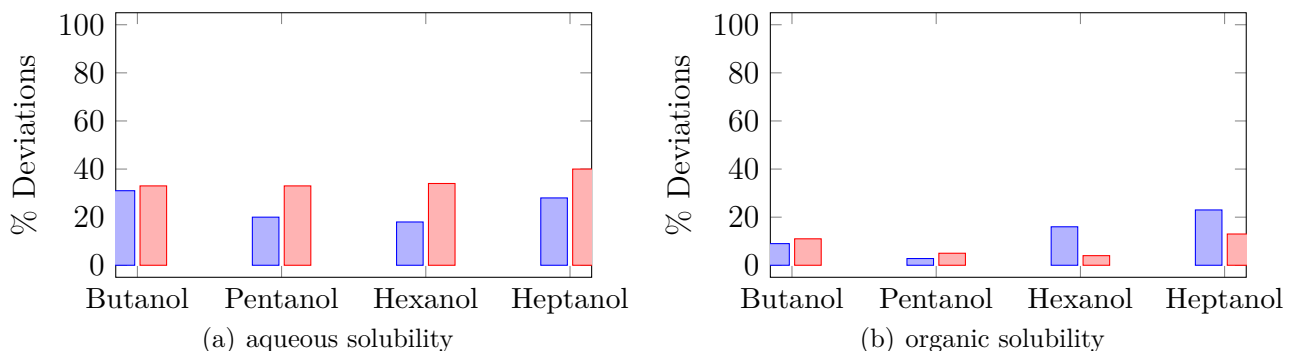


Figure 3.6: Deviations in aqueous and organic solubility of various water-alcohol mixtures from current model ■ in comparison to results from NguyenHuynh *et al.* [152] ■

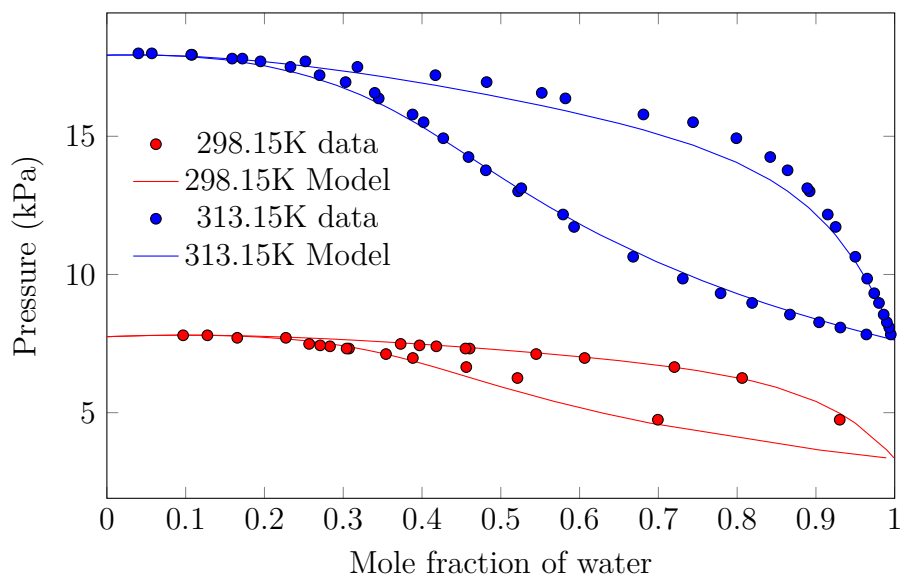


Figure 3.7: Water-Ethanol VLE at 2 different temperatures

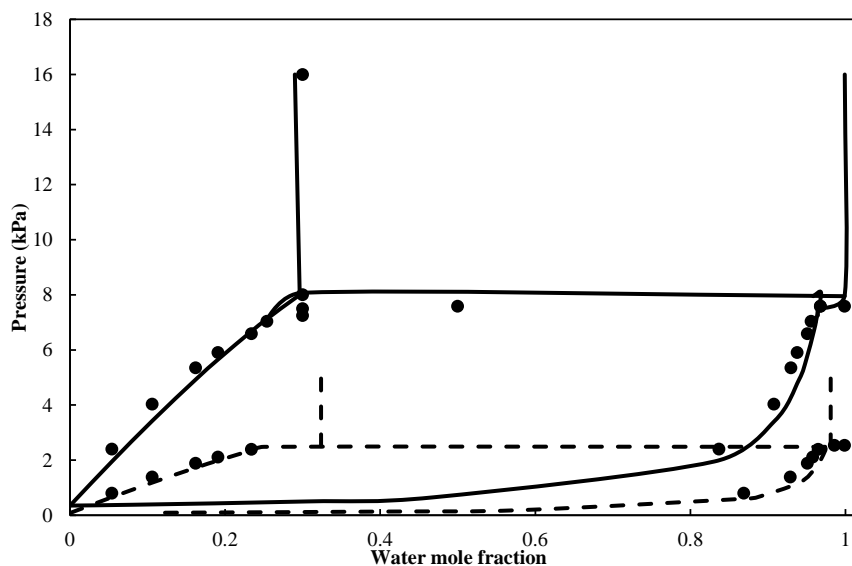


Figure 3.8: Water-hexanol vapor liquid equilibrium at 313.15K (solid line) and 294.15K (dashed line), lines are prediction from the new model and symbols are experimental data)

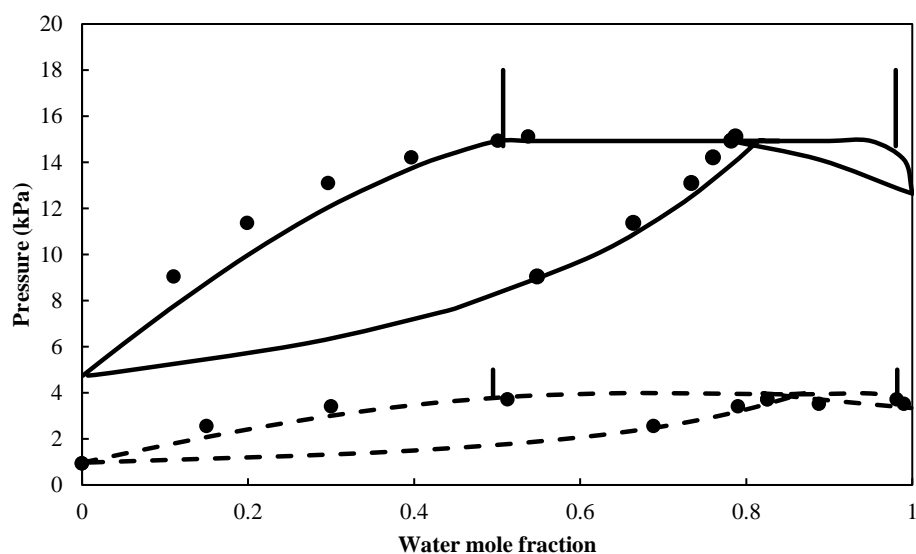


Figure 3.9: Water-butanol vapor liquid equilibrium at 323.15K (solid line) and 298.15K (dashed line), lines are prediction from the new model and symbols are experimental data)

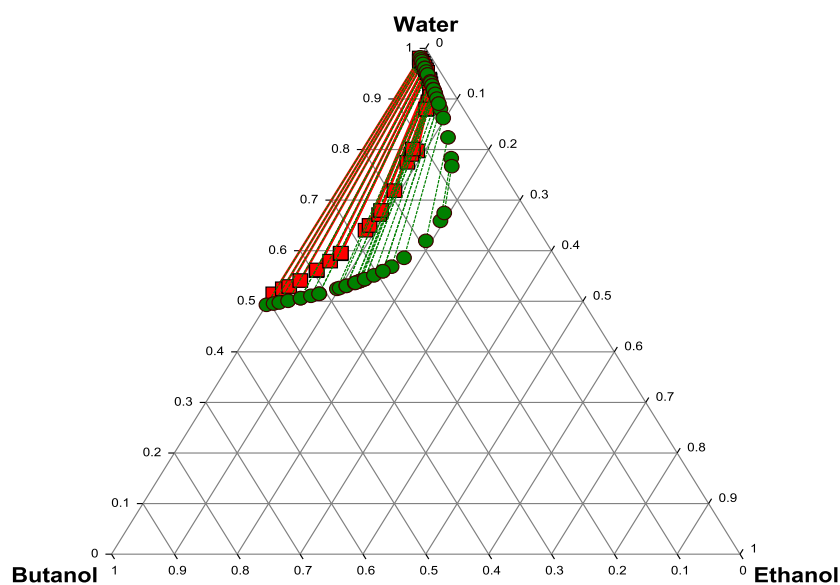


Figure 3.10: Butanol-ethanol-water liquid-liquid phase diagram at 298K, 1 bar as a comparison of model prediction with experimental data. Green circles represent the model and the red squares represent the experimental data [177]

3.4.1.4 Water - Aldehydes

Aldehydes are strongly polar molecules with a permanent dipole due to the carbon-oxygen double bond. Although aldehydes are non self-associating they have the capability of forming hydrogen bonds with water. The smaller aldehydes such as methanal and ethanal are completely miscible in water but solubility decreases with increase in chain length.

The results of regression (approach (a)) for several water-aldehyde systems are presented below in figure 3.11 and 3.12. Only the cross association parameter ε^{AB} , κ^{AB} and $l_{\alpha\beta}$ between water and the aldehyde carbonyl group (CHO) were required to be adjusted. The optimized values are $\varepsilon^{AB} = 1605.65$ and $\kappa^{AB} = 0.0586$ and $l_{\alpha\beta} = 0.03045$.

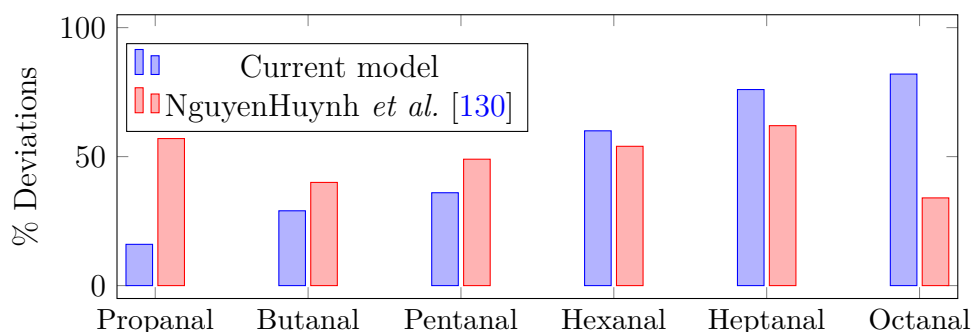


Figure 3.11: Deviations in aqueous solubility of various water-aldehyde mixtures from current model in comparison to results from NguyenHuynh *et al.* [130]

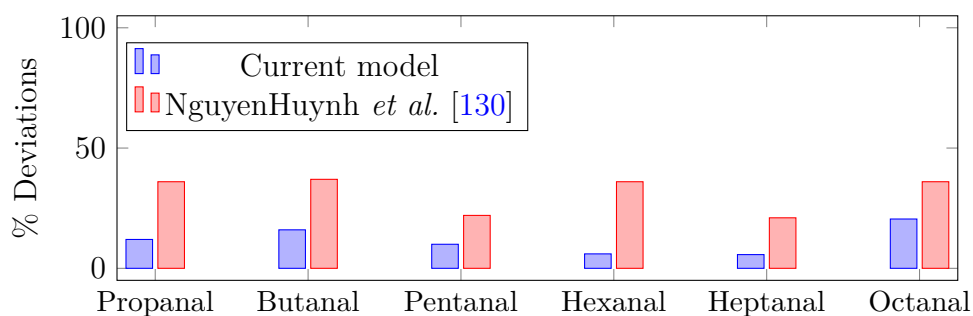


Figure 3.12: Deviations in organic solubility of various water-aldehydes mixtures from current model in comparison to results from NguyenHuynh *et al.* [130]

3.4.1.5 Water - Ketones

The simplest of the ketones, 2-propanone, is completely soluble in water. The solubility of ketones decreases with increasing chain length. Ketones are also strongly polar molecules and are capable of forming hydrogen bonds with water. The combination of strong

dispersive forces along with dipole-dipole attraction favors high solubility of ketones in water; however as chain length gets bulkier, the non-polar character increases and hence the solubility in water decreases.

After exhaustive analysis, it was observed that it was impossible to obtain satisfactory deviations of mutual solubilities by only adjusting cross association parameters between water and the ketone carbonyl group (CO) ε^{AB} and κ^{AB} . A first way to solve this problem is to regress for each ketone, a specific molecular binary interaction parameter k_{ij} (approach (b), see table 3.6) in addition to the cross-association parameters between groups ε^{AB} and κ^{AB} . For this approach, the optimized values for the cross-association parameters are $\varepsilon^{AB} = 1695.1$ and $\kappa^{AB} = 0.0368$. The drawback is that this approach is less predictive in nature because it is not possible to extrapolate the k_{ij} values to a system that is not investigated. Another approach to this problem is to include the non-additive hard sphere term developed by Trinh *et al.* [161]. This term involves a new adjustable parameter $l_{\alpha\beta}$ between water and ketone group, which is a correction for effective hard sphere diameter. With this approach, the regressed values of binary parameters between water and the ketone carbonyl group (CO) are $\varepsilon^{AB} = 1728.15$, $\kappa^{AB} = 0.03681$ and $l_{\alpha\beta} = 0.0850$. The advantage is that no more specific molecule-molecule interaction parameter is needed. The results of liquid-liquid equilibrium after incorporating this parameter are given in Figures 3.13 and 3.14. A comparison is made between this new approach versus the results obtained from previous work [130]. The deviations lie close to the previously reported deviations.

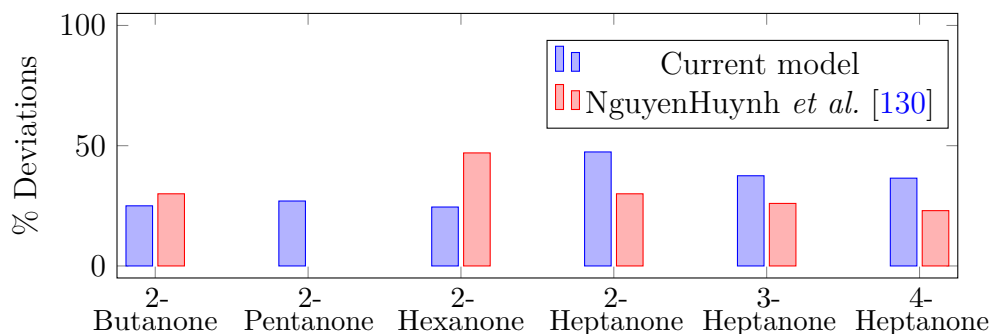


Figure 3.13: Deviations in aqueous solubility of various water-ketone mixtures from current model in comparison to results from NguyenHuynh *et al.* [130]

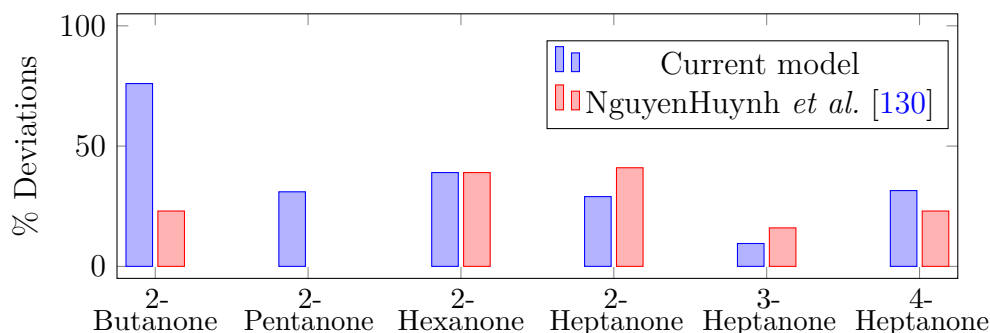


Figure 3.14: Deviations in organic solubility of various water-ketone mixtures from current model in comparison to results from NguyenHuynh *et al.* [130]

3.4.1.6 Water - Ethers

Ethers are mildly polar compounds and have the capability of forming hydrogen bonds with water but due to smaller electronegativity, the oxygen atom bearing two alkyl groups, their solubility is lower than that of alcohols but higher than alkanes. The solubility decreases with the increasing length of the hydrocarbon chain. In a similar way as for ketones, it was observed that by regressing only cross-association parameters ε^{AB} and κ^{AB} between water and the ether group -O- it was impossible to obtain correct results. As described for ketones, the first alternative is to adjust binary interaction parameter for each member of ether family. Although, adjusting binary interaction parameter k_{ij} (table 3.6) along with $\varepsilon^{AB} = 1637.68$ and $\kappa^{AB} = 0.03112$, yielded fairly good results but this approach remains non-predictive. Moreover, negative values of k_{ij} obtained remain unjustifiable. So for the purpose of predictive approach, a single $l_{\alpha\beta}$ parameter was fitted, where α stands for water and β stands for the ether group. The regressed values of the parameters are $\varepsilon^{AB} = 2275.9$, $\kappa^{AB} = 0.00406$ and $l_{\alpha\beta} = 0.10674$. A comparison is made between this last approach versus the results obtained from previous work [130] in figure 3.15 and 3.16. Some deviations are higher and some are lesser in comparison to the previous work, however, this can be a good trade-off when significant improvement in the deviation densities of water are achieved.

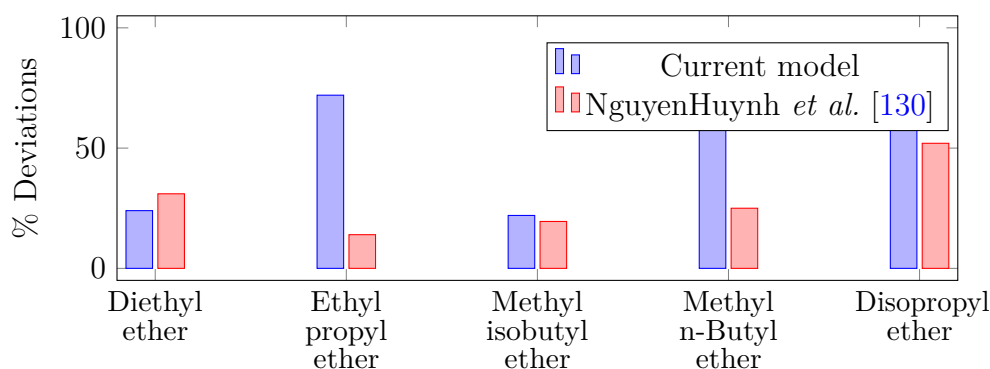


Figure 3.15: Deviations in aqueous solubility of various water-ether mixtures from current model in comparison to results from NguyenHuynh *et al.* [130]

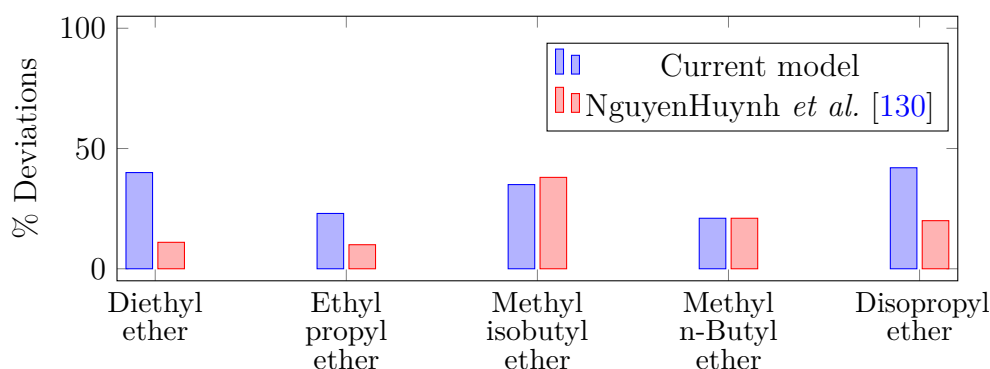


Figure 3.16: Deviations in organic solubility of various water-ether mixtures from current model in comparison to results from NguyenHuynh *et al.* [130]

3.4.1.7 Water - Esters

Esters are polar molecules and are capable of associating with water molecules although they do not self-associate. Low molecular mass esters are somewhat soluble in water and this solubility decreases drastically with increasing carbon atoms, borderline solubility occurs in esters containing three to five carbon atoms. Very low solubility of esters increases the deviation in predication when regressing only ε^{AB} and κ^{AB} . As the first alternative, the adjustment of an individual binary interaction parameters k_{ij} (table 3.6) for each member of the ester family along with cross association parameters $\varepsilon^{AB} = 1775.17$ $\kappa^{AB} = 0.03061$ (approach (b)). However, it is important to highlight that negative values of k_{ij} obtained are difficult to justify. Using approach (a) fairly good results can be obtained by incorporating $l_{\alpha\beta}$ parameter along with cross association parameters between water and the ester group. The value of these parameters are $\varepsilon^{AB} = 1577.05$, $\kappa^{AB} = 0.0630$ and $l_{\alpha\beta} = 0.04855$. In the previous work by Nguyen *et al.* [130] the average deviations

in the ester family were 70% for acetates and 30% for butyrate and propionates in the aqueous solubility. For organic solubility, these deviations were reported 25% for acetates and 20% for propionates and butyrates. The deviation of the current model, in general, didn't change sizable. However, improvements incorporating the non-additive term indicates that model is now capable of accounting for otherwise ignored perturbations while remaining predictive at the same time. A comparison is made between the approach (a) based only on group-group parameters versus the approach (b) based on regressing individual binary interaction parameter k_{ij} between each component, shown below in Figure 3.17 and 3.18 respectively.

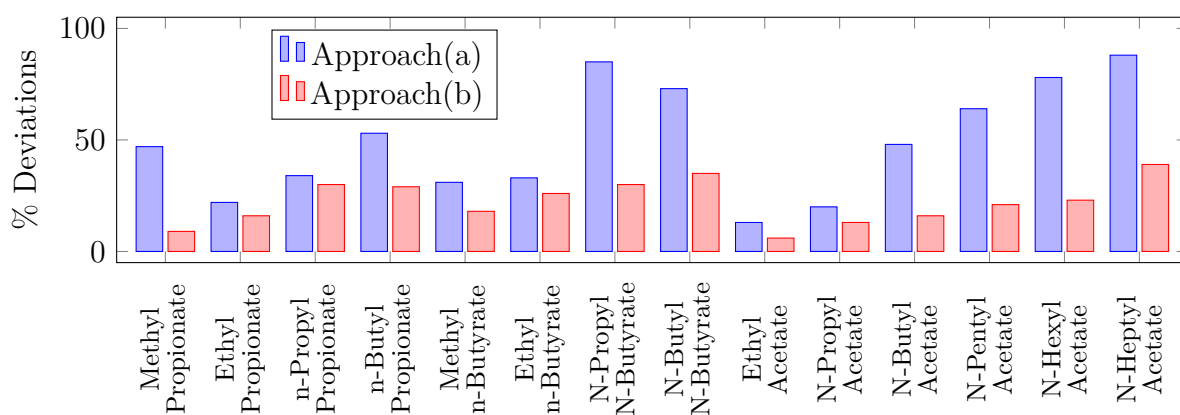


Figure 3.17: Deviations in aqueous and aqueous solubility of various water-ester mixtures from current model

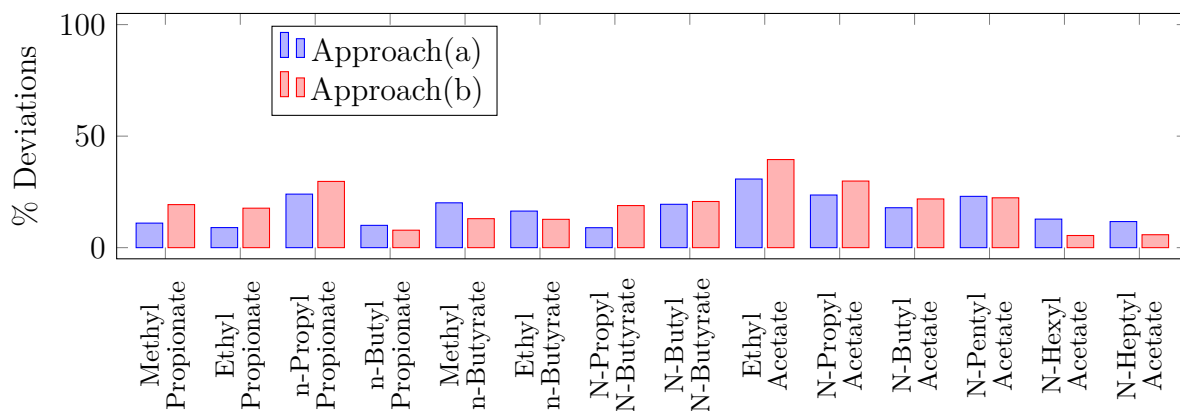


Figure 3.18: Deviations in aqueous and organic solubility of various water-ester mixtures from current model

3.4.2 Octanol/Water Partition coefficient

n-Octanol/water partition coefficients K_{OW} are interesting measurements of the solubility difference of a solute between water and an organic solvent. It is defined as:

$$K_{OW} = \frac{\gamma_i^{\infty,aq} v^{aq}}{\gamma_i^{\infty,oct} v^{oct}} \quad (3.4)$$

Where $\gamma_i^{\infty,S}$ stands for the activity coefficient of the infinitely diluted solute in the solvent S , and v^S the molar volume of the solvent S . The activity coefficient at infinite dilution is related to the fugacity coefficient given by our model by:

$$\gamma_i^{\infty} = \frac{\phi_i^{\infty}}{\phi_i^0} \quad (3.5)$$

Where $\phi_i^{\infty}, \phi_i^0$ are the fugacity coefficients of the solute at infinite dilution and of the pure solute, respectively.

Calculated K_{OW} (with the predictive approach (a)) for various families are presented in the Figure 3.19 along with the experimental values as a parity diagram. The values of various families show good coherence with experimental data.

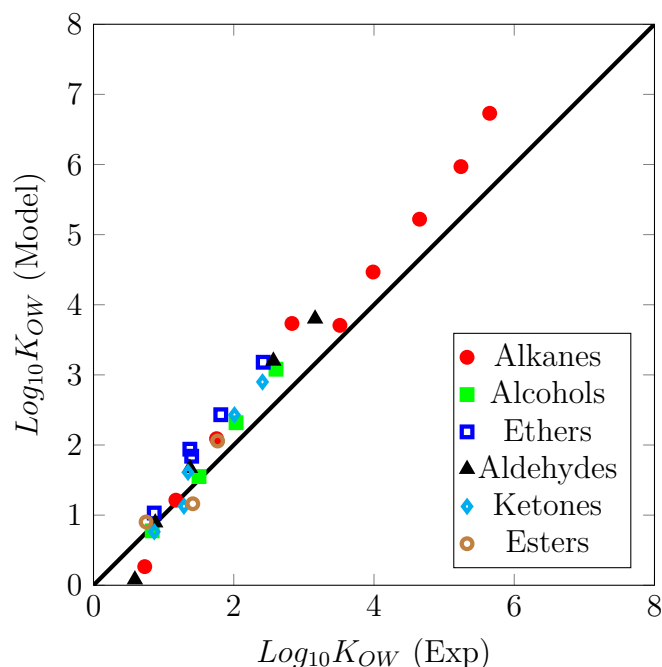


Figure 3.19: Octanol/water partition coefficient for alkanes, alcohols, aldehydes, ketones, ethers, and esters from our models compared to experimental data

The calculated values of oxygenated families such as alcohols, ketones, ethers, aldehydes remain close to the experimental values. Improvements are observed compared to the previous results of Nguyen *et al.* [130] as can be seen from table 3.7 and fig. 3.19.

Table 3.7: Average absolute deviation (%) in K_{OW} over whole hydrocarbon/oxygenate family as a comparison between Nguyen *et al.* [130] and our model

Family	AAD % in $\log K_{OW}$ (average over whole family)	
	Nguyen <i>et al.</i> [130]	<i>Our model</i>
n-alkanes	30.2	12.6
Alcohols	19.2	10.6
aldehydes	41.6	34.9
Ketones	31.4	19.5
Ethers	33.7	18.9
Esters	34.6	27.6

3.4.3 Gibbs energy of Hydrogen Bonding

The cross association parameters adjusted in the preceding sections for the various groups must be validated, to see if they have a physical significance rather than just being a corrective number. They should be in line (or close to) with the general associative behaviour exhibited by various hydrocarbon families. In order to do that the Gibbs energy of hydrogen bonding ΔG_{HB} between water and a solute is evaluated, using equation 3.6.

$$\Delta G = RT \ln \prod X_{A_i} \quad (3.6)$$

where $\prod X_{A_i}$ is the product of all non-bonded fractions at all sites of a solute. The values of ΔG_{HB} as a function of temperature are plotted on figure 3.20. In table 3.8 our results are compared at 298.15 K with the values proposed by Sedov *et al.* [178–181], which are based on a correlation involving experimental quantities such as Gibbs free energy of solvation. The values show that this model has a fair agreement with the experimentally obtained Gibbs energy of hydrogen bonding. This ΔG_{HB} conversely represents the strength of the hydrogen bond, which gives qualitative information regarding the associating capability for various families. The differences in the values of ΔG_{HB} are small hence it is difficult to quantitatively provide a clear order of hydrogen bonding strength as a function of the chemical family. However, the values conform to the qualitative behaviour and there is no departure from the general trend of association.

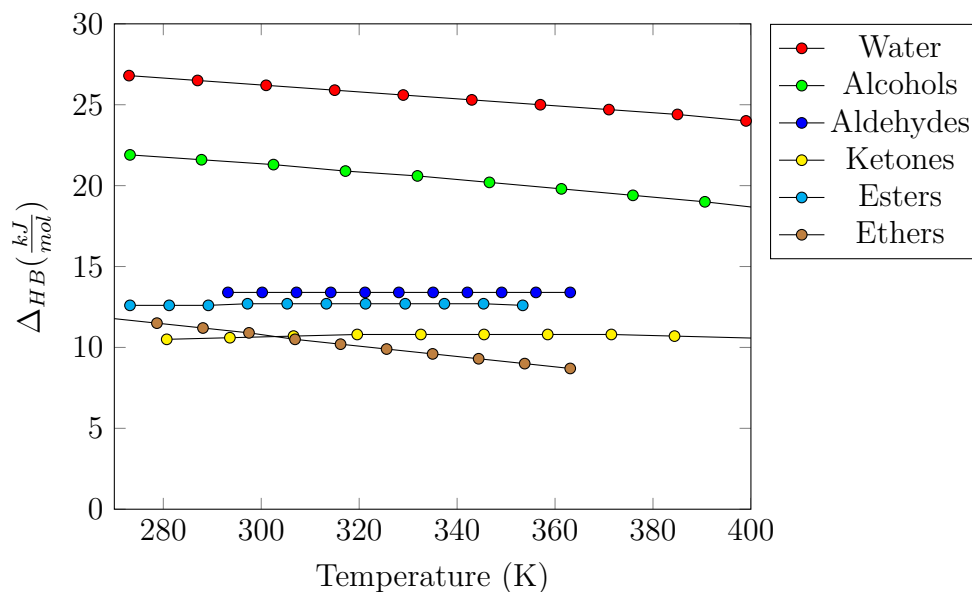


Figure 3.20: Gibbs energy of hydrogen bonding calculated with this model

Table 3.8: Comparison of Gibbs energy of hydrogen bonding between water and a solute at 298.15 K from this work (GC-PPC-SAFT model) and the experimentally-based methodology of Sedov *et al.* [178–181]

solute	$\Delta G_{HB}(\frac{kJ}{mol})$	
	Sedov <i>et al.</i> method	GC-PPC-SAFT (this work)
Water	-24.3	-26.7
2-Butanol	-17.9	-19.6
Diethyl ether	-11.2	-5.4
2-Butanone	-10.7	-5.3
Methyl propionate	-9.2	-6.3

It should be stressed that other authors tried to evaluate the quality of the hydrogen bonding using SAFT-type models, either using experimental hydrogen bonding energy data, non-bonded fraction [4, 182] or using molecular simulation data [183, 184]. Such an analysis is of the highest importance in order to validate the approach. Yet, an optimal representation of this phenomenon is not necessarily a guarantee of good quality phase equilibrium calculations. Hence, we use it here as a guideline rather than as a quality-indicator.

3.4.4 Conclusion

In the chapter, a modification for the temperature independent diameter in the GC-PPC SAFT equation of state was made for pure water. It was observed that the optimum σ -value of water depends on temperature: a correlation was then fitted on the optimized σ values. With this new approach, the GC-PPC-SAFT model accurately represented saturated liquid densities and vapour pressures of pure water (0.7% and 2.32% respectively over a wider range of temperature from 273.15 to 550 K). Deviation in liquid-liquid solubilities of water with alkanes, alkylbenzenes, alcohols, and aldehydes have been evaluated after adjusting cross association parameters between groups. Considering that the correction applies to group-group parameters, we can state that the new approach can now be used in a predictive way. However, for oxygenated mixtures such as water with ketones, ethers and esters, it was impossible to improve deviations without adding an additional improvement. A first way is to adjust individual binary interaction parameters k_{ij} between molecules. This leads naturally to better results, but the approach can be no more considered as predictive (it is impossible to predict mutual solubilities of another member of the same family). To rectify this, a non-additive hard sphere term was incorporated into the equation of state. This allows accounting for perturbations in hard sphere segment diameter using a group-group interaction parameter $l_{\alpha\beta}$. After including this term, deviations in solubilities reduced to a satisfactory range and can be used in a predictive way. A comparison between the group-group parameter approach versus the approach based on fitting k_{ij} for each component, showed that there was no large difference in deviations (less than 10% in most cases). The values of $l_{\alpha\beta}$ adjusted between groups were positive. This may indicate that cross hard sphere diameter is actually less than that was calculated previously. We speculate that this behaviour could be due to the associative nature of carbonyl groups which are strongly polar at the same time, hence there is further entanglement of molecules into one another and consequently the reduction of hard sphere diameter, which was earlier not accounted for in the model.

Chapter 4

Modeling of strong electrolytes

4.1	Abstract	70
4.2	Introduction	70
4.3	Some thoughts and arguments related to the choices made in this work	71
4.3.1	What is solvation?	71
4.3.2	Specificities related to the GC-ePPC-SAFT model	76
4.3.3	Parameters from previous work	77
4.4	Ion parameterization procedure	79
4.5	Regression Results	83
4.5.1	Correlation results for Alkali halide brines	83
4.5.2	Solvation Gibbs energies for Alkali halide brines	89
4.6	Alkanes and acid gases with brines: salting out effect in presence of organic compounds	90
4.7	Mixed solvent electrolytes	93
4.8	Conclusion	98

Modeling of mixed-solvent electrolyte systems

Fluid Phase Equilib., **2018**, 459, pp 138–157

DOI: [10.1016/j.fluid.2017.12.002](https://doi.org/10.1016/j.fluid.2017.12.002)

4.1 Abstract

Models for mixed-solvent strong electrolytes, using an equation of state (EoS) are reviewed in this work. Through the example of ePPC-SAFT (that includes a Born term and ionic association), the meaning and the effect of each contribution to the solvation energy and the mean ionic activity coefficient are investigated. The importance of the dielectric constant is critically reviewed, with a focus on the use of a salt-concentration dependent function. The parameterization is performed using two adjustable parameters for each ion: a minimum approach distance (σ_{MSA}) and an association energy (ε^{AB}). These two parameters are optimized by fitting experimental activity coefficient and liquid density data, for all alkali halide salts simultaneously, in the range 298K to 423K. The model is subsequently tested on a large number of available experimental data, including salting out of Methane/Ethane/ CO_2 / H_2S . In all cases, the deviations in bubble pressures were below 20% AADP. Predictions of vapor-liquid equilibrium of mixed solvent electrolyte systems containing methanol, ethanol are also made where deviations in bubble pressures were found to be below 10% (AADP).

4.2 Introduction

The biorefining industry involves the conversion of biomass or organic material into fuel grade bio-diesel or bio-gasoline. The pre-treated biomass (feeding bio-refinery units) is a complex mixture of oxygenated hydrocarbons and water, a strongly polar solvent which forms a non-ideal mixture with the oxygenated chemicals. Water is also responsible for the degradation of processing equipment and worsening of product quality, so it needs to be separated. Aqueous solutions of salts have shown a promising trend to aid in separation of these complex and oxygenated molecules encountered during the production processes of biofuel. The electrolyte causes a significant change in the equilibrium composition (especially liquid-liquid equilibrium), by altering the hydrogen bonding structure and other intermolecular forces. Hence, due to the addition of salt, the mutual solubilities change in either phase (aqueous phase and organic-rich phase). If the salt concentration is increased, this behaviour is called salting-out effect when the solubility

decreases, and salting-in effect when the solubility increases [185, 186]. This phenomenon is used in various industries (such as biorefining, pharmaceuticals or water treatment) for the separation of organic compounds. The use of electrolytes is however not limited to separation in process industry. They are often of interest in water treatment [29], geological, biological and petroleum industry [36, 187]. Thermodynamic information is vital for various industrial processes. More specifically, chemical engineers need to know the phase equilibrium between species and enthalpies to accurately design separation processes such as distillation column, extractive distillation, liquid-liquid extractions, etc. [5, 6, 36]. Due to a large number of species involved and varying operating conditions, accurate thermodynamic information is often missing, and leads to inefficient design both in terms of energy efficiency and product purity. In this context, the development of a predictive thermodynamic equation of state is of primary importance [6, 14–16, 36].

4.3 Some thoughts and arguments related to the choices made in this work

4.3.1 What is solvation?

The term solvation also called hydration in the case of water, is used with different meanings in the literature: either it means the phenomenon related to the forming of a specific structure around an ion or that of insertion of an ion from the ideal gas to the pure solvent. From the above discussion, it is clear that the second definition, which is better defined from a theoretical point of view, is, in fact, a combination of several elementary transformations: the discharge, the cavity formation (repulsive contribution), the charging process, and the structure-forming effect around water.

The Gibbs energy of hydration from the ideal gas is rather easy to compute using the equation of state (see also Schreckenber [\[123\]](#)):

$$\Delta G_{s,ion} = G_{s,ion}^{\infty} - G_{s,ion}^{ig}(T, V) = RT \ln \left(\varphi_{ion}^{\infty} \frac{P_s^{\sigma}}{RT \rho_{solvent}} \right) \quad (4.1)$$

where P_s^{σ} is the saturation vapor pressure. The values can then be compared to experimental values, as for example those given in ref [\[40\]](#).

In PC-SAFT, the final Helmholtz energy is the sum of various contribution such as, dispersion (attraction between molecule), hard-sphere (repulsion between molecules), chain (covalent bond energy between molecules), association (hydrogen bonding energy between two associating molecules) polar (interaction energy between polar molecules),

MSA (ion-ion long-range interactions), Born (so-called solvation energy). While calculating the fugacity coefficient as in equation 4.1 we use the net sum of all these interactions. A look at these individual terms shows the relative contribution of each phenomenon in the computation of the Gibbs energy of hydration:

$$\frac{\Delta G_{s,ion}}{RT} = \frac{\partial A^{res}(T,V)^{hc}}{\partial n_{ion}} + \frac{\partial A^{res}(T,V)^{dispersion}}{\partial n_{ion}} \quad (4.2)$$

$$+ \frac{\partial A^{res}(T,V)^{chain}}{\partial n_{ion}} + \frac{\partial A^{res}(T,V)^{assoc}}{\partial n_{ion}} \quad (4.3)$$

$$+ \frac{\partial A^{res}(T,V)^{polar}}{\partial n_{ion}} + \frac{\partial A^{res}(T,V)^{MSA}}{\partial n_{ion}} \quad (4.4)$$

$$+ \frac{\partial A^{res}(T,V)^{Born}}{\partial n_{ion}} - \ln \frac{P_s^\sigma}{RT \rho_{solvent}} \quad (4.5)$$

Figure 4.1 shows the numerical values for each of these terms at infinite dilution (the condition used for computing Gibbs energy of hydration). The value of $\frac{P_s^\sigma}{RT \rho_{solvent}}$ is provided by experiment (eg. 0.2334 at 298.15K). This term (Z in figure 4.1) is clearly insignificant for the Gibbs energy of solvation. The figure shows that the contribution of the Born term is the largest in absolute value (between 450 and 200 kJ/mol). The hard chain term reflects the contribution of cavity formation and the association the structure-forming of water molecules around the ions. The other contributions are absent or negligible in infinite dilution conditions. This validates the argument that Born contribution is essential for calculating Gibbs energy of solvation (ΔG_s) as already pointed out by [123, 124]. The calculations are made using the final parameters that are used in this work (set 1 below in table 4.6).

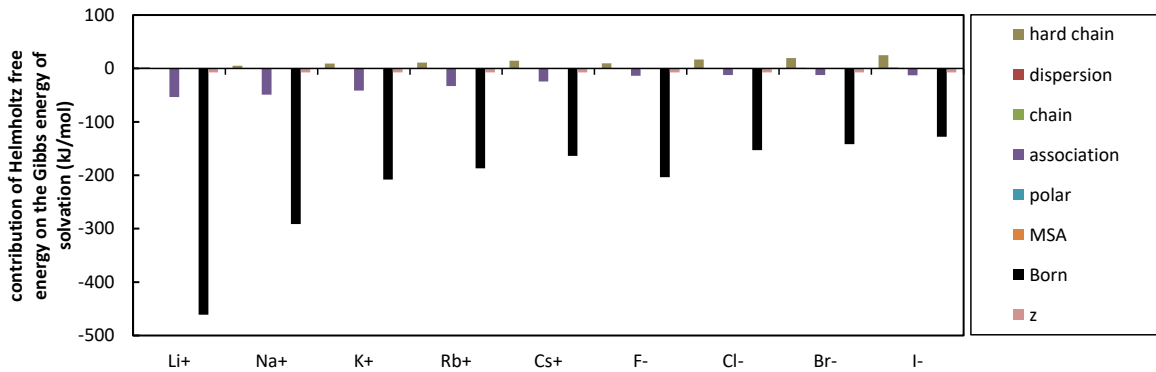


Figure 4.1: Contribution of Helmholtz free energy $\frac{\partial A^{res}}{\partial n_i}$ (Y-axis) for each term of PC-SAFT and for each ion at infinite dilution.

4.3.1.1 Should the dielectric constant be salt-composition dependent?

Both primitive MSA and the Born terms of the ePPC-SAFT model require the dielectric constant as an input. For pure compounds, the data for dielectric constant is abundantly available and hence several correlations exist [43, 188] as a function of temperature, solvent composition and density to compute their dielectric constant. In our work, we utilize the correlation proposed by Schreckenber [\[123\]](#).

Yet, it has been shown experimentally that the dielectric constant is affected by salt concentration [189, 190]. The dielectric constant of electrolyte mixture is obtained using an experimental method known as dielectric relaxation spectroscopy. This data includes the contribution of both frequency dependent complex and electric conductivities. The dielectric constant is then calculated by extrapolating the frequency dependent permittivity to zero frequency which includes effects only due to polarization [191]. While there is always some level of ambiguity associated with experimental dielectric constant due to the choice of the relaxation model, the bigger problem is due to the fact that the experimental dielectric constants contain both equilibrium and non-equilibrium contribution. The non-equilibrium contribution is what is known as kinetic depolarization. Only the equilibrium contributions are required in an electrolyte EoS. Hubbard and Onsager [192–194] discussed in detail these two contributions, the permittivity at zero frequencies ε_d (caused by dielectric saturation referred as equilibrium contributions) and the effect of kinetic depolarization $\Delta\varepsilon_d$ (non-equilibrium contribution). Kinetic depolarization is caused by the flow of the current while measurement and therefore it is not an equilibrium contribution [195].

$$\lim_{\omega \rightarrow 0} \varepsilon_d = \varepsilon_m = \varepsilon_r + \Delta\varepsilon_D \quad (4.6)$$

Most authors of industrial electrolyte models consider that the dielectric constant to be used in the MSA and Born term is independent of the salt concentration [36]. The reason for this is that the Born and MSA terms are developed in conditions of infinite dilution. They provide a corrective energy related to the charging of one ion or the ion-ion interactions. Yet, when considering the thermodynamic cycle that is presented above, it is clear that all steps bear on a system that has identical composition, temperature, and volume. Only the interactions between the species vary. Hence, when the charge is brought on the ions (charging Born term), or when the charge-charge ionic interactions are considered (MSA or DH term), the solution is not that of the infinite dilution reference state, but in terms of composition equal to that of the actual solution. This is why some [39, 70] suggest using the salt concentration-dependent dielectric constant. Recently,

Ignat and Shilov [190] used a concentration-dependent dielectric constant of several alkali halide salts to calculate their activity in an aqueous solution without any parameter adjustment which showed a semi-quantitative agreement to experimental data.

Another argument can be found in the fact that because applications generally deal with high salinities, the Born and MSA terms with infinite dilution as reference state are far beyond their application range. Hence, additional corrections would be needed anyhow. In fact, Maribo-Mogensen [189, 195] has shown that the use of such a dependency provides a non-negligible improvement on the behavior of the compositional derivative of the Helmholtz energy.

An interesting method for evaluating the effect of each term on the Mean Ionic Activity Coefficient (MIAC) (eqn. 4.16- 4.17) was provided by Inchekel *et al.* [70]. The ionic activity coefficient is defined as the ratio of fugacities in the mixture and in the reference state, generally pure water. The combination of equations 4.7 and 4.8 allow writing the mean ionic activity coefficient as follows:

$$\mu_i = \mu_i^{ref}(T, P, x) + RT \ln \varphi_i \quad (4.7)$$

$$RT \ln \varphi = \frac{\partial A^{res}(T, V)}{\partial n_i} - RT \ln(Z) \quad (4.8)$$

$$\begin{aligned} RT \ln(\gamma_{ion}) &= RT \ln\left(\frac{\varphi_{ion}}{\varphi_{ion}^*}\right) = RT \ln(\varphi_{ion}) - RT \ln(\varphi_{ion}^*) \quad (4.9) \\ &= \left(\sum \frac{\partial A^X}{\partial n_{ion}} - \sum \frac{\partial A^{*X}}{\partial n_{ion}}\right) - RT \ln\left(\frac{Z}{Z^*}\right) = \sum \left(\frac{\partial A^X}{\partial n_{ion}} - \frac{\partial A^{*X}}{\partial n_{ion}}\right) - RT \ln\left(\frac{Z}{Z^*}\right) \quad (4.10) \end{aligned}$$

Where X= all contribution from the EoS. It is then possible to plot the contribution of each of these terms to the global property. Figure 4.2 shows such a plot, with the ePPC-SAFT model discussed in section 2.5 (i.e. including a composition-dependent dielectric constant).

In the same way as already pointed out by Inchekel *et al.* [70], the figure shows clearly that the most significant contributions to the MIAC are the Born and the MSA term, which need to balance out in order to obtain the well-known curved behavior with a minimum close to 1 molal (see curve “sum”). The same plot could be shown with a model not taking into account the salt dependence of the dielectric constant. In this case, no significant change is expected from the non-electrolyte terms. The behavior of

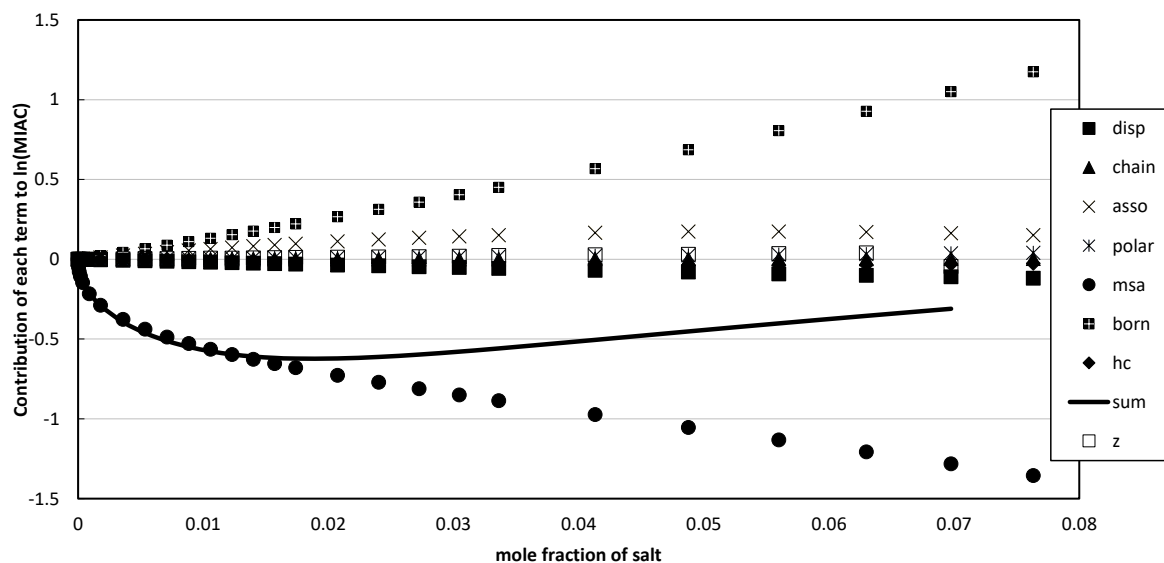


Figure 4.2: Effect of the various terms on the logarithm of the mean ionic activity coefficient (MIAC) for NaCl at 298.15K. The model used is that presented in section 3 along with the parameters presented in table 4.6

the MSA term is essentially identical, but the Born contribution would necessarily be zero. This is because:

$$\left(\frac{\partial A}{\partial n_i} - \frac{\partial A^*}{\partial n_i} \right)^{Born} = -\frac{N_A e^2}{4\pi\epsilon_0} \left[\frac{Z_i^2}{\sigma_i} \left(\frac{1}{\epsilon} - \frac{1}{\epsilon^*} \right) - \left(\sum_{j=ions} \frac{n_j Z_j^2}{\sigma_j} \right) \frac{1}{\epsilon^2} \left(\frac{\partial \epsilon}{\partial n_i} \right)_{V,T,n_i \neq i} \right] \quad (4.11)$$

where the dielectric constant, $\epsilon \neq \epsilon^*$ and its derivative with the mole fraction of ion is zero. As a consequence, another contribution should balance out with the large negative value of MSA (which is necessarily so because it doesn't contain any adjustable parameter). Most often, a large dispersive energy parameter (k_{ij}) is used such that the dispersive term is used for that purpose. Yet, an analysis of the physical significance of the above representation puts into question this choice: it can be considered that the ionic activity coefficient describes whether the ions “likes” being in salty water better than in pure water, or not. Indeed, the fugacity, or “escaping tendency” of the ion is proportional to the activity coefficient. When the activity coefficient is larger than 1 (positive logarithm), the ion prefers escaping from the salty water: it prefers pure water (the reference state). When, on the contrary, the activity coefficient is smaller than 1 (negative logarithm), the ions prefer to be in salty water.

Now, if we consider the terms individually, we see that the MSA term, which describes the long-range electrostatic interactions between ions, always has a negative contribution. This indicates that the corresponding potential makes the ions “like better” being surrounded by other ions: this is directly related to the decrease in screening length as discussed by Maribo-Mogensen [81]: the presence of other ions will tend to neutralize the strong local charge that is brought by the individual ion. Hence, the local electrostatic field strength will be reduced.

On the other hand, the observed positive contribution of the Born term can be explained by the fact that the presence of salts reduces the dielectric constant. The energy needed to charge an ion from the vacuum is directly related to this property: the larger the dielectric constant, the lower the energy needed (the dielectric continuum makes it more comfortable for the ions). Hence, from that point of view, the ions prefer being in pure water rather than in salty water.

The other terms have a much smaller impact on the “ionic happiness”. We see that the association (using our frame stating that association describes the forming of a hydration shell) tends to make that ions dislike salty water. This is because the water hydrogen bond network is disrupted as a consequence of their presence. The hard chain contribution is negative, because mixing spheres of different diameters creates entropy, thus increasing the stability of the mixture.

4.3.2 Specificities related to the GC-ePPC-SAFT model

The model used in this work is almost identical to that already discussed by Rozmus *et al.* [39]. Yet, since our objective was the treatment of mixed solvents, some modifications have been introduced.

4.3.2.1 The electrolyte terms

The terms that take into account the presence of charged species (MSA and Born) have not been modified [39]. Yet, the functional form of the dielectric constant is revisited, In the current work, the values of the dielectric constants for pure solvents are calculated using correlations eqn. 4.12 developed by Schreckenberg [123] table 4.1 and for mixtures the mixing rule is given in eqn. 4.13.

$$\varepsilon_s = 1 + \frac{\sum_i^n N}{V_{system}} d_v \left(\frac{d_T}{T} - 1 \right) \quad (4.12)$$

Table 4.1: Correlations for calculating dielectric constants of the pure solvent, regressed on experimental dielectric constant (273-423 K and densities upto 63 mol/dm³)

Component	Mol Wt.	$d_v(\frac{dm^3}{mol})$	$d_T(K)$	%AAD
Water	18.02	0.3777	1403.0	0.97
Methanol	32.05	0.5484	1011.0	0.86
Ethanol	46.07	0.9480	732.1	1.44

$$d_v = \frac{\sum_i^{solvents} n_i d_{v,i}}{\sum_i^{solvents} n_i} \quad \text{and} \quad d_T = \frac{\sum_i^{solvents} n_i d_{T,i}}{\sum_i^{solvents} n_i} \quad (4.13)$$

$$\varepsilon - 1 = (\varepsilon_s - 1) \frac{1 - \xi_3''}{1 + \xi_3''/2} \quad (4.14)$$

$$\xi_3'' = \frac{N_{Av}\pi}{6} \sum_i^{ions} \frac{n_i (\sigma_i^{HS})^3}{V} \quad (4.15)$$

In order to take into account the effect of ionic species on the dielectric constant, Pottel's [53] model is used: (eqn. 4.14 4.15).

where ε_s is the dielectric constant of the (mixed) solvent, σ_i^{HS} is the ionic diameter, V is the volume of the system.

4.3.3 Parameters from previous work

The parameters utilized in the current work are mentioned in tables (4.2-4.3). These parameters are taken from the previous work.

Table 4.2: Pure component parameters of water used in this work taken from our previous work [196].

Parameters	m	σ	T dep dia	ε/k	ε^{AB}	κ^{AB}	Association type	λ^*	J_i	μ_i	x_p
Unit and abbreviation	-	Å	-	Å	K	K	-	-	-	D	-
Parameters (current work)	1.02122	2.2423	0.51212	9904.13	201.747	1813	4C	0.203	13.65	1.85	0.276

** This parameter (softness of diameter) is fixed as 0.12 in original PC-SAFT model, however it is made adjustable in the present version of GC-PPC-SAFT.*

Table 4.3: Pure component parameters of alkanes and alcohols used in this taken from [152] work

Parameters	Segment number	Segment diameter	Dispersion energy	Association energy	Association volume	Association type ^b	Pseudo ionization energy	Dipole moment	Dipole fraction	Quadrupole moment	Quadrupole fraction
Unit and abbreviation	-	Å	K	K	-	-	eV	D	-	B	-
	m	σ	ε/k	ε^{AB}	κ^{AB}	-	J	d	x_p^d	Q	x_p^Q
Methanol	2.827	2.632	166.80	2069.09	0.2373	2B	15.55	1.7	0.35	-	-
Ethanol ^a	2.000	3.411	247.99	2143.30	0.00885	3B	15.85	1.83	0.5	-	-
Methane	1.033	3.658	147.41	-	-	-	12.61	-	-	-	-
Ethane	1.636	3.509	189.00	-	-	-	11.52	-	-	-	-
Carbon dioxide	1.846	2.984	139.97	449.71	0.0946	2B	13.78	-	-	4.3	0.5268
Hydrogen sulfide	1.302	3.416	225.05	449.71	0.0947	3B	-	-	-	-	-

^aEthanol is computed from group contribution as discussed in [130] ^bAccording to the nomenclature [197]

Table 4.4: Number of association sites (N_s) for ions in different electrolyte models

Ion	ePC-SAFT by Herzog et al. [74]	PREoS(Born) by Wu and Praunitz [94]	ePC-SAFT by Lee and Kim [198]	eSAFT-LJ by Z Liu. [199]	Number of association sites N_s			Molecular sim	Bockris et al. [201]	This work
					eEoS by Y Liu, et al. [200]	ePPC-SAFT mus et al. [39]	Roz-			
Water	2	-	4	4	4	4	-	5	7	
Li+	4	-	8	7	8	7	-	5	7	
Na+	4	6	8	7	8	7	5.64	4	7	
K+	3	-	8	7	8	7	-	3	7	
Rb+	8	-	8	8	-	7	-	3	7	
Cs+	2	-	-	10	-	7	-	4	7	
F-	0	-	-	-	-	6	-	1	6	
Cl-	0	7	7	9	6	6	6.98	1	6	
Br-	0	-	7	10	6	6	-	1	6	
I-	0	-	7	12	6	6	-	5	6	

4.4 Ion parameterization procedure

The model used in this work is almost identical to that already discussed by Rozmus *et al.* [39]. Although the results presented by Rozmus *et al.* [39] were of good accuracy, densities of alkali halides were not very well represented at low salinities. This is why the water parameters have been updated. Since the final aim of the current research is to construct an optimum model for the liquid-liquid equilibrium of electrolytes, it was necessary to have an optimal representation of the liquid densities of water. It has also been pointed by several authors that the underlying model for pure solvent must be accurate for calculating its liquid densities [123, 127]. It is thus important to re-parameterize the ions and see the performance of the new model for liquid densities.

The data used for the regression is presented in table 4.5. Mean Ionic Activity Coefficient (MIAC) equation 4.16 and solution densities (ρ) converted to Apparent Molar Volume (AMV) using equation 4.18 were used for parameterization. Their detailed description can be obtained from Rozmus *et al.* [39].

Mean Ionic Activity Coefficients (MIAC)

The mean ionic activity coefficient (MIAC) represented by γ_i is most commonly used to describe the electrolyte solution behaviour. It is calculated directly from the fugacity coefficient and is given as.

$$\gamma_{i,m} = \frac{\varphi_i(T, P, x_i)}{\varphi_i^\infty(T, P, x_i \rightarrow 0)} x_w \quad (4.16)$$

where φ_i represents the fugacity coefficient of the component i , φ_i^∞ represents the infinite dilution fugacity coefficient i , x_w represents the mole fraction of water and $\gamma_{i,m}$ is thus the activity coefficient of the component i in which 'm' stand for molal basis.

The Mean Ionic Activity Coefficient (MIAC) is given by:

$$\gamma_{\pm} = (\gamma_+^{v_+} \gamma_-^{v_-})^{1/(v_+ + v_-)} \quad (4.17)$$

where the subscripts + and - represents the cation and anion respectively. v_+ and v_- are the stoichiometric coefficients (on a full dissociation basis).

Apparent Molar Volume

The apparent molar volume (AMV) of ions is defined is given as:

$$v_{\pm} = \frac{v - x_w v_w}{(x_+ + x_-)} \quad (4.18)$$

Table 4.5: Apparent Molar Volumes (AMV), Mean Ionic Activity Coefficients (MIAC), and densities at 298 K, experimental Data, correlations, and calculations

Salt	Number of points and weight	Maximum molality	Deviation (%AAD) set #1	References			
	AMV MIAC	AMV	MIAC	AMV			
	W=0.2 for all	W=1.0 for all	MIAC	MIAC			
Lithium Halides							
LiF	17	-	0.03	7.6	-	[202]	[203]
LiCl	16	27	12.2	5	3.09	3.89	[204, 205]
LiBr	5	27	10	5	14.15	1.60	[206]
LiI	4	23	3.1	3	20.39	2.7	[207]
Sodium Halides							
NaF	24	16	0.93	1	9.85	5.85	[202]
NaCl	12	27	6.1	5	2.84	6.21	[208, 209]
NaBr	11	27	8	5	12.59	4.05	[206, 210, 211]
NaI	21	27	9.7	5	18.20	3.66	[212-214]
Potassium Halides							
KF	10	27	12.7	5	57.15	2.06	[215]
KCl	9	26	4.5	4.5	36.90	1.53	[215]
KBr	9	27	4.4	5	40.06	2.33	[216]
KI	11	26	8	4.5	40.89	1.93	[217]
Rubidium Halides							
RbF	12	24	11.7	3.5	34.77	4.42	[215]
RbCl	6	27	6	5	27.46	2.42	[218]
RbBr	7	27	4.5	5	31.66	3.10	[211]
RbI	-	27	-	5	-	4.52	[203]
Cesium Halides							
CsF	11	24	16.1	3.5	36.62	4.44	[215]
CsCl	16	27	10.6	5	24.26	7.55	[210, 215]
CsBr	13	27	4.1	5	29.73	7.20	[219]
CsI	13	23	2.3	3	32.35	5.67	[220]

where v and v_w are the molar volumes of the solution and of pure water respectively, and x_+ and x_- are the mole fractions of the cation and the anion. It is impossible to differentiate the contribution of separate ions and hence a representation of \pm is used to denote the overall AMV for the solution containing ions (anions and cations). The AMV is actually the change in the volume of the solution when salts are added into it and hence can be viewed as partial molar volume for electrolyte solutions.

The parameters that can possibly be worked on, are as following:

- The ionic diameter sigma (σ): there are in fact three: one in the hard sphere term, one in the MSA term and one in the Born term. Rozmus used a single diameter for all contributions of the SAFT EoS, equal to the Pauling diameters. However, it can be argued that the diameters to be used for the MSA term [221–223] are not the same as the hard sphere diameter to be used for the repulsive contribution. This is why in this work we kept the Pauling diameter for the hard sphere term but regressed the MSA diameter for each ion. In order to reduce the number of parameters per ion, the diameter of the Born term was taken equal to the Pauling diameter.
- The dispersive energy: while many authors use this parameter to describe the short-range interactions, we propose, as discussed above, to use the association term to describe these short-range interactions. Using both dispersive and association at once would yield too many parameters so that we follow Rozmus’s suggestion to consider the ionic dispersive energy to be zero.
- The Wertheim association requires two site-site interaction parameters (an energy, ε^{A_i} , and a volume, κ^{A_i} .) in addition to the choice of a number of association sites,

N_s . In the same way, as proposed by Rozmus, we consider the association volume equal to that of water =0.044394. The association energy is regressed individually for each ion. In literature, various authors have used different N_s , shown in table 4.4, the choice can vary widely between results from molecular dynamics calculations or experimental data (IR, spectroscopy).

The objective function used is as follows

$$OF = \sum_{j=1}^{N_{\gamma_{\pm}}} W_j \left(\frac{\gamma_{\pm,j}^{calc} - \gamma_{\pm,j}^{exp}}{\gamma_{\pm,j}^{exp}} \right)^2 + \sum_{j=1}^{N_{v_{\pm}}} W_j \left(\frac{v_{\pm,j}^{calc} - v_{\pm,j}^{exp}}{v_{\pm,j}^{calc}} \right)^2 \quad (4.19)$$

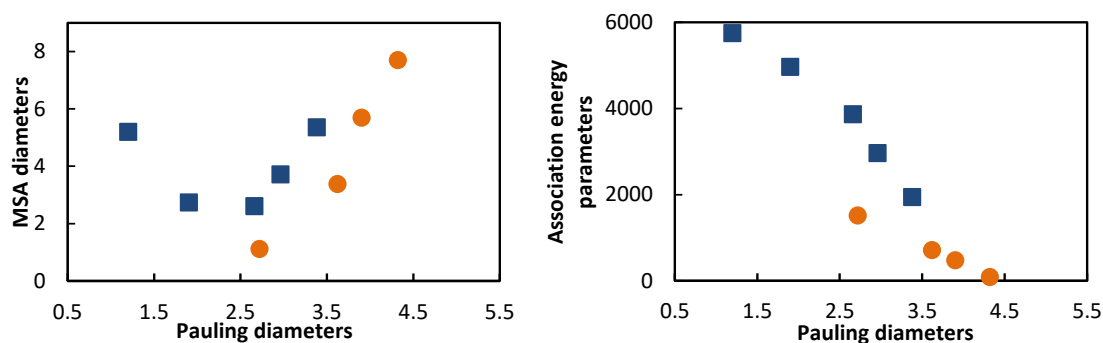
where W_j is the weight of the objective function used to select the impact of the dataset on which parameters are regressed. Their values can be found in table 4.5. The parameters σ_{MSA} and ε^{ass}/k for all ions were regressed simultaneously over MIAC and AMV of all alkali halide i.e. MX (where M is the metal ion, and X is halide ion, for eg. NaCl).

As shown in table 4.6, two sets of N_S are compared along with the final value of the ε^{A_i} and σ_{MSA} parameters. The values of N_S are smaller in set 2 as compared to set 1. In set 2 where N_S are taken from Bockris *et al.* [201], the final regressed values of ε^{A_i} were extremely high for certain ions. This is because the smaller the number of sites, the larger the energy must be to reach the same value for the association energy. In contrast, the final regressed values of ε^{A_i} in set 1 are within a reasonable range. This is clearly due to a smaller number of association sites on that ion. It can be concluded that the N_S values from Bockris *et al.* [68] cannot be used.

The final parameters used in the current work are those of set 1 in table 4.6.. The trends of the regressed diameter σ_{MSA} and association energy ε^{A_i} are shown in figure 4.3 as a comparison to Pauling diameters. It can be seen that cations and anions neatly follow a regular trend except for Li^+ . The reason for the high value of σ_{MSA} of Li^+ may be due to its small size and high charge density. The association energy ε^{A_i} of Li^+ is in decreasing order which is consistent with the decreasing charge density: the higher the charge density the higher strength of association between solvent and ion. This is an expected behavior according to work of Simonin *et al.* [224, 225]. It can be noticed that the MSA diameters optimized in this work are in good agreement with the MSA diameter values recommended in this prior publication.

Table 4.6: Final ion parameters sets, $\sigma_{HS}(\text{\AA})$ are fixed equal to Pauling diameter

Ion	Hard sphere di-	Set 1			Set 2 (Bockris <i>et al.</i> [201])		
	ameter	N_S	$\sigma_{MSA}(\text{\AA})$	$\varepsilon^{A_i}/k(K)$	N_S	$\sigma_{MSA}(\text{\AA})$	$\varepsilon^{A_i}/k(K)$
Li+	1.2	7	5.20577	5748.85	5	0.281969	23555.2
Na+	1.9	7	2.74386	4962.33	5	2.4962	4611.75
K+	2.66	7	2.61254	3869.23	4	12.398	4288.29
Rb+	2.96	7	3.72103	2967.68	3	14.4183	3806.5
Cs+	3.38	7	5.36451	1946.54	3	1.83048	3802.97
F-	2.72	6	1.12055	1516.2	4	-	-
Cl-	3.62	6	3.38508	712.074	1	1.85746	11234.5
Br-	3.9	6	5.6969	474.425	1	-	-
I-	4.32	6	7.70546	89.1208	1	-	-

**Figure 4.3:** Trend of regressed parameters in comparison to Pauling diameters. (a) MSA diameters vs Pauling diameters (b) association energy. Blue (cations), orange (anions)

4.5 Regression Results

4.5.1 Correlation results for Alkali halide brines

The regression results of MIAC and densities are presented in figure 4.4-4.6 and in table 4.5 (along with data used for regression and deviations from the model). The results of MIAC show a fairly good agreement with experimental data for 20 alkali halide salts at various temperatures. The average deviations for MIAC remain at 3.95% while it is 24% for AMV from set 1 using the current model. In contrast, the deviations observed in the work of Rozmus *et al.* [39] were 2.9% for MIAC and 30% for AMV. The mean deviations in MIAC are 1% larger than those from Rozmus *et al.* [39], however, that work did not take into account the AMV of fluorides which is difficult to correlate. Moreover, improvements in the current work are significant in correlating densities at low salinities

and infinite dilution condition which is essential for an improved mixed solvent electrolyte model [123, 127]. It can be seen that the densities of alkali halides conform fairly well at low salinities which is the capability of the model developed in our previous work [196]. The parameters for the ions that are finally used in the model are listed in table 4.6 (set 1). There are no additional parameters regressed for salt-water binary and only parameters regressed here are ion specific diameters and association energies.

Figure 4.4 is grouped according to common anions to see varying trends of salt molalities and densities. For salts of chlorides, bromides and iodides, the experimental data for MIAC and calculations from the model follow an increasing trend in the order $\text{Cs}^+ < \text{Rb}^+ < \text{K}^+ < \text{Na}^+ < \text{Li}^+$ at a given concentration and at the same temperature.

The reason for the reverse trend of MIAC in alkali fluoride solution is the "localized hydrolysis" as explained by Robinson and Harned: flour acts as a base capturing protonated thus releasing hydroxyls. Our model does not describe this chemical-equilibrium phenomena. Yet, we can try to understand the phenomena using the decomposition of the MIAC in its contributing terms which are represented in figure 4.5. This figure is drawn to see the effect of fluoride ion (for NaF), whereas figure 4.2 is drawn for NaCl. The various terms exhibit different behavior in this case: the association and hard chain terms replace the Born term in positive dominance. This is the result of various factors: the ϵ^{A_i} of F^- is bigger as compared to Cl^- ion resulting in a large association contribution. Hence, the trends for the Fluorides is for a large part driven by association. Physically, this is consistent with the explanation of the localized hydrolysis, corresponding to a strong interaction between F^- ion and water, which is related to the high charge density on fluoride ion. These interactions are correctly taken into account by the association term in the ePPC-SAFT model.

The calculation of AMV from the current model had an average AAD of 30% as compared to 24% by Rozmus *et al.* [39]. However in the work of Rozmus *et al.* AMV's of fluoride salts were not included in the regression owing to their very high deviations which could have resulted in an even higher average AAD. Likewise, the computed densities that are shown in figure 4.6 AMV of aqueous salt solutions at 298.15K have a very satisfactory behavior.

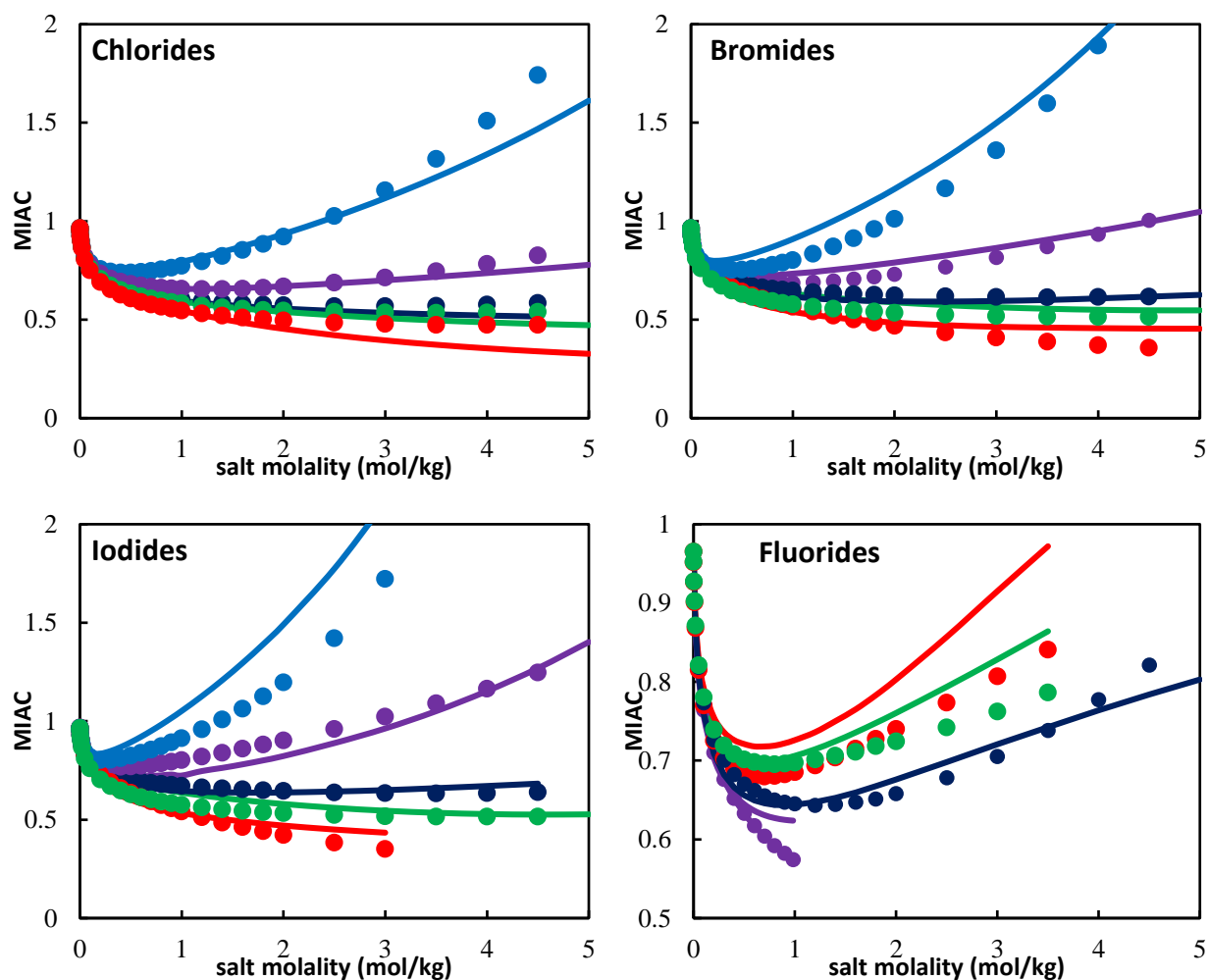


Figure 4.4: MIAC of aqueous salt solutions at 298.15K for alkali halides. The lines represent calculation from model and circles represent experimental data both in the order from top to bottom (LiX, NaX, KX, RbX, CSX) where X is the alkali halide ion except for fluorides where this order is reversed (no LiF salt not taken)

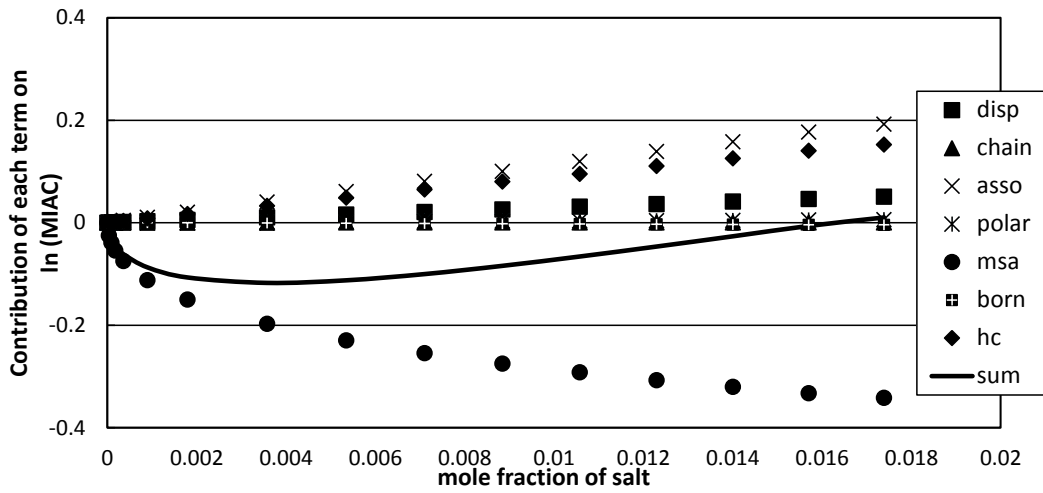


Figure 4.5: Effect of the various terms on the logarithm of the mean ionic activity coefficient (MIAC) for NaF salt

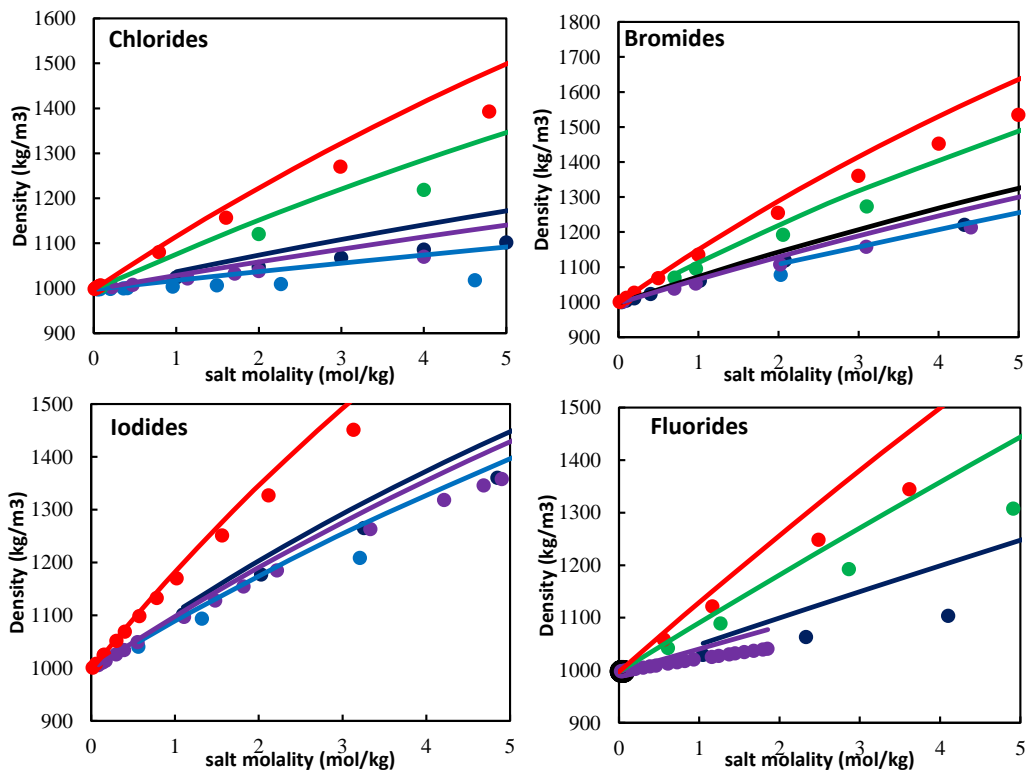


Figure 4.6: Densities (kg/m^3) (Y axis) of aqueous salt solutions at 298.15K for alkali halides. The lines represent calculation from model and circles represent experimental data both in the order from bottom to top (LiX, NaX, KX, RbX, CSX) where X is the alkali halide ion

Figure 4.7 shows the effect of the temperature on the MIAC: when temperature increases, the minimum becomes shallower and the curve levels off. It shows good results for NaCl and KCl. It is also seen that the experimentally observed trend of MIAC with respect to temperature for NaCl and KCl is reproduced.

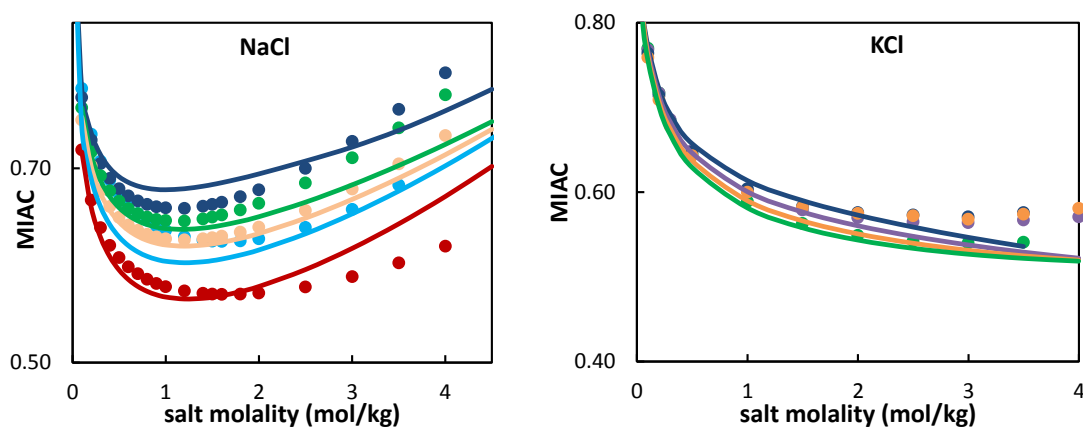


Figure 4.7: MIAC of salt aqueous solutions at various temperatures for (a) aq. NaCl (273.15K 323.15K 348.15K 373.15K 423.15K) top to bottom (b) aq. KCl (273.15K 291.15K 308.15K 323.15K) top to bottom. The lines represent calculation from model and circles represent experimental

The densities of the two salts NaCl and NaBr are also presented in the figure 4.8, a coherent trend is captured by the model that conforms fairly well to the experimental data. It may be observed that the slope of the experimental densities flattens at higher salt molalities, whereas the model does not capture this trend.

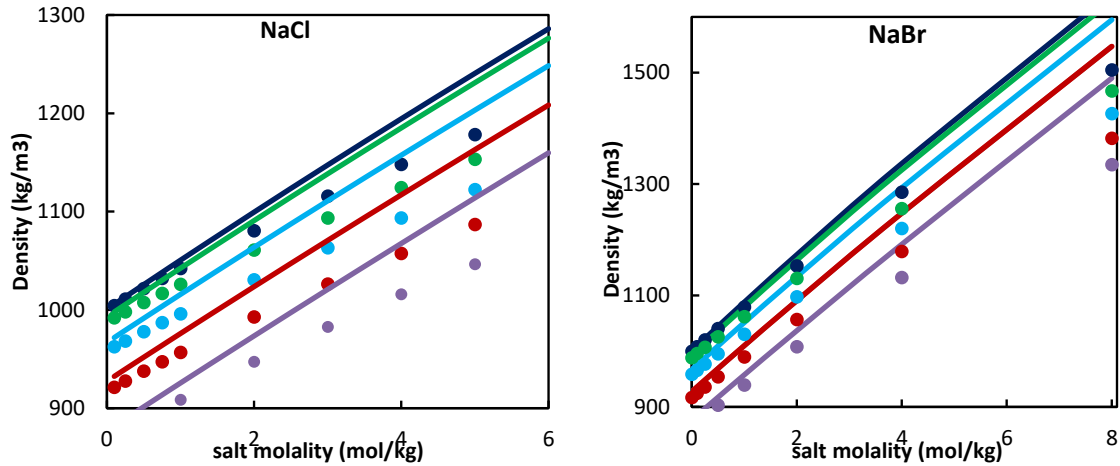


Figure 4.8: Liquid density(kg/m³) of salt aqueous solutions at various temperatures. The lines represent calculation from model and circles represent experimental.(273.15K 323.15K 373.15K 423.15K 473.15K)

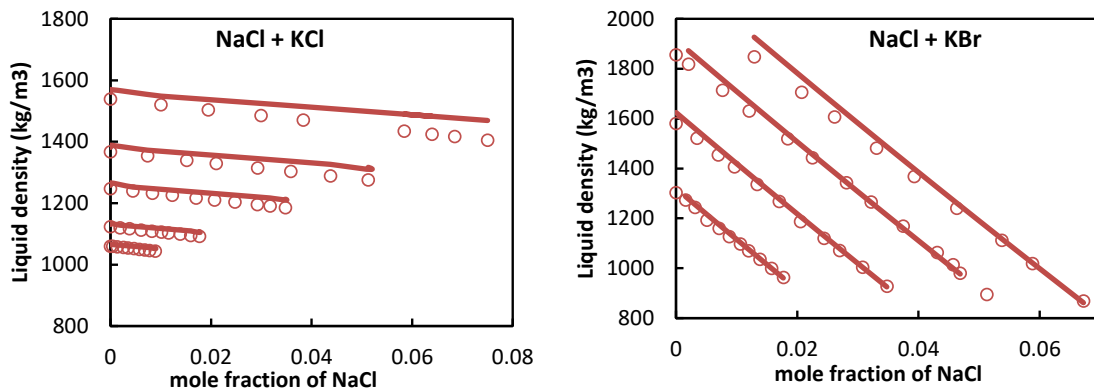


Figure 4.9: Liquid densities of aqueous (a) NaCl + KCl system and aqueous (b) NaCl + KBr system 298.15K and varying salt molalities. The figure is plotted against mole fraction of NaCl while each line is at fixed total salt concentration. Points are experimental data [226] and lines are prediction from model

In figure 4.9 multi salts (NaCl + KCl and NaCl + KBr) aqueous solution densities predictions are compared to the corresponding experimental liquid densities at 298.15K. It should be noted here the calculations are predictions from the model by using only ion specific parameters and no additional parameter was fitted for these systems. The model also correctly captures the variation in liquid density as a result of varying composition of two salts within the same system. The accuracy is rather good at low molalities (mol kg^{-1}) below 2. Above this salt concentration, the model steadily overestimates

the densities (which is in accordance with the observations of figure 4.6). The global deviation remains below around 3%.

In table 4.5, the absolute average deviation (AAD) for MIAC and AMV are summarized for all alkali halide salts at various temperatures along with the source of experimental data.

4.5.2 Solvation Gibbs energies for Alkali halide brines

The Gibbs energy of solvation discussed in section 2.3.1 is an interesting property to examine the capability of the electrolyte model to predict solvation effect and properties at infinite dilution. When ions are dissolved in water from the ideal gas, molecules of water arrange themselves around the ion which disrupts the existing hydrogen-bonded formation of water. The net change in the energy released during this process is equivalent to Gibbs energy of solvation. In table 4.7 we show that $\Delta G_{s,salt}$ predicted by the current model using parameters in table 4.6 (set 1). The $\Delta G_{s,salt}$ is defined as the sum of the ΔG_s of the cation and the anion (equation 4.20).

$$\Delta G_{s,salt} = \Delta G_{s,cation} + \Delta G_{s,anion} \quad (4.20)$$

where $\Delta G_{s,ion}$ is computed according to eqn. 4.2. The results are compared to result from Das *et al.* [127], Schreckenber *et al.* [123] and Galindo *et al.* [71]. The first work used a non-primitive model (treats solvent as molecules) while the latter two consider ions in a dielectric continuum. The results presented in table 4.7 show that the capability of the current model to describe the solvation is qualitatively good, however, the values as those obtained by Das *et al.* [127] are far better. This can be due to the fact that the current model uses only two ion specific parameters while Das *et al.* [127] used an additional water-salt binary parameter along with two other parameters per ion. As was shown in section 4.3.1, the largest contribution to the solvation energy is the Born term. The ionic diameter used in this term has obviously a large effect on the solvation Gibbs energy. Nevertheless, it was chosen to keep this diameter equal to the Pauling diameter so as to reduce the number of adjustable parameters.

Table 4.7: Gibbs energy of solvation $\Delta G_{s,salt}$ for alkali halides. Experimental data compared to calculation from the model (our model vs SAFT-VR+DE [127] vs SAFT-VRE [71] vs SAFT-VRE [123]).

Salt	Exp [221]	ePPC-SAFT (this work)		SAFT- VR+DE [127]		SAFT- VRE [71]		SAFT- VRE [123]	
		$\Delta G_{s,i}$ predicted	pre- dicted						
Lithium Halides									
LiF	-958	-1648.91						-1653	
LiCl	-833	-1523.42		-693		29		-1359	
LiBr	-807	-1496.19		-652		51		-1343	
LiI	-772	-1461.96		-596		65		-1299	
Sodium Halides									
NaF	-853	-1227.39		-712				-1341	
NaCl	-728	-1101.89		-653		-21		-1047	
NaBr	-702	-1074.66		-616		0.77		-1031	
NaI	-667	-1040.44		-568		11.61		-937	
Potassium Halides									
KF	-781	-1020.92		-685				-1227	
KCl	-656	-895.43		-630.		59		-933	
KBr	-630	-868.2		-593		81		-917	
KI	-595	-833.973		-548		94		-873	
Rubidium Halides									
RbF	-758	-968.612		-627		-		-1141	
RbCl	-633	-843.117		-579		-		-847	
RbBr	-607	-815.887		-547		-		-831	
RbI	-572	-781.66		-508		-		-787	
Cesium Halides									
CsF	-735	-910.975		-605		-		-	
CsCl	-610	-785.479		-556		-		-	
CsBr	-584	-758.249		-527		-		-	
CsI	-549	-724.023		-487		-		-	

4.6 Alkanes and acid gases with brines: salting out effect in presence of organic compounds

It is well known that the solubility of organic compounds in water decreases upon addition of salts. This is called the salting-out effect. It can be presented in the form of solubility curves (figure 4.10) or in table 4.8. The systems investigated here are water + salt + methane/ethane/CO₂/H₂S. The pure component parameter for methane, ethane, CO₂ and H₂S are listed in table 4.3. A binary parameter k_{ij} (for water-alkanes) and w_{ij} , u_{ij} (for CO₂/H₂S-alkanes) are regressed using the experimental data [227, 228] of the solubility of methane/ethane/light gases in water using the objective function given equation 4.21.

$$OF = \sum_{j=1}^{N_{P\sigma}} \left(\frac{P_{\sigma}^{calc} - P_{\sigma}^{exp}}{P_{\sigma}^{exp}} \right)^2 \quad (4.21)$$

Table 4.8 presents for each system studied the binary interaction parameters fitted and the average deviations obtained along with binary/ternary system parameters and experimental data.

When a salt like NaCl is added into the water + gas system, it decreases the solubility of the gas in water. This behavior is the so-called salting out phenomenon with the increase in salt concentration. This phenomenon is difficult to capture using electrolytes EoS [122]. The predictive capability of our model is not very accurate as it shows a systematic under-prediction of pressure. It was therefore found necessary to adjust an additional parameter between the ions and the gaseous solute. Since the ions have no dispersive energy, it is impossible to use a k_{ij} for this purpose. This is why the non-additive diameter contribution developed by Trinh and coworkers [161] was used. This correction describes the fact that the cross-diameter is different from the arithmetic average of the two pure component diameters. It was developed in the context of hydrogen dissolution in polar compounds, using the argument that due to the polarity, the shape of the hydrogen molecule would deform. It can be argued that the presence of ions is even more disturbing than a simple dipole moment for a neutral molecule. Hence, in the presence of an ionic charge, the polarizable molecule will be distorted in such a way that the arithmetic average of the diameters may need to be modified. This can be achieved using the l_{ij} binary interaction parameter.

By regressing the gas-ion l_{ij} parameters, the quality of the results is improved as shown in fig 4.10. This parameterization is performed on the ternary vapor liquid equilibrium data of several systems are given in table 4.8 along with average deviations, temperature range, and the experimental data used for regression. In order to have a transferable set of parameters for gas-ion pairs, the systems of a gas with all available salts are taken at once and all ion-gas parameters are regressed simultaneously. This gives gas-ion parameters that are not system specific and can be used when studying a system of salts having different ions.

The values of the regressed parameters l_{ij} between solvent-ion pair are not very large except for Li^+ which was fixed equal to 0.5 in order to avoid computational difficulties (which was approaching 1 during regression). Such a large value would indicate that the cross diameter of the methane and Li^+ pair is strongly reduced compared to the

arithmetic average. For remaining ions as can be seen in the table 4.8 the value of l_{ij} remains very small in absolute value. It is found to be generally positive for cations and negative for anions. The numerical values of the corrections show no clear trend, however, so that no predictive strategy could be identified.

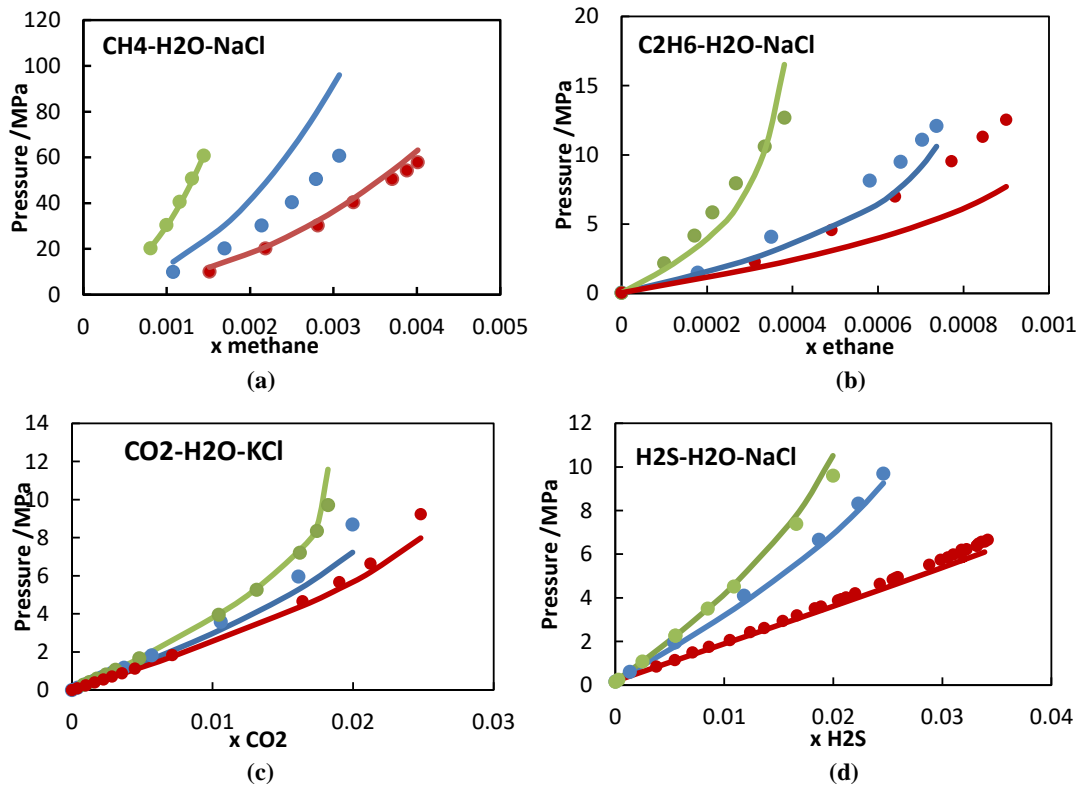


Figure 4.10: Solubility of alkanes and acid gases in water at two different salt concentrations red(0 molal) blue (1 molal) green (4 molal) for systems (a) CH₄-H₂O-NaCl system at 324 K (b) C₂H₆-H₂O-NaCl system at 353K (c) CO₂-H₂O-KCl system at 313K (d) H₂S-H₂O-NaCl system at 393K

Carbon dioxide CO₂ with brines has been investigated extensively due to the possibility of injection into saline aquifers principally for carbon capture and sequestration. Mineral rock containing salts dissolve in water and interact with CO₂. In Enhanced Oil Recovery (EOR) techniques, CO₂ is also viewed as a potential gas to pressurize the reservoir, where brines are naturally present. An increasing number of studies has been published both experimentally [229–231] and with the aid of thermodynamic models [39, 107, 232, 233] to provide an accurate representation of CO₂ brine phase equilibrium. In the current

work water + CO₂ + NaCl / KCl systems are studied (table 4.8) with our model, which gives a fairly accurate description of the phase behavior of this system.

A cross interaction parameter w_{ij} on the association energy between CO₂ and water was first fitted to obtain accurate results on salt-free system (table 4.8). Adding ionic species, because these contain association sites as well as CO₂, associative bonds will be created between them, according to the combining rules (2.50-2.51). Adjusting the cross-association parameters between CO₂ and ions did not improve the results so it was decided to work on the l_{ij} cross interaction parameter, in the same way as for alkanes (data reference and results are shown in table 4.8). It can be observed that the salting out effect can be seen with increasing concentration of salt both by the model and experimental data (figure 4.10). The results are shown at 313K. A change in slope in the bubble pressure is observed for 4.0 molal salt at 323.15K due to a shift from the vapor-liquid to the liquid-liquid region.

Another system studied in the current work is H₂S with brine at 393.15K (figure 4.10 (d)). Similar to other systems a non-additive l_{ij} binary interaction parameter between H₂S and each ion was fitted on experimental saturation pressures of salted system. The current model is able to give a fairly accurate description of the system as compared to experimental data.

4.7 Mixed solvent electrolytes

Since we have seen that the model is able to describe the salting-out phenomena in alkane or acid gas + brine systems, it can now be used to study vapor-liquid equilibrium of various mixed solvent salt systems. Pure water and several pure solvents such as methanol/ethanol/1-propanol have been already parameterized in a previous work [196] and parameters are recalled in table 4.3. Binary mixture of methanol-water were parameterized using cross interaction parameters (w_{ij} , u_{ij} and l_{ij}), here three parameters were chosen to have better accuracy in description binary of phase equilibrium (without fitting l_{ij} , deviations were close to 10% in AADP and AADY, compared to 1.8% when including this additional correction).

Several mixed solvent systems have also been studied previously by many authors [87, 114, 123, 127, 241, 242]. However, most of them rely on fitting an additional solvent-salt/ion dispersion parameter. In this work, the results are purely predictive in nature since all parameters have been determined previously.

Table 4.8: Table for AAD, binary and ternary system parameter for alkane/acid gases-water-salt systems

System	parameters	N_P	T(K) range	Average AAD (%)	Experimental data
Methane + water +	$k_{ij} = -0.027827$	94	298.15-373.15		[234]
NaCl	l_{ij} (CH ₄ -ion)	46	313, 353, 373	19.74 AADP	[235, 236]
KCl	Li ⁺ :0.5	94	313, 353	18.79 AADP	[206]
LiCl	Na ⁺ :0.1909	45	313, 353	19.03 AADP	[206]
LiBr	K ⁺ :0.00663	51	313, 353	17.08 AADP	[206]
KBr	Cl ⁻ :0.06123 Br ⁻ :0.01521	35	313, 353	16.21 AADP	[206]
Ethane + water+	$k_{ij} = -0.002845$	50	298.15-423.15	34 AADP	[237, 238]
NaCl	l_{ij} (C ₂ H ₆ -ion) Na ⁺ : 0.629 K ⁺ : 0.4790 Cl ⁻ : -0.48735	14	353	17.35 AADP	[236]
KCl		14	353	10.06AADP	[236]
H ₂ S + water +	$w_{ij} = 0.1856$	325	283-453	6.4 AADP	[239]
NaCl	l_{ij} (H ₂ S-ion) Na ⁺ : 0.00618 Cl ⁻ : -0.0964	17	393	5.8 AADP	[240]
CO ₂ + water +	$w_{ij} = 0.127$	68	298.15-353.15	14.7 AADP	[236]
NaCl	l_{ij} (CO ₂ -ion) Na ⁺ :0.0985 K ⁺ : 0.0541 Cl ⁻ : -0.2524	70	313, 353	7.07 AADP	[116]
KCl		96	313, 353	10.34 AADP	[116]

As seen in figure 4.11, the predictions from the model agree fairly well to experimental data. It is also seen that there is a systematic under-prediction of bubble temperatures at the composition of alcohols between 0.2 and 0.4 this is due to the effect of salt on the vapor-liquid equilibria of mixed solvent systems [243, 244]. Figure 4.11-4.12 show the results with mixed solvent (methanol/ethanol) salt systems. The salt molality is however rather small because the solubility in methanol is small [119]. The blue line indicates salt-free system and is evident in the figure that due to the addition of salt the phase envelop starts to change specially the bubble point is due to the emergence of separated liquid phase because of salting out effect. This trend can be seen in all the methanol-water-salt systems in figure 4.11. The similar trend is also observed in ethanol-water-salt systems in figure 4.12, where the over-estimation of the bubble curve by the model becomes here more visible.

In table 4.9 the vapor-liquid equilibrium of several alcohol-water-salt systems is presented, along with the average deviations, temperature range and the source of experimental data. For the most system, the deviations lie, in pressure below 1% and composition below 10%.

A quaternary system of CO₂-water-methanol-NaCl is also tested predictively [245]. The vapor-liquid equilibrium is predicted by the model by utilizing only binary parameters between methanol-water, CO₂-water and CO₂-ions. The average deviations in vapor pressure were 14.5% AADP, this indicated that model can predictively estimate VLE of quaternary systems with satisfactory accuracy.

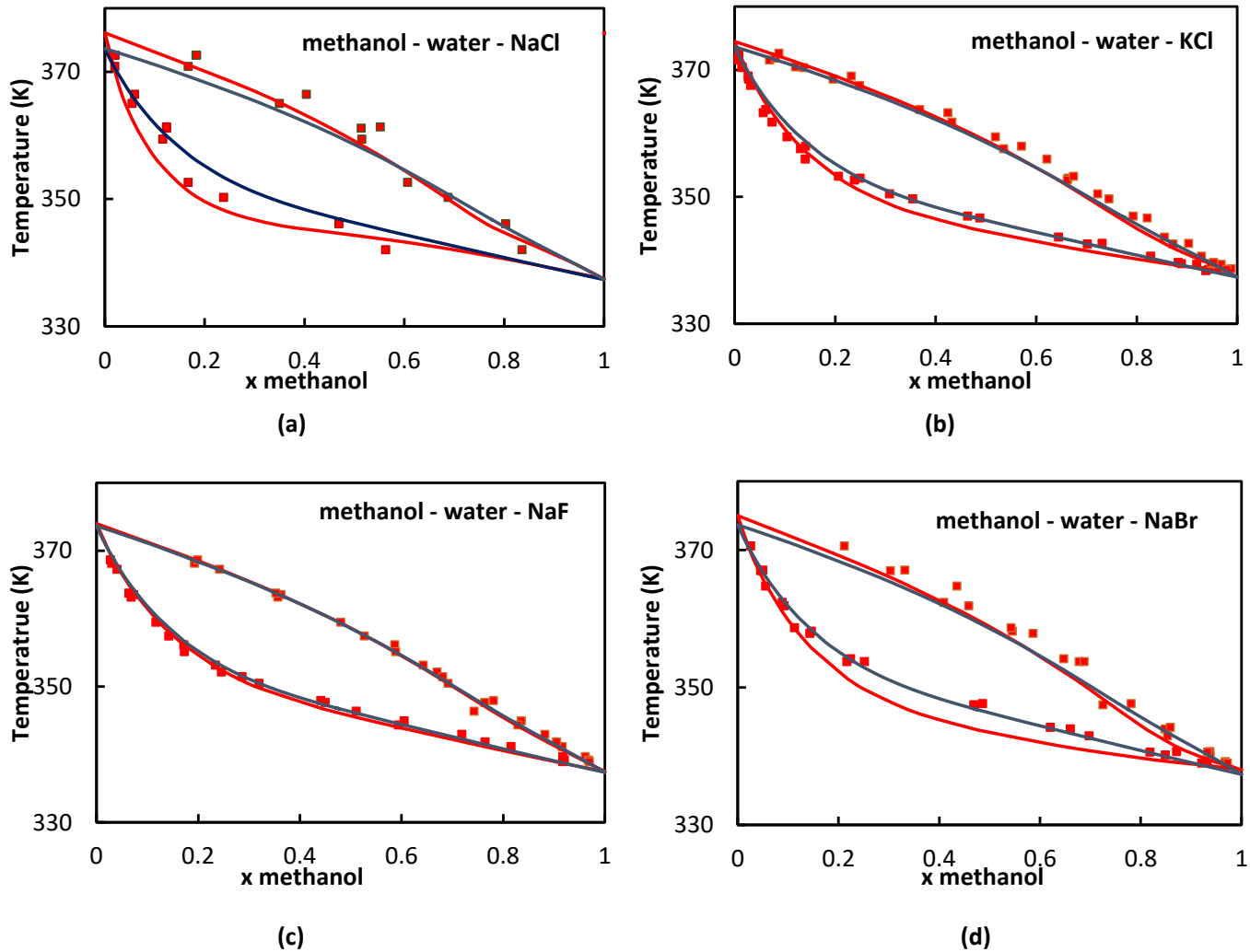


Figure 4.11: Isobaric Vapor-liquid equilibrium of Methanol-Water-salt system at 1 bar. Lines are prediction from model and point are experimental data. (a) water-methanol-NaCl system at varying salt molalities (upto 2.56 molal) (blue line indicates salt-free systems (water-methanol) (b) water-methanol-KCl system at varying salt molalities (0.1-2 molal) in experimental data the model prediction at 2 molal concentration of salt to obtain a smooth curve at uniform salt concentration. (c) water-methanol-NaF system at varying salt molalities(0.2-0.5) in experimental data but model prediction at 0.5 molal concentration of salt to obtain a smooth curve at uniform salt concentration. (d) water-methanol-NaBr system at varying salt molalities(0.01-3.5 molal) in experimental data but model prediction at 2.0 molal concentration of salt to obtain a smooth curve at uniform salt concentration

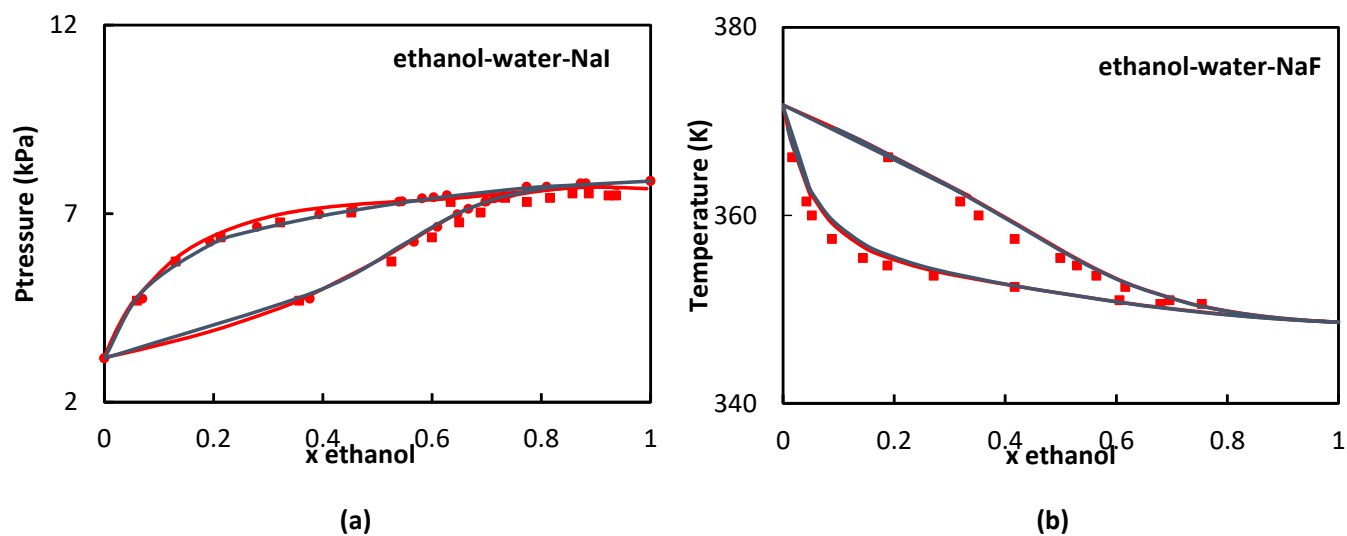


Figure 4.12: Isothermal Vapor-liquid equilibrium of Ethanol-Water-NaI system at 298.15K. Lines are prediction from model at 0.5 molal and point are experimental data at varying molalities (upto 1.35) (blue line indicates no salt systems (water-ethanol) (b) water-ethanol-NaF system at varying salt molalities (up to 0.82) at 1 bar

Table 4.9: Table for AAD, binary system parameter for VLE of alcohol-water-salt systems

System	Parameter (water-alcohol)	N_P	T(K) range	Average AAD (%)	Experimental data
Methanol + water +	$w_{ij}=0.0352$ $u_{ij}=0.0025$ $l_{ij}=0.0178$	58	298.15-403.15	1.83 AADP 1.71 AADY	[246]
LiCl	-	12	333.15	0.76 AADT 4.54 AADY	[247]
NaF	-	25	338.95-368.65	0.20 AADT 3.33 AADY	[117, 243]
NaCl	-	11	342.05-372.65	0.81 AADT 2.34 AADY	[117, 243]
NaBr	-	20	338.95-370.55	0.28 AADT 3.47 AADY	[248]
KCl	-	31	338.35-372.65	0.29 AADP 7.59 AADP	[117, 243]
Ethanol + water +	$w_{ij}=0.11628$ (water-OH group) $u_{ij}=-0.9978$ (water-OH group)	50	298.15-423.15	2.12 AADP 3.83 AADY	[249]
NaF	-	10	350.55-366.15	0.34 AADT 6.07 AADY	[243]
NaBr	-	23	351.46-356.45	0.26 AADT 3.19 AADY	[243]
KCl	-	12	352.2-354	0.41 AADT 4.22 AADY	[243]
KI	-	20	351.99-356.39	0.30 AADT 4.8 AADY	[243]
CO ₂ + Methanol + Water +	Only binary parameters and CO ₂ -ion l_{ij}	33	313.6-395.2	14.5AADP	[245]

4.8 Conclusion

This work addresses several issues related to the modeling of mixed solvent electrolytes. In a first part, the methodology of the construction of a SAFT-based electrolyte equation of state is discussed. More specifically, we investigate the meaning of solvation properties and propose using both ionic association and Born term to explain the physical phenomena occurring when bringing an ion from the ideal gas to the pure solvent. We also discuss the role of the dielectric constant and the effect of its functional form on the mean ionic activity coefficient. We conclude with the observation that a salinity dependent dielectric constant is a better choice for describing the individual contributing energies that come into the calculation of the MIAC.

Using the proposed analysis, the ePPC-SAFT electrolyte model initially proposed by Rozmus *et al.* [39] is further refined, using improved water parameters and a dielectric constant that allows working with mixed solvents. Two ion-specific parameters are fitted on activity coefficients and densities of various alkali halides.

In a final step, the model is evaluated on a larger set of VLE and density data with good success. These data include mixed salts and mixed solvent solutions. In some cases, additional binary interaction parameters had to be adjusted. For this, since the ions are considered to have negligible dispersive interactions, the algebraic average of the hard-sphere diameters was corrected using the approach proposed by Trinh *et al.* [161], with an additional adjustable parameter l_{ij} . The alcohol-water-salt systems was subsequently modeled fairly accurately in a fully predictive way (without any parameter adjustment between alcohol and ions).

Thus, it can be concluded with reasonable certainty that the current model can be used to predict and calculate VLE of mixed-solvent electrolyte systems using solvent-water binary parameters and ion-specific parameters with a reasonable accuracy.

Chapter 5

Modeling LLE of mixed-solvent electrolytes

5.1	Introduction	102
5.2	Algorithmic issue: Electroneutrality	103
5.2.1	Generalities	103
5.2.2	Current state: without electroneutrality	104
5.2.3	A new method for electroneutrality: Modifying the fugacity coefficient	104
5.3	The machinery	109
5.3.1	Prediction of the LLE by the non-parameterized model	109
5.3.2	Partition coefficient of salts	111
5.4	Parameterizing mixed solvent salt systems using available data	117
5.4.1	Dielectric constant of mixed-solvents	118
5.4.2	MIAC of mixed solvent electrolyte systems: Analysis	121
5.4.3	Approach for parameterization of mixed-solvent salt systems	122
5.4.4	Result of MIAC for mixed solvent electrolytes	126
5.4.5	Parameter for 1-Butanol-water-salt systems from LLE data	132
5.5	Final results	133
5.6	Conclusion	138

5.1 Introduction

In chapter 4, we discussed the formulation of an electrolyte thermodynamic model adapted to mixed-solvents (chapter 3). This chapter is written so as to present the results of the final objective of this research, the modeling of liquid-liquid-equilibrium for multi-solvent electrolytes (solvent-water-ions). The challenge here is that the partitioning of all compounds including ions, needs to be described. This is in contrast to the vapor-liquid equilibrium where ions are not considered in the vapor phase (a high positive value of the fugacity coefficient for ions were assigned in the vapor phase). This objective is one of the outcomes of this thesis. We believe that our electrolyte thermodynamic model is fully prepared for modeling liquid-liquid phase equilibrium of various mixed solvent salt systems.

This chapter investigates the following issues:

- Algorithmic issue related to electroneutrality: The algorithm is developed for neutral species and until now, only vapor-liquid phase equilibrium of mixed solvents were investigated (chapter 4). As ions do not migrate into the vapor phase, this constraint was not an issue. But, when dealing with a liquid-liquid phase split, ions can migrate independently from one phase to another and it is important to ensure that the bulk liquid phases remain electrically neutral. A new method to take into account this electroneutrality constraint in our model is presented in section 5.2.
- The analysis of LLE of mixed solvent salt system in terms of partitioning of species in the two phases is presented in section 5.3. This section develops an understanding of the various interactions that play a dominant role in the partitioning of salt species. It helps identifying the parameters that need to be adjusted for improving the model.
- Due to high thermodynamic non-ideality in these systems, tuning of solvent-ion parameters are required. The data and the procedure used are discussed in section 5.4. Several types of data are evaluated such as dielectric constants, Mean Ionic Activity Coefficients (MIAC) and Liquid-Liquid Equilibria (LLE).
- In the last section, the selected parameters are used on all available systems.

5.2 Algorithmic issue: Electroneutrality

5.2.1 Generalities

The computation of phase equilibria requires setting all chemical potentials, or fugacities equal in all phases. Many textbooks propose details of the algorithm that must be applied, to that end, the best known of which is Michelsen and Mollerup [43]. We describe a simplified example of such an algorithm in the next section. However, when a salt is dissolved into an aqueous system, it dissociates into ions which should be considered as independent species. The dissociated ions have the tendency to migrate into one of the two phases based on their mutual affinities with the solvent of that phase. The presence of any excess ions in a phase in comparison to the other, creates an excess charge in that phase, yet the bulk phase must remain electroneutral. Therefore, the thermodynamic model must also respect this condition of electroneutrality, either inherently, or by imposing a balance of the net amount of charges in both phases.

There are two methods used traditionally by various authors to impose the condition of electroneutrality, as shown in figure 5.1. The first method assumes no ion dissociation and considers therefore that only salt has a fugacity, and not each individual ion. Yet, as discussed at length in the previous chapter, the approach that is considered using e-PPC-SAFT makes it possible to distinguish the fugacity of each ion. We want to keep this possibility for cases where multiple salts are present simultaneously therefore making it difficult to identify which ion originated from which salt.

The second method consists of writing an additional constraint, which is the charge balance, thus effectively removing one degree of freedom from the algorithm. This would require re-writing the algorithm, which was out of the scope of this work.

The third method is detailed in section 5.2.3 and used in this work.

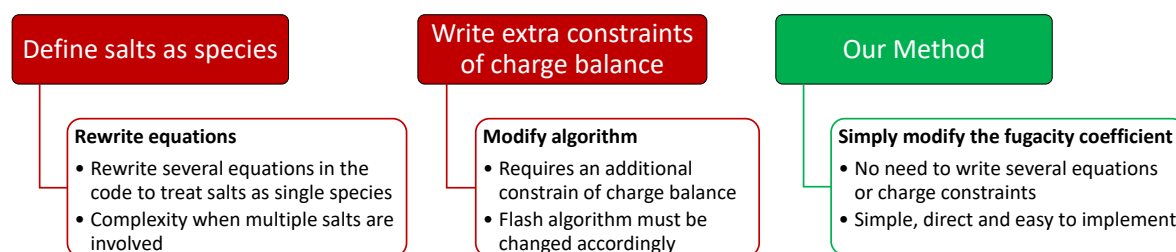


Figure 5.1: Various methods for imposing the condition of electroneutrality in a thermodynamic framework

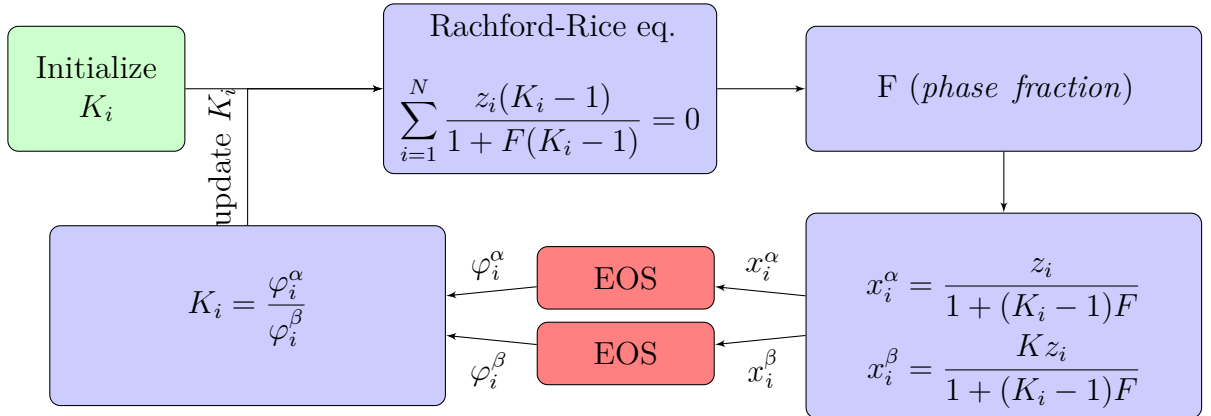


Figure 5.2: Current flash procedure without respecting electroneutrality

5.2.2 Current state: without electroneutrality

Figure 5.2 presents the flash routine without taking electroneutrality into account, this is the current state of our thermodynamic framework. The first step is the initialization (initial guess) of the partition coefficient ($K_i = \frac{x_i^\alpha}{x_i^\beta}$), which is then used in the Rachford-Rice equation ?? to calculate the phase fraction (F). The next step is to calculate the molar composition of components in the two phases (x_i^α, x_i^β) by mass balance (equation ??), where z_i is composition of the feed. The value of these molar composition is used in the equation of state (EoS) to calculate the value of the fugacity coefficient of each component in both phases ($\varphi_i^\alpha, \varphi_i^\beta$). Finally, these fugacity coefficients are used to calculate the new value of the partition coefficient (K_i). The new value of K_i is then used back in the Rachford-Rice equation ?? and the procedure is iterated until the process stabilizes.

The heart of the algorithm, which we focus on in this work is the red box. Here, the EoS takes as an input pressure, temperature and phase composition (x_i^α, x_i^β). The output is the vector of fugacity coefficients ($\varphi_i^\alpha, \varphi_i^\beta$). The formulation is identical whether the species are neutral or as ionic. Doing so, it is clear that ionic species will not be distributed evenly, leading to a violation of electroneutrality.

5.2.3 A new method for electroneutrality: Modifying the fugacity coefficient

The partition of the charged species into the different phases in liquid two-phase system (such as proteins and polymers) is studied by various authors [250–252]. The migration of these charged species results in the creation of an electrostatic potential difference between the phases. It is an interesting phenomenon and several authors have worked toward

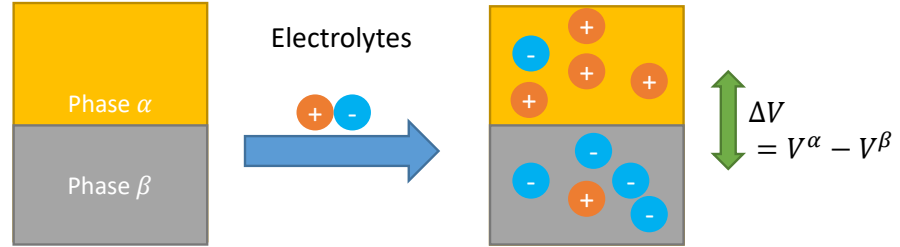


Figure 5.3: Creation of electrostatic phase potential

measuring this potential experimentally [34, 253–255]. It is of special interest in our work because with the help of this potential we can fulfill the condition of electroneutrality. A pictorial representation in fig. 5.3 which depicts the creation of this electrostatic potential difference between the phases before attaining equilibrium. A two phase liquid system is shown in fig 5.4, when a salt (say NaCl) is added into the system, it dissociates into constituent ions (Na^+ and Cl^-). These constituent ions then form individual species and similar to any other non-charged species they have the tendency to migrate into one of the two phases, depending on their mutual affinities with the respective solvents in each phase. This migration develops an electrostatic potential difference (ΔV) between the two phases. The new method for applying electroneutrality is based on deducing this hypothetical potential difference. We call it hypothetical since in reality it does not exist in our systems of investigation at equilibrium because the partitioning will be such that the bulk phases remain electroneutral.

5.2.3.1 Derivation and concept

In thermodynamics we define chemical potential (μ_i) for non-electrolyte systems and electrochemical potential ($\tilde{\mu}_i$) for electrolyte systems, which is given by equation 5.1 [256]. So, in electrostatic systems we equate not the chemical potential but the electrochemical potential to attain equilibrium.

$$\tilde{\mu}_i^\alpha = \underbrace{\mu_i^\alpha}_{\text{Chemical part}} + \underbrace{Fz_iV^\alpha}_{\text{Electrical part}} \quad (5.1)$$

where, F is the Faraday's constant, z_i is the charge, V_α is the electrostatic potential of phase α . The difference between the potential of the two phases is equal to the potential difference ΔV . Let us assume that charged species migrate in the phases in equilibrium

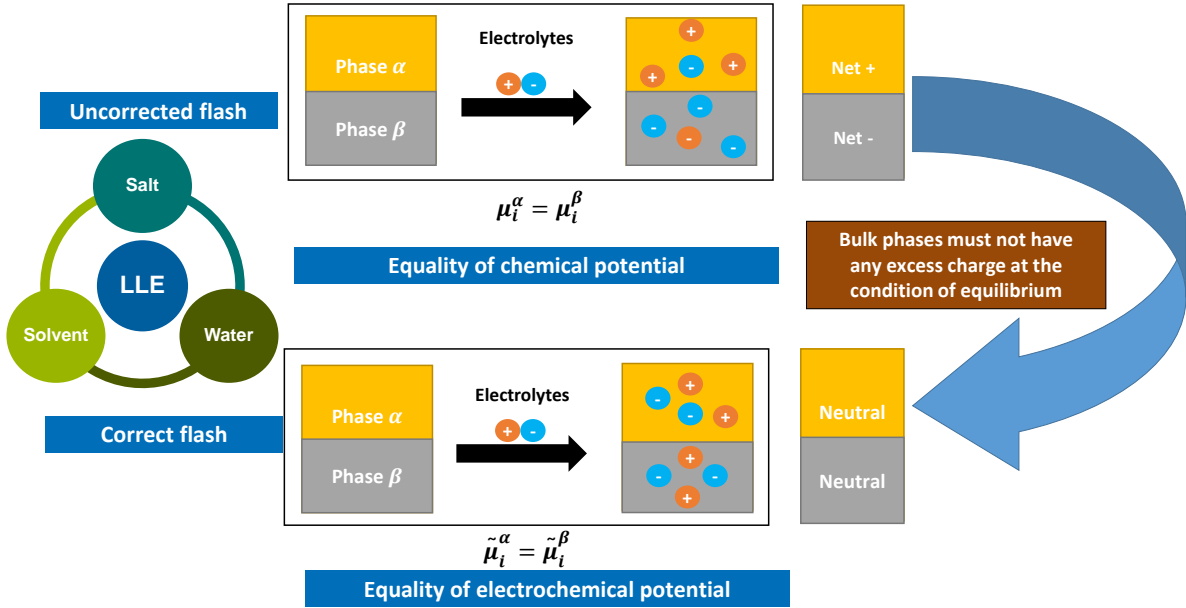


Figure 5.4: Theoretical representation of the condition of electroneutrality

without respecting the condition of electroneutrality as shown in figure 5.3. Since the distribution of ions results in excess charges in the bulk phases, a potential difference is created between the two phases. Let us re-write equation 5.1 for each of the two phases (α and β) in this case.

$$\tilde{\mu}_i^\alpha = \mu_i^\alpha + Fz_iV^\alpha \quad (5.2)$$

$$\tilde{\mu}_i^\beta = \mu_i^\beta + Fz_iV^\beta \quad (5.3)$$

This equation can be written in the form of fugacity coefficient φ as :

$$RT \ln \tilde{\varphi}_i^\alpha = RT \ln \varphi_i^\alpha + Fz_iV^\alpha \quad (5.4)$$

$$RT \ln \tilde{\varphi}_i^\beta = RT \ln \varphi_i^\beta + Fz_iV^\beta \quad (5.5)$$

The partition coefficient of a component is given by:

$$\tilde{K}^+ = \frac{\tilde{\varphi}_+^\alpha}{\tilde{\varphi}_+^\beta} \quad (5.6)$$

$$\tilde{K}^- = \frac{\tilde{\varphi}_-^\alpha}{\tilde{\varphi}_-^\beta} \quad (5.7)$$

$$\ln \tilde{K}^+ = \ln \tilde{\varphi}_+^\alpha - \ln \tilde{\varphi}_+^\beta \quad (5.8)$$

$$= \left(\ln \varphi_+^\alpha + \frac{Fz_+V^\alpha}{RT} \right) - \left(\ln \varphi_+^\beta + \frac{Fz_+V^\beta}{RT} \right) \quad (5.9)$$

$$\ln \tilde{K}^+ = \ln \frac{\varphi_+^\alpha}{\varphi_+^\beta} + \frac{Fz_+\Delta V}{RT} \quad (5.10)$$

Similarly,

$$\ln \tilde{K}^- = \ln \frac{\varphi_-^\alpha}{\varphi_-^\beta} + \frac{Fz_-\Delta V}{RT} \quad (5.11)$$

At equilibrium the condition of electroneutrality states that the partition coefficients of the two ionic species should be equal:

$$\tilde{K}^+ = \tilde{K}^- \quad (5.12)$$

Using eqn 5.10-5.11, and eqn 5.12 the following eqn 5.13 can be obtained. This equation is also famously known as Albertsson equation [250] for calculating the phase potential difference that exist in aqueous two phase systems.

$$\Delta V = \frac{RT}{F(z_- - z_+)} \ln \frac{K^-}{K^+} \quad (5.13)$$

where, K_+ and K_- are the partition coefficient of the ionic species + and – without taking into account the condition of electroneutrality (or in a non equilibrium state).

So, in order to calculate the value of the electrochemical fugacity coefficient $\tilde{\varphi}$ (eqn. 5.4), we need to know the value of the electrostatic phase potential V^α . In our model since we have not taken into account the condition of electroneutrality, the calculated fugacity coefficients are those which do not take into account electroneutrality, so their values correspond to K (the non-electroneutral partition coefficient appearing in equation 5.13). If we re-write equation 5.13 in terms of these fugacity coefficient, it is as follows:

$$\Delta V = V^\alpha - V^\beta = \frac{RT}{F(z_- - z_+)} \ln \frac{\varphi_-^\alpha \varphi_-^\beta}{\varphi_+^\beta \varphi_+^\alpha} \quad (5.14)$$

$$= \frac{RT}{F(z_- - z_+)} \left(\ln \frac{\varphi_+^\alpha}{\varphi_-^\alpha} - \ln \frac{\varphi_+^\beta}{\varphi_-^\beta} \right) \quad (5.15)$$

$$(5.16)$$

we can therefore split the potential into two contributions:

$$V^\alpha = \frac{RT}{F(z_- - z_+)} \ln \frac{\varphi_+^\alpha}{\varphi_-^\alpha} \quad (5.17)$$

$$V^\beta = \frac{RT}{F(z_- - z_+)} \ln \frac{\varphi_+^\beta}{\varphi_-^\beta} \quad (5.18)$$

Hence, the corresponding phase potential V^α and V^β can be taken from equation 5.17, 5.18 and substituted in equation 5.4. This is just a modification in existing calculation routine of the fugacity coefficient without changing the existing structure of the code. The final expression for the modified fugacity is given by equation 5.19

$$\ln \tilde{\varphi}_i^\alpha = \ln \varphi_i^\alpha + \underbrace{\frac{z_i}{z_- - z_+} \ln \frac{\varphi_+^\alpha}{\varphi_-^\alpha}}_{\text{Correction}} \quad (5.19)$$

The modified fugacity coefficient (let's say corrected fugacity coefficient) can be easily implemented in the existing code within the red EoS box as shown in figure 5.5.

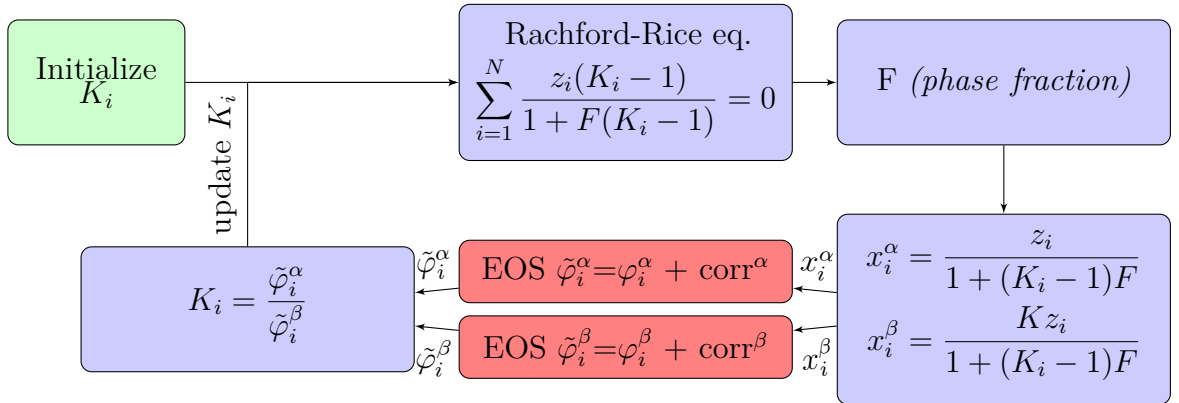


Figure 5.5: Procedure for implementing the new method of electroneutrality

The results of the partition coefficient after implementing the new method is presented in figure 5.6 as comparison to partition coefficient without any electroneutrality constraint. The figure clearly shows that the new method brings into account the electroneutrality condition as the partition coefficient of the two ions are equal.

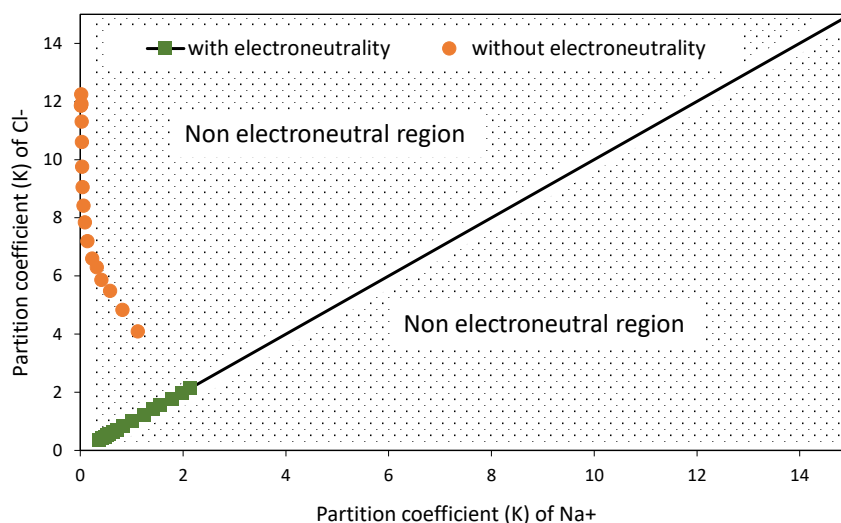


Figure 5.6: Partition coefficient of Na^+ and Cl^- in two phase ionic system before and after implementing the new method for electroneutrality

5.3 The machinery

5.3.1 Prediction of the LLE by the non-parameterized model

At this point, the current thermodynamic model is fully prepared and can be used to compute LLE of mixed solvent electrolytes. However, the predictions (fig 5.8-5.9) are still far from accurate. This behavior can be explained by the figure 5.7 where the current status of parameterization is presented. We have three types of compounds, and each binary of these three types must be fully evaluated before the full system can be investigated in a predictive fashion.

- Water + Organic compounds: has been fully described in Chapter 3
- Salt + water: has been fully described in Chapter 4
- Salt + Organic : This binary was not described yet.

The binary of salt-water is already parameterized where ion parameters were tuned on MIAC's and AMV (Chapter 4). The binary of organic solvent-water is also already parameterized (Chapter 3). But, the binary of organic solvent-salt is still not parameterized, and this is the objective of this chapter.

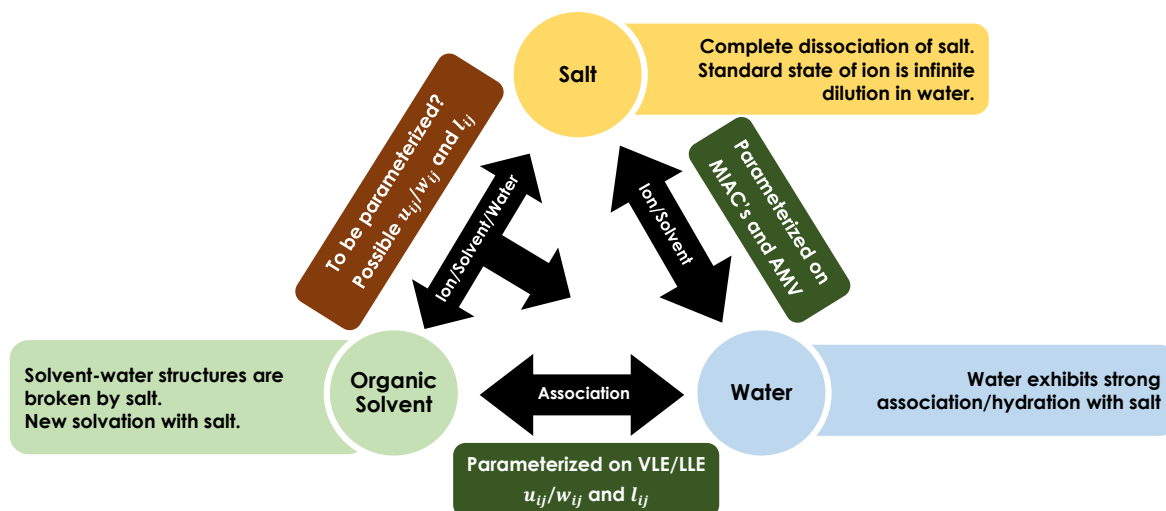


Figure 5.7: Current state of parameterization in mixed solvent electrolyte systems

5.3.1.1 Example case: 1-Butanol - Water - NaCl

The calculation from model (line) are compared to the experimental data (points) for each systems (figure 5.8-5.9). It can be seen that for small molar composition of salts, the curves are close to axes. While these calculation qualitatively captures the experimental behaviour a closer look at the partition coefficient of each component for each system reveals the deviation. It is the partition coefficient K_i (equation 5.20) that is the biggest challenge which must be better represented by the model. The following generalized observation can be inferred by analyzing these figures:

$$\ln \tilde{K}_{salt} = \ln \frac{x_{salt}^{org}}{x_{salt}^{aq}} \quad (5.20)$$

- Systematic slight over-prediction of the 1-butanol partition coefficient. However, the qualitative trend is clearly followed.
- Systematic slight over-prediction of water partition coefficients where the qualitative trend is clearly captured by the model.
- Systematic and high under-prediction of the salt partition coefficient by the model. The reason for this under prediction is due to the overprediction of the 1-butanol partition coefficients. Salts due to their inherent character like being with water as compared to that of alcohol. That means a slightly higher 1-butanol mole fraction in a phase will result in the lower concentration of salt in that phase.

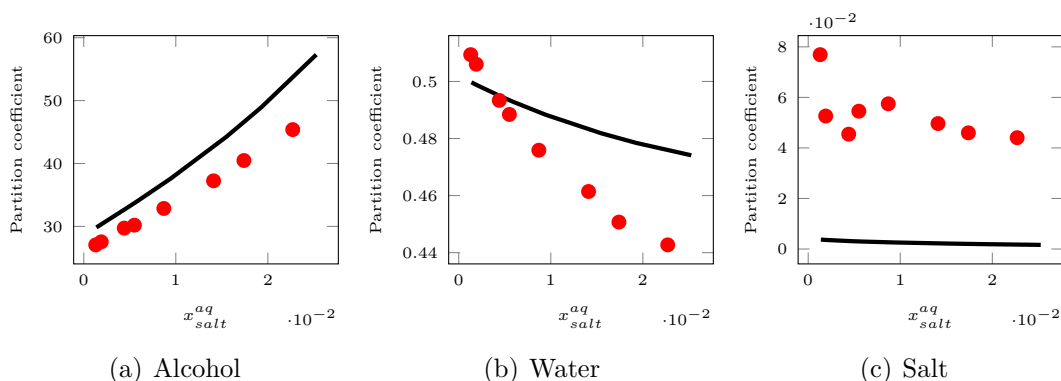


Figure 5.8: Partition coefficients of 1-Butanol - Water - CsCl system at 293.15K

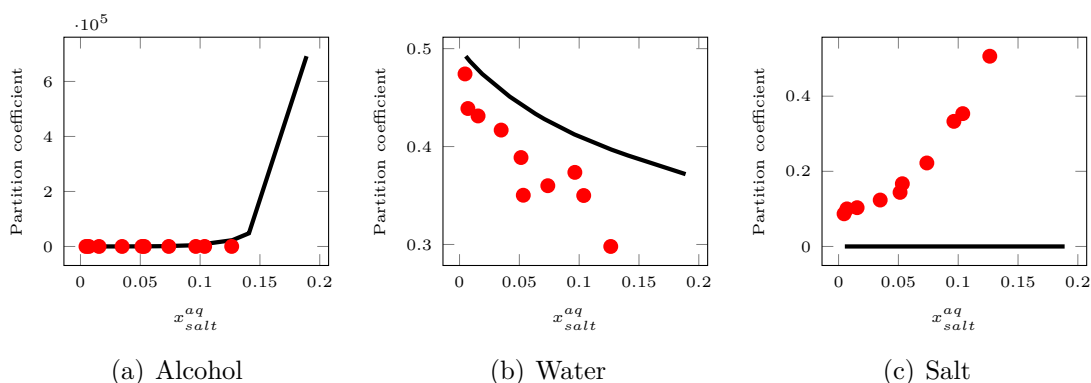


Figure 5.9: Partition coefficients of 1-Butanol - Water - LiCl system at 293.15K

Clearly, the 1-butanol-salt parameter requires adjustment and as pointed out in section 5.3.1.1 is a challenging job. The next section deals with modeling MIAC's of mixed solvent electrolytes and adjusting these parameters.

5.3.2 Partition coefficient of salts

In the analysis below, we changed the convention on the partition coefficient, now:

$$K_i = \frac{x_i^{aq}}{x_i^{org}} \quad (5.21)$$

Based on the initial results of LLE of mixed solvent electrolytes, the partition coefficients of solvent and water were satisfactory. This is expected because the binary between these species have already been optimized. However, the K_i of salt were systematically under-predicted. So, the focus of this section will be on the K_i of salt which is given by equation 5.30. The partition coefficients are calculated as the ratio of the fugacity coefficients (equation 5.29):

$$\ln \tilde{K}_i = \ln \varphi_i^{\tilde{org}} - \ln \varphi_i^{\tilde{aq}} \quad (5.22)$$

From equation (5.12) we know that the partition coefficients of both ions must be equal, hence:

$$\ln \tilde{K}_{salt} = \tilde{K}_+ = \tilde{K}_- \quad (5.23)$$

Let us take the partition coefficient of the cation as the reference, then, using equation(5.19):

$$\ln \tilde{\varphi}_+^\alpha = \ln \varphi_+^\alpha + \frac{z_+}{z_- - z_+} \ln \frac{\varphi_+^\alpha}{\varphi_-^\alpha} \quad (5.24)$$

And therefore:

$$\ln \tilde{K}_{salt} = \left(\ln \varphi_+^{org} + \frac{z_+}{z_- - z_+} \ln \frac{\varphi_+^{org}}{\varphi_-^{org}} \right) - \left(\ln \varphi_+^{aq} + \frac{z_+}{z_- - z_+} \ln \frac{\varphi_+^{aq}}{\varphi_-^{aq}} \right) \quad (5.25)$$

Since in our case, the charge of all ions is one, this is also written as:

$$\ln \tilde{K}_{salt} = \left(\ln \varphi_+^{org} - \frac{1}{2} \ln \frac{\varphi_+^{org}}{\varphi_-^{org}} \right) - \left(\ln \varphi_+^{aq} - \frac{1}{2} \ln \frac{\varphi_+^{aq}}{\varphi_-^{aq}} \right) \quad (5.26)$$

Rearranging gives,

$$\ln \tilde{K}_{salt} = \left(\frac{\ln \varphi_+^{org} + \ln \varphi_-^{org}}{2} \right) - \left(\frac{\ln \varphi_+^{aq} + \ln \varphi_-^{aq}}{2} \right) \quad (5.27)$$

Or,

$$\ln \tilde{K}_{salt} = \frac{(\ln \varphi_+^{org} - \ln \varphi_+^{aq}) + (\ln \varphi_-^{org} - \ln \varphi_-^{aq})}{2} = \frac{\ln \tilde{K}_+ + \ln \tilde{K}_-}{2} \quad (5.28)$$

This shows that we can investigate the partitioning of the salt by analyzing the average of the partitioning of ions. The ionic fugacity coefficient are computed from the Helmholtz residual energy as follows:

$$\ln \varphi_i = \ln \frac{\partial A^{res}}{\partial n_i} - \ln Z \quad (5.29)$$

where A^{res} is a sum of contribution as discussed in section 2.5.3. It is therefore possible to write the logarithm of the partition coefficient directly as the sum of the differences.

$$\ln \tilde{K}_i = \left(\sum_X \frac{\partial A^X}{\partial n_i} \right)^{org} - \left(\sum_X \frac{\partial A^X}{\partial n_i} \right)^{aq} - \ln \frac{Z^{org}}{Z^{aq}} \quad (5.30)$$

where Z is the compressibility factor and X refers to the terms of the ePPC-SAFT equation.

Table 5.1: Dominant PC-SAFT contribution in partitioning of salt in LLE of mixed solvent electrolytes and their parameter

Term	Non-modifiable parameter ¹	Modifiable parameter ²	Discussed in
Born	ε	D_{ij}	(sec 5.4.1)
MSA	ε	D_{ij}	(sec 5.4.1)
HC	$\sigma_{alc}, \sigma_{ion}$	l_{ij}	(Chapter 3 and 4)
Association	$\varepsilon^{AB}/k_{alc}, \varepsilon^{AB}/k_{ion}$	u_{ij} / w_{ij}	(Chapter 3 and 4)

¹ We call these parameters non-modifiable because at this stage they cannot be changed, they are already obtained on the respective binary systems.

² We call these parameters modifiable because they can be changed depending on the parameterization strategy that is adapted. However, D_{ij} may not be changed once its value is fixed for certain solvent-water system

In order to focus on the partitioning of the salt, the analysis below uses the half sum of the derivative by equation below:

$$\ln \tilde{K}_{salt} = \frac{1}{2} \sum_X \left[\left(\frac{\partial A^{X,org}}{\partial n_+} + \frac{\partial A^{X,aq}}{\partial n_+} \right) + \left(\frac{\partial A^{X,org}}{\partial n_-} + \frac{\partial A^{X,aq}}{\partial n_-} \right) \right] - \ln \frac{Z^{org}}{Z^{aq}} \quad (5.31)$$

5.3.2.1 Individual PC-SAFT contributions and their impact on K_i

The next step is to look at the individual contribution of PC-SAFT and how their values impact the partitioning of salt species.

The plots of the various individual contribution to the partition coefficient $\frac{\partial A}{\partial n_i}$ of ePPC-SAFT are shown for several 1-Butanol - water - salt systems (figure 5.10-5.16) for salt, cation and anion in that order. These plots will help us understand which contribution has the dominant effect on the value of the partition coefficient. As this is a qualitative analysis the actual numbers (for $\frac{\partial A}{\partial n_i}$) have little significance, however, it is their qualitative trend that makes sense. Rewriting equation 5.32 for all the terms we can see the mathematical contribution of each term on the partition coefficient, the way it is computed. The equation 5.32 represents the combined contribution by cation and anion for the two phases (organic and aqueous). For each figure fig 5.10-5.16, the contribution of each ion is plotted as well as the final contribution for the salt.

$$\ln K_{salt} = \frac{1}{2} \sum_X \left[\left(\frac{\partial A^{X,org}}{\partial n_+} - \frac{\partial A^{X,aq}}{\partial n_+} \right) + \left(\frac{\partial A^{X,org}}{\partial n_-} - \frac{\partial A^{X,aq}}{\partial n_-} \right) \right] - \ln \frac{Z^{org}}{Z^{aq}} \quad (5.32)$$

It can be seen in figures (5.10-5.16) that contributions (polar, dispersion, chain) are always least dominant. The contribution in which we are particularly interested in, are, Hard chain, Association, MSA and Born and their corresponding parameters that affect their values (table 5.1).

The figures (5.10-5.16) have been constructed as follows:

- A LLE calculation was performed to determine the adequate composition of both phases
- At equilibrium, the various contributions (equation 5.32) are computed.

Whenever the contribution is found to be positive, it means that it tends to increase K_{salt} and therefore to pump the salt into the aqueous phase. When the contribution is negative, on the contrary, it will rather pull the salt in the organic phase.

The figures show that the partition coefficients result from the balance of different forces (contributions). The most significant ones are the association, the hard chain and the Born contributions. The coulombic ion-ion interactions (MSA) have no significant effect on the ionic partition coefficient.

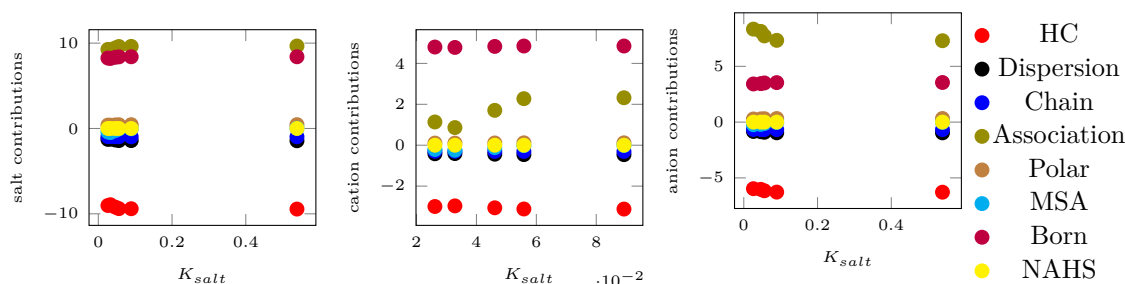


Figure 5.10: Contributions of the various terms on the partition coefficient of salts, cations and anions for 1-Butanol-water-KCl at 298.15K

By looking at the various figures one can observe that some contributions are positive while others are negative. The positive contributions are those that increase the value of K_i while the negative contributions are those that decrease the value of K_i . Since, by our calculation we observe a systematic under-prediction of the partition coefficient of salt, thus our aim is to increase its value. In other words, we need to shift the net contribution to positive regions to pull out more ions from the aqueous regions and bring them into the organic region. The parameter that can help bring this change are mentioned in table 5.1.

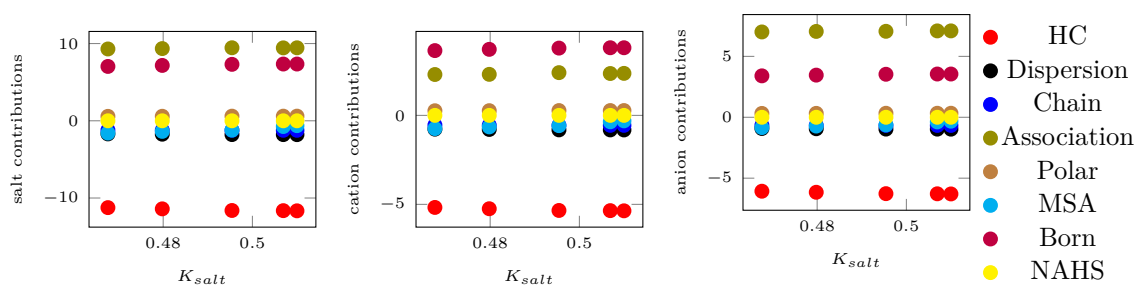


Figure 5.11: Contributions of the various terms on the partition coefficient of salts, cations and anions for 1-Butanol-water-CsCl at 298.15K

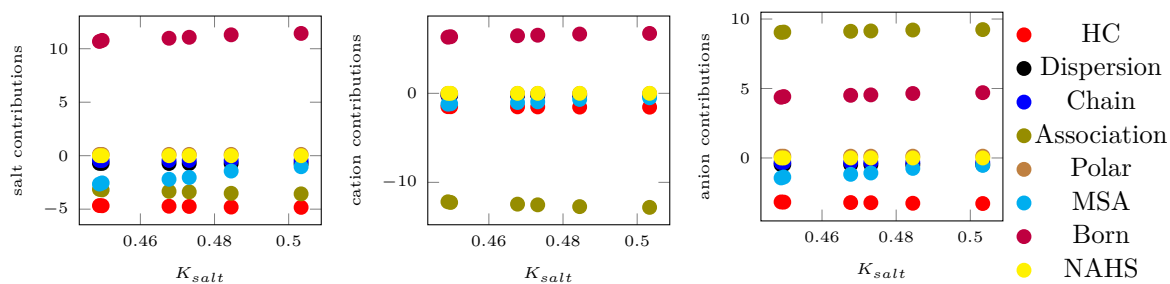


Figure 5.12: Contributions of the various terms on the partition coefficient of salts, cations and anions for 1-Butanol-water-NaF at 298.15K

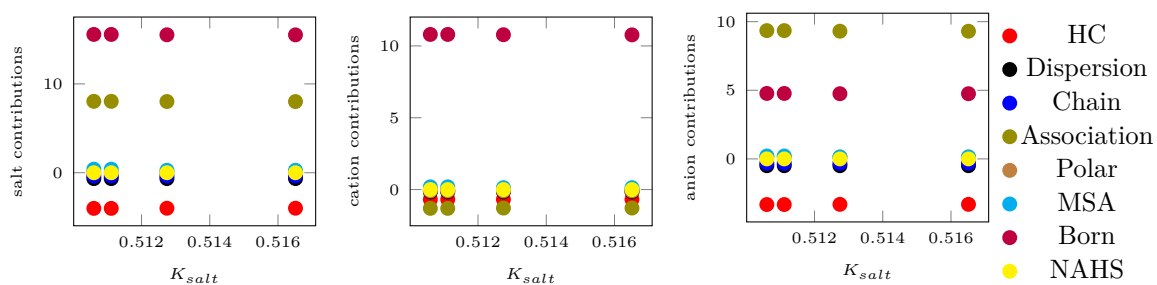


Figure 5.13: Contributions of the various terms on the partition coefficient of salts, cations and anions for 1-Butanol-water-LiF at 298.15K

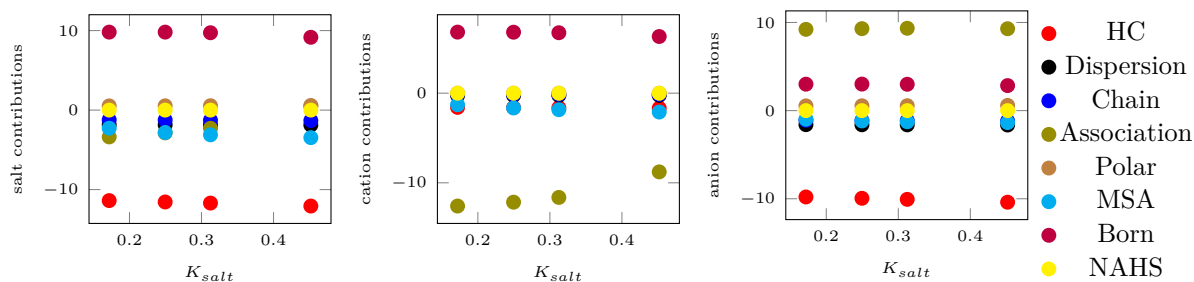


Figure 5.14: Contributions of the various terms on the partition coefficient of salts, cations and anions for 1-Butanol-water-NaI at 298.15K

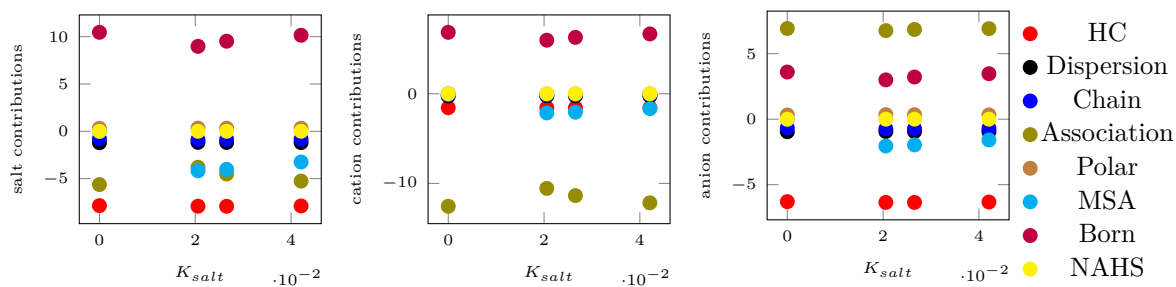


Figure 5.15: Contributions of the various terms on the partition coefficient of salts, cations and anions for 1-Butanol-water-NaCl at 298.15K

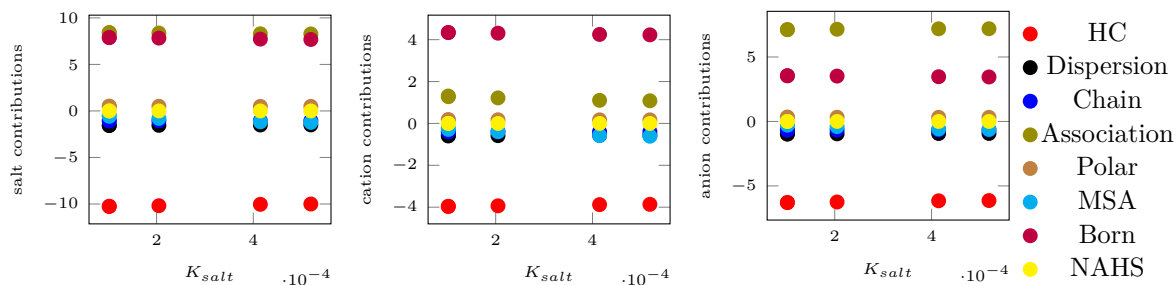


Figure 5.16: Contributions of the various terms on the partition coefficient of salts, cations and anions for 1-Butanol-water-RbCl at 298.15K

The hard chain contribution is often negative although in some cases it can be very small. This can be explained by noting that the organic phase has more free volume (less dense) than the aqueous phase. As a result, any small species will prefer migrating to the organic phase. This is an entropic effect, as it is only related to the size of the compounds. Notice that another entropic term, NAHS, which describes the non additivity of the sphere diameter has zero effect on the plots for the simple reason that the interaction parameter, l_{ij} is taken as zero. However, this parameter between ions and alcohols could be adjusted so as to create either a positive or a negative effect on these plots. If l_{ij} (alcohol-ion) >0 , this meant that the cross diameter is reduced, resulting in a lower repulsion between ions and alcohols. The expected consequence is a negative effect, the ions will prefer going into the organic phase.

The association contribution describes the structure forming. It may be both positive or negative. In fact we notice that it is often negative for cations and positive for anions. This would indicate that cations are more solvated in the organic phase, which is not to be expected. The strength of these interaction should much stronger with water than with the alcohol. The association strength can be tuned using interactions parameters as explained in chapter 3. By adjusting either u_{ij} or w_{ij} , we will be able to improve the quantitative results.

The Born term is seen to always have a positive effect. This is clearly explained by the difference in the dielectric constant between the two phases. The aqueous phase that contains mostly water has a very large dielectric constant, while the organic phase has a small one. The ions prefer the high dielectric constant medium. Hence, another tuning parameter might be the mixing rule on D . This is further discussed in the section 5.4.1.

Table 5.1 summarizes the effect of the terms and the various interaction parameters that can be tuned in order to improve the salt partitioning. The analysis is used as the basis for the parameterization in the next section

5.4 Parameterizing mixed solvent salt systems using available data

In the previous section we have made attempts to understand the ion-solvent interactions in LLE for mixed solvent systems. Since, the K_i of salts showed systematic deviations, there is a need to correctly parameterize the ion-solvent interaction. To this end, we will use a range of data that helps understand this phenomena.

- Dielectric constant data: these are essential since we have seen that the dielectric constant has a strong impact on the partitioning.
- MIAC data for mixed-solvent electrolytes (section 5.4.3).
- Individual partition coefficients as obtained from LLE data and observe a individual trends (section 5.3.2.1).

5.4.1 Dielectric constant of mixed-solvents

In our thermodynamic framework we need the value of the dielectric constant to calculate the electrolyte contribution (MSA and Born term). For single solvent mixture, they can be modeled using temperature and density dependent correlation for the pure solvent as discussed in chapter 4. In this work we used the equation proposed by Sreckengerg [123].

Table 5.2: Correlations for calculating dielectric constants of the pure solvent [123]

Component	Mol Wt.	$d_v(\frac{dm^3}{mol})$	$d_T(K)$
Water	18.02	0.3777	1403.0
Methanol	32.05	0.5484	1011.0
Ethanol	46.07	0.9480	732.1
1-Propanol	60.10	1.269	641.7
2-Propanol	60.10	1.667	550.1
1-Butanol	74.12	1.515	593.3
2-Butanol	74.12	2.555	461.6

$$\varepsilon_s = 1 + \frac{\sum_i^n N}{V_{system}} d_v \left(\frac{d_T}{T} - 1 \right) \quad (5.33)$$

Note that the $\sum \frac{N}{V_{system}}$ is the molar density as calculated by the SAFT EoS. The parameters, listed in table 5.2, have been determined on the dielectric constant data for pure components [123].

For mixed solvent salt systems, calculating this property requires a mixing rule. It also becomes more important since the value of the dielectric constant affects the Born and MSA term which in turn will rule the chemical potential of ions in each phase. The higher the value of dielectric constant the more "comfortable" the ions will be in the given phase as discussed in section 5.3.2. Initially, we have tried a simple mixing rule

(equation 5.34)

$$\varepsilon_s = \sum_i^{\text{solvent}} \varepsilon_i x_i \quad (5.34)$$

where ε_s is the dielectric constant of the mixed solvent. This mixing rule showed inconsistent result when compared to experimental data.

Then a more complex rule given by Wang and Anderko (eq 5.35). Again, doing so the computed dielectric constant showed an inconsistency.

$$p = \frac{(\varepsilon - 1)(2\varepsilon + 1)}{9\varepsilon} \quad (5.35)$$

$$p_m = \frac{\sum_i^n x_i v_i p_i}{\sum_i^n x_i v_i} \quad (5.36)$$

The reason for failure in both these mixing rules is that when the solvent composition is altered, the molar density also changes such that $\varepsilon_i(V_{\text{mix}}) \neq \varepsilon_i(V_{\text{pure}})$. This is why another option was chosen with equation 5.38, that provides the mixing rule on the equation parameters.

A third option is to use a mixing rule on the equation parameters (similar to section 4.3.1.1) d_T and d_v , we used:

$$d_v = \sum_i^{\text{solvent}} \sum_j^{\text{solvent}} x_i x_j \frac{d_{vi} + d_{vj}}{2} (1 - D_{ij}) \quad (5.37)$$

$$d_T = \frac{\sum_i^{\text{solvents}} n_i d_{T,i}}{\sum_i^{\text{solvents}} n_i} \quad (5.38)$$

The mixing rule based on equations 5.37 and 5.38 is simple and the prediction of dielectric constant for methanol and ethanol are good when $D_{ij} = 0$ (figure 5.17 a and b). The figure shows that the dielectric constant of small alcohols with water behaves more linearly than that of larger alcohols. This may be related to the fact that small molecules are more mobile and can therefore align their dipoles along the electric field much easier than large molecules. The consequence of this non-linear behavior is that a correction parameter D_{ij} needs to be introduced so that the model can reproduce the observation (equation 5.37). The value of $D_{ij}=0.7$ used in this work was set arbitrarily in such a way that model provides acceptable results.

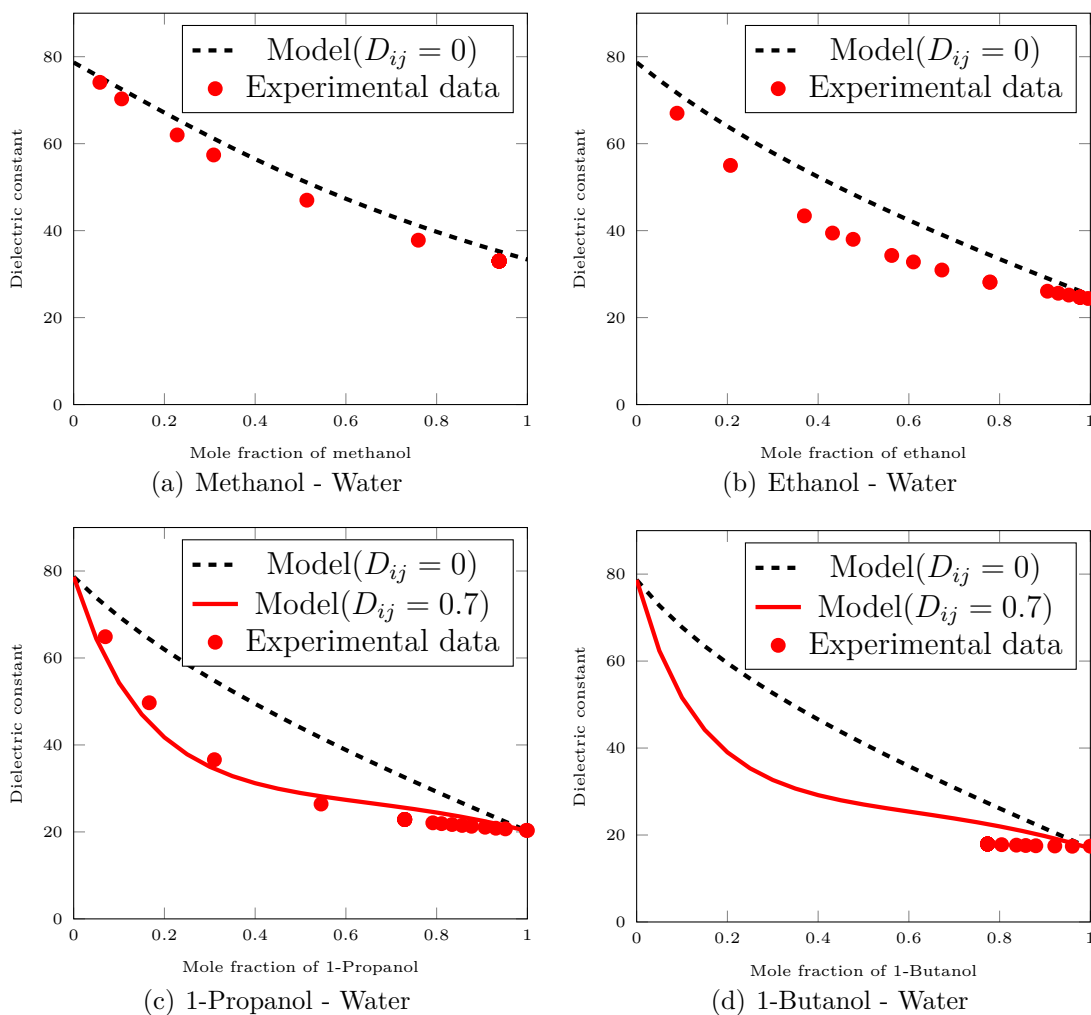


Figure 5.17: Dielectric constant of Alcohol-water mixture at 298.15K, comparison from model vs experimental data (adjusted binary parameter D_{ij} for model)

After utilizing the new correction parameter on the new mixing rule 5.37, the current model for dielectric constant correctly correlates the dielectric constant for propanol and butanol. So, we continue to use this value $D_{ij} = 0.7$ for all propanol/butanol systems and $D_{ij} = 0$ for methanol ethanol systems.

In order to take into account the effect of ionic species on the dielectric constant, Pottel's [53] model is used: (equation 5.39). The value of the solvent dielectric constant that is thus found, is next introduced into the Pottel equation 5.39-5.40 to find the solution dielectric constant, needed for the Born and the MSA terms of ePPC-SAFT.

$$\varepsilon - 1 = (\varepsilon_s - 1) \frac{1 - \xi_3''}{1 + \xi_3''/2} \quad (5.39)$$

$$\xi_3'' = \frac{N_{Av}\pi}{6} \sum_i^{ions} \frac{n_i (\sigma_i^{HS})^3}{V} \quad (5.40)$$

where σ_i^{HS} is the ionic diameter, V is the volume of the system.

5.4.2 MIAC of mixed solvent electrolyte systems: Analysis

Electrolyte systems are characterized by high thermodynamic non-ideality. Thus, the study of the mean ionic activity coefficients of mixed-solvent electrolyte systems of alcohol-water-salts can provide an insight into the actual interaction that play a dominant role in the non-ideality. The ionic activity coefficients $\gamma_{i,m}$ are defined as the ratio of the ionic fugacity coefficients and its value in the reference state (eq 5.41).

$$\gamma_{i,m} = \frac{\varphi_i(T, P, x_i)}{\varphi_i^\infty(T, P, x_i \rightarrow 0)} x_{solvent} \quad (5.41)$$

The definition of the reference state is infinite dilution of the ion in the solvent. It is important in the case of mixed solvent as the reference state is not pure water but the actual mixed solvent mixture.

Because ionic coefficients cannot be measured, only mean ionic activity coefficients (MIAC) data are reported in the literature. They are defined by eqn. 5.42.

$$\gamma_{\pm} = (\gamma_+^{v_+} \gamma_-^{v_-})^{1/(v_+ + v_-)} \quad (5.42)$$

At this stage, it is important to understand the underlying interactions that affect the MIAC's of mixed solvents before attempting to parameterize these systems. The trend of MIAC's of water-salt systems is already discussed in chapter 4, which is already well described by our model. It was shown how the balance between the various phenomena explain the observed behavior, characterized by a sharp initial drop with increasing salt molality, followed by a minimum and a subsequent rise of the activity coefficient. This is consistent with the explanation provided earlier (Chapter 4): the rise in the curve results from the structure-forming effect (sometimes called solvation) of the solvent around ions. When a second solvent (alcohol) is added the minimum in the curve goes deeper, shown in fig 5.18. Yet, when water is replaced by alcohol, such structures are much weaker and the rise therefore only at much high concentrations, if at all.

Comparing plots in figure 5.18 for methanol, ethanol, propanol, and butanol it can also be observed that the nature of the solvent affects the behavior.

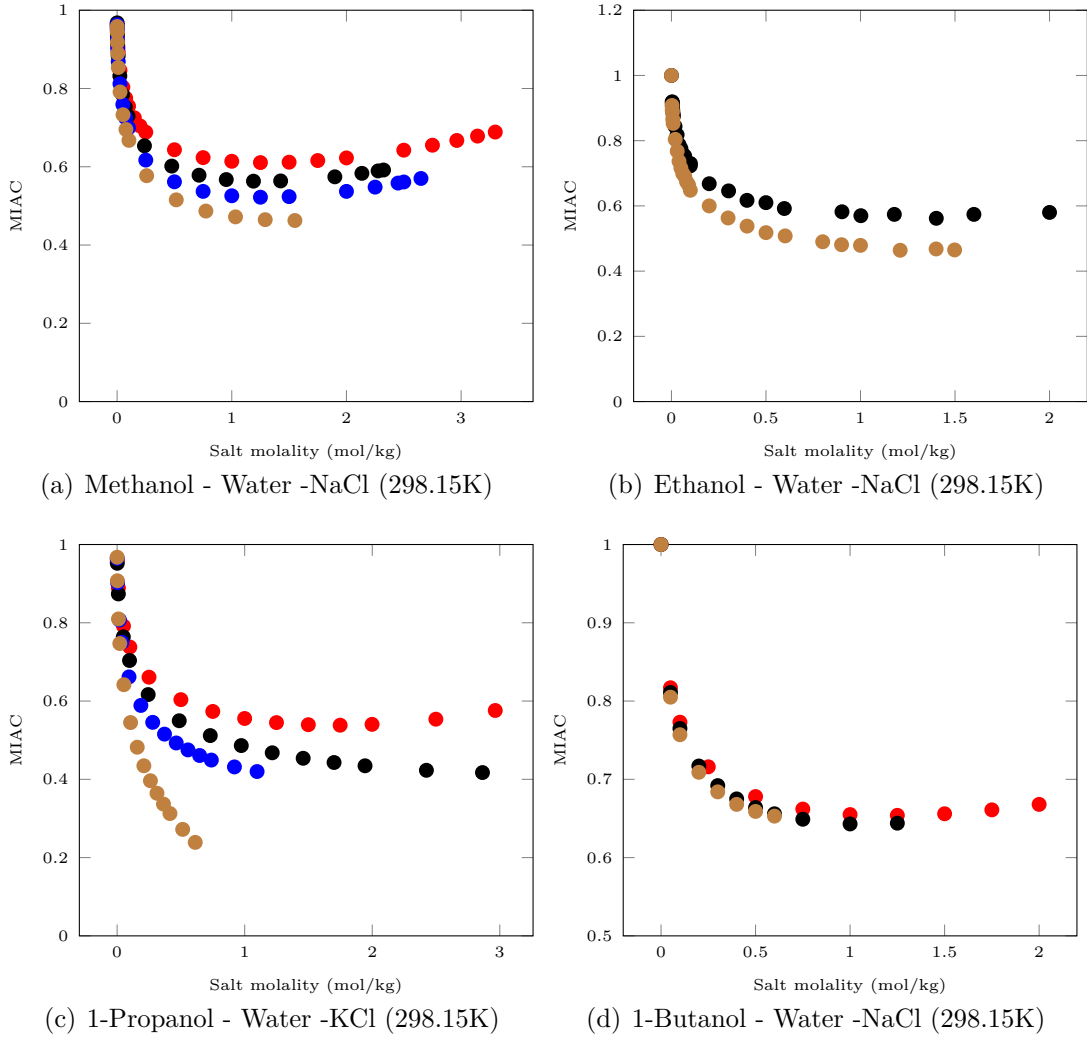


Figure 5.18: Mean Ionic activity coefficients experimental data trend for mixed solvent methanol, ethanol, 1-Propanol, and butanol - salt systems systems at varying weight fraction (w_m) (10% —, 20% —, 30% —, 40% —)

5.4.3 Approach for parameterization of mixed-solvent salt systems

Since the aim is to find parameters independent of salt, the parameterization must be done with all available experimental data of MIAC simultaneously, for a common solvent. The objective function used in this parameterization is given by eq 5.43 and the experimental data is mentioned in table 5.3.

$$OF = \sum_{j=1}^{N_{\gamma_{\pm}}} \left(\frac{\gamma_{\pm,j}^{calc} - \gamma_{\pm,j}^{exp}}{\gamma_{\pm,j}^{exp}} \right)^2 \quad (5.43)$$

Considering the analysis above, two types of interaction parameters can be considered for tuning. The most obvious one is the parameters regulating association between ions and alcohols (see eqn 2.5.6). We selected the u_{ij} parameter as most data is given at around room temperature so that it didn't seem reasonable to modify the temperature dependent term.

The second interaction parameter is l_{ij} which affects the entropic contribution through the NAHS term (see Chapter 5). Note that in all cases we consider group-group parameter. Most molecular species are considered as single group except propanol and 1-butanol which are constructed using the group contribution scheme by NguyenHuynh [130]. As such the same OH group is used for both of these molecules.

Three scenarios are tested:

- Case(a) Table 5.4 : Association parameter (u_{ij}) tuning : In this case , u_{ij} between each solvent-ion pair is tuned on MIAC data where $l_{ij}=0$. A negative value of u_{ij} indicates higher association in the model whereas a positive value is an indication of lower association strength.
- Case(b) Table 5.5 : Repulsion parameter (l_{ij}) tuning : In this case, association interactions are turned off ($u_{ij}=1$), and l_{ij} between each solvent-ion pair is tuned on MIAC data. A negative value of l_{ij} indicates higher ionic diameter i.e more repulsion that accounted in the model, whereas a positive value indicates lesser repulsion.
- Case(c) Table 5.6 : Both association parameter u_{ij} and repulsion parameter l_{ij} are tuned simultaneously between each solvent-ion pair.

The deviation obtained for each system is available in table 5.3. While the parameters obtained through these approaches may or may not work successfully for LLE modeling, their qualitative trend will reveal the nature of the interactions these systems have. To this end, the values of the regressed parameters are plotted against Pauling diameter to observe a trend in fig 5.19 - fig 5.20 for cases (a), (b) and (c).

In case (a): For methanol, the u_{ij} parameters are high and negative (for cations), this indicates that there are actually higher association interactions than it was accounted earlier in the model, this is also true since Li^+, Na^+ have higher charge density than other cations and they like forming solvated structures with the solvent. In contrast, the anions do not take part as much in the solvation as cations. Hence their association strength is

Table 5.3: Experimental MIAC data at 298.15K of mixed solvent salt systems used for ion-solvent parameter regression, deviations from calculation using case(c) are reported in % AAD of MIAC

System	weight fraction(%) alcohol	molality range	% AAD	Ref
Methanol-Water-NaF	10,20,30	0-0.1	3.3	[257]
Methanol-Water-NaCl	10,20,30	0-1.5	2.5	[258]
Methanol-Water-RbCl	10,20,30,40	0-3	7.9	[259]
Methanol-Water-CsCl	10,20,30,40	0-3	9.8	[259]
Ethanol-Water-LiCl	20,40	0-4	2.6	[260]
Ethanol-Water-NaF	20,30,40	0-0.2	10.7	[261]
Ethanol-Water-NaCl	20,40	0-2	9.5	[262]
Ethanol-Water-NaBr	10,20,40	0-5	7.1	[263]
Ethanol-Water-CsCl	10,20,30,40	0-0.8	7.0	[264]
1-Propanol-Water-KCl	10,20,30,40	0-3	6.9	[242]
2-Propanol-Water-NaF	10,20,30,40	0-0.5	3.3	[257]
2-Propanol-Water-NaBr	10,20,40	0-0.2	2.7	[265]
1-Butanol-Water-NaCl	10,20,40	0-2	3.9	[266]

thus low as compared to cations. Although, clear and coherent trend is not exhibited by the parameters, this is due to scarce data and unavailable for all salts.

For ethanol, parameters are adjusted between the OH (group of ethanol) and ions. The parameters follow a similar trend for cation parameters as in methanol. However, for anions the values are negative except for F^- , this is the reversal of the expected behaviour, it exhibits that anions also take part in solvation structure formation along with cations. This could be due to fact that since ethanol is bulkier than methanol, it is easier for anions to break the existing hydrogen bonded structure between water and ethanol thus separating out free ethanol for solvation.

For propanol and 1-butanol, parameters again show a similar trend for cations as well as for anions, moreover, the values are more negative than those in ethanol. This is a validation to previous hypothesis that due to bulkier structure of propanol/1-butanol, anions can easily break the hydrogen bonded structure between water and alcohol, thus liberating alcohol for solvation.

In case (b): For methanol, the parameters l_{ij} are positive for Li^+ and goes further negative for Na^+ and higher cations. This indicates that the effective cross diameter of the alcohol solvent and cation is smaller, and so the repulsion are lower than those accounted in the model. This then corresponds to an effective attraction.

Table 5.4: Solvent-ion parameters for mixed-solvent salt systems (Case a: Association parameter tuning u_{ij})

	Li ⁺	Na ⁺	K ⁺	Rb ⁺	Cs ⁺	F ⁻	Cl ⁻	Br ⁻	I ⁻
Methanol	-11.807	-14.537	-	-6.840		0.9	0.903	-	-
Ethanol (OH-group)	-4.431	-0.391	-	-	0.599	0.615	-0.890	-2.258	-
Propanol Butanol (OH-group)	-	-11.647	0.465	-	-	0.623	-3.383	0.989	-

Table 5.5: Solvent-ion parameters for mixed-solvent salt systems (Case b: Repulsion parameter tuning l_{ij})

	Li ⁺	Na ⁺	K ⁺	Rb ⁺	Cs ⁺	F ⁻	Cl ⁻	Br ⁻	I ⁻
Methanol	0.977	-0.623	-	-1.306	-0.572	-2.191	0.202	-	-
Ethanol	-1.238	-2.511			-3.428	-2.524	0.689	0.998	
Propanol Butanol (OH-group)	-	0.99	0.99	-	-	-2.1	-0.99	-0.157	-

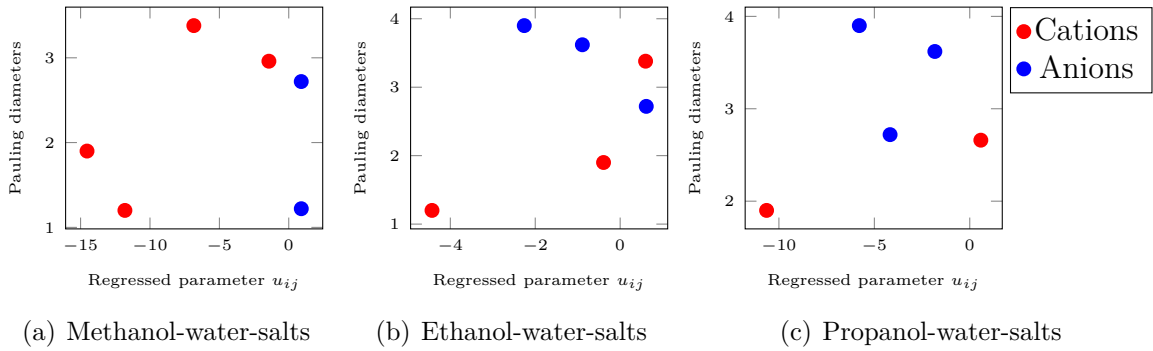
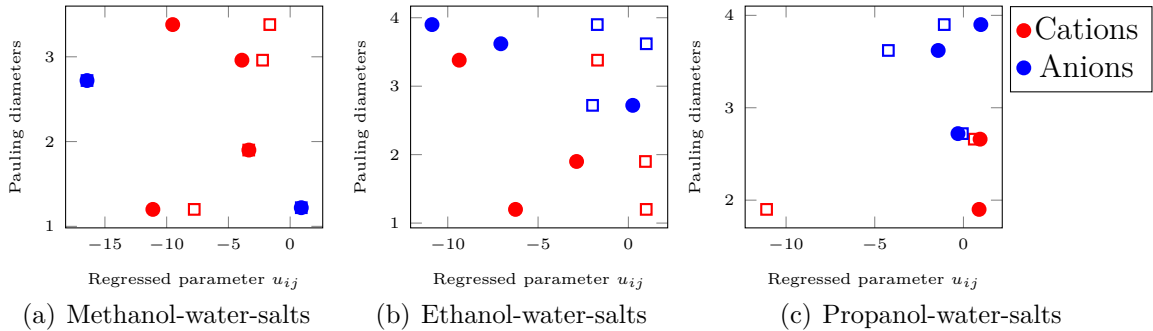
For ethanol we also observe a similar trend where the negative value for l_{ij} for Li⁺ goes further negative for cations Na⁺ and Cs⁺

For propanol/1-butanol we observe that this does not hold true and we believe this case has clearly failed in case of propanol/butanol mixed solvent salt systems.

In case (c): This is the case where both l_{ij} and u_{ij} parameters were adjusted simultaneously for all available MIAC data for respective mixed solvent salt systems. Although, we found that the deviation are lower as compared to the previous two cases, for propanol/butanol the parameter do not follow an expected trend.

Table 5.6: Solvent-ion parameters for mixed-solvent salt systems (Case c: Association parameter u_{ij} and Repulsion parameter tuning l_{ij})

		Li ⁺	Na ⁺	K ⁺	Rb ⁺	Cs ⁺	F ⁻	Cl ⁻	Br ⁻	I ⁻
Methanol	u_{ij}	-11.117	-3.342	-	-3.906	-9.513	0.902	-16.449	-	-
	l_{ij}	-7.766	-3.354	-	-2.232	-1.649	0.899	0.789	-	-
Ethanol (OH-group)	u_{ij}	-6.246	-2.868	-	-	-9.366	0.243	-7.061	-10.872	-
	l_{ij}	0.989	0.945	-	-	-1.708	-1.983	0.991	-1.721	-
Propanol Butanol (OH-group)	u_{ij}	-	0.882	0.940	-	-	-1.424	0.981	-0.308	-
	l_{ij}	-	-11.099	0.612	-	-	-4.233	-1.082	-0.06	-

**Figure 5.19:** Plot of the regressed alcohol-ion parameter u_{ij} against Pauling diameters: Case(a)**Figure 5.21:** Plot of the regressed alcohol-ion parameter l_{ij} (red circles) and u_{ij} (red squares) against Pauling diameters: Case(b)

5.4.4 Result of MIAC for mixed solvent electrolytes

The plot of MIAC for all systems that are studied is presented in this section: The case (c) obviously provides the best representation among all approaches, since it has more

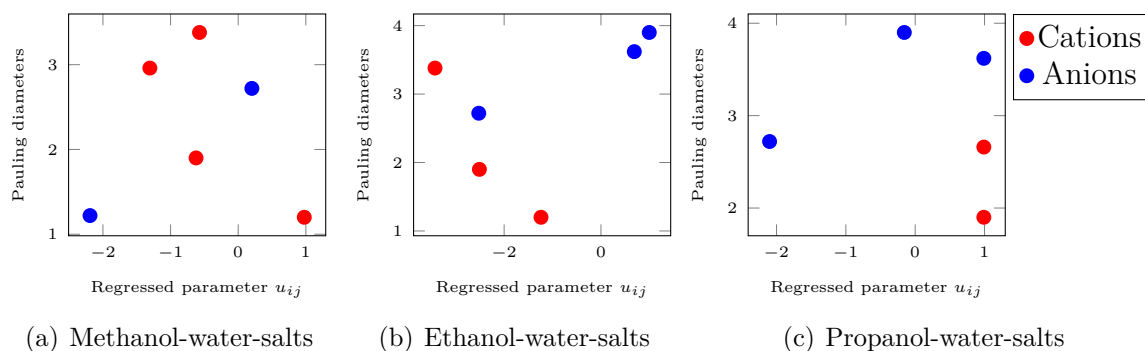


Figure 5.20: Plot of the regressed alcohol-ion parameter l_{ij} against Pauling diameters: Case(b)

flexibility in terms of parameterization. The plots are drawn for this case by full thick lines, while experimental data is represented by points.

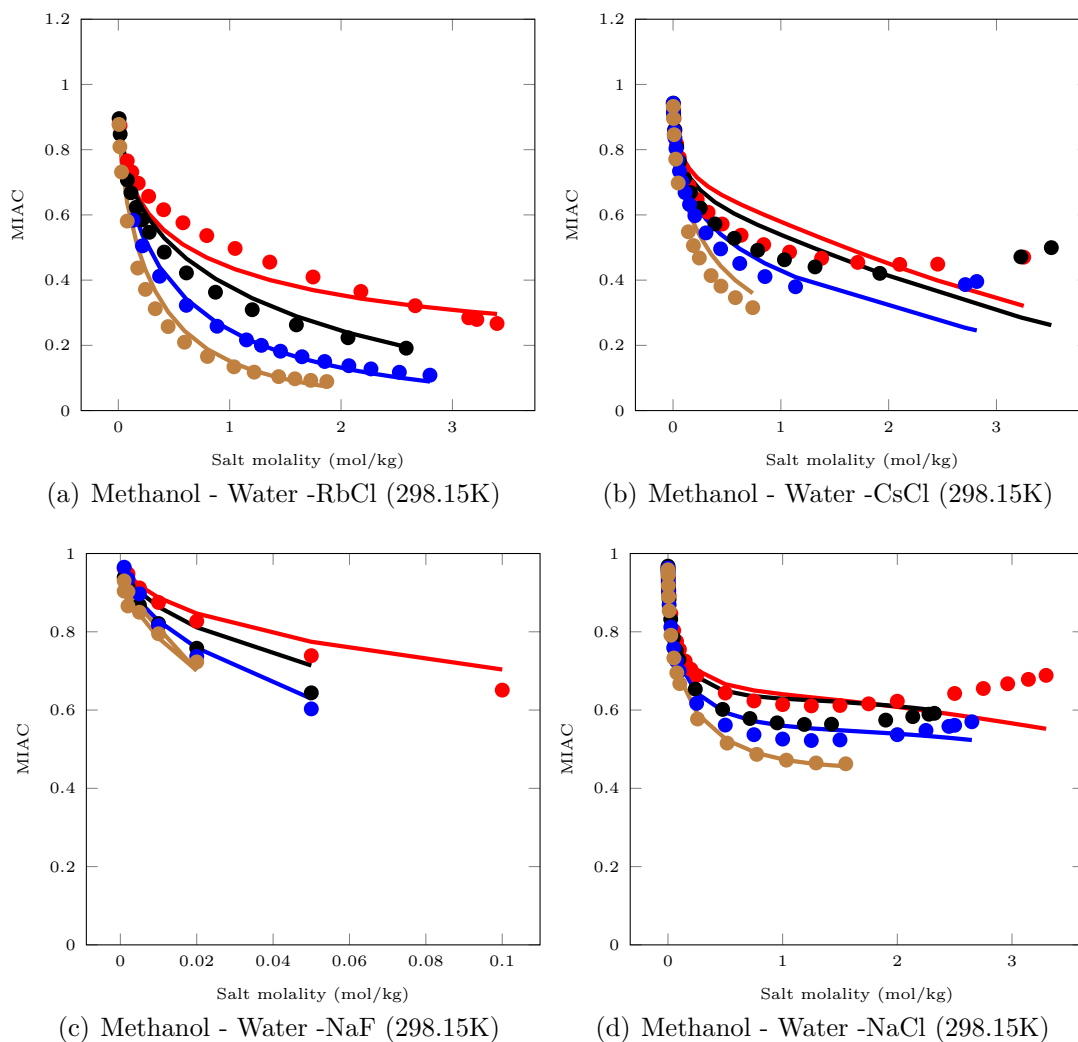


Figure 5.22: Mean Ionic activity coefficients of Methanol-water-NaCl systems at varying weight fraction (w_m) (10% —, 20% —, 30% —, 40% —), points: experimental data, full lines: case (c)

The model is able to represent the activity coefficients for methanol-water-salts systems with satisfactory accuracy as whole using case (c). However, there are systematic deviations at higher salt molalities (larger than 2m), where the theory could not capture the upward trend as exhibited by the experimental data. The reason for this behavior could be further analyzed by evaluating the behavior of each term of the equation, as illustrated in chapter 4. It is well known that thermodynamic models have difficulties describing high salinities. At high salinities, dielectric constant by Pottel may not be correctly represented, resultingly, the Born term is being reduced because dielectric constant is reduced.

The model is also able to represent the trend of varying alcohol weight fraction, where each curve represents a different fixed weight fraction of alcohol. The higher the alcohol concentration, the deeper the curve goes which is already observed previously in this chapter. The fact that the theory can correctly correlate this phenomenon provides an evidence that the change in interaction by varying alcohol-water concentration is captured. The MIAC's of ethanol-water-salt systems are also correctly represented by the theory using parameter set (c). The similar trend was observed and can be explained with similar argument that were made for methanol-water-salt systems. In this case the ethanol is bulkier than methanol, resulting in weaker hydrogen bonded structure between water and ethanol as compared to water and methanol. Since salt can now break the water-alcohol at smaller molalities, we see the minimum in the curves come at lower molalities, but in some cases flattens out at higher molalities.

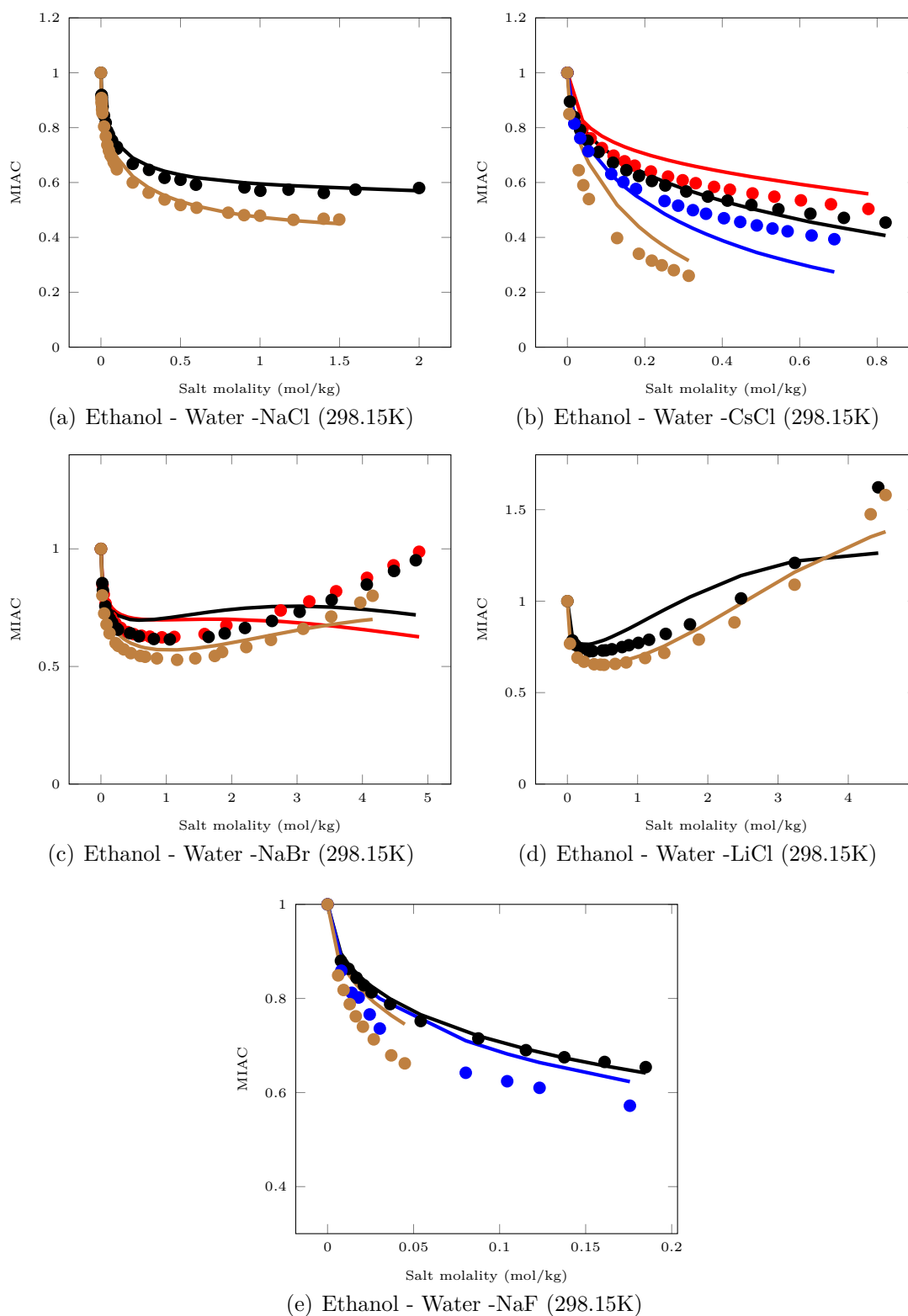


Figure 5.23: Mean Ionic activity coefficients of Ethanol-water-NaCl systems at varying weight fraction (w_m) (10% —, 20% —, 30% —, 40% —), points: experimental data, full lines: case (c)

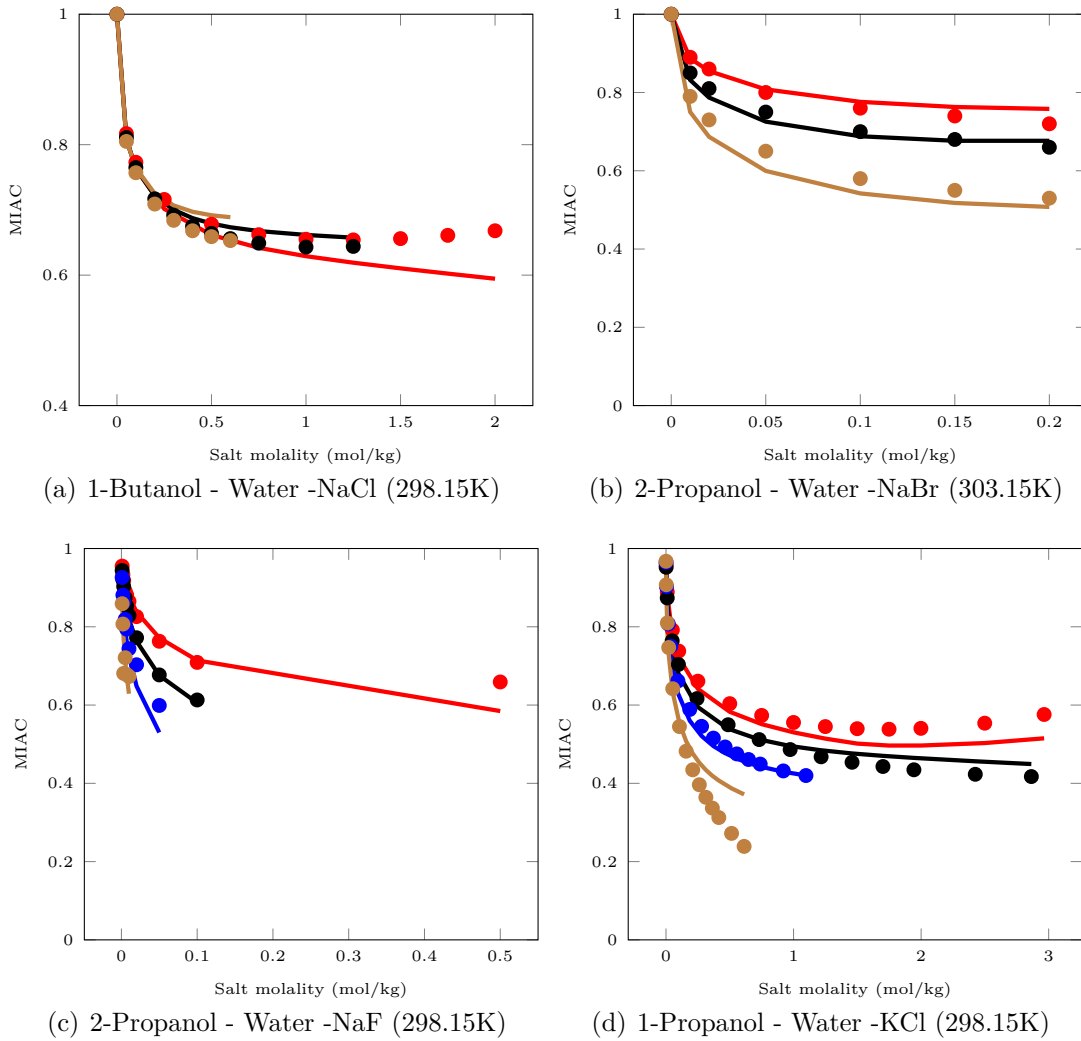


Figure 5.24: Mean Ionic activity coefficients of Propanol/ Butanol-water-NaCl systems at varying weight fraction (w_m) (10% —, 20% —, 30% —, 40% —), points: experimental data, full lines: case (c)

The MIAC's of propanol/butanol-water-salt system are crucial since with the parameter set obtained for these systems the LLE of these systems will be modeled. The problem is that data are very scarce and sometimes available for small range of salt molalities. Therefore it is challenging to correctly tune the parameters that would better represent the LLE of these systems. Nonetheless, with case (c) the MIAC's are correctly represented by the theory, where the result follow the qualitative trend of varying salt concentration as well as varying salt molalities.

Since the MIAC data for 1-butanol/propanol-water-salt systems were not adequate, it was difficult to obtain a parameter set that could correctly capture the interactions

between ion-solvent. Furthermore, these parameters (case (c)) are less likely to give good prediction of LLE since there is no data that corresponds to alcohol concentration for organic region.

5.4.5 Parameter for 1-Butanol-water-salt systems from LLE data

It is interesting to note that many investigations that focus on LLE predictions show the quality of the phase diagrams (phase behavior) calculation. Yet, in industrial practice the true property of interest is the partition coefficients: when designing an extraction column, engineers want to know how well the target compounds are transferred from one phase to the other phase. This is why in this work we want to improve the prediction of this property. Let us first look at the data. The references used in this work are summarized in table 5.7. The experimental partition coefficients are shown in figures 5.34. Some systematic trends are observed.

Table 5.7: Experimental LLE data of mixed solvent salt systems used in the current work

System	T(K)	Dev %AAD (K_i)			Ref
		Alc	Water	Salt	
1-Butanol-Water-CsCl	293.15	12.9	3.6	21.7	[267]
1-Butanol-Water-LiCl	293.15	32.1	17	59	[267]
1-Butanol-Water-KCl	298.15	11.2	20.8	39	[268]
1-Butanol-Water-KCl	293.15	7.4	12.6	95.1	[267]
1-Butanol-Water-NaCl	298.15	16.4	10.2	35.7	[269, 270]
1-Butanol-Water-NaF	293.15	25.0	5.6	62.5	[271]
1-Butanol-Water-NaI	293.15	8.1	2.4	95.9	[272]
1-Butanol-Water-LiF	293.15	20.74	10	70.1	[271]
1-Butanol-Water-KF	293.15	19.5	5.0	42.6	[271]
1-Butanol-Water-RbCl	293.15	30.8	26.7	48.2	[267]

Upon the addition of salts, the aqueous phase becomes richer in water and the organic phase loses its water ($K_{alcohol} = \frac{x^{org}}{x^{aq}}$ increases where K_{water} decreases). Simultaneously the salt partitioning, which is generally very small but not negligible, decreases.

The observation can be readily understood from a theoretical perspective. The ionic species have a closer preference to be surrounded by water rather than by alcohol. Hence, when salt is added to the systems, the ions that are preferentially in the aqueous phase, will push the alcohol away into the organic phase, while it will attract all water it can from the organic phase. Doing so, the organic phase becomes poor in water and therefore has a worse solvating power for ions. The partitioning coefficients of salts should always follows that of water.

We chose to work on our second proposition for parameterization, to look at the various contributions of the ePPC-SAFT terms on the partition coefficient K_{salt} and see their qualitative trend. The calculation are made using the parameter set obtained for case (a) in the last section. The choice to use these parameters for this study is to draw a conclusion as to how well the model extrapolate to very high alcohol contents: MIAC data generally go up to 40% alcohol, while LLE modeling requires computation of activities in the organic phase that may contain up to 80% alcohol.

Table 5.8: Final solvent ion-parameters for propanol/butanol - water - salt systems

	Li ⁺	Na ⁺	K ⁺	Rb ⁺	Cs ⁺	F ⁻	Cl ⁻	Br ⁻	I ⁻
(OH-group)	-3.0	0.1	0.35	0.8	0.9	-0.9	0.8	0.9	0.99

The parameters presented in table 5.8 have been adjusted manually. The deviation on the partition coefficients are given in table 5.7. We do not claim that this is best possible parameter set. It should also be noted here that as there was no data for systems containing Br⁻ we could not verify the partition coefficient of Bromides.

The results of liquid-liquid equilibrium using this parameter set is presented in the next section for all the available mixed solvent electrolyte systems (figure 5.25-5.34).

The parameters obtained using this procedure were tested back on the MIAC of propanol/1-butanol-water-salt systems. Interestingly, MIAC of 1-butanol-water-NaCl were correctly predicted (7% AAD), but the MIAC's of 1-Propanol and 2-propanol salt systems had deviations upto 90% AAD with the same parameters. Obviously, this is due to the fact that the parameters from this approach are obtained focusing on 1-butanol-water-salt LLE (K_i). Whereas, the MIAC's were more focused on 1-propanol and 2-propanol (only one set of data for 1-butanol-water-NaCl). The deviation are most probably due to the assumption that the same interaction parameters can be used propanol ion and butanol ion interactions. In fact, the interactions propanol-ion and 1-butanol-ion seem quite different, and the group contribution concept cannot be applied.

5.5 Final results

The results of partition coefficients (figures 5.25-5.34) clearly show that the problem of systematic under prediction of the salt partition coefficient is resolved up to significant level as compared to these results presented in the section 5.3.1.1. However, for certain systems the partition coefficients are under-predicted. Theoretically, the curves (K_{salt})

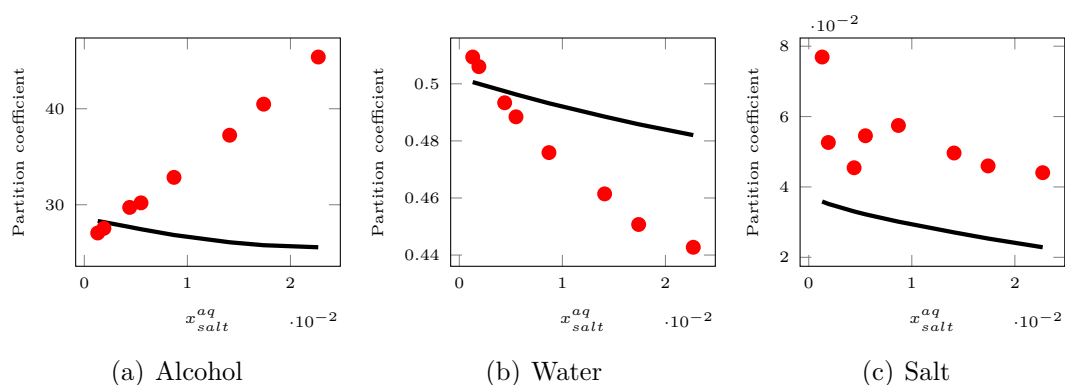


Figure 5.25: Partition coefficients of 1-Butanol - Water - CsCl system at 293.15K

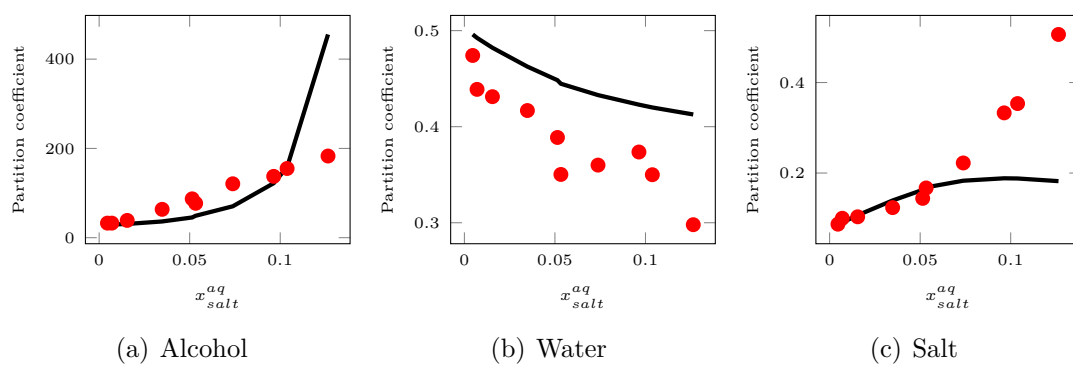


Figure 5.26: Partition coefficients of 1-Butanol - Water - LiCl system at 293.15K

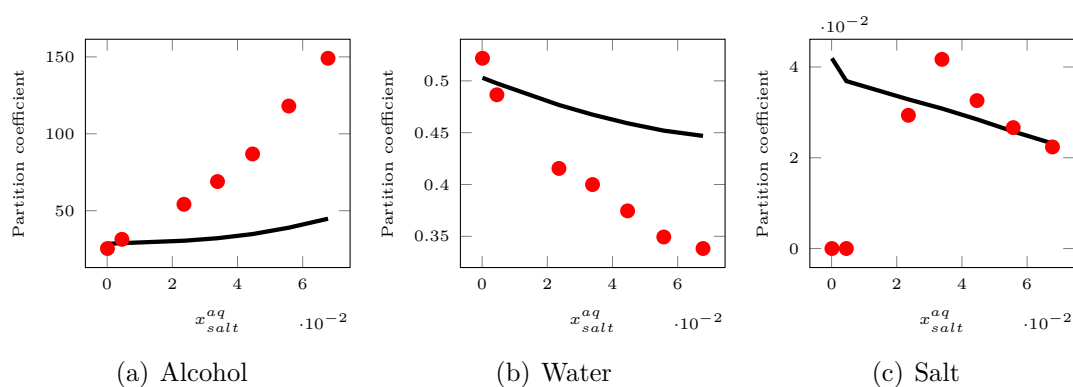


Figure 5.27: Partition coefficients of 1-Butanol - Water - KCl system at 298.15K

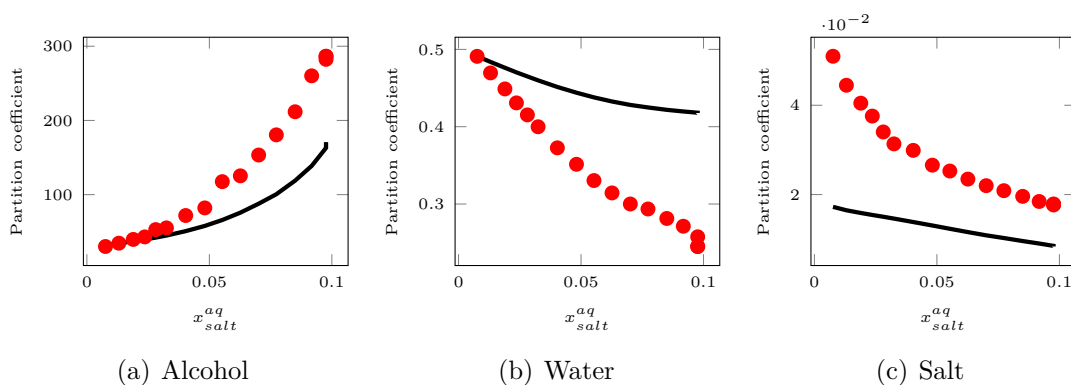


Figure 5.28: Partition coefficients of 1-Butanol - Water - NaCl system at 293.15K and 303.15K

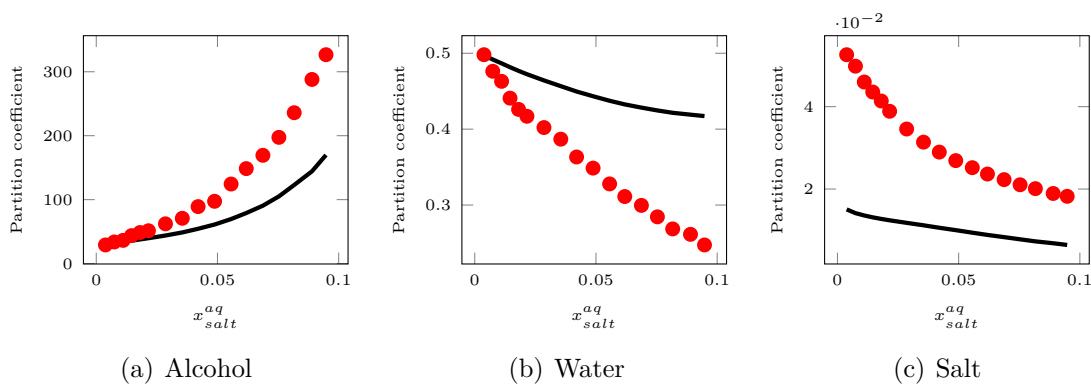


Figure 5.29: Partition coefficients of 1-Butanol - Water - NaCl system at 298.15K

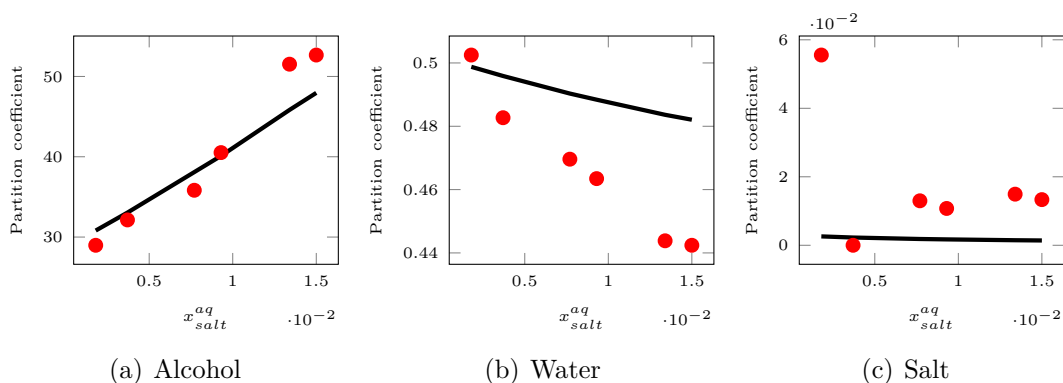


Figure 5.30: Partition coefficients of 1-Butanol - Water - NaF system at 293.15K

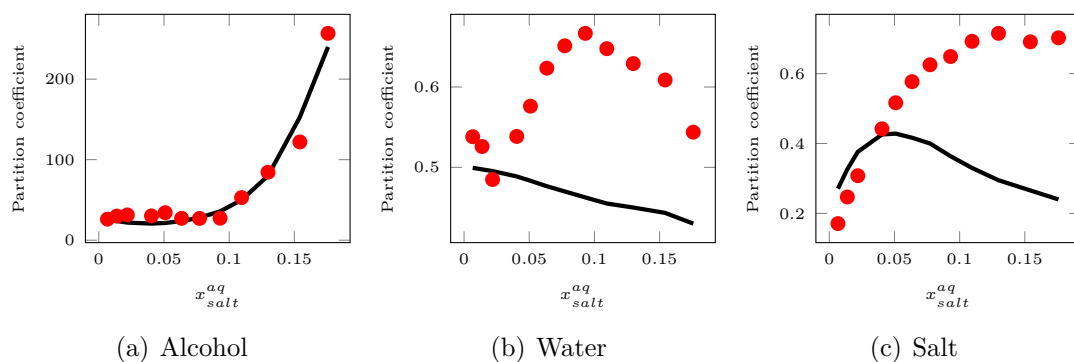


Figure 5.31: Partition coefficients of 1-Butanol - Water - NaI system at 293.15K

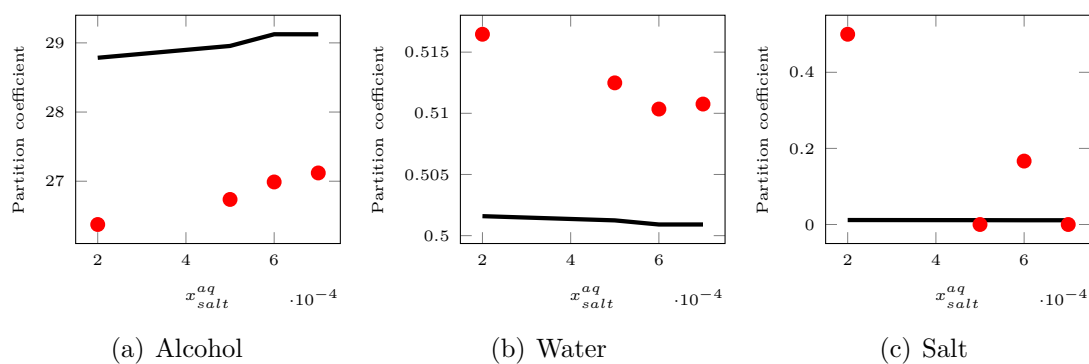


Figure 5.32: Partition coefficients of 1-Butanol - Water - LiF system at 293.15K

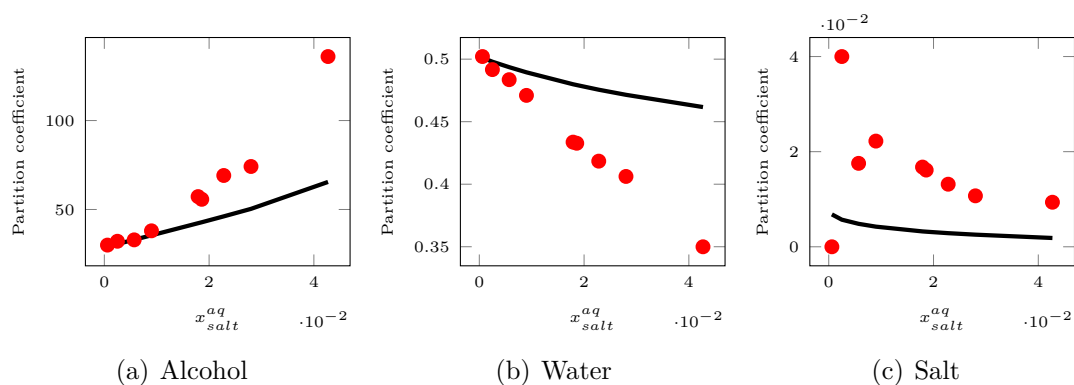


Figure 5.33: Partition coefficients of 1-Butanol - Water - KF system at 293.15K

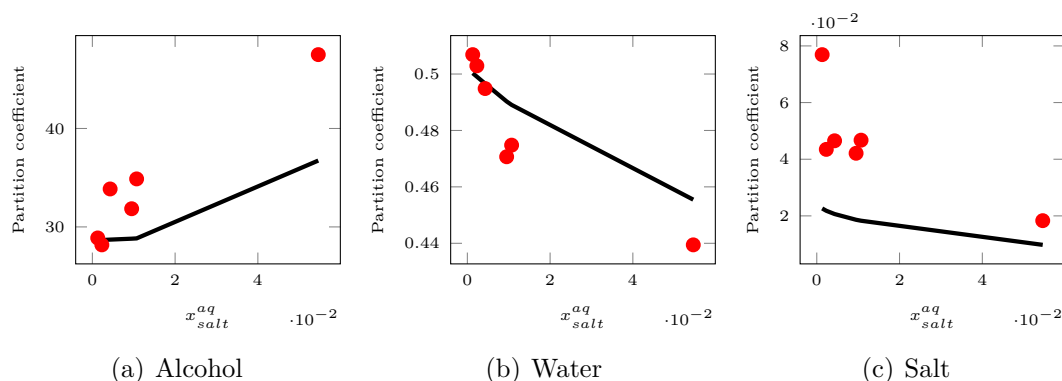


Figure 5.34: Partition coefficients of 1-Butanol - Water - RbCl system at 293.15K

should show an upward trend because the more salt in the system, the more contrast among the phases (organic contains more alcohol and aqueous contains more water).

For the CsCl system, the calculated alcohol partition coefficient incorrectly decreases the model. The model under-predicts the amount of 1-butanol in the organic phase, while it over-predicts the amount of water in organic phase, the salt partition coefficient has qualitatively improved since the last results. The reason for this may be the overestimation of the ion alcohol association, such that the salt has a salting-in effect rather than the expected salting-out effect.

For LiCl system, the partition coefficient of alcohol and water is represented correctly. The experimental salt partitioning trend is however unexpected. Here, increasing salt content results in more salt in the organic phase, despite a reduction of the amount of water in that phase. The model can reproduce the trend at the prices of a very large interaction between Li^+ and alcohol. The partition coefficient of salt is also qualitatively represented but at higher salt concentration of alcohol in organic phase increases after certain composition and we see the partition coefficient plot flattens out. This is again due to same fact that a higher alcohol composition, the proportional amount of salt does not remain in organic phase and prefers to go into the aqueous phase.

For KCl systems the global salt concentration is very small. We see an under-prediction in partition coefficients of alcohol but this time the degree of under-prediction is lower as compared to that of CsCl and the trend (increasing $K_{alcohol}$ with salt content) is respected. It is in between LiCl and CsCl, thus, the similar reasoning holds as given for the preceding two systems that K^+ has a charge density and ionic radii in between Li^+ Rb^+ . The solvation structures are stronger than CsCl but weaker and less likely than LiCl.

For NaCl systems, the similar arguments can be used to explain the trend in the partition coefficients, which is slightly under-predicted for alcohols, slightly over-predicted for water, and under-predicted for salts.

For NaF systems this problem was to lesser degree and it can be observed that the partition coefficients are correctly represented with good level of accuracy.

For NaI system the partition coefficient of NaI was observed to be extremely large (up to 1.6) and suggesting a trend that is clearly opposite to the expected one, the more salt in the systems, the more it goes in the organic phase, while this phase clearly contains more alcohol. In order to be able to model this trend, it was needed to almost deactivate the I^- 1-butanol interaction ($u_{ij} = 0.99$). The result is maximum in the K_{salt} : at low salt content, increasing the amount of salt will draw more salt into the organic phase, while at high salt content, the opposite expected behavior will take over. This is the reason I^- ion prefer to stay with water rather than 1-butanol according to our model.

For LiF system, only very few data are available and at very small salt molalities. The scatter on the salt partitioning is also very large, so it is very difficult to reach a final conclusion.

For RbCl system, the results of the partition coefficients can be explained by the same explanation which is drawn for other chloride systems. In this system too under-prediction of alcohol partition coefficient and under-prediction of salt partition are apparent.

5.6 Conclusion

Modeling LLE of mixed solvent electrolyte systems invite several challenges. Even the most advanced thermodynamic EoS face several shortcomings when modeling such systems. First challenge was the imposition of electroneutrality law in the model. A new methodology was proposed which is consistent for any single salt system. With the help of this method, the electroneutrality was taken into account by simple modification of the calculated fugacity coefficients.

The second challenge was to identify the most effective parameters to improve the partition coefficients and specifically, that of salts. The analysis of the effect of the various ePPC-SAFT terms on this property showed that three terms drive this phenomena (Hard chain, Born, and association): the entropic or hard chain term, no interaction parameter is available for this term, but the use of an additional, non-additive hard sphere term (NAHS) makes it possible to modify this contribution.

The Born term is driven by the difference in the dielectric constant between the two phases. Data on the dielectric constant of mixed solvent exist and a mixing rule was

designed so as to correlate these data. With almost little or no data of dielectric constant for mixed solvent salt systems and no clear existing model to calculate this property, the current thermodynamic framework relies on the efficiency of the mixing rule. Moreover, the effect of ions on the dielectric constant also cannot be ignored. Therefore, Pottel's model for ion-effects to calculate dielectric constant was implemented. Evidently, this gave satisfactory result of dielectric constant for mixed solvent, however, the effect of ions cannot be verified with data. Nonetheless, this property plays a crucial role in the partitioning of species in the two phases. Ions like to be in the phase where the dielectric constant is higher. The association term that mimics the structure forming effect of the ions. The association strength between ions and alcohols is a parameter that can be used and has effectively a great impact on the results.

The third challenge was the parameterization of ion-solvent parameters. In order to parameterize these systems, MIAC of mixed solvent electrolytes were used, which were satisfactorily represented by the model. However, those parameters tuned on MIAC's failed to give correct representation of LLE. The partition coefficients of salt were systematically under predicted. Therefore, a new parameterization strategy was adapted based on analyzing partition coefficients of individual species. This analysis brought into focus the various contributions that played a dominant role in the deviations for partition coefficients. Based on this analysis, the values of parameters were predicted so as to improve these partition coefficient. Finally, a parameter set was found which could satisfactorily represent the experimental values of the partition coefficient of salts, alcohols and water.

Chapter 6

Conclusions and recommendations for future work

6.1 Conclusion

The objective of this work is to holistically develop a predictive and advanced equation of state such as PC-SAFT to model LLE of mixed solvent electrolytes. The current research was performed to do exactly that. eGC-PPC-SAFT EoS was adapted and enhanced to model the liquid-liquid equilibrium of the mixed solvent electrolyte systems. This objective was achieved by systematic study and modeling of, first non-electrolyte systems, then single solvent electrolyte systems and finally mixed-solvent electrolyte systems. During the course of this research, the model was critically evaluated and enhanced at several stages so as to achieve a predictive model for LLE of mixed solvent electrolytes. While modeling of electrolytes and mixed solvent electrolytes is not new and is being studied by many research group, the current research stands out due to the following reasons.

- **First step:** The model was made accurate for water. The prominent and ubiquitous solvent water was studied and it was found necessary to improve the deviation in liquid densities and vapor pressure for pure water. Thus, a modification was introduced which then successfully yielded an improved model for water, hydrocarbons and oxygenates mixtures. This was verified by modeling VLE, VLLE and LLE of various mixed solvent systems which showed a good agreement to experimental data. This was thus a clear indication that deviations in mixed solvents are correctly taken into account by the model. Since the current model uses group contribution approach, there are fewer parameters (one per family) to model the systems. This is a significant advantage in terms of predictive capability.
- **Second step:** The improved model was then utilized to model the aqueous salt systems for MIAC's, liquid densities and VLE. This model is based on the primitive

version of non-restricted MSA and uses a Born term. This primitive MSA term gives flexibility in accounting only the requisite interactions specific to electrolytes in our thermodynamic framework. The Born term is essential in accounting the effect of changing the dielectric constant when they are transferred from one phase to another. Both these contributions were shown to be crucially important in modeling electrolyte systems. The dependence of the dielectric constant on the solvent composition is vital when using a primitive MSA or Born term. To this end, a model for dielectric constant that depend on temperature density and salt content is utilized in the current work. Finally, the thermodynamic framework was ion-specifically parameterized on 20 monovalent salts for their association parameter (ϵ^{AB}/k) and MSA diameters (σ_{MSA}). The parameterization was a challenging task since it was ion specific, included the difficult salts such as fluorides, and it was necessary to have physically meaningful trend on the optimized parameters. Subsequent to this parameterization, several VLE of alkane/alcohol and acid gases with aqueous salt systems were successfully modeled along with the evidence to show the salting-out effect. Parameters for certain systems were tuned on their VLE and the results showed a good agreement with the experimental data for most systems.

- **Third step:** The modeling of LLE of mixed solvent electrolyte systems was a challenging task, specially when there was a scarce amount of data to parameterize the interaction parameters. The initial modeling of LLE by our model without parameterization on ternary systems was able to qualitatively represent the partition coefficients of solvent and water, but systematic under-prediction were seen for salts. The reason is that the alcohol content in the organic phase is generally much higher than what is found in systems for which MIAC data exists. The parameterization of solvent-ion binaries was then attempted on whatever MIAC data was available for mixed-solvent electrolytes. But, still these parameters failed to improve the partition coefficient of salts. Finally, a methodology was proposed to predict the solvent-ion parameter that successfully represented the partition coefficients of salts for various mixed solvent electrolytes.

Through the research carried out in this work on the mixed solvent electrolytes, the following facts are concluded.

The e-PPC-SAFT approach where the residual Helmholtz energy is computed as a sum of contributions, each referring to a specific type of interaction is a tool that can be used to understand the balance of forces yielding the observed physical behavior. The traditional contribution for non-electrolytes are well-know. When it comes to systems that contain ionic species, additional contribution must be included. The following choices have been made.

- The Coulombic ion-ion interaction are modeled using a non-restricted primitive mean spherical approximation (MSA). This version includes only ion-ion interactions as opposed to three different interactions (ion-ion, ion-dipole and dipole-dipole) in its non-primitive counterpart.
- The effect of variable dielectric constant on the ion energy is described using a Born term. An adequate description of the dielectric constant is key for application, and more work can probably be done to further improve the model.

The current framework defines ions as associating species with association sites like any other associating hard sphere. This provided the capability to allow ions to interact with the neighbouring solvent molecules (polar hard spheres) and other ions.

Since we used a non-restricted primitive MSA, that describes each ion of different diameters, the correct parameterization of these diameter was essential. In addition, we used association for ions, so association parameter (ε^{AB}/k) was also needed to be parameterized. Our choice of ion-based parameterization proved better in term of predictive capability. This also provided ability to model any system of different salts with the same ion parameters.

LLE of mixed-solvent electrolyte systems are difficult to model and the underlying theoretical model for the solvent must be as accurate as possible. In the absence of such accuracy, even a small amount of deviation in the partitioning of solvent or water in the two phases can significantly affect the partitioning of salt species. These partitioning of salt species are then difficult to improve since there are restricted number of parameters that can be tuned. Therefore, it is necessary to have an accurate model as much as possible for water and solvent mixtures.

6.2 Recommendations for future work

This work hints at a possible methodology for improving such complex systems. Using an improved tuning of the dielectric constant with the salt concentration, it should

be possible to catch both the dilute alcohol as the concentrated alcohol salt activities, As a consequence, it should be possible to describe both MIAC and LLE. Also, each alcohol should have its own binary parameter with each one (the hydroxyl group cannot be considered equivalent in all cases)

The current model is extensible and can be used to study the following.

Multivalent salts: Bivalent and trivalent salt systems can be parameterized using the same methodology and parameterization schemes as developed in this work. Only the parameters for the new set of ions would be required to be tuned on MIAC's and AMV for their respective salts.

Weak electrolytes: The weak electrolytes are those that do not get fully dissociated in the aqueous state. There exist an equilibrium dissociation constant that provides the ration of ions to the un-dissociated salts. Those systems require additional parameter between solvent and undissociated salts. The current model can be extended to model these systems.

Reactive mixed solvent salt systems: Organic aqueous amine solution with CO_2 and H_2S that are present in carbon capture and acid gas treatment process can be modeled using the present model. However, these systems are reactive and require taking into account their kinetic as well as physico-chemical properties.

Aqueous two phase systems: The current model can be extended to model the partitioning of protein and macro-molecules in aqueous two phases systems that find wide use in pharmaceutical and bio-science industry.

Bibliography

- [1] Otto. Redlich and J. N. S. Kwong. On the thermodynamics of solutions. v. an equation of state. fugacities of gaseous solutions. *Chemical Reviews*, 44(1):233–244, 1949.
- [2] Waals, J. D. van der and J. S. Rowlinson. *J.D. van der Waals: On the continuity of the gaseous and liquid states / edited with an introductory essay by J.S. Rowlinson*, volume vol.14 of *Studies in statistical mechanics*. North-Holland, Amsterdam, 1988.
- [3] Ding-Yu Peng and Donald B. Robinson. A new two-constant equation of state. *Industrial & Engineering Chemistry Fundamentals*, 15(1):59–64, 1976.
- [4] Georgios M. Kontogeorgis, Ioannis Tsivintzelis, Nicolas von Solms, Andreas Grenner, David Bøgh, Michael Frost, Anders Knage-Rasmussen, and Ioannis G. Economou. Use of monomer fraction data in the parametrization of association theories. *Fluid Phase Equilibria*, 296(2):219–229, 2010.
- [5] Kaj Thomsen. *Electrolytes Notes*. 2009.
- [6] Eric Hendriks, Georgios M. Kontogeorgis, Ralf Dohrn, Jean-Charles de Hemptinne, Ioannis G. Economou, Ljudmila Fele Žilnik, and Velisa Vesovic. Industrial requirements for thermodynamics and transport properties. *Industrial & Engineering Chemistry Research*, 49(22):11131–11141, 2010.
- [7] Denis S. Abrams and John M. Prausnitz. Statistical thermodynamics of liquid mixtures: A new expression for the excess gibbs energy of partly or completely miscible systems. *AIChE Journal*, 21(1):116–128, 1975.
- [8] Chau-Chyun Chen, Costas P. Bokis, and Paul Mathias. Segment-based excess gibbs energy model for aqueous organic electrolytes. *AIChE Journal*, 47(11):2593–2602, 2001.
- [9] Chau-Chyun Chen, H. I. Britt, J. F. Boston, and L. B. Evans. Local composition model for excess gibbs energy of electrolyte systems. part i: Single solvent, single completely dissociated electrolyte systems. *AIChE Journal*, 28(4):588–596, 1982.
- [10] C.-C. Chen. Some recent developments in process simulation for reactive chemical systems. *Pure and Applied Chemistry*, 59(9), 1987.
- [11] Aage Fredenslund, Russell L. Jones, and John M. Prausnitz. Group-contribution estimation of activity coefficients in nonideal liquid mixtures. *AIChE Journal*, 21(6):1086–1099, 1975.
- [12] R. Dohrn and O. Pfohl. Thermophysical properties—industrial directions. *Fluid Phase Equilibria*, 194-197:15–29, 2002.

- [13] John P. O'Connell, Rafiqul Gani, Paul M. Mathias, Gerd Maurer, James D. Olson, and Peter A. Crafts. Thermodynamic property modeling for chemical process and product engineering: Some perspectives. *Industrial & Engineering Chemistry Research*, 48(10):4619–4637, 2009.
- [14] Sunmish Gupta and James D. Olson. Industrial needs in physical properties. *Industrial & Engineering Chemistry Research*, 42(25):6359–6374, 2003.
- [15] Paul M. Mathias. Applied thermodynamics in chemical technology: current practice and future challenges. *Fluid Phase Equilibria*, 228-229:49–57, 2005.
- [16] Karen Huff. Applied thermodynamics for process modeling. *AIChE Journal*, 48(2):194–200, 2002.
- [17] Bjørn Maribo-Mogensen. Development of an electrolyte cpa equation of state for applications in the petroleum and chemical industries, phd thesis, technical university of denmark. 2014.
- [18] A. Groysman and N. Erdman. A study of corrosion of mild steel in mixtures of petroleum distillates and electrolytes. *Corrosion*, 56(12):1266–1271, 2000.
- [19] A. Groysman. Corrosion problems and solutions in oil, gas, refining and petrochemical industry. *Koroze a ochrana materialu*, 61(3):905, 2017.
- [20] M.D Jager, C.J Peters, and E.D Sloan. Experimental determination of methane hydrate stability in methanol and electrolyte solutions. *Fluid Phase Equilibria*, 193(1):17 – 28, 2002.
- [21] Pankaj D. Dholabhai, J. Scott Parent, and P. Raj Bishnoi. Equilibrium conditions for hydrate formation from binary mixtures of methane and carbon dioxide in the presence of electrolytes, methanol and ethylene glycol. *Fluid Phase Equilibria*, 141(1):235 – 246, 1997.
- [22] Peter Englezos. Clathrate hydrates. *Industrial & Engineering Chemistry Research*, 32(7):1251–1274, 1993.
- [23] Ahmadun Fakhru'l-Razi, Alireza Pendashteh, Luqman Chuah Abdullah, Dayang Radiah Awang Biak, Sayed Siavash Madaeni, and Zurina Zainal Abidin. Review of technologies for oil and gas produced water treatment. *Journal of Hazardous Materials*, 170(2):530 – 551, 2009.
- [24] Soraya Honarparvar, Sina Hassanjani Saravi, Danny Reible, and Chau-Chyun Chen. Comprehensive thermodynamic modeling of saline water with electrolyte nrtl model: A study on aqueous $\text{Ba}_2^+ \text{-Na}^+ \text{-Cl-SO}_4^{2-}$ quaternary system. *Fluid Phase Equilibria*, 447:29–38, 2017.
- [25] J.C.M. Pires, F. G. Martins, M.C.M. Alvim-Ferraz, and M. Simões. Recent developments on carbon capture and storage: An overview. *Chemical engineering Research and design*, 89(9):1446–1460, 2011.
- [26] Nikolaos I. Diamantonis and Ioannis G. Economou. Evaluation of statistical associating fluid theory (SAFT) and perturbed chain-SAFT equations of state for the calculation of thermodynamic derivative properties of fluids related to carbon capture and sequestration. *Energy & Fuels*, 25(7):3334–3343, 2011.

- [27] John J. Carroll. *Acid gas injection and carbon dioxide sequestration*. Wiley-Scrivener, Salem, Mass., 2010.
- [28] Abolghasem Jouyban. *Handbook of solubility data for pharmaceuticals*. CRC Press, Boca Raton, 2010.
- [29] R. M. Enick and S. M. Klara. Effects of CO₂ solubility in brine on the compositional simulation of co2 floods. *SPE Reservoir Engineering*, 7(02):253–258, 2013.
- [30] J. Krissmann M. Luckas. *Thermodynamik der Elektrolytlösungen: Eine einheitliche Darstellung der Berechnung komplexer Gleichgewichte*. Springer Berlin Heidelberg, Berlin, Heidelberg, 2001.
- [31] A. D. Diamond and J. T. Hsu. Fundamental studies of biomolecule partitioning in aqueous two-phase systems. *Biotechnology and bioengineering*, 34(7):1000–1014, 1989.
- [32] Ioannis G. Sargantanis and M. N. Karim. Prediction of aqueous two-phase equilibrium using the flory–huggins model. *Industrial & Engineering Chemistry Research*, 36(1):204–211, 1997.
- [33] Toshiaki Hino and John M. Prausnitz. Lattice thermodynamics for aqueous salt-polymer two-phase systems. *Journal of Applied Polymer Science*, 68(12):2007–2017, 1998.
- [34] Hans-Olof Johansson, Gunnar Karlström, Folke Tjerneld, and Charles A. Haynes. Driving forces for phase separation and partitioning in aqueous two-phase systems. *Journal of Chromatography B: Biomedical Sciences and Applications*, 711(1-2):3–17, 1998.
- [35] Justyna Rozmus. Predictive electrolyte equation of state for co2 capture, phd thesis, pierre and marie curie university and ifp energies nouvelles.
- [36] Georgios M. Kontogeorgis and Georgios K. Folas. *Thermodynamic models for industrial applications: From classical and advanced mixing rules to association theories*. Wiley, Hoboken, N.J., 2010.
- [37] José O. Valderrama. The state of the cubic equations of state. *Industrial & Engineering Chemistry Research*, 42(8):1603–1618, 2003.
- [38] Jean-Charles de Hemptinne and Jean-Marie Ledanois. *Select Thermodynamic models for Process simulation: A Practical Guide using a Three Steps Methodology, IFP Energies nouvelles, Editions Technip, 2012*.
- [39] Justyna Rozmus, Jean-Charles de Hemptinne, Amparo Galindo, Simon Dufal, and Pascal Mougin. Modeling of strong electrolytes with eppc-saft up to high temperatures. *Industrial & Engineering Chemistry Research*, 52(29):9979–9994, 2013.
- [40] Kenneth S. Pitzer. Thermodynamics of electrolytes. i. theoretical basis and general equations. *The Journal of Physical Chemistry*, 77(2):268–277, 1973.
- [41] Kenneth S. Pitzer, editor. *Activity coefficients in electrolyte solutions*. CRC, Boca Raton, 2 edition, 1991.

- [42] Andrzej Anderko and Kenneth S. Pitzer. Equation-of-state representation of phase equilibria and volumetric properties of the system NaCl-H₂O above 573 K. *Geochimica et Cosmochimica Acta*, 57(8):1657–1680, 1993.
- [43] Michael L. Michelsen and Jørgen M. Møllerup. *Thermodynamic models: Fundamentals & computational aspects*. Tie-Line Publications, Holte, Denmark, 2nd ed. edition, 2007.
- [44] Yi Lin, Kaj Thomsen, and Jean-Charles de Hemptinne. Multicomponent equations of state for electrolytes. *AIChE Journal*, 53(4):989–1005, 2007.
- [45] Peiming Wang, Andrzej Anderko, and Robert D. Young. A speciation-based model for mixed-solvent electrolyte systems. *Fluid Phase Equilibria*, 203(1-2):141–176, 2002.
- [46] Jerzy J. Kosinski, Peiming Wang, Ronald D. Springer, and Andrzej Anderko. Modeling acid–base equilibria and phase behavior in mixed-solvent electrolyte systems. *Fluid Phase Equilibria*, 256(1-2):34–41, 2007.
- [47] Lin, Yi, Thomsen, and Kaj. Development of an equation of state for solution containing electrolytes, phd thesis. 2007.
- [48] Sugata P. Tan, Hertanto Adidharma, and Maciej Radosz. Recent advances and applications of statistical associating fluid theory. *Industrial & Engineering Chemistry Research*, 47(21):8063–8082, 2008.
- [49] M. S. Wertheim. Fluids with highly directional attractive forces. i. statistical thermodynamics. *Journal of Statistical Physics*, 35(1-2):19–34, 1984.
- [50] M. S. Wertheim. Fluids with highly directional attractive forces. ii. thermodynamic perturbation theory and integral equations. *Journal of Statistical Physics*, 35(1-2):35–47, 1984.
- [51] M. S. Wertheim. Fluids with highly directional attractive forces. iii. multiple attraction sites. *Journal of Statistical Physics*, 42(3-4):459–476, 1986.
- [52] M. S. Wertheim. Fluids with highly directional attractive forces. iv. equilibrium polymerization. *Journal of Statistical Physics*, 42(3-4):477–492, 1986.
- [53] Masoud Sadeghi, Christoph Held, Cyrus Ghotbi, Mohammad Jafar Abdekhodaie, and Gabriele Sadowski. Thermodynamic properties of aqueous glucose–urea–salt systems. *Journal of Solution Chemistry*, 43(6):1110–1131, 2014.
- [54] Christoph Held, Thomas Reschke, Sultan Mohammad, Armando Luza, and Gabriele Sadowski. ePC-SAFT revised. *Advances in Thermodynamics for Chemical Process and Product Design*, 92(12):2884–2897, 2014.
- [55] Thomas Reschke, Christoph Brandenbusch, and Gabriele Sadowski. Modeling aqueous two-phase systems: I. polyethylene glycol and inorganic salts as atps former. *Fluid Phase Equilibria*, 368:91–103, 2014.
- [56] Thomas Reschke, Christoph Brandenbusch, and Gabriele Sadowski. Modeling aqueous two-phase systems: II. inorganic salts and polyether homo- and copolymers as atps former. *Fluid Phase Equilibria*, 375:306–315, 2014.

- [57] Thomas Reschke, Christoph Brandenbusch, and Gabriele Sadowski. Modeling aqueous two-phase systems: III. polymers and organic salts as atps former. *Fluid Phase Equilibria*, 387:178–189, 2015.
- [58] Christopher J. Cramer and Donald G. Truhlar. A universal approach to solvation modeling. *Accounts of Chemical Research*, 41(6):760–768, 2008.
- [59] S. Mohammad, G. Grundl, Rainer Müller, W. Kunz, G. Sadowski, and C. Held. Influence of electrolytes on liquid-liquid equilibria of water/1-butanol and on the partitioning of 5-hydroxymethylfurfural in water/1-butanol. *Fluid Phase Equilibria*, 428:102–111, 2016.
- [60] Luca F. Cameretti, Gabriele Sadowski, and Jørgen M. Møllerup. Modeling of aqueous electrolyte solutions with perturbed-chain statistical associated fluid theory. *Industrial & Engineering Chemistry Research*, 44(9):3355–3362, 2005.
- [61] Christoph Held, Gabriele Sadowski, Aristides Carneiro, Oscar Rodríguez, and Eugénia A. Macedo. Modeling thermodynamic properties of aqueous single-solute and multi-solute sugar solutions with PC-SAFT. *AIChE Journal*, 59(12):4794–4805, 2013.
- [62] Justyna Rozmus, Isabelle Brunella, Pascal Mougin, and Jean-Charles de Hemptinne. Isobaric vapor–liquid equilibria of tertiary amine and n -alkane/alkanol binary mixtures: Experimental measurements and modeling with GC-PPC-SAFT. *Journal of Chemical & Engineering Data*, 57(11):2915–2922, 2012.
- [63] M. Born. Volumen und hydrationswärme der ionen. *Zeitschrift für Physik*, 1(1):45–48, 1920.
- [64] Henri Renon. Electrolyte solutions. *Fluid Phase Equilibria*, 30:181–195, 1986.
- [65] You-Xiang Zuo and Tian-Min Guo. Extension of the patel—teja equation of state to the prediction of the solubility of natural gas in formation water. *Chemical Engineering Science*, 46(12):3251–3258, 1991.
- [66] Jason A. Myers, Stanley I. Sandler, and Robert H. Wood. An equation of state for electrolyte solutions covering wide ranges of temperature, pressure, and composition. *Industrial & Engineering Chemistry Research*, 41(13):3282–3297, 2002.
- [67] Rémi Fauve, Xavier Guichet, Véronique Lachet, and Nicolas Ferrando. Prediction of H₂S solubility in aqueous NaCl solutions by molecular simulation. *Journal of Petroleum Science and Engineering*, 157:94–106, 2017.
- [68] J. O’M Bockris and Amulya K. N. Reddy. *Ionics*, volume v.1 of *Modern electrochemistry*. Kluwer Academic, New York, 2. ed. edition, 1998.
- [69] W. Fürst and H. Renon. Representation of excess properties of electrolyte solutions using a new equation of state. *AIChE Journal*, 39(2):335–343, 1993.
- [70] Radia Inchekel, Jean-Charles de Hemptinne, and Walter Fürst. The simultaneous representation of dielectric constant, volume and activity coefficients using an electrolyte equation of state. *Fluid Phase Equilibria*, 271(1-2):19–27, 2008.

- [71] Amparo Galindo, Alejandro Gil-Villegas, George Jackson, and Andrew N. Burgess. Saft-vre: Phase behavior of electrolyte solutions with the statistical associating fluid theory for potentials of variable range. *The Journal of Physical Chemistry B*, 103(46):10272–10281, 1999.
- [72] S. Mohammad, C. Held, E. Altuntepe, T. Köse, T. Gerlach, I. Smirnova, and G. Sadowski. Salt influence on MIBK/water liquid–liquid equilibrium: Measuring and modeling with ePC-SAFT and COSMO-RS. *Fluid Phase Equilibria*, 416:83–93, 2016.
- [73] Christoph Held, Luca F. Cameretti, and Gabriele Sadowski. Modeling aqueous electrolyte solutions. *Fluid Phase Equilibria*, 270(1-2):87–96, 2008.
- [74] Stefanie Herzog, Joachim Gross, and Wolfgang Arlt. Equation of state for aqueous electrolyte systems based on the semirestricted non-primitive mean spherical approximation. *Fluid Phase Equilibria*, 297(1):23–33, 2010.
- [75] Peter Debye and Hans Falkenhagen. Dispersion of the conductivity and dielectric constants of strong electrolytes. *Zeitschrift für Elektrochemie*, 24:562ff, 1928.
- [76] J. L. Lebowitz and J. K. Percus. Mean spherical model for lattice gases with extended hard cores and continuum fluids. *Physical Review*, 144:251–258, 1966.
- [77] Patrice Paricaud, Amparo Galindo, and George Jackson. Recent advances in the use of the saft approach in describing electrolytes, interfaces, liquid crystals and polymers. *Fluid Phase Equilibria*, 194-197:87–96, 2002.
- [78] B. Behzadi, B. H. Patel, A. Galindo, and C. Ghotbi. Modeling electrolyte solutions with the SAFT-VR equation using yukawa potentials and the mean-spherical approximation. *Fluid Phase Equilibria*, 236(1-2):241–255, 2005.
- [79] P. K. Jog and W. G. Chapman. Application of wertheim’s thermodynamic perturbation theory to dipolar hard sphere chains. *Molecular Physics*, 97(3):307–319, 1999.
- [80] PRASANNA K. JOG, Sharon G. Sauer, Jorg Blaesing, and Walter G. Chapman. Application of dipolar chain theory to the phase behavior of polar fluids and mixtures. *Industrial & Engineering Chemistry Research*, 40(21):4641–4648, 2001.
- [81] Bjørn Maribo-Mogensen, Georgios M. Kontogeorgis, and Kaj Thomsen. Comparison of the debye–hückel and the mean spherical approximation theories for electrolyte solutions. *Industrial & Engineering Chemistry Research*, 51(14):5353–5363, 2012.
- [82] Lars Onsager. Theories of concentrated electrolytes. *Chemical reviews*, 13(1):73–89, 1933.
- [83] Gang Jin and Marc D. Donohue. An equation of state for electrolyte solutions. 3. aqueous solutions containing multiple salts. *Industrial & Engineering Chemistry Research*, 30(1):240–248, 1991.
- [84] Allan H. Harvey and John M. Prausnitz. Dielectric constants of fluid mixtures over a wide range of temperature and density. *Journal of Solution Chemistry*, 16(10):857–869, 1987.

- [85] Pinsky, M.L. Takano, K. *Computer Aided Chemical Engineering: Chapter 8: Property estimation for electrolyte systems*. Elsevier, Denmark, 2004.
- [86] Sugata P. Tan, Hertanto Adidharma, and Maciej Radosz. Statistical associating fluid theory coupled with restricted primitive model to represent aqueous strong electrolytes. *Industrial & Engineering Chemistry Research*, 44(12):4442–4452, 2005.
- [87] Bjørn Maribo-Mogensen, Kaj Thomsen, and Georgios M. Kontogeorgis. An electrolyte cpa equation of state for mixed solvent electrolytes. *AIChE Journal*, 61(9):2933–2950, 2015.
- [88] W. G. Chapman, K. E. Gubbins, G. Jackson, and M. Radosz. Saft: Equation-of-state solution model for associating fluids. *Fluid Phase Equilibria*, 52:31–38, 1989.
- [89] Joachim Gross and Gabriele Sadowski. Perturbed-chain saft: An equation of state based on a perturbation theory for chain molecules. *Industrial & Engineering Chemistry Research*, 40(4):1244–1260, 2001.
- [90] Henri Renon and J. M. Prausnitz. Local compositions in thermodynamic excess functions for liquid mixtures. *AIChE Journal*, 14(1):135–144, 1968.
- [91] Gang Jin and Marc D. Donohue. An equation of state for electrolyte solutions. 1. aqueous systems containing strong electrolytes. *Industrial & Engineering Chemistry Research*, 27(6):1073–1084, 1988.
- [92] You-Xiang Zuo and Walter Fürst. Prediction of vapor pressure for nonaqueous electrolyte solutions using an electrolyte equation of state. *Fluid Phase Equilibria*, 138(1):87 – 104, 1997.
- [93] Hans-Günter Simon, Hans Kistenmacher, John M. Prausnitz, and Dieter Vortmeyer. An equation of state for systems containing electrolytes and nonelectrolytes. *Chemical Engineering and Processing: Process Intensification*, 29(3):139–146, 1991.
- [94] Jianzhong Wu and John M. Prausnitz. Phase equilibria for systems containing hydrocarbons, water, and salt: An extended peng–robinson equation of state. *Industrial & Engineering Chemistry Research*, 37(5):1634–1643, 1998.
- [95] Anders Schlaikjer, Kaj Thomsen, and Georgios M. Kontogeorgis. Simultaneous description of activity coefficients and solubility with ecpa. *Industrial & Engineering Chemistry Research*, 56(4):1074–1089, 2017.
- [96] Hooman Haghghi, Antonin Chapoy, and Bahman Tohidi. Freezing point depression of electrolyte solutions: Experimental measurements and modeling using the cubic-plus-association equation of state. *Industrial & Engineering Chemistry Research*, 47(11):3983–3989, 2008.
- [97] Luca F. Cameretti, Gabriele Sadowski, and Jørgen M. Møllerup. Modeling of aqueous electrolyte solutions with perturbed-chain statistical association fluid theory. *Industrial & Engineering Chemistry Research*, 44(23):8944, 2005.
- [98] Christoph Held and Gabriele Sadowski. Modeling aqueous electrolyte solutions. part 2. weak electrolytes. *Fluid Phase Equilibria*, 279(2):141–148, 2009.

- [99] Sugata P. Tan, Xiaoyan Ji, Hertanto Adidharma, and Maciej Radosz. Statistical associating fluid theory coupled with restrictive primitive model extended to bivalent ions. SAFT2: 1. single salt + water solutions. *The journal of physical chemistry. B*, 110(33):16694–16699, 2006.
- [100] Xiaoyan Ji, Sugata P. Tan, Hertanto Adidharma, and Maciej Radosz. Statistical associating fluid theory coupled with restrictive primitive model extended to bivalent ions. SAFT2: 2. brine/seawater properties predicted. *The Journal of Physical Chemistry B*, 110(33):16700–16706, 2006.
- [101] Xiaoyan Ji and Hertanto Adidharma. Ion-based SAFT2 to represent aqueous single- and multiple-salt solutions at 298.15K. *Ind. Eng. Chem. Res.*, 45(22):7719–7728, 2006.
- [102] Xiaoyan Ji and Hertanto Adidharma. Ion-based statistical associating fluid theory (saft2) to represent aqueous single-salt solutions at temperatures and pressures up to 473.15 k and 1000 bar. *Ind. Eng. Chem. Res.*, 46(13):4667–4677, 2007.
- [103] Xiaoyan Ji and Hertanto Adidharma. Ion-based saft2 to represent aqueous multiple-salt solutions at ambient and elevated temperatures and pressures. *Chemical Engineering Science*, 63(1):131 – 140, 2008.
- [104] Bong-Seop Lee and Ki-Chang Kim. Modeling of aqueous electrolyte solutions based on perturbed-chain statistical associating fluid theory incorporated with primitive mean spherical approximation. *Korean Journal of Chemical Engineering*, 26(6):1733–1747, 2009.
- [105] Wen-bin Liu, Yi-gui Li, and Jiu-fang Lu. A new equation of state for real aqueous ionic fluids based on electrolyte perturbation theory, mean spherical approximation and statistical associating fluid theory. *Fluid Phase Equilibria*, 158-160:595–606, 1999.
- [106] Zhi-Ping Liu, Yi-gui Li, and Jiu-fang Lu. Low-density expansion of the solution of mean spherical approximation for ion–dipole mixtures. *The Journal of Physical Chemistry B*, 106(20):5266–5274, 2002.
- [107] Xiaoyan Ji, Sugata P. Tan, Hertanto Adidharma, and Maciej Radosz. Statistical associating fluid theory coupled with restricted primitive model to represent aqueous strong electrolytes: Multiple-salt solutions. *Industrial & Engineering Chemistry Research*, 44(19):7584–7590, 2005.
- [108] Azam Najafloo, Farzaneh Feyzi, and Ali Taghi Zoghi. Development of electrolyte SAFT-HR equation of state for single electrolyte solutions. *Korean Journal of Chemical Engineering*, 31(12):2251–2260, 2014.
- [109] Azam Najafloo, Farzaneh Feyzi, and Ali T. Zoghi. Modeling solubility of co2 in aqueous mdea solution using electrolyte saft-hr eos. *Journal of the Taiwan Institute of Chemical Engineers*, 58:381–390, 2016.
- [110] Yoshinori Adachi, Benjamin C.-Y. Lu, and Hidezumi Sugie. A four-parameter equation of state. *Fluid Phase Equilibria*, 11(1):29 – 48, 1983.
- [111] Kim Aasberg-Petersen, Erling Stenby, and Aage Fredenslund. Prediction of high-pressure gas solubilities in aqueous mixtures of electrolytes. *Ind. Eng. Chem. Res.*, 30:2180–2185, 1991.

- [112] Pedro J. Carvalho, Luís M.C. Pereira, Neusa P.F. Gonçalves, António J. Queimada, and João A.P. Coutinho. Carbon dioxide solubility in aqueous solutions of nacl: Measurements and modeling with electrolyte equations of state. *Fluid Phase Equilibria*, 388:100–106, 2015.
- [113] T.-J. Chou and A. Tanioka. Predicting the effect of dissolved salt on the vapour-liquid equilibria for alcohol-water-salt systems. *Chemical engineering Research and design*, 77(4):329–334, 1999.
- [114] Chul Soo Lee, Sung Bin Park, and Yon Sik Shim. A unified and predictive model for mixed-electrolyte, aqueous mixed-solvent systems using parameters for ions and solvents. *Industrial & Engineering Chemistry Research*, 35(12):4772–4780.
- [115] Anil Rastogi and Dimitrios Tassios. Thermodynamics of a single electrolyte in a mixture of two solvents. *Industrial & Engineering Chemistry Research*, 26(7):1344–1351, 1987.
- [116] Shu-Xin Hou, Geoffrey C. Maitland, and J. Martin P. Trusler. Phase equilibria of (CO₂+H₂O+NaCl) and (CO₂+H₂O+KCl): Measurements and modeling. *The Journal of Supercritical Fluids*, 78:78–88, 2013.
- [117] R. W. Rousseau and J. E. Boone. Vapor-liquid equilibrium for salt containing systems: Correlation of binary solvent data and prediction of behavior in multi-component solvents. *AIChE Journal*, 24(4):718–725, 1978.
- [118] Philip L. Fosbøl, Kaj Thomsen, and Erling H. Stenby. Modeling of the mixed solvent electrolyte system CO₂-Na₂CO₃-NaHCO₃-Monoethylene Glycol-Water. *Industrial & Engineering Chemistry Research*, 48(9):4565–4578, 2009.
- [119] Maria C. Iliuta, Kaj Thomsen, and Peter Rasmussen. Extended uniquac model for correlation and prediction of vapour-liquid-solid equilibria in aqueous salt systems containing non-electrolytes. part a. methanol-water-salt systems. *Chemical Engineering Science*, 55(14):2673–2686, 2000.
- [120] Allan H. Harvey and John M. Prausnitz. Thermodynamics of high-pressure aqueous systems containing gases and salts. *AIChE Journal*, 35(4):635–644, 1989.
- [121] Xiaoyan Ji, Sugata P. Tan, Hertanto Adidharma, and Maciej Radosz. SAFT1-RPM approximation extended to phase equilibria and densities of CO₂-H₂O and CO₂-H₂O-NaCl systems. *Industrial & Engineering Chemistry Research*, 44(22):8419–8427, 2005.
- [122] B. H. Patel, P. Paricaud, A. Galindo, and G. C. Maitland. Prediction of the salting-out effect of strong electrolytes on water + alkane solutions. *Industrial & Engineering Chemistry Research*, 42(16):3809–3823, 2003.
- [123] Jens M.A. Schreckenber, Simon Dufal, Andrew J. Haslam, Claire S. Adjiman, George Jackson, and Amparo Galindo. Modelling of the thermodynamic and solvation properties of electrolyte solutions with the statistical associating fluid theory for potentials of variable range. *Molecular Physics*, 112(17):2339–2364, 2014.
- [124] Daniel K. Eriksen, Georgia Lazarou, Amparo Galindo, George Jackson, Claire S. Adjiman, and Andrew J. Haslam. Development of intermolecular potential models for electrolyte solutions using an electrolyte SAFT-VR Mie equation of state. *Molecular Physics*, 114(18):2724–2749, 2016.

- [125] Monir Hosseini Anvari, Gholamreza Pazuki, Saeed Seyfi Kakhki, and Babak Bonakdarpour. Application of the soft-VR equation of state in estimation of physico-chemical properties of amino acid solutions. *Journal of Molecular Liquids*, 184:24–32, 2013.
- [126] Gaurav Das, Stepan Hlushak, and Clare McCabe. A soft-VR+DE equation of state based approach for the study of mixed dipolar solvent electrolytes. *Fluid Phase Equilibria*, 416:72–82, 2016.
- [127] Gaurav Das, Stepan Hlushak, dos Ramos, M. Carolina, and Clare McCabe. Predicting the thermodynamic properties and dielectric behavior of electrolyte solutions using the SAFT-VR+DE equation of state. *AIChE Journal*, 61(9):3053–3072, 2015.
- [128] D. NguyenHuynh, J.-P. Passarello, P. Tobaly, and J.-C. de Hemptinne. Application of GC-SAFT EOS to polar systems using a segment approach. *Fluid Phase Equilibria*, 264(1-2):62–75, 2008.
- [129] D. NguyenHuynh, J.-P. Passarello, J.-C. de Hemptinne, and P. Tobaly. Extension of polar GC-SAFT to systems containing some oxygenated compounds: Application to ethers, aldehydes and ketones. *Fluid Phase Equilibria*, 307(2):142–159, 2011.
- [130] Thanh-Binh Nguyen, Jean-Charles de Hemptinne, Benoit Creton, and Georgios M. Kontogeorgis. Improving GC-PPC-SAFT equation of state for LLE of hydrocarbons and oxygenated compounds with water. *Fluid Phase Equilibria*, 372:113–125, 2014.
- [131] D. NguyenHuynh, J.-P. Passarello, J.-C. de Hemptinne, F. Volle, and P. Tobaly. Simultaneous modeling of VLE, LLE and VLLE of CO₂ and 1, 2, 3 and 4 alkanol containing mixtures using GC-PPC-SAFT EOS. *The Journal of Supercritical Fluids*, 95:146–157, 2014.
- [132] Nguyen-Huynh Dong, de Hemptinne Jean-Charles, Lugo Rafael, Passarello Jean-Philippe, and Tobaly Pascal. Simultaneous liquid–liquid and vapour–liquid equilibria predictions of selected oxygenated aromatic molecules in mixtures with alkanes, alcohols, water, using the polar GC-PC-SAFT. *Chemical engineering Research and design*, 92(12):2912–2935, 2014.
- [133] Joachim Gross and Gabriele Sadowski. Application of perturbation theory to a hard-chain reference fluid: an equation of state for square-well chains. *Fluid Phase Equilibria*, 168(2):183–199, 2000.
- [134] Alejandro Gil-Villegas, Amparo Galindo, Paul J. Whitehead, Stuart J. Mills, George Jackson, and Andrew N. Burgess. Statistical associating fluid theory for chain molecules with attractive potentials of variable range. *The Journal of Chemical Physics*, 106(10):4168, 1997.
- [135] Alexandros Lymperiadis, Claire S. Adjiman, Amparo Galindo, and George Jackson. A group contribution method for associating chain molecules based on the statistical associating fluid theory (soft- γ). *The Journal of Chemical Physics*, 127(23):234903, 2007.
- [136] Yuan-Hao Fu and Stanley I. Sandler. A Simplified-SAFT equation of state for associating compounds and mixtures. *Industrial & Engineering Chemistry Research*, 34(5):1897–1909, 1995.

- [137] Ioannis G. Economou. Statistical associating fluid theory: A successful model for the calculation of thermodynamic and phase equilibrium properties of complex fluid mixtures. *Industrial & Engineering Chemistry Research*, 41(5):953–962, 2002.
- [138] Ya Song Wei and Richard J. Sadus. Equations of state for the calculation of fluid-phase equilibria. *AIChE Journal*, 46(1):169–196, 2000.
- [139] John M. Prausnitz and Frederico W. Tavares. Thermodynamics of fluid-phase equilibria for standard chemical engineering operations. *AIChE Journal*, 50(4):739–761, 2004.
- [140] N. Von Solms, I. Kouskoumvekaki, M.L. Michelsen, G.M. Kontogeorgis. Capabilities, limitations and challenges of a simplified pc-saft equation of state. *Fluid Phase Equilibria*, 241:344, 2006.
- [141] W. Arlt, O. Spuhl, A. Klamt. Challenges in thermodynamics. *Chemical Engineering and Processing*, 43:221, 2004.
- [142] Dong Nguyen Huynh, M. Benamira, J.-Philippe Passarello, Pascal Tobaly, and J.-Charles de Hemptinne. Application of GC-SAFT EOS to polycyclic aromatic hydrocarbons. *Fluid Phase Equilibria*, 254(1-2):60–66, 2007.
- [143] Erich A. Müller and Keith E. Gubbins. Molecular-based equations of state for associating fluids: A review of saft and related approaches. *Industrial & Engineering Chemistry Research*, 40(10):2193–2211, 2001.
- [144] Feely Tumakaka and Gabriele Sadowski. Application of the perturbed-chain saft equation of state to polar systems. *Fluid Phase Equilibria*, 217(2):233–239, 2004.
- [145] Joachim Gross. An equation-of-state contribution for polar components: Quadrupolar molecules. *AIChE Journal*, 51(9):2556–2568, 2005.
- [146] Eirini K. Karakatsani and Ioannis G. Economou. Perturbed chain-statistical associating fluid theory extended to dipolar and quadrupolar molecular fluids. *The journal of physical chemistry. B*, 110(18):9252–9261, 2006.
- [147] Matthias Kleiner and Gabriele Sadowski. Modeling of polar systems using pcp-saft: An approach to account for induced-association interactions †. *The Journal of Physical Chemistry C*, 111(43):15544–15553, 2007.
- [148] Sofiane Tamouza, J.-Philippe Passarello, Pascal Tobaly, and de Hemptinne, J.-Charles. Group contribution method with saft eos applied to vapor liquid equilibria of various hydrocarbon series. *Proceedings of the Fifteenth Symposium on Thermophysical Properties*, 222–223:67–76, 2004.
- [149] D. NguyenHuynh, A. Falaix, J.-P. Passarello, P. Tobaly, and J.-C. de Hemptinne. Predicting VLE of heavy esters and their mixtures using GC-SAFT. *Fluid Phase Equilibria*, 264(1-2):184–200, 2008.
- [150] Thanh-Binh Nguyen, Jean-Charles de Hemptinne, Benoit Creton, and Georgios M. Kontogeorgis. Gc-ppc-saft equation of state for vle and lle of hydrocarbons and oxygenated compounds. sensitivity analysis. *Industrial & Engineering Chemistry Research*, 52(21):7014–7029, 2013.

- [151] J. Rozmus, J.-C. de Hemptinne, and P. Mougin. Application of GC-PPC-SAFT EoS to amine mixtures with a predictive approach. *Fluid Phase Equilibria*, 303(1):15–30, 2011.
- [152] Dong Nguyen-Huynh, Jean-Charles de Hemptinne, Rafael Lugo, Jean-Philippe Passarello, and Pascal Tobaly. Modeling liquid–liquid and liquid–vapor equilibria of binary systems containing water with an alkane, an aromatic hydrocarbon, an alcohol or a gas (methane, ethane, CO₂ or H₂S), using group contribution polar perturbed-chain statistical associating fluid theory. *Industrial & Engineering Chemistry Research*, 50(12):7467–7483, 2011.
- [153] M. Mourah, D. NguyenHuynh, J. P. Passarello, J. C. de Hemptinne, and P. Tobaly. Modelling lle and vle of methanol+n-alkane series using gc-pc-saft with a group contribution kij. *Fluid Phase Equilibria*, 298(1):154–168, 2010.
- [154] A. Barreau, I. Brunella, J.-C. de Hemptinne, V. Coupard, X. Canet, and F. Rivollet. Measurements of liquid–liquid equilibria for a methanol + glycerol + methyl oleate system and prediction using group contribution statistical associating fluid theory. *Industrial & Engineering Chemistry Research*, 49(12):5800–5807, 2010.
- [155] Tran, T. K. S., D. NguyenHuynh, N. Ferrando, J.-P. Passarello, J.-C. de Hemptinne, and P. Tobaly. Modeling vle of H₂ + hydrocarbon mixtures using a group contribution SAFT with a k_{ij} correlation method based on london’s theory. *Energy & Fuels*, 23(5):2658–2665, 2009.
- [156] Stephen S. Chen and Aleksander Kreglewski. Applications of the augmented van der waals theory of fluids.: I. pure fluids. *Berichte der Bunsengesellschaft für physikalische Chemie*, 81(10):1048–1052, 1977.
- [157] Walter G. Chapman, George Jackson, and Keith E. Gubbins. Phase equilibria of associating fluids spherical molecules with multiple bonding sites. *Molecular Physics*, 65(1):1–31, 1988.
- [158] Tomá Boublik. Perturbation theory of pure quadrupolar hard gaussian overlap fluids. *Molecular Physics*, 69(3):497–505, 1990.
- [159] G. A. Mansoori. Equilibrium thermodynamic properties of the mixture of hard spheres. *The Journal of Chemical Physics*, 54(4):1523, 1971.
- [160] Prasanna K. JOG, Sharon G. Sauer, Jorg Blaesing, and Walter G. Chapman. Application of dipolar chain theory to the phase behavior of polar fluids and mixtures. *Industrial & Engineering Chemistry Research*, 40(21):4641–4648, 2001.
- [161] Thi-Kim-Hoang Trinh, Jean-Philippe Passarello, Jean-Charles de Hemptinne, Rafael Lugo, and Veronique Lachet. A non-additive repulsive contribution in an equation of state: The development for homonuclear square well chains equation of state validated against monte carlo simulation. *The Journal of chemical physics*, 144(12):124902, 2016.
- [162] A. O. Malakhov and V. V. Volkov. Phase behavior of polymer mixtures with nonadditive hard-sphere potential. *Polymer Science Series A*, 49(6):745–756, 2007.

- [163] Lyra Paredes, Márcio Luis, dos Reis, Rodrigo Azevedo, and Frederico Wanderley Tavares. Inner segment radial distribution functions at contact point for chain-like molecules. *Journal of Molecular Liquids*, 147(3):198–210, 2009.
- [164] Samer O. Derawi, Georgios M. Kontogeorgis, Michael L. Michelsen, and Erling H. Stenby. Extension of the cubic-plus-association equation of state to glycol–water cross-associating systems. *Industrial & Engineering Chemistry Research*, 42(7):1470–1477, 2003.
- [165] Aleksandër Dhima, Jean-Charles de Hemptinne, and Gérard Moracchini. Solubility of light hydrocarbons and their mixtures in pure water under high pressure. *Fluid Phase Equilibria*, 145(1):129 – 150, 1998.
- [166] Allan H. Harvey and J. M. H. Levelt Sengers. Correlation of aqueous henry’s constants from 0°c to the critical point. *AIChE Journal*, 36(4):539–546, 1990.
- [167] Vlnayak N. Kadi and Ronald P. Danner. A modified soave-redlich-kwong equation of state for water-hydrocarbon phase equilibria. *Industrial & Engineering Chemistry Research*, 24:537–541, 1985.
- [168] Ingolf Søreide and Curtis H. Whitson. Peng-robinson predictions for hydrocarbons, co₂, n₂, and h₂ s with pure water and naci brine. *Fluid Phase Equilibria*, 77(Supplement C):217 – 240, 1992.
- [169] Iakovos V. Yakoumis, Georgios M. Kontogeorgis, Epaminondas C. Voutsas, Eric M. Hendriks, and Dimitrios P. Tassios. Prediction of phase equilibria in binary aqueous systems containing alkanes, cycloalkanes, and alkenes with the cubic-plus-association equation of state. *Industrial & Engineering Chemistry Research*, 37(10):4175–4182, 1998.
- [170] Georgios M. Kontogeorgis, Michael L. Michelsen, Georgios K. Folas, Samer Derawi, Nicolas von Solms, and Erling H. Stenby. Ten years with the cpa (cubic-plus-association) equation of state. part 1. pure compounds and self-associating systems. *Industrial & Engineering Chemistry Research*, 45(14):4855–4868, 2006.
- [171] Georgios M. Kontogeorgis, Georgios K. Folas, Núria Muro-Suñé, Nicolas von Solms, Michael L. Michelsen, and Erling H. Stenby. Modelling of associating mixtures for applications in the oil & gas and chemical industries. *Fluid Phase Equilibria*, 261(1-2):205–211, 2007.
- [172] Aleksandra Dominik, Walter G. Chapman, Matthias Kleiner, and Gabriele Sadowski. Modeling of polar systems with the perturbed-chain saft equation of state. investigation of the performance of two polar terms. *Industrial & Engineering Chemistry Research*, 44(17):6928–6938, 2005.
- [173] Sofiane Tamouza, J.-Philippe Passarello, Pascal Tobaly, and J.-Charles de Hemptinne. Application to binary mixtures of a group contribution saft eos (gc-saft). *Fluid Phase Equilibria*, 228-229:409–419, 2005.
- [174] G. H. Hudson and J. C. McCoubrey. Intermolecular forces between unlike molecules. a more complete form of the combining rules. *Transactions of the Faraday Society*, 56:761, 1960.

- [175] Justyna Rozmus, Jean-Charles de Hemptinne, Nicolas Ferrando, and Pascal Mougin. Long chain multifunctional molecules with gc-ppc-saft: Limits of data and model. *Fluid Phase Equilibria*, 329:78–85, 2012.
- [176] Xiaodong Liang, Ioannis Tsivintzelis, and Georgios M. Kontogeorgis. Modeling water containing systems with the simplified pc-saft and cpa equations of state. *Industrial & Engineering Chemistry Research*, 53(37):14493–14507, 2014.
- [177] Mos van Berlo, Michael T. Gude, van der Wielen, Luuk A. M., and Luyben, Karel Ch. A. M. Partition coefficients and solubilities of glycine in the ternary solvent system 1-butanol + ethanol + water. *Industrial & Engineering Chemistry Research*, 36(6):2474–2482, 1997.
- [178] Igor A. Sedov and Boris N. Solomonov. Determining the gibbs energies of hydrogen-bonding interactions of proton-accepting solutes in aqueous solutions from thermodynamic data at 298K with regard to the hydrophobic effect. *Journal of Chemical & Engineering Data*, 56(4):1438–1442, 2011.
- [179] Igor A. Sedov and Boris N. Solomonov. Distinctive thermodynamic properties of solute–solvent hydrogen bonds in self-associated solvents. *Journal of Physical Organic Chemistry*, 25, 2012.
- [180] Igor A. Sedov and Boris N. Solomonov. Gibbs free energy of hydrogen bonding of aliphatic alcohols with liquid water at 298K. *Fluid Phase Equilibria*, 315:16–20, 2012.
- [181] Igor A. Sedov and Boris N. Solomonov. Hydrogen bonding in neat aliphatic alcohols: The gibbs free energy of self-association and molar fraction of monomer. *Journal of Molecular Liquids*, 167:47–51, 2012.
- [182] Georgios M. Kontogeorgis, Georgios K. Folas, Núria Muro-Suñé, Nicolas von Solms, Michael L. Michelsen, and Erling H. Stenby. Modelling of associating mixtures for applications in the oil gas and chemical industries. *Fluid Phase Equilibria*, 261(1):205 – 211, 2007.
- [183] Wael A. Fouad, Le Wang, Amin Haghmoradi, D. Asthagiri, and Walter G. Chapman. Understanding the thermodynamics of hydrogen bonding in alcohol-containing mixtures: Cross-association. *The journal of physical chemistry. B*, 120(13):3388–3402, 2016.
- [184] Nicolas Ferrando, Jean-Charles de Hemptinne, Pascal Mougin, and Jean-Philippe Passarello. Prediction of the pc-saft associating parameters by molecular simulation. *The journal of physical chemistry. B*, 116(1):367–377, 2012.
- [185] Michael J. Hey, Daniel P. Jackson, and Hong Yan. The salting-out effect and phase separation in aqueous solutions of electrolytes and poly(ethylene glycol). *Polymer*, 46(8):2567–2572, 2005.
- [186] Paul M. Gross. The salting out of non-electrolytes from aqueous solutions. *Chemical Reviews*, 13(1):91–101, 1933.
- [187] Georgios M. Kontogeorgis, Michael L. Michelsen, Georgios K. Folas, Samer Derawi, Nicolas von Solms, and Erling H. Stenby. Ten years with the cpa (cubic-plus-association) equation of state. part 1. pure compounds and self-associating systems. *Industrial & Engineering Chemistry Research*, 45(14):4855–4868, 2006.

- [188] M. Uematsu and E. U. Frank. Static dielectric constant of water and steam. *Journal of Physical and Chemical Reference Data*, 9(4):1291–1306, 1980.
- [189] Bjørn Maribo-Mogensen, Georgios M. Kontogeorgis, and Kaj Thomsen. Modeling of dielectric properties of complex fluids with an equation of state. *The journal of physical chemistry. B*, 117(12):3389–3397, 2013.
- [190] Ignat Yu Shilov and Andrey K. Lyashchenko. The role of concentration dependent static permittivity of electrolyte solutions in the debye-hückel theory. *The journal of physical chemistry. B*, 119(31):10087–10095, 2015.
- [191] G. H. Haggis, J. B. Hasted, and T. J. Buchanan. The dielectric properties of water in solutions. *The Journal of Chemical Physics*, 20(9):1452, 1952.
- [192] J. Hubbard and L. Onsager. Dielectric dispersion and dielectric friction in electrolyte solutions. i. *The Journal of Chemical Physics*, 67(11):4850, 1977.
- [193] J. B. Hubbard. Dielectric dispersion and dielectric friction in electrolyte solutions. ii. *The Journal of Chemical Physics*, 68(4):1649, 1978.
- [194] Joseph B. Hubbard, Peter Colonomos, and Peter G. Wolynes. Molecular theory of solvated ion dynamics. iii. the kinetic dielectric decrement. *The Journal of Chemical Physics*, 71(6):2652, 1979.
- [195] Bjørn Maribo-Mogensen, Georgios M. Kontogeorgis, and Kaj Thomsen. Modeling of dielectric properties of aqueous salt solutions with an equation of state. *The journal of physical chemistry. B*, 117(36):10523–10533, 2013.
- [196] Saifuddin Ahmed, Nicolas Ferrando, Jean-Charles de Hemptinne, Jean-Pierre Simonin, Olivier Bernard, and Olivier Baudouin. A new pc-saft model for pure water, water–hydrocarbons, and water–oxygenates systems and subsequent modeling of vle, vll, and lle. *Journal of Chemical & Engineering Data*, 61(12):4178–4190, 2016.
- [197] Stanley H. Huang and Maciej Radosz. Equation of state for small, large, polydisperse and associating molecules. *Industrial & Engineering Chemistry Research*, 29:2284–2294, 1990.
- [198] Bong-Seop Lee and Ki-Chang Kim. Study on the activity coefficients and solubilities of amino acids in aqueous solutions with perturbed-chain statistical associating fluid theory. *Korean Journal of Chemical Engineering*, 27(1):267–277, 2010.
- [199] Zhiping Liu, Wenchuan Wang, and Yigui Li. An equation of state for electrolyte solutions by a combination of low-density expansion of non-primitive mean spherical approximation and statistical associating fluid theory. *Fluid Phase Equilibria*, 227(2):147–156, 2005.
- [200] Yuanhui Liu, Minqiang Hou, Guanying Yang, and Buxing Han. Solubility of CO_2 in aqueous solutions of NaCl, KCl, CaCl_2 and their mixed salts at different temperatures and pressures. *The Journal of Supercritical Fluids*, 56(2):125–129, 2011.
- [201] J. O’M. Bockris and Harold Egan. The salting-out effect and dielectric constant. *Transactions of the Faraday Society*, 44:151, 1948.

- [202] Torben Graves Pedersen, Christian Dethlefsen, and Aase Hvidt. Volumetric properties of aqueous solutions of alkali halides. *Carlsberg Research Communications*, 49(3):445–455, 1984.
- [203] Walter J. Hamer and Yung-Chi Wu. Osmotic coefficients and mean activity coefficients of uni-univalent electrolytes in water at 25°C. *Journal of Physical and Chemical Reference Data*, 1(4):1047–1100, 1972.
- [204] Grinnell Jones and Benjamin C. Bradshaw. The transference number of lithium chloride as a function of the concentration. *Journal of the American Chemical Society*, 54(1):138–150, 1932.
- [205] Ernesto Vercher, Solange Solsona, M. Isabel Vázquez, and Antoni Martínez-Andreu. Apparent molar volumes of lithium chloride in 1-propanol + water in the temperature range from 288.15 to 318.15 K. *Fluid Phase Equilibria*, 209(1):95–111, 2003.
- [206] Jörn Kiepe, Sven Horstmann, Kai Fischer, and Jürgen Gmehling. Experimental determination and prediction of gas solubility data for methane + water solutions containing different monovalent electrolytes. *Industrial & Engineering Chemistry Research*, 42(21):5392–5398, 2003.
- [207] I. M. Abdulagatov and N. D. Azizov. Densities and apparent molar volumes of aqueous LiI solutions at temperatures from (296 to 600)K and at pressures up to 30MPa. *The Journal of Chemical Thermodynamics*, 36(10):829–843, 2004.
- [208] F. A. Gonçalves and J. Kestin. The viscosity of NaCl and KCl solutions in the range 25–50°C. *Berichte der Bunsengesellschaft für physikalische Chemie*, 81(11):1156–1161, 1977.
- [209] Lisa A. Romankiw and I. Ming Chou. Densities of aqueous sodium chloride, potassium chloride, magnesium chloride, and calcium chloride binary solutions in the concentration range 0.5–6.1 m at 25, 30, 35, 40, and 45 degree.c. *Journal of Chemical & Engineering Data*, 28(3):300–305, 1983.
- [210] P. S. Nikam, Mehdi Hasan, R. P. Shewale, and A. B. Sawant. Limiting ionic partial molar volumes of Cs^+ , Na^+ , Ca^{2+} , NH_4^+ , Cl^- , Br^- , I^- , BPh_4^- in aqueous acetone at 298.15 K. *Journal of Solution Chemistry*, 32(11):987–995, 2003.
- [211] M. Kh. Karapetyants, V. A. Vasilev, B. V. Mikhailin, Strakhov, V. N. Karapetyants, M. Kh., V. A. Vasilev, B. V. Mikhailin, and V. N. Strakhov. Heat capacity and density of aqueous NaBr and RbBr solutions at 25°C. *Russian Journal of Physical Chemistry A*, 53(1):207–209, 1979.
- [212] G. V. Roshkovskii, N. V. Penkina, and G. M. Poltoratskii. Viscometric study of the system water - sodium iodide.
- [213] Duncan A. MacInnes and Margaret O. Dayhoff. The partial molal volumes of potassium chloride, potassium and sodium iodides and of iodine in aqueous solution at 25°. *Journal of the American Chemical Society*, 74(4):1017–1020, 1952.
- [214] A. B. Zdanovskii. Partial heats of dilution for aqueous solutions of salts. *Russian Journal of Physical Chemistry*, 68(4):556–561, 1994.

- [215] S. Lengyel, J. Giber, Holerit J, and J. Tamas. Study of viscosity of aqueous alkali halide solutions. *Acta chimica Academiae Scientiarum Hungaricae*, 40(2):125–143, 1964.
- [216] Grinnell Jones and Charles F. Bickford. The conductance of aqueous solutions as a function of concentration. i. potassium bromide and lanthanum chloride. *Journal of the American Chemical Society*, 56:602–611, 1934.
- [217] R. E. Gibson. The calculation of the solubility of certain salts in water at high pressures from data obtained at low pressures. *Journal of the American Chemical Society*, 56(4):865–870, 1934.
- [218] Frank T. Gucker, David Stubley, and David J. Hill. The isentropic compressibilities of aqueous solutions of some alkali halides at 298.15K. *The Journal of Chemical Thermodynamics*, 7(9):865–873, 1975.
- [219] Mikhajlin, B.V., Vorob'ev, A.F., & Vasilev, V.A. Heat capacity and density of aqueous solutions of cesium and copper bromides at 298,15 k. *Russian Journal of Physical Chemistry A*, 56(8):1937–1940, 1982.
- [220] Grinnell Jones and Holmes J. Fornwalt. The viscosity of aqueous solutions of electrolytes as a function of the concentration. iii. cesium iodide and potassium permanganate. *Journal of the American Chemical Society*, 58(4):619–625, 1936.
- [221] W. Ronald Fawcett. Thermodynamic parameters for the solvation of monatomic ions in water. *The Journal of Physical Chemistry B*, 103(50):11181–11185, 1999.
- [222] Yizhak Marcus. Ionic radii in aqueous solutions. *Chemical Reviews*, 88(8):1475–1498, 1988.
- [223] L. Blum and W. R. Fawcett. Application of the mean spherical approximation to describe the gibbs solvation energies of monovalent monoatomic ions in polar solvents. *The Journal of Physical Chemistry*, 96(1):408–414, 1992.
- [224] Jean-Pierre Simonin, Olivier Bernard, and Lesser Blum. Real ionic solutions in the mean spherical approximation. 3. osmotic and activity coefficients for associating electrolytes in the primitive model. *The Journal of Physical Chemistry B*, 102(22):4411–4417, 1998.
- [225] Jean-Pierre Simonin, Lesser Blum, and Pierre Turq. Real ionic solutions in the mean spherical approximation. 1. simple salts in the primitive model. *The Journal of Physical Chemistry*, 100(18):7704–7709, 1996.
- [226] V. S. Patwardhan and Anil Kumar. Thermodynamic properties of aqueous solutions of mixed electrolytes: A new mixing rule. *AIChE Journal*, 39(4):711–714, 1993.
- [227] A. Michels, J. de Gruyter, and F. Niesen. Isotherms of ethylene between 0° and 150° and at pressures from 20 to 270 atm. *Physica*, 3(5):346–351, 1936.
- [228] Lu-Kun Wang, Guang-Jin Chen, Guang-He Han, Xu-Qiang Guo, and Tian-Min Guo. Experimental study on the solubility of natural gas components in water with or without hydrate inhibitor. *Fluid Phase Equilibria*, 207(1-2):143–154, 2003.

- [229] Jiawen Hu, Zhenhao Duan, Chen Zhu, and I-Ming Chou. PVTx properties of the co₂-h₂o and co₂-h₂o-nacl systems below 647 k: Assessment of experimental data and thermodynamic models. *Chemical Geology*, 238(3-4):249–267, 2007.
- [230] Wei Yan, Shengli Huang, and Erling H. Stenby. Measurement and modeling of co₂ solubility in nacl brine and co₂-saturated nacl brine density. *International Journal of Greenhouse Gas Control*, 5(6):1460–1477, 2011.
- [231] Danlu Tong, J. P. Martin Trusler, and David Vega-Maza. Solubility of co₂ in aqueous solutions of cacl₂ or mgcl₂ and in a synthetic formation brine at temperatures up to 423 k and pressures up to 40 mpa. *Journal of Chemical & Engineering Data*, 58(7):2116–2124, 2013.
- [232] Rui Sun and Jean Dubessy. Prediction of vapor-liquid equilibrium and PVTx properties of geological fluid system with SAFT-LJ EOS including multi-polar contribution. part II: Application to H₂O-NaCl and CO₂-H₂O-NaCl system. *Geochimica et Cosmochimica Acta*, 88:130–145, 2012.
- [233] Xiaoyan Ji and Chen Zhu. A saft equation of state for the quaternary h₂s-co₂-h₂o-nacl system. *Geochimica et Cosmochimica Acta*, 91:40–59, 2012.
- [234] O. L. Culberson and J. J. McKetta. Phase equilibria in hydrocarbon-water systems iii - the solubility of methane in water at pressures to 10,000 psia. *Journal of Petroleum Technology*, 3(08):223–226, 2013.
- [235] Thomas D. O’Sullivan and Norman Obed Smith. Solubility and partial molar volume of nitrogen and methane in water and in aqueous sodium chloride from 50 to 125.deg. and 100 to 600 atm. *The Journal of Physical Chemistry*, 74(7):1460–1466, 1970.
- [236] Denis Krotov. *Weiterentwicklung der Gruppenbeitragszustandsgleichung VTPR zur Beschreibung von Elektrolyt- und Polymersystemen*. Phd, Universität Oldenburg, 2014.
- [237] O. L. Culberson and J. J. McKetta. Phase equilibria in hydrocarbon-water systems ii - the solubility of ethane in water at pressures to 10,000 psi. *Journal of Petroleum Technology*, 2(11):319–322, 2013.
- [238] Allen Dupree King and C. R. Coan. Solubility of water in compressed carbon dioxide, nitrous oxide, and ethane. evidence for hydration of carbon dioxide and nitrous oxide in the gas phase. *Journal of the American Chemical Society*, 93(8):1857–1862, 1971.
- [239] Jong Lee, II and Alan E. Mather. Solubility of hydrogen sulfide in water. *Berichte der Bunsengesellschaft für physikalische Chemie*, 81(10):1020–1023, 1977.
- [240] Jianzhong Xia, Álvaro Pérez-Salado Kamps, Bernd Rumpf, and Gerd Maurer. Solubility of hydrogen sulfide in aqueous solutions of the single salts sodium sulfate, ammonium sulfate, sodium chloride, and ammonium chloride at temperatures from 313 to 393 k and total pressures up to 10 mpa. *Industrial & Engineering Chemistry Research*, 39(4):1064–1073, 2000.

- [241] Matthew A. Clarke and P. R. Bishnoi. Development of a new equation of state for mixed salt and mixed solvent systems, and application to vapour-liquid and solid (hydrate)-vapour-liquid equilibrium calculations. *Fluid Phase Equilibria*, 220(1):21–35, 2004.
- [242] Bahram Ghalami-Choobar, Maryam Shekofteh-Gohari, and Fatemeh Sayyadi-Nodehi. Thermodynamic study of ternary electrolyte kcl +1-proh+water system based on pitzer and pitzer – simonson – clegg models using potentiometric measurements. *Journal of Molecular Liquids*, 188:49–54, 2013.
- [243] David Meranda and William F. Furter. Vapor-liquid equilibrium in alcohol-water systems containing dissolved halide salts and salt mixtures. *AIChE Journal*, 18(1):111–116, 1972.
- [244] David Meranda and William F. Furter. Salt effects on vapor-liquid equilibrium: Some anomalies. *AIChE Journal*, 20(1):103–108, 1974.
- [245] Álvaro Pérez-Salado Kamps, Michael Jödecke, Jianzhong Xia, Mathias Vogt, and Gerd Maurer. Influence of salts on the solubility of carbon dioxide in (water + methanol). part 1: Sodium chloride. *Industrial & Engineering Chemistry Research*, 45(4):1505–1515, 2006.
- [246] V. T. Zharov and O. K. Pervukhin. Liquid vapor equilibrium diagrams in systems with chemical interaction. ii. the methanol - formic acid - methyl formate - water system. *Russ. J. Phys. Chem.*, 46(8):1130–1132, 1972.
- [247] Jia Yao, Haoran Li, and Shijun Han. Vapor-liquid equilibrium data for methanol-water-nacl at 45°C. *Fluid Phase Equilibria*, 162(1-2):253–260, 1999.
- [248] N. M. Baron and K. P. Mishenko. Investigation of the composition and the vapor pressures over the solutions of sodium bromide in the binary solvent methanol - water. *Zhurnal Obshchei Khimii*, 18(12):2067–2079, 1948.
- [249] B. Kolbe and J. Gmehling. Thermodynamic properties of ethanol + water. i. vapour-liquid equilibria measurements from 90 to 150°C by the static method. *Fluid Phase Equilibria*, 23(2-3):213–226, 1985.
- [250] Per Åke Albertsson. Partition of cell particles and macromolecules in polymer two-phase systems. volume 24 of *Advances in Protein Chemistry*, pages 309 – 341. Academic Press, 1970.
- [251] A. Pfennig and A. Schwerin. Analysis of the electrostatic potential difference in aqueous polymer two-phase systems. *Fluid Phase Equilibria*, 108(1-2):305–315, 1995.
- [252] J. Bringmann, B. Keil, and A. Pfennig. Partition of dipeptides in aqueous polymer two-phase systems as a function of ph in the presence of salts. *Fluid Phase Equilibria*, 101:211–225, 1994.
- [253] Richard Reitherman, Steven D. Flanagan, and Samuel H. Barondes. Electromotive phenomena in partition of erythrocytes in aqueous polymer two phase systems. *Biochimica et Biophysica Acta (BBA) - General Subjects*, 297(2):193 – 202, 1973.

- [254] C. A. Haynes, J. Carson, H. W. Blanch, and J. M. Prausnitz. Electrostatic potentials and protein partitioning in aqueous two-phase systems. *AIChE Journal*, 37(9):1401–1409, 1991.
- [255] Donald E Brooks, Kim A Sharp, Stephan Bamberger, Cherry H Tambllyn, Geoffrey V.F Seaman, and Harry Walter. Electrostatic and electrokinetic potentials in two polymer aqueous phase systems. *Journal of Colloid and Interface Science*, 102(1):1 – 13, 1984.
- [256] Allen J. Bard and Larry R. Faulkner. *Electrochemical methods and applications*. Wiley-Interscience, New York and London, 2nd ed. edition, 2000.
- [257] S. I. Dermeleva, E. N. Glazkova, and A. A. Kireev. Solubility and thermodynamics of solvation of sodium fluoride in water - methanol and water - propan-2-ol mixtures. *Visn. Khark. Natsional. Univ. Khim.*, 596(10):147–154, 2003.
- [258] Jia Yao, Wei-dong Yan, Yi-jin Xu, and Shi-jun Han. Activity coefficients for nacl in meoh + h2o by electromotive force measurements at 308.15 k and 318.15 k. *Journal of Chemical & Engineering Data*, 44(3):497–500, 1999.
- [259] Rui-Fang Cui, Man-Cheng Hu, Li-Hua Jin, Shu-Ni Li, Yu-Cheng Jiang, and Shu-Ping Xia. Activity coefficients of rubidium chloride and cesium chloride in methanol–water mixtures and a comparative study of pitzer and pitzer–simonson–clegg models (298.15k). *Fluid Phase Equilibria*, 251(2):137 – 144, 2007.
- [260] Felipe Hernández-Luis, Héctor R. Galleguillos, Teófilo A. Graber, and María E. Taboada. Activity coefficients of licl in ethanol–water mixtures at 298.15 k. *Industrial & Engineering Chemistry Research*, 47(6):2056–2062, 2008.
- [261] Felipe Hernández-Luis, Mario V. Vázquez, and Miguel A. Estesó. Activity coefficients for naf in methanol-water and ethanol-water mixtures at 25°C. *Journal of Molecular Liquids*, 108(1-3):283–301, 2003.
- [262] Miguel A. Estesó, Oscar M. Gonzalez-Diaz, Felipe F. Hernandez-Luis, and Luis Fernandez-Merida. Activity coefficients for nacl in ethanol-water mixtures at 25°C. *Journal of Solution Chemistry*, 18(3):277–288, Mar 1989.
- [263] O. M. González-Díaz, L. Fernández-Mérida, F. Hernández-Luis, and M. A. Estesó. Activity coefficients for nabr in ethanol-water mixtures at 25°C. *Journal of Solution Chemistry*, 24(6):551–563, Jun 1995.
- [264] Mancheng Hu, Ruifang Cui, Shu'ni Li, Yucheng Jiang, and Shu Ping Xia. Determination of activity coefficients for cesium chloride in methanol–water and ethanol–water mixed solvents by electromotive force measurements at 298.15 k. *Journal of Chemical & Engineering Data*, 52(2):357–362, 2007.
- [265] J. Radošević and I. Mekjavić. Thermodynamic studies of sodium bromide in 2-propanol–water mixtures (10, 30 and 50 wt.%) from electromotive force measurements. *Electrochimica Acta*, 28(10):1435–1438, 1983.

- [266] N.M. Konstantinova, M.S. Motornova, M.N. Mamontov, D.I. Shishin, and I.A. Uspenskaya. Partial and integral thermodynamic properties in the sodium chloride–water–1-butanol(iso-butanol) ternary systems. *Fluid Phase Equilibria*, 309(1):20 – 29, 2011.
- [267] Norio Yui and Yoichi Kurokawa. Equilibrium compositions of 1-butanol-water-mcl (m= li, na, k, rb, cs and nh4). *Nippon kagaku zasshi*, 87(11):1138–1143,A65, 1966.
- [268] Vicente Gomis, Francisco Ruiz, Juan Carlos Asensi, and María Dolores Saquete. Liquid–liquid–solid equilibria for the ternary systems butanols + water + sodium chloride or + potassium chloride. *Journal of Chemical & Engineering Data*, 41(2):188–191, 1996.
- [269] Louis A. Reber, Wallace W. McNabb, and Walter W. Lucasse. The effect of salts on the mutual miscibility of normal butyl alcohol and water. *The Journal of Physical Chemistry*, 46(4):500–515, 1942.
- [270] R. de Santis, L. Marrelli, and P. N. Muscetta. Liquid–liquid equilibria in water—aliphatic alcohol systems in the presence of sodium chloride. *The Chemical Engineering Journal*, 11(3):207–214, 1976.
- [271] Norio Yui and Yoichi Kurokawa. Equilibrium compositions of 1-butanol-water-mf (m= li, na, k and nh4). *Nippon kagaku zasshi*, 87(11):1143–1146,A65, 1966.
- [272] M. I. Bakeev and I. P. Akimova. *Phase equilibrium in the MeA - Water - organic liquids systems*. 1976.
- [273] L. Blum. Mean spherical model for asymmetric electrolytes. *Molecular Physics*, 30(5):1529–1535, 1975.
- [274] R. J. Baxter. Ornstein–zernike relation and percus–yevick approximation for fluid mixtures. *The Journal of chemical physics*, 52(9):4559–4562, 1970.
- [275] L. Blum and J. S. Hoeye. Mean spherical model for asymmetric electrolytes. 2. thermodynamic properties and the pair correlation function. *The Journal of Physical Chemistry*, 81(13):1311–1316, 1977.
- [276] Henri Planche and Henri Renon. Mean spherical approximation applied to a simple but nonprimitive model interaction for electrolyte solutions and polar substances. *The Journal of Physical Chemistry*, 85(25):3924–3929, 1981.
- [277] Simon L. Clegg and Kenneth S. Pitzer. Thermodynamics of multicomponent, miscible, ionic solutions: Generalized equations for symmetrical electrolytes. *The Journal of Physical Chemistry*, 96(8):3513–3520, 1992.
- [278] Xiao-hua Lu and G. Maurer. Model for describing activity coefficients in mixed electrolyte aqueous solutions. *AIChE Journal*, 39(9):1527–1538, 1993.
- [279] L. Blum. Solution of a model for the solvent–electrolyte interactions in the mean spherical approximation. *The Journal of chemical physics*, 61(5):2129–2133, 1974.
- [280] Dongqing Wei and Lesser Blum. The mean spherical approximation for an arbitrary mixture of ions in a dipolar solvent: Approximate solution, pair correlation functions, and thermodynamics. *The Journal of chemical physics*, 87(5):2999–3007, 1987.

-
- [281] Tzu-Jen Chou, Akihiko Tanioka, and Hsieng-Cheng Tseng. Salting effect on the liquid–liquid equilibria for the partially miscible systems of n -propanol–water and i -propanol–water. *Industrial & Engineering Chemistry Research*, 37(5):2039–2044, 1998.
- [282] Jianguo Wang, Yaming Zhang, and Yanru Wang. Liquid–liquid equilibria for 1-propanol (or 2-propanol)–water systems containing potassium fluoride. *Journal of Chemical & Engineering Data*, 47(1):110–112, 2002.
- [283] Vicente Gomis, Francisco Ruiz, Guillermo de Vera, Eladio López, and M.Dolores Saquete. Liquid-liquid-solid equilibria for the ternary systems water-sodium chloride or potassium chloride-1-propanol or 2-propanol. *Fluid Phase Equilibria*, 98:141–147, 1994.
- [284] Jing Tang, Mancheng Hu, Shu’ni Li, Ruifang Cui, and Lihua Jin. Measurement and correlation of liquid-liquid equilibria for ternary systems of water + rubidium chloride + propanol. *Chemical Engineering Communications*, 195(8):925–933, 2008.

Appendix A

Variants of the MSA theory

A.1 Mean spherical approximation (MSA) theory

A.1.1 Primitive MSA

The MSA theory is derived from the solution of Ornstein-Zernike (OZ) equation using mean-spherical approximation which can then be applied to system of real fluids containing ionic species. The primitive version of MSA accounts for ion-ion interaction and does not define solvent as dipolar hard sphere rather defines them as a dielectric continuum.

A.1.2 Non-restricted primitive

Blum *et al.* [273] derived the solution of the complete MSA from the Ornstein-Zernike (OZ) equation for charged hard spheres which is repeated below.

The mixture of “charged hard spheres” (ions) are immersed in a dielectric continuum of dielectric constant ε and the system is assumed to be electroneutral by the imposition (eqn. A.1), such that the net charge on the overall system is zero.

$$\sum_{i=1}^n \rho_i z_i = 0 \quad (\text{A.1})$$

where ρ_i is the numerical density and z_i is the charge of ionic species i containing n different types of ions.

The pair correlation function is $c_{ij}(r)$, and the indirect correlation function is $h_{ij}(r)$, for a pair of ions (i, j) . The closure equations are given by the equations A.2-A.3.

$$h_{ij}(r) = g_{ij}(r) = -1 \quad ; r \leq \sigma_{ij} \quad (\text{A.2})$$

$$c_{ij} = -\beta u_{ij}(r) = -\frac{\beta z_i z_j e^2}{4\pi\varepsilon_0\varepsilon_r r_{ij}} \quad ; r > \sigma_{ij} \quad (\text{A.3})$$

where, σ_{ij} is the distance of the closes approach for a pair i, j .

$$\sigma_{ij} = \frac{1}{2}(\sigma_i + \sigma_j) \quad (\text{A.4})$$

and u_{ij} is the electrostatic potential defined as,

$$u_{ij} = \frac{e^2}{\varepsilon_0} \frac{z_i z_j}{r} \quad (\text{A.5})$$

where, e is the elementary charge on the ‘‘charged hard sphere’’, and ε_0 is the permittivity of the vacuum.

The solution of the OZ equation is then given in terms of the factor correlation function [274, 275] by $\mathbf{Q}(\mathbf{r})$. The long derivation is omitted from here.

$$\mathbf{Q}_{ij}(r) = \lim_{\mu \rightarrow 0} [(r - \sigma_{ij})Q'_{ij} + 0.5(r - \sigma_{ij})^2 Q''_j - z_i a_j e^{-\mu r}] \quad ; \lambda_{ji} < r \leq \sigma_{ij} \quad (\text{A.6})$$

$$\mathbf{Q}_{ij}(r) = \lim_{\mu \rightarrow 0} (-z_i a_j e^{-\mu r}) \quad ; r > \sigma_{ij} \quad ; \lambda_{ji} = 0.5(\sigma_j - \sigma_i) \quad (\text{A.7})$$

The numeric coefficients Q'_{ij} , Q'_j and a_j are given as:

$$Q_{ij'} = \frac{2\pi}{\Delta} \left(\sigma_{ij} + \frac{\pi}{4\Delta} \sigma_i \sigma_j \zeta_2 \right) - \frac{2\Gamma^2}{\alpha^2} a_i a_j \quad (\text{A.8})$$

$$Q_{j'} = \frac{2\pi}{\Delta} \left(1 + \zeta_{2j} \left(\frac{\pi}{2\Delta} + \frac{1}{2} a_j P_n \right) \right) \quad (\text{A.9})$$

$$a_j = \frac{\alpha^2}{2\Gamma(1 + \Gamma\sigma_j)} \left(z_j - P_n \sigma_j^2 \frac{\pi}{2\Delta} \right) \quad (\text{A.10})$$

$$(\text{A.11})$$

where,

$$P_n = \frac{1}{\Omega} \sum_k \frac{\rho_k \sigma_k z_k}{(1 + \Gamma\sigma_k)} \quad (\text{A.12})$$

$$\Omega = 1 + \frac{\pi}{2\Delta} \sum_k \frac{\rho_k \sigma_k^3}{1 + \Gamma\sigma_k} \quad (\text{A.13})$$

$$\zeta_n = \sum_k \rho_k (\sigma_k)^n \quad ; n = 0, 1, 2, 3 \quad (\text{A.14})$$

$$\Delta = 1 - \pi \frac{\zeta_3}{6} \quad (\text{A.15})$$

$$\alpha^2 = 4\pi\beta \frac{e^2}{\varepsilon_0} \quad (\text{A.16})$$

The shielding parameter Γ can be obtained by analytically solving the above equations:

$$\Gamma = \frac{1}{2}\alpha \sqrt{\left[\sum_i^n \rho_i \left\{ \frac{\left(z_i - \frac{\pi}{2\Delta} \sigma_i^2 P_n \right)}{(1 + \Gamma\sigma_i)} \right\}^2 \right]} \quad (\text{A.17})$$

In the simplified version of MSA, P_n is taken as zero.

The value of the shielding parameter Γ is obtained by iteration where it can be seen that each “charged hard sphere” (ion) has its own characteristic diameter σ_i . This is the non-restricted primitive version, which is utilized in our thermodynamic framework.

A.1.3 Restricted primitive

To reduce the complexity, a restricted version can be formed by using an average diameter σ as the same diameter for each ion $\sigma = \frac{\sigma_+ + \sigma_-}{2}$. This is the so-called restricted version and does not require an iterative solution for Γ and the equation of reduces to:

$$\Gamma = -\frac{1}{2} \left[\frac{(1 - \sqrt{(1 + 2\alpha\sigma)\sqrt{\sum_i \rho_i z_i^2}})}{\sigma} \right] \quad (\text{A.18})$$

A.1.4 Helmholtz energy expression

The solution obtained for MSA can be conveniently applied to derive relationship for thermodynamic properties such activity coefficients and internal energy. Planche and Renon [276] developed an analytical expression to develop a primitive electrolyte EoS using the Blum formalism and taken into account the effect of neutral solvent molecules. The equation was further simplified by Fürst and Renon [69]. This is the version that we incorporated in our thermodynamic EoS, we use the non-restricted case (ions of different diameter) is given as:

$$\frac{A^{MSA}}{RT} = -\frac{e^2 N_A}{4\pi\epsilon_0 DRT} \left[\Gamma \sum_i \frac{n_i z_i^2}{1 + \Gamma\sigma_i} \right] + \frac{V\Gamma^3}{3\pi N_A} \quad (\text{A.19})$$

$$4\Gamma^2 = -\frac{e^2 N_A^2}{\epsilon_0 DRT} \sum_i \frac{n_i}{V} \left[\frac{z_i}{1 + \Gamma\sigma_i} \right]^2 \quad (\text{A.20})$$

where, D is the dielectric constant of the solvent, z_i si the cahrg on the ion, e is the electronic charge.

In the case when ions are treated as spheres of identical σ (the restricted case) or some call it a explicit case, the Helmholtz free energy is given by:

$$\frac{A^{MSA}}{RT} = -\frac{2\Gamma^3 V}{3\pi N_A} \left[1 + \frac{3}{2}\Gamma\sigma \right] \quad (\text{A.21})$$

$$\Gamma = \frac{1}{2\sigma} \left[\sqrt{1 + 2\sigma\kappa} - 1 \right] \quad (\text{A.22})$$

$$\kappa = \left(\frac{e^2 N_A^2}{\epsilon_0 DRTV} \sum_i n z_i^2 \right) \quad (\text{A.23})$$

A.2 Non-Primitive MSA

In non-primitive MSA the solvent molecules are treated as dipolar hard sphere having a hard sphere diameter. This version is used by several authors [9, 277, 278] in their electrolyte EoS. This version of MSA includes three different types of interactions, ion-ion, ion-dipole, and dipole-dipole. This is in contrast to the primitive version which has only ion-ion interaction.

$$u_{ij}^{id}(r) = -\frac{z_i e \mu_j}{r^2} (\vec{r}_{ij} \vec{\mu}_{ij}) \quad (\text{A.24})$$

$$u_{ij}^{dd}(r) = -\frac{\mu_i \mu_j}{r^3} [3(\vec{\mu}_i \vec{r}_{ij})(\vec{\mu}_j \vec{r}_{ij}) - \vec{\mu}_i \vec{\mu}_j] \quad (\text{A.25})$$

$$u_{ij}^{ii}(r) = \frac{z_i z_j e^2}{r} \quad (\text{A.26})$$

The solution of the OZ equation was presented by Blum *et al.* [279] for the restricted case where all ion and dipoles case same diameter.

Here we present the case for restricted non-primitive MSA, where the residual Helmholtz energy contribution is obtained after solving systems of six non-linear equations. These equation are repeated from Blum and Wei [280] without derivation. The equations for the semi-restricted non-primitive MSA are repeated below Herzog *et al.* [74], this version utilizes a common ion diameter σ_{ion} and different diameter for dipolar hard spheres σ_{solv} fo solvent molecules. In contrast to the restricted non-primitive MSA, the only difference here is that $\sigma_{solv} \neq \sigma_{ion}$.

A set of non-linear algebraic equation are solved which yield three different energy parameters, b_0 for ion-ion, b_1 for ion-dipole, b_2 for dipole-dipole.

$$a_1^2 + a_2^2 + d_0^2 = 0 \quad (\text{A.27})$$

$$a_1 k_{10} - a_2(1 - k_{11}) - d_0 d_2 = 0 \quad (\text{A.28})$$

$$k_{10}^2 + (1 - k_{11})^2 - y_1^2 - d_2^2 = 0 \quad (\text{A.29})$$

where the parameter d_0^2 and d_2^2 are calaculted by,

$$d_0^2 = \frac{4\pi}{kT} e^2 \sigma_{ion} \sum_j^{ions} \rho_j z_j^2 \quad (\text{A.30})$$

$$d_2^2 = \frac{4\pi}{3kT} \mu_{D,solv}^2 \rho_{solv} \quad (\text{A.31})$$

For solving equations A.27-A.29, some other parameters are required such as $a_1, a_2, k_{10}, k_{11}, y_1$, their relations are given below

$$\beta_3 = 1 + \frac{b_2}{3} \quad \beta_6 = 1 - \frac{b_2}{6} \quad \beta_{12} = 1 + \frac{b_2}{12} \quad (\text{A.32})$$

$$\lambda = \frac{\beta_3}{\beta_6} \quad \Delta = \frac{b_1^2}{4} + \beta_6^2 \quad y_1 = \frac{\beta_6}{\beta_{12}^2} \quad (\text{A.33})$$

$$(\text{A.34})$$

$$D_F = 0.5 \left(\beta_6(1 + b_0) - \frac{b_1^2 \sigma_{solv}}{12 \sigma_{ion}} \right) \quad (\text{A.35})$$

$$a_1 = \frac{1}{2D_F^2} (\Delta - 2\beta_6 D_F) \quad (\text{A.36})$$

$$a_2 = \frac{-b_1}{2\beta_6 D_F^2} \left(\frac{\Delta}{2} - 2D_F \beta_3 \frac{\sigma_{ion}}{\sigma_{solv}} \right) \quad (\text{A.37})$$

$$\Lambda = 0.5(1 + b_0) + \frac{\beta_6 \sigma_{solv}}{6 \sigma_{ion}} \quad (\text{A.38})$$

$$k_{10} = \frac{\sigma_{solv}}{\sigma_{ion}} \frac{b_1}{2\Delta} (1 + a_1 \Lambda) \quad (\text{A.39})$$

$$k_{11} = 1 - \frac{1}{\Delta} \left(\beta_3 - a_2 b_1 \Lambda \frac{\sigma_{solv}}{2 \sigma_{ion}} \right) \quad (\text{A.40})$$

The initial guess for solving these equation can be used as given below

$$b_0 = \frac{-2d_0(1 + d_0)}{4 + 8d_0 + 3d_0^2} F_H^{0.5} \quad (\text{A.41})$$

$$b_2 = \frac{3d_2^2}{2 + d_2^2} F_H \quad (\text{A.42})$$

$$b_1 = b_0(2b_2)^{0.5} \quad (\text{A.43})$$

$$F_H = 1 - 1.5x_{ion}x_{solv} \sqrt{\frac{\pi}{6} \frac{N_{total}}{V} \sum_i \sigma_i^3} \quad (\text{A.44})$$

After deducing the parameters b_0 , b_1 , and b_2 the following expression can be used for calculating the contribution to residual Helmholtz energy by np-MSA term.

$$\frac{A^{ion-ion}}{RT} = \frac{1}{12\pi\rho\sigma_{ion}^3} (2d_0^2 b_0 - [Q'_{ion-ion}]^2) \quad (\text{A.45})$$

$$\frac{A^{ion-dipole}}{RT} = \frac{1}{12\pi\rho\sigma_{ion}^3} \left(-2d_0 d_2 b_1 \frac{\sigma_{ion}}{\sigma_{solv}} - \left[1 + \frac{\sigma_{ion}}{\sigma_{solv}} \right] \frac{\sigma_{ion}}{\sigma_{solv}} [Q'_{ion-dipole}]^2 \right) \quad (\text{A.46})$$

$$\frac{A^{dipole-dipole}}{RT} = -\frac{1}{12\pi\rho\sigma_{solv}^3} ([Q'_{dipole-dipole}]^2 + 2(q')^2) \quad (\text{A.47})$$

where,

$$Q'_{ion-ion} = -a_1 - 2 + \frac{\beta_6}{D_F} \quad (\text{A.48})$$

$$Q'_{ion-dipole} = \frac{b_1}{\beta_6^2 D} [(\beta_3 + a_1(3\Lambda - 2D_F))] \quad (\text{A.49})$$

$$D = 1 + \frac{b_1^2}{4\beta_6^2} \quad (\text{A.50})$$

$$Q'_{dipole-dipole} = \frac{2}{\Delta} (\beta_3^2 - (\frac{\sigma_{solv}}{\sigma_{ion}} b_1 a_2 (3\Lambda - 2D_F))) - 2 \quad (\text{A.51})$$

$$q' = b_2 \frac{1 - b_2/24}{\beta_{12}^2} \quad (\text{A.52})$$

where $\rho_i = \frac{N_i}{V}$

Final Helmholtz energy expression is given as the sum of the three contributions:

$$\frac{A^{MSA}}{RT} = \frac{A^{ion-ion}}{RT} + \frac{A^{ion-dipole}}{RT} + \frac{A^{dipole-dipole}}{RT} \quad (\text{A.53})$$

Appendix B

LLE phase diagrams of mixed-solvent salt systems

B.1 1-Butanol-water-salts

The result of the ternary phase diagram of liquid-liquid equilibrium(LLE) of 1-Butanol-water- salt systems are presented here (figure B.1).

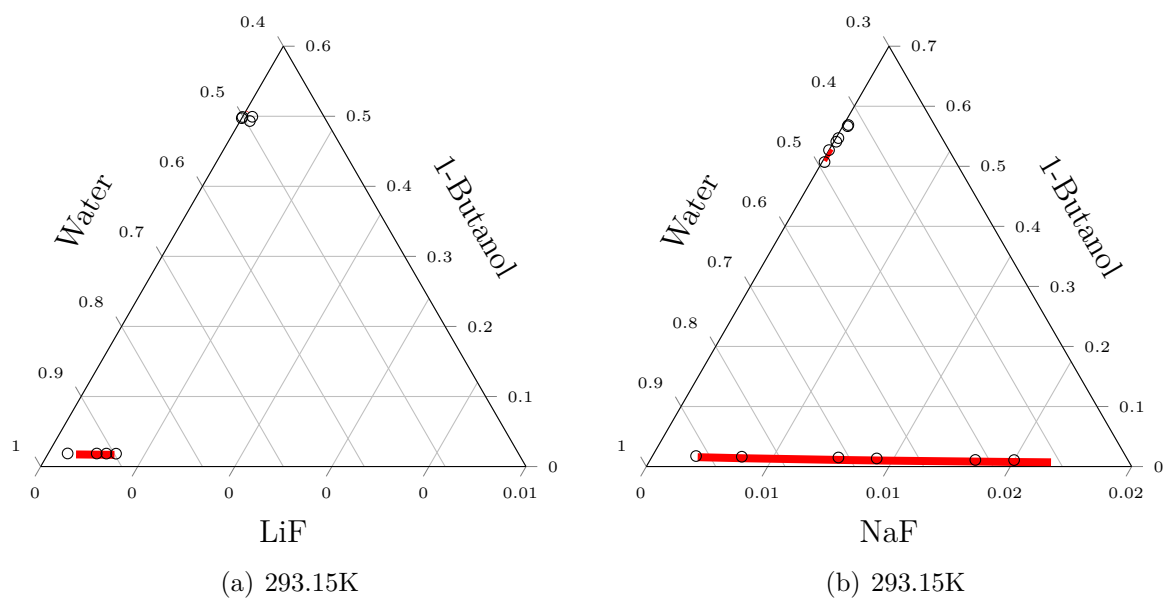
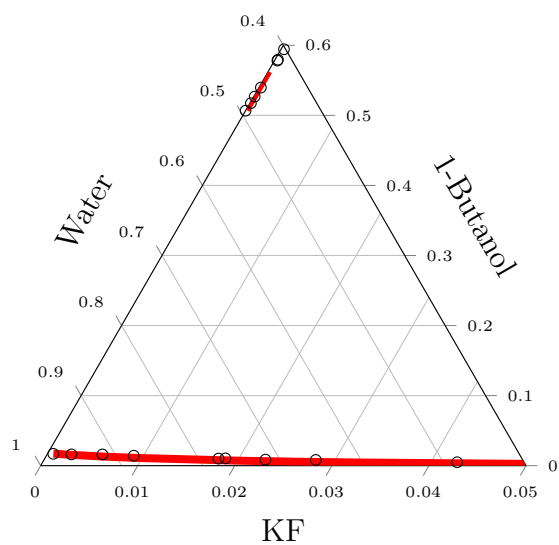
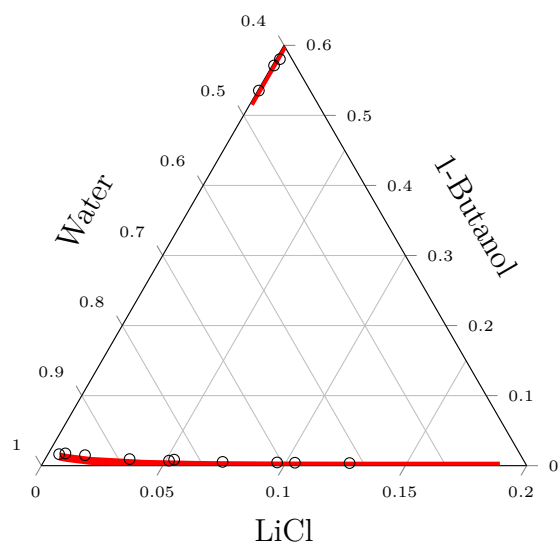


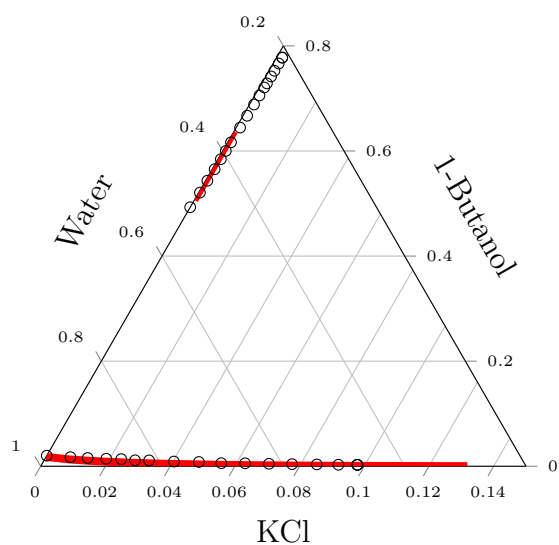
Figure B.1: Liquid-Liquid equilibrium in 1-Butanol-Water-Salt systems at various temperatures, Points are experimental data, line is the calculation from model. Axes represent the mole fraction of the respective component, some axes are scaled.



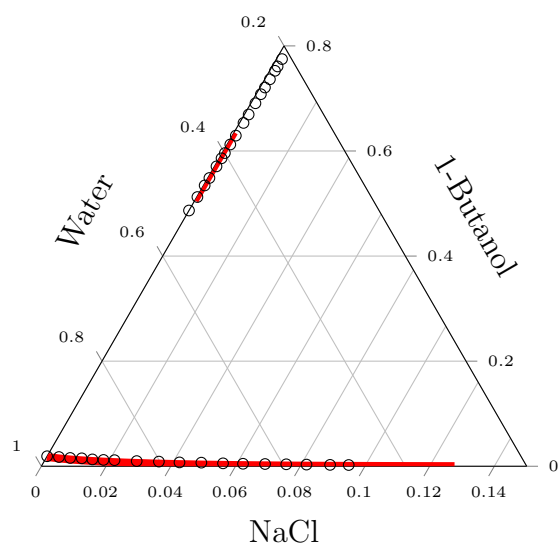
(a) 293.15K



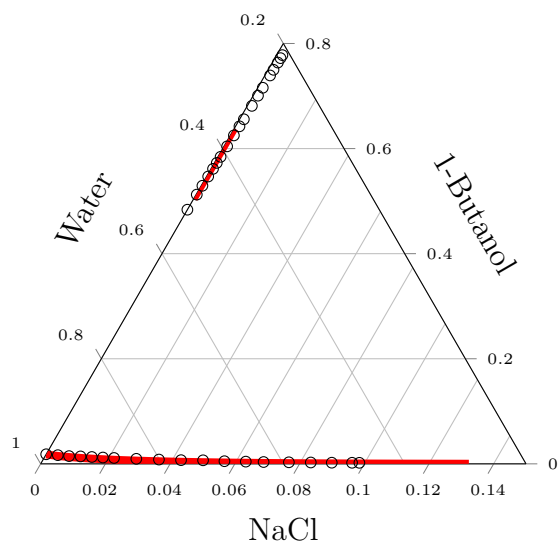
(b) 293.15K



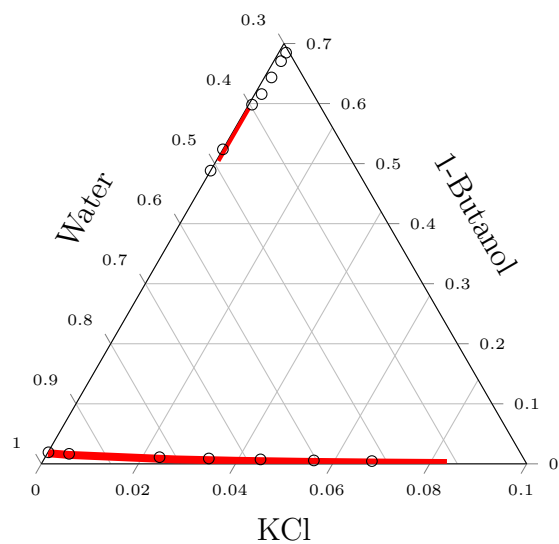
(c) 293.15K



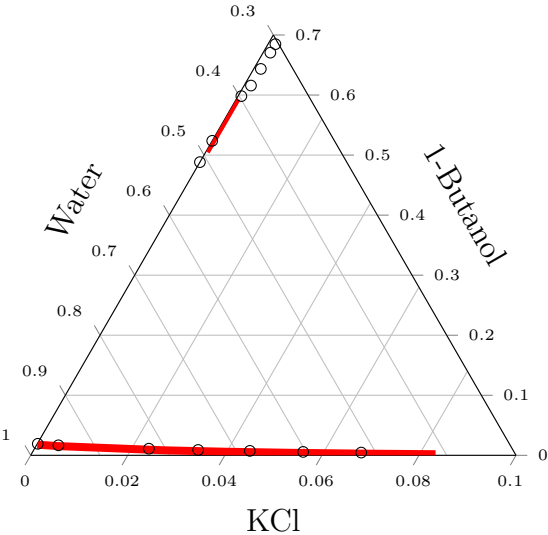
(d) 298.15K



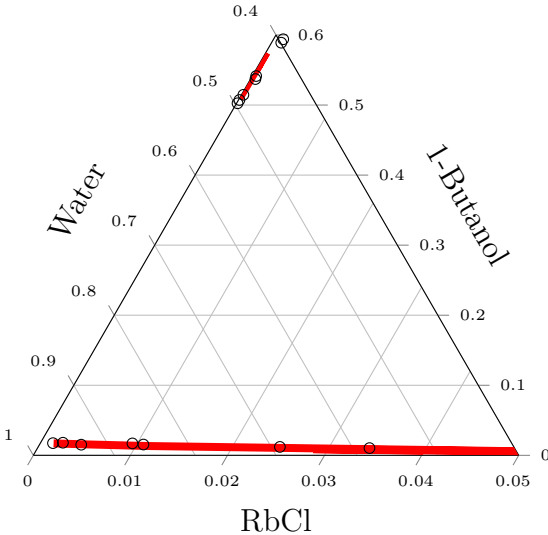
(e) 303.15K



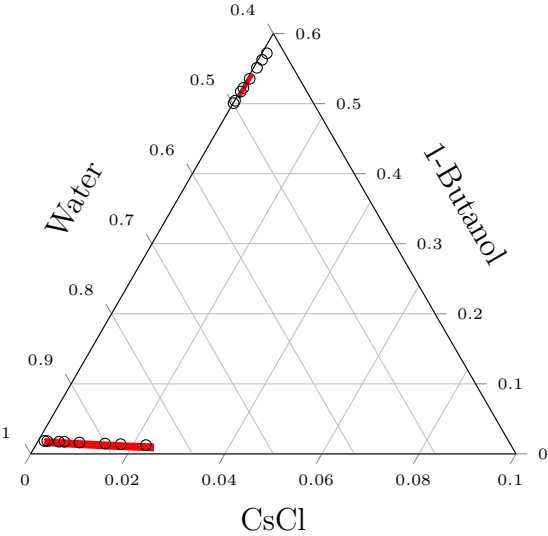
(f) 293.15K



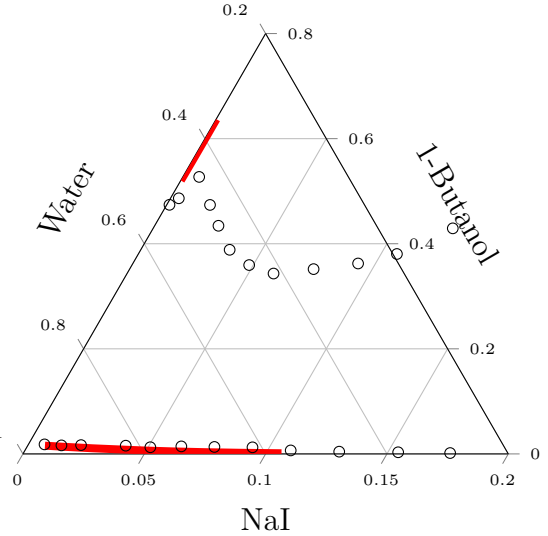
(g) 298.15K



(h) 293.15K



(i) 293.15K



(j) 293.15K

B.2 2-Butanol-water-salts

The result of the ternary phase diagram of liquid-liquid equilibrium (LLE) of 2-Butanol-water-salt systems are presented here (figure B.2). The parameter used for predicting LLE of this systems are same as those used for 1-Butanol-water-salt systems. There are higher deviation as compared 1-Butanol-water-salt systems, the salt is underpredicted in the organic region. The reason as pointed out in chapter 5 that it is due to use of same OH-ion parameter(of 1-Butanol-ions) for predicting 2-butanol. Moreover, the dielectric constant parameter $D_{ij} = 0.7$ used in this case should change as the dielectric constant of 2-butanol-water-salts is different from 1-butanol-water-salts

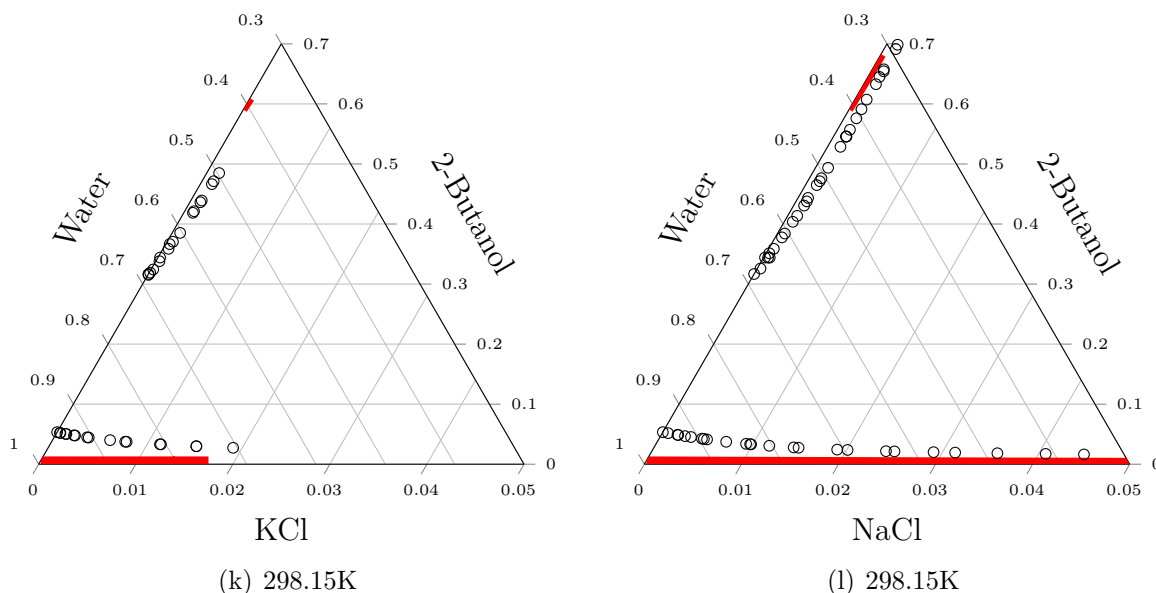


Figure B.2: Liquid-Liquid equilibrium in 2-Butanol-Water-Salt systems at 298.15K, Points are experimental data (NaCl [268], KCl [268]) line is the calculation from model. Axes represent the mole fraction of the respective component, some axes are scaled.

B.3 Propanol-water-salts

The result of the ternary phase diagram of liquid-liquid equilibrium (LLE) of 1-propanol-water-salt systems are presented here (figure B.3). These results are calculated using the same parameters as obtained for 1-butanol-water-salt systems.

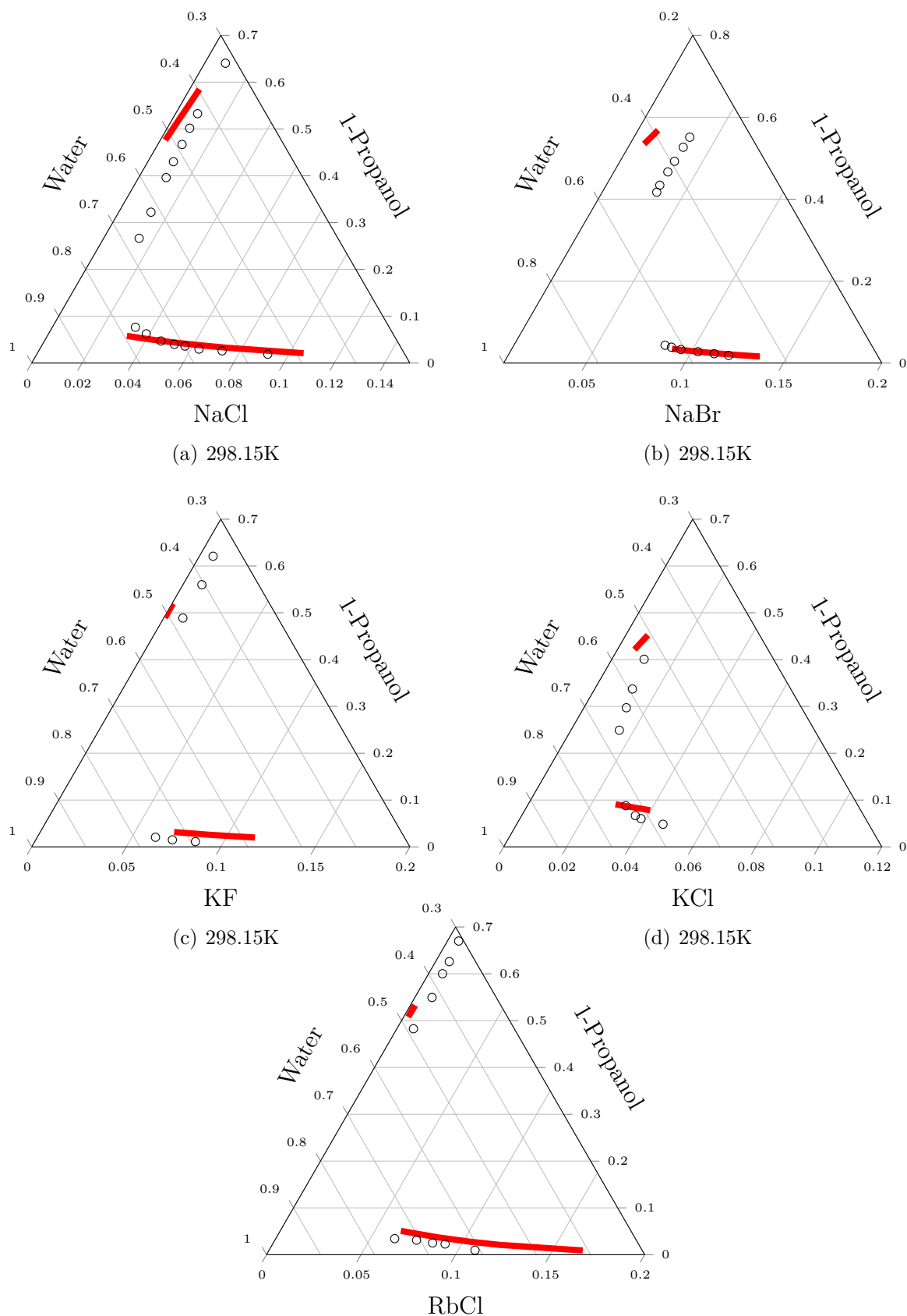


Figure B.3: Liquid-Liquid equilibrium in 1-Propanol-Water-Salt systems at 298.15K, Points are experimental data(NaCl [281], NaBr [281], KF [282],KCl [283]), RbCl [284]) line is the calculation from model. Axes represent the mole fraction of the respective component, some axes are scaled.

